Cellular localization, pro-oxidant/antioxidant effects of natural products and organometallics in normal and tumor cells

By

AMIT KUNWAR

BHABHA ATOMIC REASERCH CENTRE

A thesis submitted to the
Board of Studies in Chemical Sciences Discipline

In partial fulfillment of requirements

For the Degree of

DOCTOR OF PHILOSOPHY

of

HOMI BHABHA NATIONAL INSTITUTE

September, 2009

Homi Bhabha National Institute

Recommendations of the Viva Voce Board

As members of the Viva Voce Board, we certify that we have read the dissertation prepared by **Amit Kunwar** entitled "**Cellular localization, pro-oxidant/antioxidant effects of natural products and organometallics in normal and tumor cells**" and recommend that it may be accepted as fulfilling the dissertation requirement for the Degree of Doctor of Philosophy.

Chairman-	**(Dr. S. Chattopadhyay)**	Date: 12/04/2010
Convener-	**(Dr. K. I. Priyadarsini)**	Date: 12/04/2010
Member 1-	**(Dr. R. K. Bhattacharya)**	Date: 12/04/2010
Member 2-	**(Dr. M. Krishna)**	Date: 12/04/2010
Member 3-	**(Dr. D. B. Naik)**	Date: 12/04/2010
Member 4-	**(Dr. T. P. A. Devasagayam)**	Date: 12/04/2010

Final approval and acceptance of this dissertation is contingent upon the candidate's submission of the final copies of the dissertation to HBNI.

We hereby certify that we have read this dissertation prepared under our direction and recommend that it may be accepted as fulfilling the dissertation requirement.

Guide – **Dr. K. I. Priyadarsini** Date: 12/04/2010

Co-guide – **Dr. M. Krishna** Date: 12/04/2010

STATEMENT BY AUTHOR

This dissertation has been submitted in partial fulfillment of requirements for an advanced degree at Homi Bhabha National Institute (HBNI) and is deposited in the library to be made available to borrowers under rules of the HBNI.

Brief quotations from this dissertation are allowable without special permission, provided that accurate acknowledgement of source is made. Requests for permission for extended quotation from or reproduction of this manuscript in whole or in part may be granted by the Competent Authority of HBNI when in his or her judgment the proposed use of the material is in the interests of scholarship. In all other instances, however, permission must be obtained from the author.

Amit Kunwar

DECLARATION

I, hereby declare that the investigations presented in the thesis have been carried out by me. The work is original and has not been submitted earlier as a whole or in part for a degree / diploma at this or any other Institution / University.

Amit Kunwar

Dedicated to my parents

ACKNOWLEDGEMENTS

I wish to record my deep sense of gratitude and sincere thanks to my research guide Dr. (Mrs) K. I. Priyadarsini, Head, Radiation Chemistry Section, RPC Division for her unstinted inspiration, invaluable guidance, encouragement, keen interest, good wishes and valuable suggestions throughout my entire research tenure. I am also grateful to her for critically reviewing this thesis.

It gives me immense pleasure to acknowledge to my research co-guide Dr. (Mrs) M. Krishna, Head, Radiation Signaling Section, RB&HS Division for critically evaluating my research activities time to time and also for providing the laboratory facilities and several valuable suggestions for completion of this work.

It is also my great pleasure to thank Drs. T. Mukherjee, Director, Chemistry Group, K. B. Sainis, Director, Bio-medical Group and S. K. Sarkar, Head, RPC Division BARC for their encouragement and support in carrying out the research work.

It is my great privilege to acknowledge Drs. S. K. Ghosh, Head, TCS, S. Chattopadhyay, Head, Bio-organic Division, D. B. Naik, RPC Division and T. P. A. Devasagayam, RB&HS Division for critically evaluating my research activities time to time as members of the HBNI doctoral committee and providing valuable suggestions for completion of this work.

I express my sincere thanks to Dr. M. K. Unnikrishnan and Mr. P. Bansal of Manipal College of Pharmaceutical Sciences, for their help in carrying out the in vivo experiments at Manipal, India.

I convey my sincere thanks to Drs. R. C. Chaubey, S. K. Sandur, R. Pandey and H. Narang of RB&HS Division and V. K. Jain, Chemistry Division, for providing laboratory facilities and moral support time to time.

I also wish to thank my senior lab colleagues Drs. A. Barik and B. Mishra for helping me in experimental work and providing constructive suggestions throughout the work. It is a great pleasure to acknowledge my lab mates U. Singh, P. P. Bag, B. Santosh kumar, E. Simon and Elizabeth Thomas for their kind support and encouragement during my research work. I am also thankful to all my RPCD colleagues and staff members for their support at different times.

I wish to express my sincere gratitude and indebtedness to my parents, parents-in-law for their blessings, brother and other family members for their love and support to me. I am extremely thankful to my wife Anshu for all her love and understanding.

Last but not the least, I also wish to thank all my friends especially S. Verma, A. Srivastava, S. Jayakumar, Y. S. Rajpurohit, S. Bihani, S. Roy, N. Rawat and B. S. Rajpurohit for their constant unconditional support.

September, 2009 *Amit Kunwar, RPCD, BARC*

CONTENTS

SYNOPSIS

Preamble

Recent focus on antioxidant research is to develop multifunctional compounds having antioxidant activity along with other important pharmacological activities such as anti-tumor, anti-inflammatory activities, radioprotection etc. Natural products and herbal extracts derived from the plant sources are considered pharmacologically safe since they are consumed regularly as part of the diet. Therefore, such compounds are the first choice of researchers for the exploration of their antioxidant property; accordingly several plant derived polyphenols are in different stages of evaluation as new therapeutic antioxidants. There has also been a growing interest among researchers for exploring new derivatives of natural antioxidants and synthetic compounds as novel class of drugs with multiple activities and target specificity.

The main hurdle in developing such compounds as therapeutic agents is that they switch over from antioxidant to pro-oxidant behavior depending on the dosage and type of the target cell. This antioxidative or pro-oxidative activity of a compound has its own significance like for example: the antioxidative property may be useful to protect the normal cells from oxidative stress while pro-oxidative property may confer the molecule selective toxicity to tumor cells. It is therefore, necessary to identify the conditions under which such compounds show differential activities in order to take full advantage of their therapeutic potential.

With this aim, in the present thesis, curcumin a natural product from *Curcuma longa L*, its copper complex that acts as a superoxide dismutase (SOD) mimic, and a synthetic selenocystine derivative having glutathione peroxidase (GPx) activity have been evaluated for antioxidant/pro-oxidant activity. Wherever possible, they have also been examined for their ability to offer protection against radiation induced oxidative

stress (radioprotector) in different biological models. Details of the above mentioned studies including general introduction and experimental techniques have been arranged in four different chapters of the thesis.

Chapter I

This is an introductory chapter and describes the literature related to various terminologies such as free radicals, oxidative stress, antioxidants and radioprotection linked to the research problem and also about the current status of research on different pharmacological aspects of curcumin and organoselenium compounds.

Free radicals are highly reactive molecules or atoms having one or more unpaired electrons.[1,2] In cells, reactive free radicals like $O_2^{\bullet -}$, $^{\bullet}OH$, $ROO^{\bullet}$, $RO^{\bullet}$, $NO^{\bullet}{}_2$ are derived from oxygen or nitrogen and are generally known by the collective term reactive oxygen species (ROS).[1,2] ROS have been recognized for playing a dual role since they can be either harmful or advantageous to living systems.[1,2] Beneficial effects of ROS occur at low/moderate concentrations and involve physiological roles in cellular responses to defense against infectious agents and in the activation of cellular signaling network as observed during induction of a mitogenic response.[3] Oxidative stress occurs in biological systems when there is an overproduction of ROS on one side and a deficiency of enzymatic antioxidants such as SOD, catalase, GPx and non-enzymatic antioxidants like vitamin E, vitamin C, glutathione (GSH), pyruvate etc. on the other.[1,2] In other words, oxidative stress represents a disturbance in the equilibrium status of pro-oxidant/antioxidant levels in living organisms. Excess ROS can damage cellular lipids, proteins and DNA, thereby inhibiting their normal function. Because of this, oxidative stress has been implicated in the onset of a number of diseases such as cancer, atherosclerosis, ageing, diabetics, neurological diseases, etc. as well as in the ageing process.[4] Antioxidants are molecules that

neutralize free radicals mainly by scavenging them and converting them to less reactive species, thereby preventing or slowing down the deleterious effect of these reactive species to the cellular components.[2] Hence supplementation of exogenous antioxidants that can act either as free radical scavenger or as antioxidant enzyme mimic is being examined to offset this oxidative challenge.

Exposure of ionizing radiation to cells also causes similar effect as oxidative stress.[5] Interaction of ionizing radiation is non-selective and water being the major constituent in cells undergoes radiolysis, producing radicals that react with cellular organelles, similar to those produced by oxidative stress. Due to the similarity between oxidative stress and radiation injury, an antioxidant in principle can also act as an agent that can reduce the damaging effects of radiation and such compounds are termed as radioprotectors.[5] In this background, the focus of the researchers has been to develop new antioxidants based on natural plant products as well as synthetic compounds that showed improved efficacy and selectivity. For the present thesis work curcumin and organoselenium compound were selected.

Curcumin is the major yellow pigment obtained from the root of *Curcuma longa L*, belonging to the *zingeberacea* family. It constitutes nearly 2-8% of the dry weight of turmeric. The chemical structure of curcumin has been shown in scheme -1.

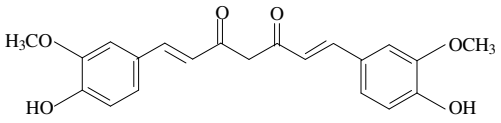

Scheme-1: *Curcumin*

Curcumin exhibits a variety of pharmacological properties such as antioxidant, anti-inflammatory, anti-carcinogenic, anti-microbial, neuro-protective, cardio-protective, thrombo-suppressive and anti-diabetic actions.[6,7] Interestingly, while contended to

have antioxidant effects, reports are now steadily appearing about apparently contradictory investigations of curcumin showing its pro-oxidative effects in transformed cells in culture.[7]

The trace element selenium is a well established micronutrient for both humans and animals.[8] The biochemical role of selenium in mammals has been clearly established by the discovery that it is part of the catalytic group within active site of the redox active enzymes like GPx and thioredoxin reductase (TRx).[8] The GPx is an antioxidant enzyme, playing a crucial role in combating oxidative stress and thus is primarily responsible for the antioxidant action shown by selenium.[8] The effects of selenium on the organism are sensitive to the dosage, ranging from essential to antioxidant to pro-oxidant resulting in to limited therapeutic utility.[8] In general organoselenium compounds have less toxicity than inorganic selenium.[9] Therefore, design and development of new water-soluble, stable, and non-toxic organoselenium compounds with therapeutic potential as antioxidant, GPx mimics, radioprotector, immunomodulators, chemopreventive and antitumor agents is of current interest to researchers.

Chapter II

This chapter gives details of experimental methods used in different studies. The cell lines used for different studies included RAW 264.7 (mouse macrophage cell line), MCF7 (breast cancer cells of human origin), EL4 (T cell lymphoma of murine origin) and NIH3T3 (mouse fibroblast cells). The human RBCs (erythrocytes) and mouse spleen lymphocytes were freshly isolated. The free radical scavenging activity of curcumin or organoselenium compounds was studied by following their reaction with peroxyl radicals using pulse radiolysis set up and kinetic spectrometry. The antioxidant activity in RBCs was studied in terms of their ability to inhibit peroxyl

radicals induced membrane lipid peroxidation, hemolysis and K^+ ion leakage as assessed by the formation of thiobarbituric acid reactive substances (TBARS), absorbance of hemoglobin at 532 nm and flame photometry respectively.

The pro-oxidant effect of curcumin in cells was studied by monitoring the intracellular ROS studied by the oxidation sensitive probe dichlorofluorescein diacetate (DCF-DA) and non protein thiol levels using 5,5'-dithiobis-2-nitrobenzoic acid (DTNB) reagent. The expression of antioxidant genes at mRNA level was checked by reverse transcription – polymerase chain reaction (RT-PCR) while the post translational modification of signal transduction proteins was checked by western blotting. The cytotoxicity was evaluated by trypan blue dye exclusion test using a hemocytometer and 3-[4,5-dimethylthiazole-2-yl]-2,5-diphenyl tetrazolium bromide dye conversion assay. The γ-radiation induced apoptosis in cells was estimated by DNA fragmentation assay and by cell cycle analysis using flow cytometry. The uptake of curcumin by cells was calculated by estimation of curcumin extracted in to methanol from cell lysate. The intracellular localization of curcumin was confirmed by confocal microscopy using an Olympus Fluoview 500 confocal laser-scanning microscope (Olympus, Tokyo, Japan) equipped with a multi-Argon laser for excitation at 458, 488 and 515 nm.

In vitro GPx activity of organoselenium compound was assessed by employing hydroperoxides as substrate and thiols as co-substrate. GPx activity was measured by monitoring the glutathione reductase catalyzed NADPH oxidation at 340 nm at 37ºC. The *in vivo* radioprotection studies of organoselenium compound were done in Swiss albino mice with strict adherence to the ethical guidelines laid down by the institutional animal ethics committee of BARC. For γ-irradiation ^{60}Co γ-source (Theratron –780) at a dose rate of 0.52Gy/min as measured by standard Fricke

dosimeter was used. Animals were sacrificed at different time intervals post irradiation and antioxidant enzyme activities were estimated in liver homogenate using standard assays. DNA damage was checked in peripheral leukocytes by single cell gel electrophoresis (comet assay). The survival studies were carried out at Department of Pharmacology, Manipal University using the ^{60}Co γ-source (Theratron teletherapy unit, dose rate of 1.66 Gy/min) of Kasturba Medical College, Manipal, India, after approval from the institutional animal ethics committee.

The results have been presented as mean ± S.E.M. for two independent experiments run in triplicates. The statistical analysis of the data was done by student's "t" test, one-way and two-way ANOVA of Origin software (version 6.0.0)

Chapter III

This chapter discusses about the antioxidant activity, pro-oxidative toxicity, uptake and localization of curcumin in cells. This chapter also discuses about the radioprotection studies of transition metal complex of curcumin having SOD like activity in cells. This chapter has been divided in to three sections; section I describes differential antioxidant/pro-oxidant behavior of curcumin in human RBCs and murine macrophage cell line (RAW 264.7), section II describes the radioprotective effects of 1:1 copper-curcumin complex in spleen lymphocytes and section III describes the differential cellular uptake and localization of curcumin in normal vs. tumor cells.

Section-I: Oral usage of curcumin results in its systemic distribution to peripheral blood circulation before reaching to target cell. The peripheral blood vascular system possesses different kind of cells including erythrocytes or red blood cells (RBCs) and leukocytes such as monocytes and lymphocytes. Curcumin exhibits both antioxidant and pro-oxidant behavior depending on dosage, cell type and oxidative stress, it

becomes essential to investigate the effect of concentration on the antioxidant and pro-oxidant activity of curcumin in above type of cells.

(a) Studies in human RBCs - The RBCs are the most important cells as they carry oxygen to different parts of body. However, these cells are highly sensitive to oxidative stress and undergo hemolysis. In recent years oxidative hemolysis of RBCs induced by free radicals and its inhibition by compounds are being used as a model system to screen the antioxidant behavior of a test compound. Free radical reaction is initiated with the help of an azo compound, 2,2'-azobis (2-amidinopropane) hydrochloride (AAPH) in the presence of oxygen. RBC membranes are rich in polyunsaturated fatty acids, which are susceptible to free radical-mediated peroxidation leading to damage of the membrane, release of hemoglobin (hemolysis), release of intracellular K^+ ions and depletion of GSH. The pretreatment of RBCs with curcumin (1-50 μM) showed concentration dependant decrease in levels of TBARS and hemolysis. The IC_{50} values for lipid peroxidation and hemolysis were estimated to be 23.2 ± 2.5 and 43 ± 5.0 μM respectively. However, in contrast to above mentioned effects, curcumin in similar concentration range, did not prevent release of intracellular K^+ ions during the process of hemolysis, rather curcumin itself induced its release even in the absence of AAPH. The ability of curcumin to prevent oxidation of intracellular GSH due to AAPH showed mixed results. At low concentrations of curcumin (≤10 μM), it prevented GSH depletion and at higher concentrations, the GSH levels decreased gradually. Curcumin also scavenged the peroxyl radicals generated from AAPH with bimolecular rate constant of 63.4 ± 12.7 M^{-1} s^{-1}. These results indicate that curcumin while acting as an antioxidant, also exhibits pro-oxidant activity at higher concentrations.

(b) Studies in RAW 264.7 cells - Apart from treatment concentrations several other factors such as ability to differentially modulate the redox environment either through promoting the intracellular production of free radicals or by free radical quenching, activation of cytoprotective or cytotoxic signaling pathways and expressions of ROS scavenging enzymes in different cell types may contribute to curcumin action as antioxidant or a pro-oxidant. Since mature RBCs do not have the transcriptional and translational machinery to synthesize antioxidant enzymes, the effect of curcumin on the expression of above enzymes cannot be studied in these cells. The macrophage cells which represent the differentiated monocytes, are better for such studies as these cells are highly responsive to oxidative stress induced inflammation through transcriptional and translational modulation of antioxidant enzymes.[10] In order to understand the antioxidant and pro-oxidant behavior of curcumin in similar type of cells, the effects of treatment concentration and incubation time on intracellular ROS generation, non protein thiol levels and mRNA expression of antioxidant enzymes was evaluated in RAW 264.7 cells. Treatment of cells with curcumin (1 – 25 μM) elevated ROS levels accompanied by a decrease in levels of intracellular non-protein thiols at 2 h after its addition to cells indicating that curcumin provoked oxidative stress early after its addition. However, the ROS levels decreased and non-protein thiols content increased at 18 h after its addition suggesting that the pro-oxidant activity of curcumin was only transient. The investigations on the expression of antioxidant enzymes at 6 and 18 h after treatment with 5 or 25 μM curcumin, showed induction of *GPx*, *catalase*, *heme oxygenase (HO-1)* and *Cu,Zn –SOD* genes with increasing time and concentration. A striking observation of the present study was that curcumin reduced the *Mn-SOD* gene expression in a concentration dependant manner. The cell viability was significantly reduced at high concentration (25 μM) of

curcumin treatment but not at low concentration (5 μM). The observed loss of cell viability after treatment of 25 μM curcumin was also evident in terms of the decrease in expression of antiapoptotic genes such as *Bcl-2* and *Bcl-XL*, which are required for cell survival. These results provide a line of evidence to support the existence of a concentration and time dependent differential changes in oxidative stress and antioxidant gene expression levels as part of the molecular mechanism leading to either beneficial or cytotoxic actions as caused by curcumin. Since recent approach of antioxidant therapy is to use a combination of antioxidants to achieve desired therapeutic potential, the effects of water soluble thiol antioxidants such as GSH or NAC on curcumin-mediated cellular modifications were also studied by pre-treating the cells with GSH or NAC. Interestingly, pretreatment with GSH (1mM) inhibited curcumin induced oxidative stress and antioxidant effects at 2 and 18 h respectively. However, NAC pretreatment at the same concentration inhibited the pro-oxidant effects of curcumin at early time point (2 h) and augmented the antioxidant effects at 18 h. GSH also lowered the curcumin induced expressions of *GPx*, *Cu,Zn-SOD* and *HO-1* genes and increased the expression of *Mn-SOD* gene. While, NAC increased the curcumin induced expression of *GPx* and reduced the expression of all the other genes examined. Pretreatment with GSH or NAC inhibited curcumin induced cell death however; NAC was more effective than GSH. This differential modulation of curcumin action by thiols could be due to their ability to inhibit cellular uptake of curcumin as GSH is impermeable to cells. Our experiments indeed showed that GSH significantly inhibited the cellular uptake of curcumin; however, pretreatment with NAC did not affect curcumin uptake by cells. These studies hence conclude that thiols can be employed to modulate curcumin action in cells to achieve the desired therapeutic effects.

Section-II: As discussed earlier curcumin is a potent antioxidant at low doses (≤10 μM) and one of the mechanisms of its antioxidant action is the ability to chelate metal ions. However, this property of curcumin can also be used to design SOD mimics.[11,12] SOD is an endogenous enzymatic antioxidant that converts toxic superoxide radical to hydrogen peroxide and oxygen. Hydrogen peroxide is further reduced to water by catalase enzyme.

$$2O_2^{\bullet -} + 2H^+ \xrightarrow{SOD} O_2 + H_2O_2$$

$$2H_2O_2 \xrightarrow{catalase} 2H_2O + O_2$$

SOD is being used as a therapeutic agent to reduce oxidative stress.[11] However due to limitations in the supplementation with native exogenous SOD, new SOD mimics are being developed.[11,12] Most of the SOD mimics are designed with a redox active metal centre, like copper, manganese etc. similar to the active metal site of the native SOD. SOD mimics made by complexation of metals with functional ligands like antioxidants are preferred as they have additive effects.[11,12] With this background a copper (II)-curcumin complex with the stoichiometry of 1:1 was synthesized in our laboratory. It was reported to exhibit SOD mimetic activity and free radical scavenging capability better than curcumin.[11,12] The chemical structure of 1:1 copper-curcumin complex has been shown in scheme -2.

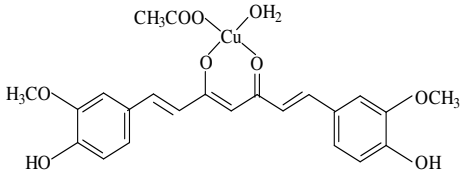

Scheme-2: 1:1 *Copper-Curcumin Complex*

Since exposure of cells to high energy radiation leads to acute depletion of intracellular antioxidants, the supplementation with exogenous antioxidants in form of

SOD mimic prior to irradiation is expected to protect the cells against free radicals induced oxidative stress. With this view, we investigated the modulation of γ-radiation induced oxidative stress by the complex in freshly isolated spleen lymphocytes and compared these results with those for curcumin. The lymphocytes were pretreated with curcumin or the complex at 10 μM and then exposed to γ-radiation at an absorbed dose of 2 to 8 Gy. The oxidative stress parameters like lipid peroxidation, protein carbonylation and intracellular antioxidant levels were estimated within one hour post irradiation to check the ability of the complex to prevent the initial radiochemical events through free radical scavenging mechanisms. The complex showed effective protection against radiation-induced suppression of antioxidant enzymes activities including GPx, catalase and SOD as compared to curcumin. Both curcumin and the complex protected the cells against radiation induced protein carbonylation and lipid peroxidation with the complex showing better protection than curcumin. The oxidative damage caused to cellular components soon after irradiation forces cell to undergo apoptosis and hence for a chemical agent to be an effective radioprotectant, it must inhibit the apoptosis. Accordingly in this study the complex showed better overall protection by decreasing the radiation-induced apoptosis as estimated by flow cytometry analysis. Curcumin is known to be involved in the activation or inhibition of various signaling pathways, such as protein kinase C delta (PKCδ) and nuclear factor - κB (NF-κB). PKCδ is a signal transduction protein which in phosphorylated form leads to upregulation of cytoprotective gene like *HO-1*.[10] NF-κB is a redox sensitive transcription factor and is translocated to nucleus following degradation of its inhibitory protein (IκB) in cytoplasm.[12-14] In the nucleus, NF-κB induces transcription of several genes related to cell survival and proliferation. Therefore, activation of PKCδ and NF-κB favors cell survival. In order to understand

how the complex could influence their activation in comparison with curcumin, studies were carried out on the phosphorylation of PKCδ and nuclear translocation of NF-κB. The lymphocytes pretreated with the complex showed extensive phosphorylation of PKCδ and nuclear translocation of NF-κB at 60 min post irradiation in comparison to curcumin pretreated cells indicating that the complex is more efficient than curcumin in activating cytoprotective pathways after the initial damage. All these results suggest that the complex in comparison to curcumin is better antioxidant or radioprotective agent at cellular level. The *in vivo* testing of the complex to act as radioprotector was not followed in study because of its solubility limitations however; the *in vitro* studies definitely conclude that the synthesis of a stable water soluble SOD mimic from antioxidants like curcumin may be a promising research area to look upon with an aim to use them for therapeutic application as radioprotector.

Section-III: Curcumin exhibits selective toxicity towards tumor cells and several mechanisms like its ability to enhance ROS production, disrupt redox homeostasis and mitochondrial function and to inhibit transcription factor like NF-κB have been reported to be responsible for its remarkable selective toxicity to tumor cells.[6,7] The concentration dependant pro-oxidant or antioxidant activity of curcumin prompted us to hypothesize that probably the differential cellular uptake of curcumin as well as localization in normal vs tumor cells might have role in deciding its selective toxicity to tumor cells. To address this we performed cellular uptake measurements in four different cell types, such as two normal cells, *viz.*, mouse spleen lymphocytes, NIH3T3, and two tumor cell lines, *viz.*, EL4 and MCF7. Mouse spleen lymphocytes and EL4 cells grow in suspension and are of lymphoid origin, while NIH3T3 and MCF7 are adherent cell lines. These cells were incubated with curcumin for four

hours and the cells after repeated washings were lysed and the curcumin loaded into the cells was extracted into methanol and estimated by absorption spectrometry. Typically 20 to 40 pmoles of curcumin could be loaded per million cells. A linear dependency on the uptake was observed with treatment concentration of curcumin in each cell type. Tumor cells showed higher curcumin uptake as compared to normal cells. The fluorescence spectrum and intensity of curcumin showed distinct changes depending on the cell type. For e.g. suspension cells (lymphocytes and EL4) showed fluorescence maximum at 500-505 nm, while adherent cells (NIH3T3 and MCF7 cells) showed fluorescence maximum at 520-535 nm. Also curcumin loaded in tumor cells showed higher fluorescence intensity as compared to that in normal cells. Since maximum uptake was observed in MCF-7 cells, these cells loaded with curcumin were fractionated and curcumin from each fraction was extracted into methanol and estimated by absorption spectrometry. The results indicated that maximum localization of curcumin in the cell membrane followed by cytoplasm and nucleus. Using laser confocal microscopy, fluorescence images of curcumin treated MCF7 cells was captured after exciting cellular curcumin at 458 nm. The images confirmed intracellular localization of curcumin including a fraction in the nucleus of the cells. Cytotoxicity studies in different cell lines indicated that the toxicity of curcumin increased with increasing uptake and curcumin was more toxic to tumor cells compared to their respective normal cells. This is in correlation with our studies that curcumin acts as a pro-oxidant at higher concentration and therefore may be responsible for higher toxicity in tumor cells.

Chapter IV

This chapter discusses about the antioxidant and radioprotection studies of an organoselenium compound synthesized in our laboratory. The most effective

radioprotective drug possessing antioxidative properties developed till date, and the only agent approved by the FDA for use in the protection of normal tissues in patients treated with radiation is a thiol (sulfur) based compound amifostine (*S*-2-[3-aminopropylamino] ethylphosphorothioic acid). However, inherent toxicity of this agent at the radioprotective concentration warranted further search of nontoxic and effective radio-protectors. Selenium an essential trace element for both animals and humans belongs to the same group in periodic table as sulfur. Selenium has similar properties as sulphur, and is easier to undergo oxidation as compared to sulfur. Therefore, selenium compounds are expected to show better free radical scavenging activity and thereby repairing cellular damage. In the last few decades, there has been an increasing interest in antioxidant and chemopreventive application of organoselenium compounds specifically selenoaminoacids as they are non toxic in nature and show GPx mimetic activity.[9] With this view 3,3'-Diselenodipropionic acid (DSePA), a water soluble derivative of selenocystine was synthesized and tested for antioxidant, GPx mimetic activity and radio protective properties. The chemical structure of DSePA is shown scheme -3.

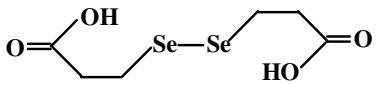

Scheme -3: *3,3'-Diselenodipropionic acid (DSePA)*

(a) *In vitro* antioxidant studies: The antioxidant properties of DSePA were studied by evaluating its ability to protect human RBCs from AAPH induced oxidative damage. The IC_{50} values for inhibition of lipid peroxidation, hemolysis and K^+ leakage were estimated to be in the range of 20-75 μM. DSePA is a good peroxyl radical scavenger and the bimolecular rate constant for the reaction of DSePA with $CCl_3O_2^{\bullet}$ was determined to be 2.7 x 10^8 M^{-1} s^{-1}. In a cell free system, DSePA showed

catalytic reduction of hydroperoxides in presence of GSH in a similar manner as that of native GPx enzyme with K_m and V_{max} values of 10.2 x 10^{-3} M and 4.8 µmol/min respectively for GSH and 0.14 x 10^{-3} M and 2.24 µmol/min respectively for hydroperoxide. The cytotoxicity of DSePA was studied in lymphocytes and EL4 tumor cells and the results showed that DSePA is non-toxic to these cells upto 500 µM concentration.

(b) *In vivo* studies: The acute toxicity studies of DSePA in mice revealed its maximum tolerable dose (MTD) value as ~ 8 mg/kg body weight for i.p mode of administration from which the safest dose for *in vivo* studies was estimated to be ≤ 2 mg/kg body weight. This dosage is employed for further studies. Radiation exposure to whole body causes cell killing and altered cell-to-cell communication leading to inflammatory responses and injury to normal tissue. The most sensitive organ to radiation induced injury is gonad followed by hematopoietic, gastrointestinal and central nervous system.[5] Therefore a chemical agent to act as an effective radioprotector, it must provide protection in a broad range of cellular and tissue systems. With this aim the *in vivo* radioprotection studies of DSePA were carried out in mice exposed to whole body γ-radiation (3 to 10 Gy) with special emphasis on protection of hepatic, gastrointestinal tract and hematopoietic organs. These studies indicated that supplementation with DSePA (2 mg/kg body weight, i.p.) for 5 consecutive days prior to γ-irradiation significantly prevented the hepatic lipid peroxidation, protein carbonylation and loss of hepatic function. DSePA was also found to influence the depletion of endogenous antioxidants viz., GSH, GPx, SOD, catalase, thiols in livers of the irradiated mice. Pre-administration of DSePA protected the villi height, increased the number of crypt cells and protected the intestine from acute radiation effects. DSePA also protected the hematopoietic system as assessed by

endogenous spleen colony assay, contributing to the overall radioprotective ability. The single cell gel electrophoresis of peripheral blood leukocytes indicated that DSePA prevented the radiation induced DNA damage. In order to know whether the DSePA mediated protection to cellular DNA is because of its ability to modulate the DNA repair pathway, we looked at the mRNA expression levels of *p21* and *GADD45α* genes. The translational product of *p21* and *GADD45α* genes regulate the cell arrest (G1/S and G2/M respectively) and DNA repair.[13] The gene expression analysis by RT-PCR revealed that that pre-administration of DSePA augmented the radiation induced increase in mRNA expression of *GADD45α* while attenuated that of *p21* at early time point indicating the involvement of DSePA in DNA repair. Pre-administration of DSePA also improved the 30 day survival by 30% with a dose reduction factor of about 1.10. These findings suggest that the protective effect of DSePA against whole body γ-radiation may be due to its free radical scavenging effects, antioxidant activity, GPx mimetic activity and DNA repair. These studies confirmed that this simple organoselenium compound possesses promising radioprotective effects.

Conclusions:

The major findings of the present thesis have been summarized below:

1) Curcumin, a natural polyphenol from turmeric exhibits both antioxidant and pro-oxidant effects in human RBC model system. While curcumin protected RBCs from free radical induced hemolysis and lipid peroxidation in the entire concentration range studied from 1 to 50 μM, it induced depletion of intracellular GSH levels and leakage of K^+ ions at concentrations > 10 μM indicating its pro-oxidant behaviour.

2) The dual antioxidant and pro-oxidant effects of curcumin were reconfirmed in macrophage cells (RAW 264.7). In these cells, even though curcumin increased the

expression of antioxidant genes with increasing concentration from 5 to 25 μM, it induced ROS generation, contributing to the cytotoxicity at higher concentration.

3) In the same macrophage cells, both cell permeable and impermeable thiols such as NAC and GSH respectively reduced the curcumin induced pro-oxidative effects. While NAC inhibited the curcumin induced expression of most of the antioxidant genes, GSH lowered the magnitude of induction of the genes indicating differential modulation by thiols to curcumin action in cells. These effects are attributed to differential cellular uptake of curcumin in presence of thiols suggesting that thiols can be employed to modulate desired therapeutic applications of curcumin.

4) A 1:1 copper-curcumin complex exhibiting SOD mimicking activity showed antioxidant effects in lymphocytes after exposure to γ-radiation, as seen by the activation of cytoprotective pathways, reduction of oxidative stress parameters and decrease in apoptosis. Under similar experimental conditions, when compared with curcumin the complex was found to be more effective. The studies can be explored to develop such compounds as radioprotectors in future.

5) Employing absorption and fluorescence spectroscopic properties of curcumin, a method has been developed to quantitatively estimate its uptake in different cells. Tumor cells (EL4 and MCF7) showed much higher uptake of curcumin, as compared to normal (lymphocytes, NIH3T3) cells, which could be directly correlated with its selective cytotoxicity to tumor cells.

6) The intracellular localization in MCF7 cells was confirmed by confocal fluorescence microscopic imaging. The subcellular fractionation of these cells indicated maximum localization of curcumin in the cell membrane followed by cytoplasm and nucleus. The nuclear localization indicates its probable direct

interaction with genomic DNA, which is valuable to recognize the molecular actions of curcumin.

7) 3,3'-Diselenodipropionic acid a water soluble selenocystine derivative having GPx like activity showed protection to RBCs against free radical induced hemolysis, lipid peroxidation, and K^+ ions leakage indicating its antioxidant activity at cellular level. It was not toxic to toxic to normal spleen lymphocytes and EL4 tumor cells up to concentration of 500 μM.

8) When administered in to mice at a non-toxic dose of 2 mg/kg body weight, i.p., for 5 consecutive days prior to γ-irradiation, DSePA showed radioprotection. It prevented irradiation induced lipid peroxidation, decreased expression of antioxidant enzymes and inhibited DNA damage. It showed excellent protection to organs that are sensitive to radiation like hematopoietic and gastrointestinal systems. At the same dosage, DSePA improved the 30 day survival of mice after whole body γ-irradiation at a lethal absorbed dose of 9 Gy by 30% and the dose reduction factor is about 1.10. The studies confirmed the potent radioprotection ability of DSePA in animal models.

References

1. Halliwell, B.; Gutteridge, J. M. C. Free radicals in biology and medicine (3rd ed), Oxford University Press, **1999**.

2. Valko, M.; Rhodes, C. J.; Moncol, J.; Izakovic, M.; Mazur, M. *Chem. Biol. Int.* **2006**, 160, 1-40.

3. Suzuki, Y. J.; Forman, H. J.; Sevanian, A. *Free Radic. Biol. Med.* **1997**, 22, 269-285.

4. Gate, L.; Paul, J.; Nguyen, Ba G.; Tew, K. D.; Tapiero, H. *Biomed. Pharmacother.* **1999**, 53, 169-180.

5. Riley, P.A. *Int. J. Radiat. Biol.* **1994**, 65, 27-33.

6. Strimpakos, A. S.; Sharma, R. A. *Antioxidants Redox Signaling* **2008**, 10**,** 512-534.

7. Aggarwal, B. B.; Sung, B. *Trends Pharmacol Sci.* **2009**, 30**,** 85-94.

8. Papp, L. V.; Lu, J.; Holmgren, A.; Khanna, K. K. *Antioxidants Redox Signaling* **2007**, 9, 776-793.

9. Nogueira, C. W.; Zeni, G.; Rocha, J. B. *Chem. Rev.* **2004**, 104, 6255–6285.

10. Rushworth, S. W.; Ogborne, R. M.; Charalambos, C. A.; O'Connell, M. A. *Biochem. Biophys. Res. Commun.* **2006**, 341, 1007-1016.

11. Vajragupta, O.; Boonchoong, P.; Berliner, L. J. *Free Radic. Res.* **2004**, 38, 303-314.

12. Barik, A.; Mishra, B.; Shen, L.; Mohan, H.; Kadam, R. M.; Dutta, S.; Zhang, H-Y.; Priyadarsini, K. I. *Free Radic. Biol. Med.* **2005**, 39, 811-822.

13. Smith, M. L.; Kontny, H. U.; Zhan, Q.; Sreenath, A.; O'Connor, P. M.; Fornace, A. J. Jr. *Oncogene* **1996**, 13, 2255-63.

LIST OF FIGURES

LIST OF TABLES

CHAPTER 1

INTRODUCTION

Oxidants are generated in aerobic organisms as byproduct of normal cellular metabolism. Oxidants have both beneficial and deleterious effects, like while they are essential for normal life, their excessive production has been linked to disease development. Oxidants are both molecular and free radical in nature. By definition a free radical is any atom, molecule or ion with one or more unpaired electrons and is capable of independent existence. Free radicals are produced during oxidation/reduction reaction involving one electron transfer, or when a covalent bond is broken and one electron from each pair remains with each group. Due to the presence of unpaired electron(s), free radicals are considerably more reactive and participate in a number of physiological and patho-physiological functions.[1] The most important class of radical species generated in living systems are oxygen derived radicals, which are referred as reactive oxygen species (ROS). Antioxidants are substances, which inhibit damages induced by the oxidants. Although aerobic organisms have evolved their own antioxidant defenses against free radicals induced damages, under pathological conditions exogenous antioxidant supplementation becomes unavoidable. However, primary concern during the development of antioxidants is that under some favorable condition these agents may also act as pro-oxidants (induce ROS production). Therefore careful understanding of the effect of antioxidant compounds on ROS, intracellular redox status, antioxidant and pro-oxidant activities and their interconnectivity is the basic requirement. With this background, all these relevant details have been discussed in brief in the subsequent sections of this chapter.

1.1 Generation of ROS

Oxygen is an essential molecule for all aerobic forms of life for chemical energy production (ATP). Various energy sources like fatty acids, glucose, lactate, ketones, and amino acids consumed by the living organisms are metabolized by oxidative pathways producing acetyl-CoA, nicotine adenine dinucleotide (NADH) and flavin adenine dinucleotide ($FADH_2$). The acetyl-CoA enters the tricarboxylic acid pathway in mitochondria, producing more NADH and $FADH_2$. The resultant NADH and $FADH_2$ donate electrons to the electron transport chain present on the inner membrane of mitochondria, which generates ATP by oxidative phosphorylation.[2] ATP is finally utilized by cellular machineries to meet their energy requirement. Oxygen also serves as the terminal electron acceptor in the electron transport chain, and in the absence of sufficient oxygen, electron transport ceases and cellular energy demands are not met. The complete reduction of oxygen by four electrons as a terminal event in the electron transport chain results in formation of water. However, sequential donation of electrons to oxygen during this process can generate ROS as intermediates, and electron leakage can also contribute to the formation of ROS.[1,3,4] Molecular oxygen (dioxygen) is having two unpaired electrons therefore it is considered as a free radical. The addition of one electron to dioxygen forms the superoxide anion radical ($O_2^{\bullet -}$). Past studies on the measurement of the efficiency of electron transport during mitochondrial respiration suggest an upper limit of 1–3% of all electrons in the transport chain leaking to generate superoxide instead of contributing to the reduction of oxygen to water.[5] The electron transport chain of mitochondria consists of four major multi-subunit protein complexes designated as NADH-Coenzyme Q (CoQ) reductase (Complex I), succinate-CoQ

reductase (Complex II), ubiquinol-cytochrome c reductase (Complex III) and cytochrome c oxidase (Complex IV). Recently it has been demonstrated that superoxide is produced from both complexes I and III of the electron transport chain in mitochondria.[6] In addition to this, superoxide radical is also formed by auto-oxidation of hydroquinones, catecholamines, thiols, etc. Purine metabolism in vertebrates also produces superoxide as by product during the conversion of xanthine to uric acid.[7] Additionally, phagocytic cell such as the neutrophil has the ability of recognizing the foreign particle and undergoing a series of reactions called the respiratory burst. NAD(P)H oxidase is the best characterized enzyme in the neutrophil, which after activation produces superoxide radicals necessary for bacterial destruction.[8]

Superoxide radical is considered the "primary" ROS, which subsequently generates "secondary" ROS, either directly or indirectly through enzyme or metal-catalyzed processes. In plant and animal cells superoxide is converted into hydrogen peroxide (H_2O_2) by the enzyme called superoxide dismutase (SOD).[9] Hydrogen peroxide is a weak oxidising agent and can cross the cell membrane and inactivate enzymes directly by oxidation of essential thiol groups. The transition metal ions like Fe^{2+} and Cu^{2+} convert hydrogen peroxide into reactive hydroxyl radical ($^{\bullet}OH$) by Haber-Weiss and Fenton reactions according to equations 1.1 and 1.2 respectively.[10,11] The hydroxyl radical has a very short *in vivo* half-life of ~ 10^{-9} s.

Haber-Weiss reaction: $$H_2O_2 + O_2^{\bullet -} + 2H^+ \xrightarrow{Fe^{3+},Cu^{2+}} {}^{\bullet}OH + OH^- + O_2 \qquad (1.1)$$

Fenton reaction: $$H_2O_2 + Fe^{2+} \longrightarrow {}^{\bullet}OH + OH^- + Fe^{3+} \qquad (1.2)$$

This enables only trace levels of Fe^{3+} to catalyze the formation of potentially large quantities of hydroxyl radicals from superoxide. The most realistic *in vivo* production of

hydroxyl radical according to the Fenton reaction occurs in presence of iron or copper. Thus the intracellular levels of free metal ions, particularly iron and copper, are critical in defining the extent of hydroxyl radical production from superoxide and hydrogen peroxide. Other important ROS that can be formed in living systems are singlet oxygen ($^1O_2$) and peroxyl radical ($ROO^{\bullet}$). Singlet oxygen is generated in immunologically stimulated neutrophil by the reaction between hypochlorous acid (HOCl) and hydrogen peroxide. Neutrophils synthesize hypochlorous acid from hydrogen peroxide in a myeloperoxidase (MPO) catalyzed reaction.[1] Singlet oxygen is a highly reactive, electrophilic and non-radical molecule. The peroxyl radicals are formed by the reaction of hydroxyl radical and singlet oxygen with organic molecule like lipid. The simplest peroxyl radical is $HOO^{\bullet}$, which is the protonated form (conjugate acid; pKa ~ 4.8) of superoxide and is termed as hydroperoxyl radical.[1,6] Thus only ~ 0.3% of any superoxide present in the cytosol of a typical cell is in the protonated form. The major pathways of ROS formation in living system are outlined in scheme 1.1.

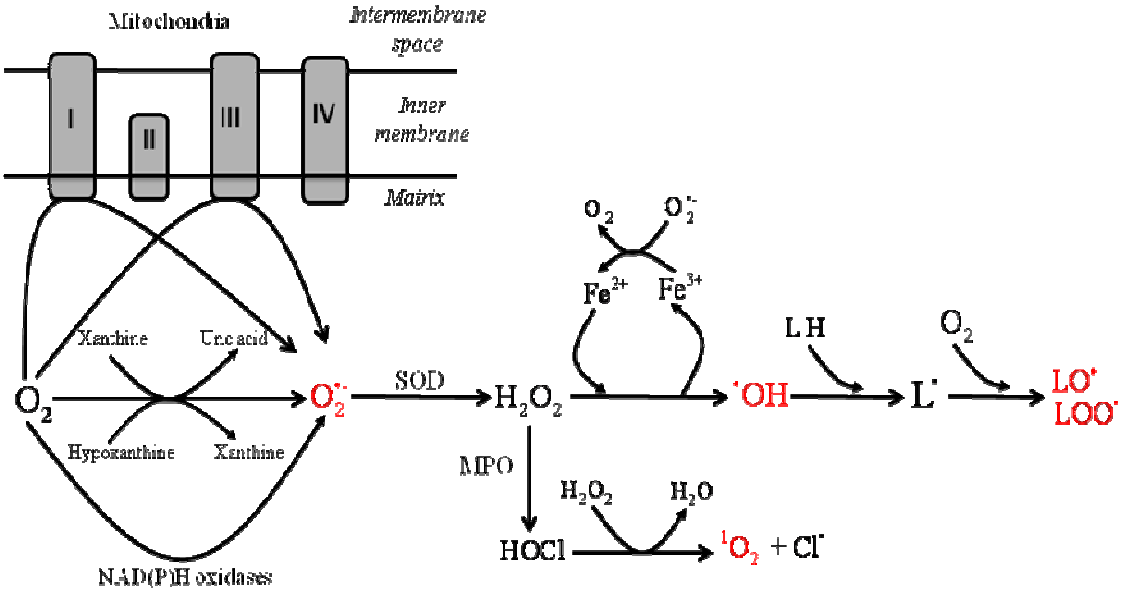

Scheme1.1: *Formation of reactive oxygen species via different routes*

1.1.1 ROS in normal physiology

Typically, low concentration of ROS is essential for normal physiological functions like gene expression, cellular growth and defense against infection. Sometimes they also act as the stimulating agents for biochemical processes within the cell.[12,13] ROS exert their effects through the reversible oxidation of active sites in transcription factors such as nuclear factor-kappa B (NF-kB) and activator protein-1 (AP-1) leading to gene expression and cell growth.[14] ROS can also cause indirect induction of transcription factors by activating signal transduction pathways.[15] One example of signal transduction molecules activated by ROS is the mitogen activated protein kinases (MAPKs). ROS also appear to serve as secondary messengers in many developmental stages. For example, in sea urchins ROS levels are elevated during fertilization. Similarly prenatal and embryonic development in mammals has also been suggested to be regulated by ROS.[16] Apart from these, ROS also participate in the biosynthesis of molecules such as thyroxin, prostaglandin which accelerates developmental processes. It is noteworthy that in thyroid cells, regulation of hydrogen peroxide concentration is critical for thyroxine synthesis as it is needed to catalyze the binding of iodine atoms to thyroglobulin.[16] Finally, ROS are also used by the immune system. For example, ROS have been shown to trigger proliferation of T cells through NF-κB activation. Macrophages and neutrophils generate ROS in order to kill certain bacteria that they engulf by phagocytosis. Furthermore, tumor necrosis factor (TNF-α) mediates cytotoxicity of tumor and virus infected cells through ROS generation and induction of apoptosis.[16] The various physiological roles of ROS are shown in scheme 1.2.

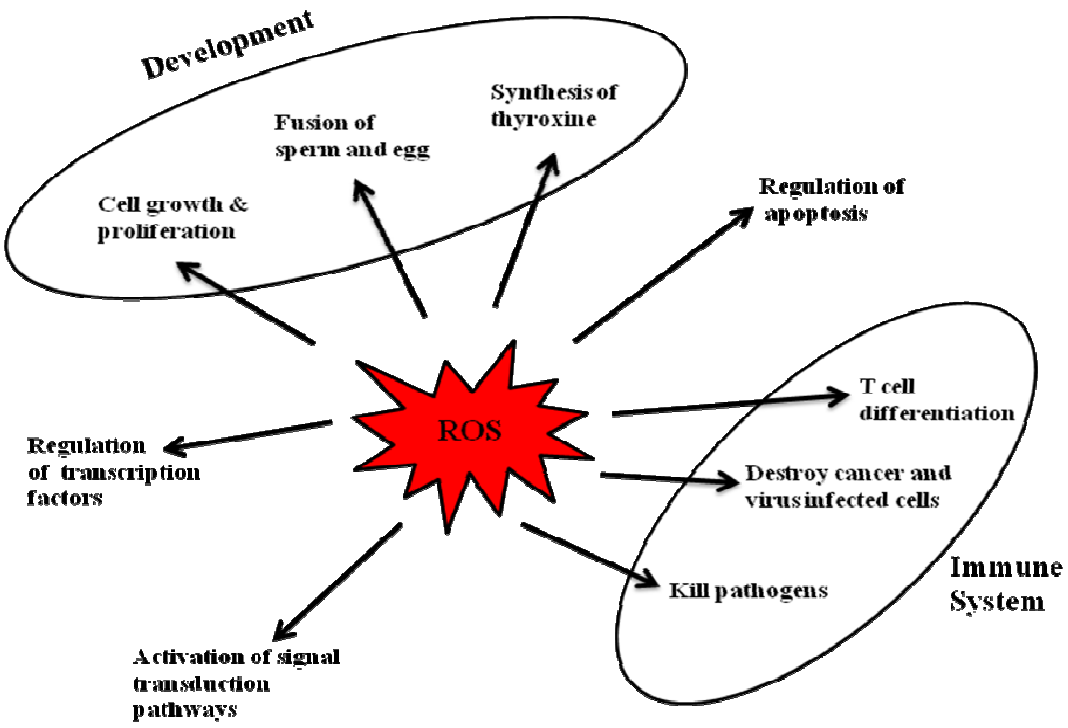

Scheme1.2: *ROS in normal cellular functions*

1.1.2 ROS induced oxidative damages

At high concentrations, ROS can be important mediators of damage to macromolecules such as nucleic acids (DNA), lipids, proteins and may have a role in pathophysiology of several diseases.

Lipids

Cellular membranes in general are vulnerable to oxidation due to their high concentration of unsaturated fatty acids. The damage to lipids, usually called lipid peroxidation, occurs in three stages.[1] The first stage, initiation, involves the attack of ROS capable of abstracting a hydrogen atom from an active methylene group in the lipid (LH). The presence of a double bond adjacent to the methylene group weakens the bond between the hydrogen and carbon atoms so that it can easily be removed from the molecule.

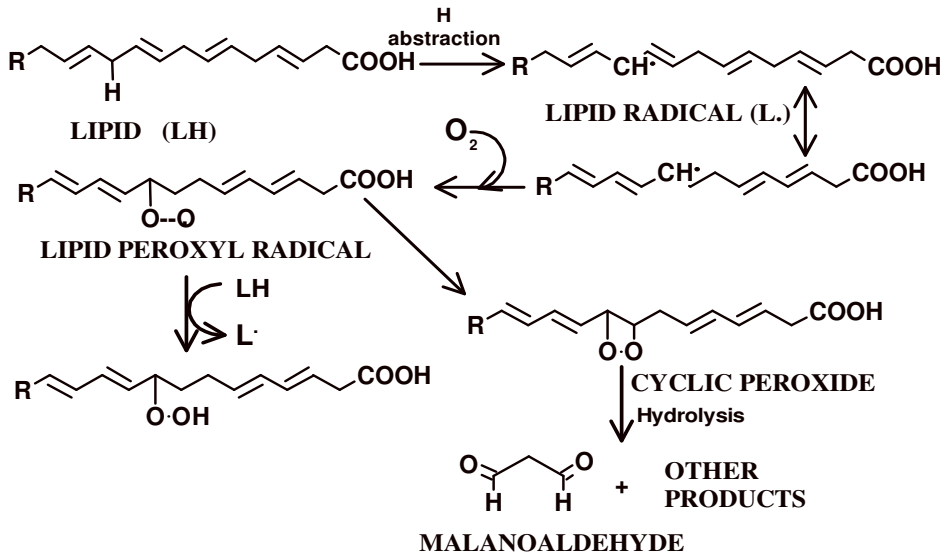

Scheme1.3: *Reactions involved in lipid peroxidation*

Following hydrogen abstraction, the remaining lipid radical ($L^{\bullet}$) retains one electron and is stabilized by rearrangement of the molecular structure to form a conjugated diene. When oxygen is present in sufficient concentration in the surroundings, the lipid radical will react with it to form lipid peroxyl radical ($LOO^{\bullet}$) during the propagation stage. These radicals themselves are capable of abstracting another hydrogen atom from a neighboring lipid molecule, which leads again to the production of lipid radicals that undergo the same reactions rearrangement and propagation. The propagation stage allows the reaction to continue. The overall reactions involved in lipid oxidation are given in scheme 1.3. A single initiation can lead to a chain reaction resulting in peroxidation of all the reactive lipids in the membrane resulting in formation of lipid hydroperoxide (LOOH). It can further decompose to an aldehyde such as malonaldehyde, 4- hydroxy nonenal (4HNE) or form cyclic endoperoxide, isoprotans, and hydrocarbons. The consequences of lipid peroxidation are cross linking of membrane proteins, change in membrane fluidity and

formation of lipid-protein, lipid-DNA adduct which may be detrimental to the functioning of the cell.[7]

Proteins

Proteins, other major constituents of cell, can serve as possible targets for attack by ROS. Proteins can undergo direct and indirect damage following interaction with ROS resulting in to peroxidation, changes in their tertiary structure, proteolytic degradation, protein-protein cross linkages and fragmentation.[17-19] The side chains of all amino acid residues of proteins, in particular tryptophan, cysteine and methionine residues of proteins are susceptible to oxidation by ROS. Protein oxidation products are usually carbonyls such as aldehydes, and ketones as shown in scheme 1.4.

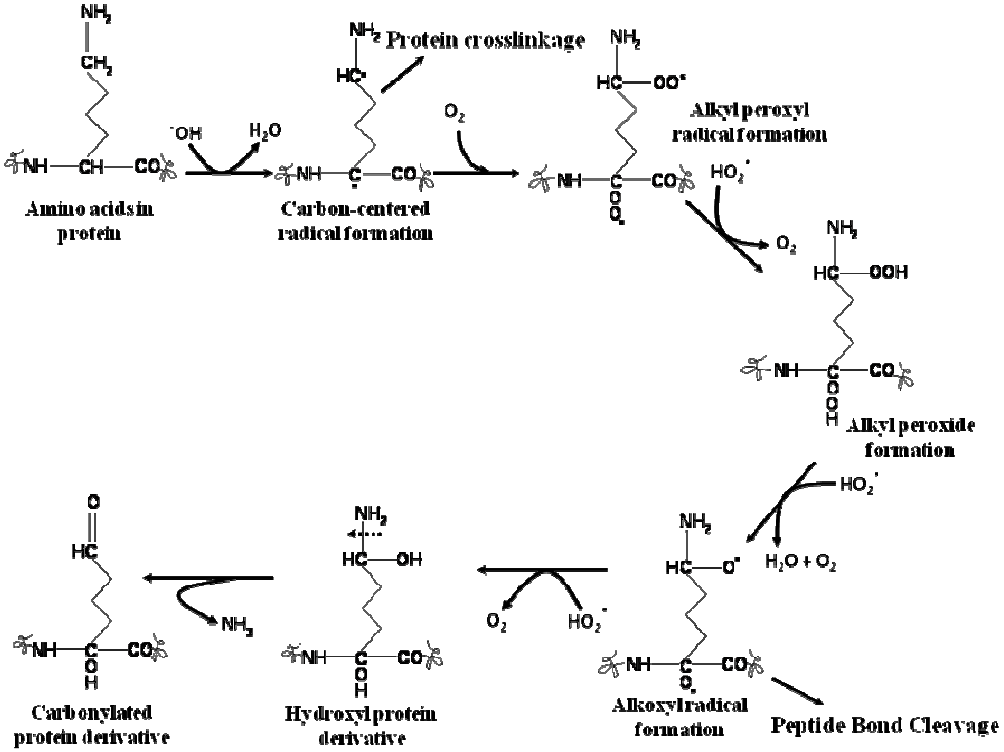

Scheme 1.4: *ROS mediated oxidation of proteins*

The consequences of protein damage are loss of enzymatic activity, altered cellular functions such as energy production, and inactivation/activation of transcription factors, changes in the cellular redox potential.

DNA

Although DNA is a stable, well-protected molecule, ROS can interact with it and cause several types of damage such as modification of DNA bases, single and double strand DNA breaks, loss of purines (apurinic sites), damage to the deoxyribose sugar, DNA-protein cross-linkage and damage to the DNA repair system.[20,21] Not all ROS can cause DNA damage and most of the ROS induced damages to DNA are attributable to the hydroxyl radical. A variety of adducts are formed on reaction of hydroxyl radical with DNA. The hydroxyl radical can attack purine and pyrimidine bases to form hydroxyl radical adducts, which are both oxidizing and reducing in nature.

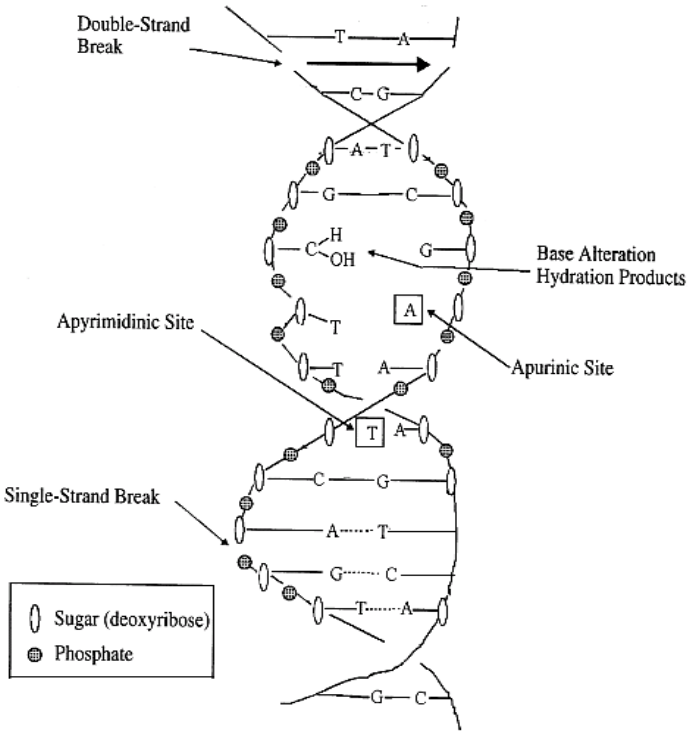

Figure1.1: *DNA damage induced by ROS*

This induces base modifications and sometimes release of bases. Some of the important base modifications include 8-hydroxydeoxyguanosine (8-OHdG), 8 (or 4-, 5-)-hydroxyadenine, thymine peroxide, thymine glycols and 5-(hydroxymethyl) uracy.[17,20,21] ROS can also attack the sugar moiety, which can produce sugar peroxyl radicals and subsequently inducing strand brakeage. The various kinds of damages that are induced in DNA molecule by ROS are shown in figure 1.1. The consequences of DNA damage is the modification of genetic material resulting in to cell death, mutagenesis, carcinogenesis and ageing.

1.2 Defenses from ROS induced damages

Continuous generation of ROS during normal metabolism can lead to the accumulation of ROS which is detrimental to the cells. Therefore, cells have evolved defense mechanisms for protection against ROS mediated oxidative damage to keep a check on the generation of ROS. These include antioxidant defenses and repair mechanisms.

1.2.1 Antioxidant defenses

Among the various defense mechanisms, the one involving direct removal of free radicals by antioxidants is considered to be important as it can provide maximum protection to biological site. Antioxidant can be defined as any substance present at low concentrations compared to that of an oxidizable substrate, significantly delays or prevents oxidation of the oxidizable substrate.[6,7,22] Antioxidants are effective because they can donate their own electrons to free radicals and thereby preventing the chain reaction. In general, an antioxidant in the body may work at three different levels: (a) prevention - keeping formation of reactive species to a minimum, (b) interception -

scavenging reactive species either by using catalytic and noncatalytic molecules and (c) repair - repairing damaged target molecules.[7] The antioxidant systems are classified into two major groups, enzymatic antioxidants and non enzymatic antioxidants.

1.2.1.1 Enzymatic antioxidants

Enzyme antioxidants are present in the body and they act as body's first line of defense against free radicals. They convert reactive free radicals into less reactive or inert species (Scheme 1.5). Enzymatic antioxidants present in the body include superoxide dismutase (SOD), catalase, and glutathione peroxidase (GPx).[23] NADPH helps in converting the oxidized thiol (GSSG) produced as byproduct during catalytic cycle of GPx to glutathione (GSH) in a glutathione reductase (GRed) catalyzed reaction.

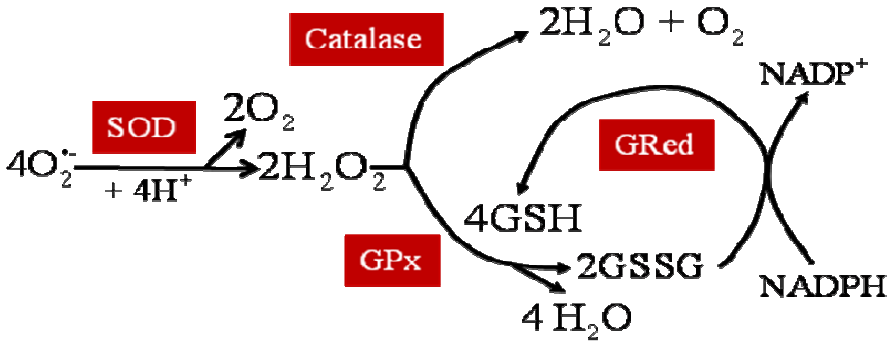

Scheme1.5: *Removal of different reactive oxygen species by antioxidant enzymes*

SOD

SOD was first isolated by Mann and Keilin from bovine blood in 1938 and its catalytic function was discovered in 1969 by McCord and Fridovich.[24] SOD is a metalloenzyme whose active center is occupied by copper and zinc, sometimes by iron and manganese. Copper/zinc SOD has been found in eukaryotic cells, while the iron SOD has been observed in prokaryotic cells. Manganese SOD has been found in both the type of cells.[23] In humans three forms of superoxide dismutase are present. SOD1 is located in

the cytoplasm, SOD2 in the mitochondria and SOD3 is extracellular. The first is a dimer (consists of two units), while the others are tetramers (four subunits). SOD1 and SOD3 contain copper and zinc, while SOD2 has manganese in its reactive centre. SOD plays major role in the protection of cells against superoxide toxicity. SOD catalyzes the dismutation of superoxide into oxygen and hydrogen peroxide.[24] SOD has the highest rate constant (~7 x 10^9 M^{-1} s^{-1}) of any known enzyme.

$$2O_2^{\bullet -} + 2H^+ \xrightarrow{SOD} O_2 + H_2O_2 \qquad (1.5)$$

Catalase

Catalase is located in a cell organelle called the peroxisome. Peroxisomes in animal cells are involved in the oxidation of fatty acids, synthesis of cholesterol and bile acids. Hydrogen peroxide is a byproduct of fatty acid oxidation. Catalase present in the peroxisomes serves to protect the cell from the toxic effects of hydrogen peroxide. It catalyses the conversion of hydrogen peroxide into molecular oxygen and water without the production of free radicals.[23] It was first crystallized in 1973 from beef liver by Sumner and Dounce.[25] Catalase is present in all major body organs, mainly in liver.

$$2H_2O_2 \xrightarrow{catalase} 2H_2O + O_2 \qquad (1.6)$$

Catalase has a molecular weight of about 240 kD, and is composed of four identical subunits, each containing a protoporphyrin ring and a central iron (Fe^{3+}) atom as observed in hemoglobins, cytochromes, chlorophylls etc. The heme group is responsible for enzymatic activity of catalase. In catalytic sense, it is the most efficient enzyme known, one molecule of catalase converts 5 x 10^6 molecules of hydrogen peroxide to water and oxygen each minute.[2]

GPx

GPx is a mammalian antioxidant selenoenzyme, which protects biomembranes and other cellular components from oxidative damage by catalyzing the reduction of a variety of hydroperoxides, using glutathione (GSH) as the reducing substrate.[23]

$$H_2O_2 + 2GSH \xrightarrow{GPx} 2H_2O + GSSG \quad (1.7)$$

GPx is a four subunit selenoenzyme with a molecular weight of 88 kD.[26] Four distinct species of GPx have been identified in mammals to date, the classical cytosolic GPx (cGPx), phospholipid hydroperoxide GPx (PHGPx), plasma GPx (pGPx), and gastrointestinal GPx (GI-GPx), all of which require selenium in their active sites for the catalytic activity.[23,27] The reactivity of these enzymes differs considerably depending upon the hydroperoxide and thiol cofactors. The classical cGPx catalyses reduction of hydrogen peroxide and a limited number of organic hydroperoxides such as cumene hydroperoxide and *tert*-butyl hydroperoxide. The PHGPx is active on all phospholipid hydroperoxides, fatty acid hydroperoxides, cumene hydroperoxide, *tert*-butyl hydroperoxide, cholesterol hydroperoxides and hydrogen peroxide.[26] Although pGPx and GI-GPx can reduce hydrogen peroxide and organic hydroperoxides, these are less active than the cGPx.

1.2.1.2 Low molecular weight or non enzymatic antioxidants

Several low molecular weight molecules present inside the cell provide secondary defense against ROS. A few examples of such molecules include GSH, α-tocopherol, ascorbate, bilirubin, etc. GSH is a water soluble thiol containing tripeptide, L-γ-glutamyl-L-cysteinyl-glycine, synthesized endogenously in both animals and plants. GSH is highly abundant in the cytosol (1–11 mM), nuclei (3–15 mM), and mitochondria (5–11 mM) and

is the major soluble antioxidant in these cell compartments.[6,22,28,29] It acts as a cofactor for the enzyme peroxidase, thus serving as an indirect antioxidant donating the electrons necessary for the decomposition of hydrogen peroxide. This compound is also involved in many other biochemical pathways and cellular functions including metabolism, maintenance of communication between cells, prevention of oxidation in SH protein groups and copper transport. GSH can act as a chelating agent for copper ions and prevent them from participating in the Haber-Weiss reaction. GSH also serves as a cofactor for several enzymes, such as glyoxylase and those involved in leukotriene biosynthesis; and play a role in protein folding, degradation, and cross-linking.[7,26] In addition to its biochemical functions, it can scavenge ROS directly and help in regeneration of antioxidant by reducing their radical species. Ascorbic acid (vitamin C) is another important water soluble antioxidant synthesized mainly by plants. Animals don't have enzymes to synthesize it endogenously and therefore depend completely on dietary sources to obtain it. Similar to GSH, ascorbic acid takes part in various physiological processes.[7] As an antioxidant it is an efficient scavenger or capable of donating its electron to ROS and eliminating them. It is a cofactor for many enzymes such as proline hydroxylase and dopamine-β-hydroxylase. It also takes part in the repair of lipid soluble antioxidant radicals, like vitamin E radical. Finally ascorbate radical is converted back to ascorbate by reduction with NADPH. Tocopherol (vitamin E) is lipid soluble chain breaking antioxidant present in the cell membrane and plasma lipoproteins and thus protects the lipids from ROS mediated oxidation.[7] There are eight members in the Vitamin E family including d-α, d-*β*, d-*γ*, and d-*δ* tocopherols and d-*α*, d-*β*, d-*γ*, and d-*δ* tocotrienols.[7] Among these the most effective form in animals is d-α tocopherol.

Tocopherols scavenge peroxyl radicals to inhibit the lipid peroxidation and in this process tocopherol radicals are formed. Tocopherol radical is reconverted to α-tocopherol by reaction with ascorbate or GSH. Some of the physiologically important non enzymatic antioxidants are listed in table 1.1.

Table 1.1: *Important non enzymatic physiological antioxidants*

Non -enzymatic antioxidants	**Location**	**properties**
Vitamin C	Aqueous phase of cell	Acts as free radical scavenger and recycles vitamin E
Vitamin E	Cell membrane	Major chain-breaking antioxidant in cell membrane
Uric acid	Product of purine metabolism	Scavenger of ˙OH radicals
Glutathione	Non-protein thiol in cell	Serves multiple roles in the cellular antioxidant defense
α-Lipoic acid	Endogenous thiol	Effective in recycling vitamin C, effective glutathione substitute
Carotenoids	Lipid soluble antioxidants, located in membrane tissue	Scavengers of reactive oxygen species, singlet oxygen quencher
Bilirubin	Product of heme metabolism in blood	Extracellular antioxidant
Ubiquinones	Mitochondria	Reduced form are efficient antioxidants
Metals ions sequestration: transferrin, ferritin, lactoferrin,	Cytoplasm of cell	Chelating of metals ions, responsible for Fenton reactions
Nitric oxide	Serum and cell	Free radical scavenger, Signal transduction

Apart from the molecules discussed above, there are also some compounds which are generated as excretory products in the cell, can also act as antioxidants, example bilirubin, which is the yellow breakdown product of normal heme catabolism. Heme is found in hemoglobin, a principal component of red blood cells. The degradation of heme

is catalyzed by Heme oxygenase (HO) producing biliverdin, iron, and carbon monoxide.[30] Biliverdin is subsequently converted to bilirubin by biliverdin reductase. Under normal physiological conditions, the activity of HO is highest in the spleen, where aged erythrocytes are sequestered and destroyed.[31] There are three known isoforms of HO. HO-1 is an inducible isoform in response to stress such as oxidative stress, hypoxia, heavy metals, cytokines, etc. HO-2 is a constitutive isoform which is expressed under homeostatic conditions. Both HO-1 and HO-2 are ubiquitously expressed and catalytically active. A third HO-3 is not catalytically active, but is thought to work in oxygen sensing. Bilirubin acts as an efficient free radical scavenger. Another important excretory molecule having free radical scavanging capability is uric acid. Uric acid is produced as end product of purine metabolism in animals. Uric acid under physiological condition reacts with ROS producing a stable urate radical that can be regenerated by ascorbate.[7] Urate can also chelate metals ions like copper and iron and prevent them from participating in generation of ROS. In addition to all these low molecular weight molecules, cells are also equipped with metal binding proteins such as lothionein, ceruloplasmin, ferritin, lactoferrin, transferring, metallothionein, etc.[7] These proteins prevent the production of ROS through sequestration of redox active metals (iron and copper)

1.2.2 Repair mechanisms

One of the most efficient defense mechanisms present in both prokaryotic and eukaryotic organisms to cope with the ROS mediated DNA damage is repair system. Though evidence for DNA repair mechanisms in mammals including humans is growing, the detailed information has emerged from prokaryotes.[2] More than 100 genes participate

in various aspects of DNA repair, even in organisms with very small genomes. The various repair mechanisms are photoreactivation, base excision and nucleotide excision repair.[2] Although cells possess a large number of different types of repair systems, each is relatively specific for a certain type of DNA damage. For example thymine dimers are repaired by photoreactivation mechanisms involving photolyases enzymes.[2] Oxidized bases are repaired by base excision repair system involving base specific glycosylases such as uracil-DNA, hydroxymethyl DNA, thymine glycol-DNA, N-methylpurine-DNA and 8-hydroxyguanine-DNA, which remove damaged bases from genome.[2,32,33] Nucleotide excision repair is a versatile and sophisticated mechanism that can eliminate a wide range of unrelated lesions. It repairs bulky adducts like benzo(a)pyrene-guanine and pyrimido[1,2-α]purin-10(3H)-one (M1G) adducts formed during oxidative stress.[32,33] It involves incision, one on each side of lesion to release an oligonucleotide carrying the damage. Further, DNA synthesis occurs to fill in the gap and ligation to restore strand integrity. In prokaryotes NER is carried out by Uvr-ABC endonuclease enzyme complex, however in eukaryotes a battery of proteins are involved in this process such as Xeroderma Pigmentosum (XPA, XPB, XPC, XPD, XPE, XPF, and XPG), radiation and DNA damage (RAD23 and RAD52), growth arrest DNA damage (GADD45), DNA polymerase δ, DNA ligases, etc.[2,34,35]

1.3 Redox state and oxidative stress

All forms of life maintain a steady state concentration of ROS determined by the balance between their rates of production and their rates of removal by various antioxidants. Thus each cell is characterized by a particular concentration of reducing species like GSH, NADH, FADH, etc. stored in many cellular constituents and is referred

as redox state of a cell.[6] By definition redox state is a total of the reduction potential or the reducing capacity of all the redox couples such as GSSG/2GSH, NAD+/NADH, $Asc^{\bullet-}$/$AcsH^{-}$, etc found in biological fluids, organelles, cells or tissues.[28] In recent years the term "redox state" is not only used to describe the state of a redox pair, but also to describe the redox environment of a cell. Under normal conditions, the redox state of biological system is maintained towards more negative redox potential values. However, with increase in ROS generation or decrease in antioxidant protection within cells, it is shifted towards less negative values resulting in the oxidizing environment (scheme 1.6). The oxidizing environment can cause toxic effects by initiating damage to cellular components such as proteins, lipids, and DNA. This shift from reducing status to oxidizing status is referred as oxidative stress.[6,26,28] During elevated oxidative stress, there is loss of mitochondrial functions, which results in to ATP depletion and necrotic cell death, while moderate oxidation can trigger apoptosis. There are a few recent reports indicating that the induction of apoptosis or necrosis during oxidative stress is actually determined by the redox state of cell.[28] For example it has been reported that an increase in reduction potential of +72 mV in HL-60 cells (i.e., from -239 ± 6 to -167 ± 9 mV) or an increase of +65 mV in murine hybridoma cells (i.e., from -235 ± 5 to -170 ± 8 mV) would cause induction of apoptosis.[28] Oxidative stress has been implicated in a number of human diseases like cancer, artherosclerosis, diabetics, neurological diseases such as Alzheimer's disease, Parkinson's disease etc. as well as in the ageing process.

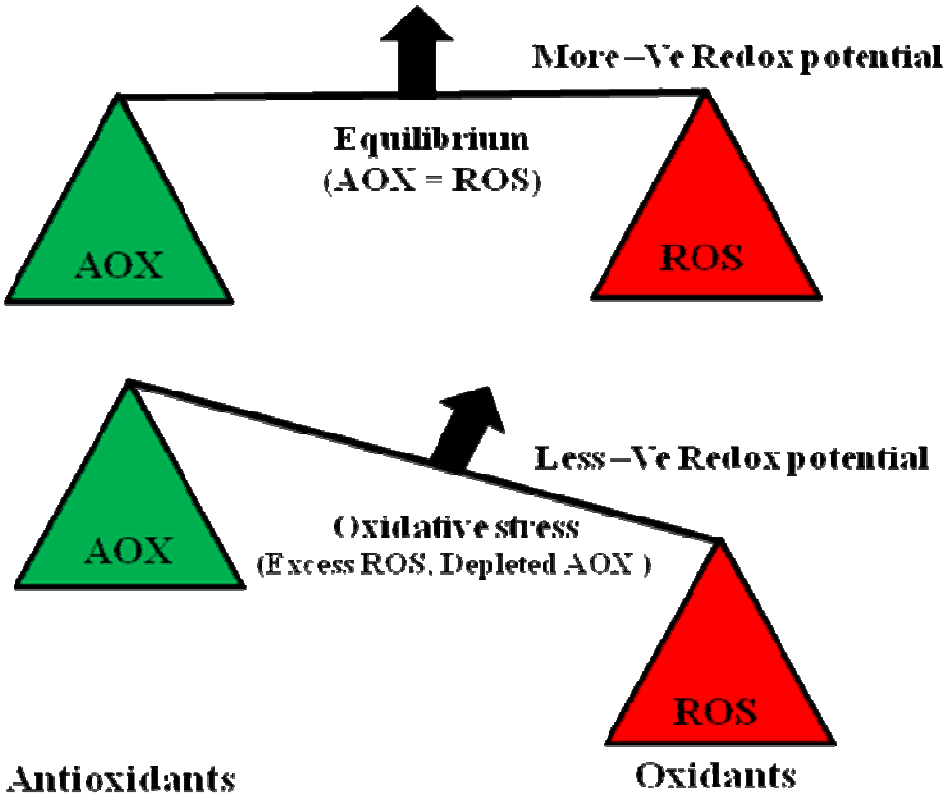

Scheme1.6: *Balance between oxidant and antioxidant defines oxidative stress*

1.4 Antioxidant supplementation

Although cells are equipped with an impressive repertoire of antioxidant enzymes as well as small antioxidant molecules, these agents may not be enough to normalize the redox status under oxidative stress.[36] Under such conditions supplementation with exogenous antioxidants is required to restore the redox homeostasis in cells. Several epidemiological studies performed in last few decades have shown inverse correlation between the levels of established antioxidants (vitamin E and C)/phytonutrients present in tissue/blood samples and occurrence of cardiovascular disease, cancer or mortality due to these diseases.[37-39] Since all of these diseases are initiated due to oxidative stress in cells, it is presumed that antioxidants supplementation through dietary sources may possibly protect against the oxidative stress mediated disease development. Therefore as an effort

to maintain the optimal body function, antioxidant supplementation has become a more and more popular practice nowadays all over the world. In this background, the focus of the researchers has been to develop new antioxidants based on natural plant products and synthesize new derivatives with improved efficacy and selectivity.

1.4.1 Natural products as antioxidants

A variety of dietary plants including grams, legumes, fruits, vegetables, tea, wine etc. have antixodiants. The disease preventive abilities of dietary plants have been attributed to the antioxidants/polyphenols present in them. Polyphenols with over 8000 structural variants are secondary metabolites of plants and represent a huge gamut of substances having aromatic ring(s) bearing one or more hydroxyl moieties.[40] Polyphenols are effective free radical scavengers and metal chelators; which is mediated by the presence of multiple hydroxyl groups. Some of the examples of polyphenolic natural antioxidants derived from plant sources include vitamin E, flavonoids, cinnamic acid derivatives, curcumin, caffeine, catechins, gallic acid derivatives, salicylic acid derivatives, chlorogenic acid, resveratrol, folate, anthocyanins and tannins.[40-45] Apart from polyphenols there are also some plant derived non-phenolic secondary metabolites such as melatonin, carotenoids, retinal, thiols, jasmonic acid, eicosapentaenoic acid, ascopyrones and allicin that show excellent antioxidant activity.[45-47] Additionally, vitamin C is the most effective water soluble natural vitamin, which belongs to class of both phenolic and non-phenolic antioxidant.[7] Both vitamin E and C exhibit the highest free radical scavenging activity and are used as standards for evaluating the antioxidant capacity of new molecules.[7]

1.4.2 Synthetic compounds as antioxidants

The usage of synthetic compounds having antioxidant activity for the preservation of cosmetic, pharmaceutical and food products has been a regular practice. The most commonly used synthetic antioxidants in the food industry are butylated 4-hydroxytoluene (BHT) and butylated 4-hydroxyanisole (BHA).[48] However, the supplementation with synthetic antioxidants for the health benefits have not been appreciated much. The obvious reason is toxicity associated with synthetic compounds.[48] However, there are numerous reports indicating that polyphenols which are the major constituent of most of the natural antioxidants are poorly bio-absorbed and the concentrations achieved in the target tissues are much lower than the range at which they are effective *in vitro*.[49] These findings have shifted the attention of researches towards development of synthetic, water soluble, stable and nontoxic compounds with potent antioxidant activity and therapeutic application. Many different antioxidants and antioxidant compositions have been developed over the years based on their mechanism of action.

One group of such antioxidants includes molecules that prevent the production of ROS through metal ions sequestration, free radical scavenging or by inhibiting the ROS producing enzymes. For example, desferrioxamine an iron chelator have been tested for preventing ROS formation in a myocardial stunning model system following hemorrhagic and endotoxic shock.[50] The allopurinol and other pyrazolopyrimidines, which are inhibitors of xanthin oxidase, have also been tested under similar disease model system and have been found to be very effective. Several congeners of GSH have been used in various animal models to attenuate ROS induced injury. For example, *N*-2-

mercaptopropionylglycine has been found to confer protective effects in a canine model of myocardial ischemia and reperfusion and N- acetylcysteine (NAC) has been used to treat endotoxin toxicity in sheep. Dimethyl thiourea (DMTU) and butyl-phenylnitrone (BPN) are believed to scavenge hydroxyl radical, and have been shown to reduce ischemia reperfusion injury in rat myocardium and in rabbits.[51-54]

Another important group of synthetic antioxidants includes molecules that act as antioxidant enzyme mimic and catalytically remove the ROS. For example, the complex formed between the chelator, desferroxamine and manganese possesses SOD activity and has shown some activity in biological models, but the instability of the metal ligand complex apparently precludes its pharmaceutical use. Porphyrin-manganese and curcumin-transition metal complexes have also shown SOD activity and are under development as SOD mimetic drugs.[55,56] Ebselen an organoselenium compound exhibits GPx activity and has been even tested in clinic as anti-inflammatory drug.[57]

Based on these studies, it is clear that a need exists for antioxidant agents which are efficient at removing dangerous ROS and which are inexpensive to manufacture, stable, and possess advantageous pharmacokinetic properties, such as the ability to cross the blood-brain barrier and penetrate tissues. Such versatile antioxidants would find use as pharmaceuticals and possibly as dietary supplements.

1.4.3 Limitations of antioxidant supplementation

The primary concern for the antioxidant supplementation is the potentially deleterious effects of these agents on free radical production (pro-oxidant action) especially when precise modulation of free radical levels are needed to allow normal cell function.[58] In fact, some reports of negative effects of antioxidant use, especially

concerning dietary supplementation with flavanoids, carotenoids, vitamin C and synthetic compounds has also emerged in last few decades.[38,39,59] Mechanistic investigation has revealed that antioxidants may exhibit pro-oxidant activity depending on the specific set of conditions. Some of the conditions that are important include their concentration and also the presence of free transition metals in cellular milieu.[60] For example, ascorbate, a well-known antioxidant in the presence of high concentration of ferric iron is a potent potentiator of lipid peroxidation. Recent studies suggest that ascorbate sometimes increases DNA damage in humans. Similarly β-carotene also can behave as a pro-oxidant in the lungs of smokers. Apart from this, natural antioxidant compounds also face problems of bioavailability. Thus, the main hurdle emerging in the development of exogenous antioxidants as therapeutic agents is their dual behavior of antioxidant and pro-oxidant in biological systems. It is therefore necessary to examine in details the differential activities of natural and synthetic compounds before considering them for therapeutic or pharmacological application as antioxidant.

1.5 Exposure to ionizing radiation, an important environmental risk

High-energy radiations (KeV to MeV range) such as short wavelength electromagnetic radiations (X-rays & γ-rays) and particle radiations (fast electrons, α-particles, protons, deuterons, neutrons, etc) are considered hazardous to human health.[61] These radiations ionize the medium through which they pass and hence they are called as ionizing radiation. Since the discovery of X-rays by Roentgen in 1895 and radioactivity by Bacquerel in 1896, ionizing radiation has been used increasingly in medicine both for diagnosis and treatment.[62] However, its deleterious effects on human health became more evident after study of the health related abnormalities in Japanese atom bomb survivors

of 1945. Since then understanding the mechanisms of radiation induced injury to living cells has been a key research area of radiation biologists and radiation chemists.[63] Today it is well established that radiation exposure initiates injury at cellular level.

When ionizing radiation interacts with living cell, water being a major (70%) constituent of the cell, undergoes radiolysis producing highly reactive free radical species, viz. hydrogen radicals, hydroxyl radicals, hydroperoxyl radicals and superoxide radicals. In addition to this, other molecular species like hydronium ions (H_3O^+) and hydrogen peroxide are also produced.[64-66]

$$H_2O \sim\sim\sim\sim\sim\sim\rightarrow e_{aq}^-, {}^{\bullet}OH, H^{\bullet}, H_2O_2, H_2, H_3O^+ \qquad (1.8)$$

The relative yields of these species vary with the linear energy transfer (LET) of the radiation. The excess generation of free radicals within cells after radiation exposure leads to oxidative stress, which finally initiates cellular damages. Among the various radical species, hydroxyl radicals have been considered to be primarily responsible for most of the radiation induced cellular damage.[65,66] Cellular damage is considered to be the origin of tissue and organ damage leading to acute radiation syndrome and mortality. Depending on the type and dose of radiation exposure, all these events occur within hours to weeks. Sometimes delayed effects are observable even many months after the exposure. The extent of radiation injury after whole body exposure depends on the absorbed dose.[67,68] Absorbed dose is the energy absorbed per unit mass of the irradiated material on passing of ionizing radiation through a medium. The absorbed dose is usually expressed in the units of Gray (Gy). One Gy is equal to one joule of energy deposition in one kilogram (1 J/kg) of the material.[69]

Whole body exposure to low doses of radiation (i.e., ≤ 2 Gy) over an extended period of time generally does not cause an immediate problem to any body organ, but results in to long term effects and such doses are referred as sub lethal doses. For example, exposure to low doses of radiation in range of 0.05 to 1 Gy has been reported to cause cancer, birth anomalies, erythema, and dysfunctions to almost all organs.[67,70] On the other side, whole body exposure to high doses of radiation (i.e., ≥ 2 Gy) over short periods of time tends to kill cells causing acute or short term health hazards and such doses are referred as lethal doses. For example, if the exposure dose is in between 2 and 5 Gy, the death of exposed individual takes a relatively longer time (i.e., within 30 days) and is due to the loss of bone marrow cells, and the characteristic features include onset of chills, fatigue, petechial hemorrhages in the skin, ulceration of mouth and pharynx, and epilation. If the exposure dose is still higher (i.e., 5-10 Gy), it causes the gastrointestinal syndrome, and death of the individual occurs between 3 to 10 days due to failure of the gastrointestinal tract. It is characterized by fever, vomiting, anorexia, diarrhea, infection, dehydration, weight loss, diminishing food and water intake and decrease in gastric retention and intestinal absorption.[67,71-73] However, if the exposure dose is very high (i.e., ≥ 10 Gy), it causes death within minutes or up to 48 h because of the severe damage to central nervous system (CNS) and this phenomenon is called as radiation induced CNS syndrome.[67,68,71] It is characterized by ataxia, uncoordinated aberrant movements and tremors, response to stimuli with convulsions, vomiting, repeated defecation, watery diarrhea, nystagmus, meningismus, and intermittent seizures.

In addition to the absorbed dose, the sensitivity of the different organs equally determines the manifestation of radiation injury. For example, organs like brain, bone,

muscle, thyroid, pituitary, adrenal, and liver are radioresistant, whereas others like the lymphoid organs, reproductive organs, bone marrow, and intestinal crypts are radiosensitive.[65,68,71] Hence, radiation exposures present an enormous health risk in the event of planned exposures or radiation accidents/incidents.

1.5.1 Radioprotector

A radioprotector is a chemical compound capable of minimizing the damaging effects of ionizing radiation to normal cells. The potential application of radioprotective chemicals in the event of planned exposures or radiation accidents/incidents has been investigated from the beginning of the nuclear era.[74] However, with the recognition that normal tissue protection during radiotherapy is as important as the destruction of the cancer cells, the focus of radioprotection research became more therapy oriented.[62] An ideal radioprotector should be able to protect against the deleterious effect of radiation during therapeutic procedures as well as during nuclear accidents, space flight, etc. Additionally, a radioprotector should be inexpensive, have no toxic implications, and can be orally administered, with rapid absorption and a reasonably good dose modifying factor (DMF).[75]

The efficacy of any agent to act as radioprotector is studied in animal models using distinct endpoints like protection against radiation-induced lethality due to hematopoietic or gastrointestinal (GI) injury, apoptosis, mutagenesis, and carcinogenesis.[72,76] The most reliable procedures for evaluating the efficacy of a radioprotector involve determination of a DMF. In animal studies, DMFs are typically determined by irradiating mice with and without administered agents at a range of radiation doses and then comparing the endpoint of interest.[76] However, this parameter is

the subject of variation depending on radiation dose, dosage of radioprotective chemical, time and schedule of treatment, animal strain and dose rate of irradiation.

The first *in vivo* studies on the protective effects of a sulphur containing amino acid against ionizing radiation were conducted by Patt & co-workers.[77] They reported that cysteine, a sulfur-containing amino acid, could protect rats from a lethal dose of X-rays. Subsequently Bacq et al. (1951) reported that cysteamine, the decarboxylated form of cysteine, could also protect rats against lethal doses of X-rays.[78] When radioprotective effect of cysteamine was compared with N-acetylcysteine a water soluble antioxidant, both provided similar protection against the immunosuppressive effect of sub lethal radiation exposure in mice.[79] However, protection against radiation induced lethality was greater after cysteamine treatment compared with the results for N-acetylcysteine treatment, but the lethal toxicity and behavioural toxicity of cysteamine is much greater.[80]

In the last one decade, several synthetic sulfhydryl compounds have also been screened for their radioprotective ability.[81] However, the most effective radioprotective drug developed till date, and the only agent approved by the FDA for use in the protection of normal tissues in patients treated with radiation is amifostine (*S*-2-[3-aminopropylamino] ethylphosphorothioic acid).[82-84] It is a complex aminothiol, which is reported to exhibit multiple biochemical properties like free radical scavenging activity, high affinity for DNA and the structural similarity with cellular polyamine.[85] Although, amifostine is a clinically approved radioprotector, it exhibits considerable toxicity at radioprotective doses, warranting the search for new effective and non-toxic radioprotectors.[80] Therefore, extensive research on modulation of radiation-induced changes by competent agents using *in vitro* and *in vivo* models is required.

1.5.2 Antioxidant as radioprotector

Due to the similarity between oxidative stress and radiation injury, the free radical scavenging is one of the most important criteria required for a compound to be good radioprotector and thus an antioxidant in principle can also act as an agent that can reduce the damaging effects of radiation.[86] Among dietary antioxidants vitamins E, vitamin A, vitamin C and β-carotene have been extensively studied for radioprotection. Srinivasan et al. (1983) reported that the survival of irradiated mice enhanced with diets containing vitamin E (a-tocopherol acetate) three times the minimal dietary allowance for mice (0.036% of the diet).[87] Injectable form of vitamin E (α-tocopherol), showed further improvement in post-irradiation survival than its dietary administration.[88] Vitamin E injected subcutaneously, either 1 h before or within 15 min after irradiation, significantly increased 30-day post-irradiation survival in CD2F1 mice. Similarly, radioprotection by dietary vitamin A and β carotene in mice exposed to localized or whole body irradiation have been reported. For example, in a study by Friedenthal et al. (1991), dietary vitamin A (150000 IU/kg of diet vs. three times the minimal dietary allowance for control group) provided protection against localized radiation exposure to the esophagus (29 Gy) or intestine (13 Gy, whole body) in mice.[89] In another study by Okunieff, (1991) involving mice transplanted with fibrosarcomas, vitamin C (4.5 g/kg i.p.) administered 50 min before whole body irradiation protected against lethality and skin desquamation.[90] It has also been reported to protect against radiation induced chromosomal damage in mice even when administered after irradiation.

In addition to the nutrient antioxidants, a large number of phytochemicals obtained from plant sources have been reported to be radioprotective in various model

systems. For example, caffeine administration at a dosage of 80 mg/kg body weight has been shown to enhance the survival of mice irradiated at radiation doses causing hematopoietic or GI injury.[91] Similarly, the flavonoids orientin and vicenin extracted from *ocimum sanctum* (Indian holy basil, tulasi) have been extensively studied for radioprotection in animal models. These compounds provided significant protection against chromosome aberrations, haematopoietic syndrome and lethality when administered to mice at nontoxic dose (50 mg/kg body weight orally) before radiation exposure.[92] In addition to this, curcumin a well known antioxidant and antitumor agent obtained from rhizome of *curcuma longa* has also been tested against radiation. Although, curcumin treatment did not show consistent protection against radiation induced lethality, it exhibited other radioprotective effects like prevention of chromosoml aberration, induction of antioxidant enzymes and inhibition of apoptosis in rodents and cell lines.[93] In a separate study, alginate, a water-soluble marine polysaccharide with antioxidative properties has been reported to protect bone marrow stem cells in a mouse model following high dose irradiation. It is also useful for the removal of internally deposited radionuclides.[94]

All these reports support the argument that dietary antioxidants have great potential to be developed as radioprotectors. It is also worth mentioning that antioxidant nutrients and phytochemicals have the advantage of low toxicity, therefore, they might be more easily and safely used in patients undergoing radiotherapy than other radioprotective chemicals.

The work in this thesis deals with studies on curcumin and organic selenium compounds, therefore a brief introduction about these compounds is given in the subsequent sections.

1.6 Curcumin

Curcumin is the yellow spice derived from the rhizomes of the plant *Curcuma longa*. The *Curcuma* genus belongs to the division of *Magnoliophyta*, class of *liliopsyda*, subclass of *zinziberidae*, order of *zinziberales* and family *zinziberaceae*.[95,96] *Curcuma longa* is a short-stemmed perennial herb, which grows to about 100 cm in height. It has curved leaves and oblong, ovate or cylindrical rhizomes as shown in figure 1.2. Turmeric grows naturally throughout the Indian subcontinent and in tropical countries, particularly South-East Asia.

Figure 1.2: *Plant of Curcuma longa*

Turmeric has been used in Asian cookery and traditional medicines for thousands of years. More recently, they have been used by the food industry as additives (e.g., in Curry

in the U.K.), flavoring, preservatives and coloring agents (e.g. in mustard, margarine, soft drinks and beverages). Curcumin is listed as a safe coloring agent in the international numbering system for food additives with the code E100.[96] Curcumin was first extracted in impure form in 1815 by Vogel and Pelletier but, it was prepared in pure and crystalline form in 1870 by Daube.[97] Roughley and Whiting determined its chemical structure in 1973.[98] Curcumin and turmeric products have been certified as safe by health authorities such as the Food and Drug Administration (FDA) in United States of America, the Natural Health Products Directorate of Canada, and the Expert Joint Committee of the Food and Agriculture Organization/World Health Organization (FAO/WHO) on food additives (JECFA). Turmeric is Generally Recognized as Safe ("GRAS") by the U.S. FDA, and curcumin has been granted an acceptable daily intake (ADI) level of 0.1–3 mg/kg-body weight by the Joint FAO/WHO expert committee on food additives, 1996.[96] At the time of writing this thesis, more than 3000 scientific articles have been published in the National Centre for Biotechnology Information (NCBI) website.

The turmeric preparations from rhizomes of *curcuma longa* contain volatile (essential) and non-volatile oils, protein, fat, minerals, carbohydrates and moisture in addition to curcumin. Curcumin is one of the non-volatile constituents of turmeric.[95] The aromatic properties of curcumin are attributed to its volatile oils, while its coloring characteristics are due to non-volatile oils, particularly the curcuminoids including curcumin.[95] The physico-chemical properties of curcumin are listed in table 1.2. The curcuminoids, which constitute approximately 2-8 % of most turmeric preparations, are a mixture of curcumin, desmethoxycurcumin and bisdesmethoxycurcumin.[96]

Table 1.2: *Physico-chemical properties of curcumin*

Curcumin	**Properties**
Molecular weight (MW)	368.38
Melting point	179–183°C
Molecular formula	$C_{21}H_{20}O_6$
pK_a	7.75 (Enolic proton), 8.55 (Phenolic proton1) and 9.05 (Phenolic proton2)
Appearance	Yellow-orange crystalline powder
Solubility	Insoluble in water at neutral pH
Specific gravity	0.9348 (59.0° F)

Curcumin is a diferuloylmethane having two methoxyl groups, two phenolic hydroxyl groups and a β-diketone moiety. Curcumin can exist in both enolate and di-keto form in equilibrium, however the enolate form predominates in solution.[99] Curcumin is more soluble in ethanol, dimethylsulfoxide (DMSO), methanol and acetone than in water. The maximal light absorption by curcumin occurs at 420 nm in most of the solvents. In methanol, its molar extinction coefficient at 428 nm is ~ 48000 $M^{-1}cm^{-1}$. The keto-enol tautomerism of curcumin has been shown in scheme 1.7.[99]

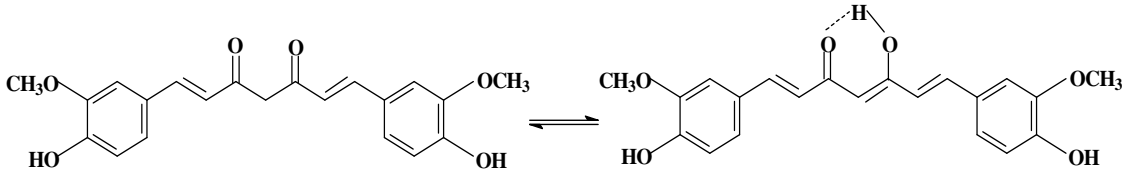

Keto form **Enol form**

Scheme1.7: *Keto-enol tautomerism of curcumin*

1.6.1 Pharmacokinetics and metabolism of curcumin

The pharmacokinetic properties of curcumin have been studied in rodent models since the 1970s. Most of these studies revealed that majority of oral administered curcumin are excreted in feces.[100] About 35% is excreted unchanged, while the remaining

65% is excreted as metabolites of curcumin.[101] Most of the ingested curcumin is metabolized very rapidly (*i.e*., within minutes) before being absorbed via the intestine and then is also subjected to transformation by liver. Using high resolution analytical techniques like high pressure liquid chromatography (HPLC) and liquid chromatography mass spectroscopy (LCMS), the different curcumin metabolites have been identified from biological samples like feces, urine, serum, bile, etc. The metabolites include curcumin glucuronide, curcumin sulphate, tetrahydrocurcumin, hexahydrocurcumin and hexahydrocurcumin glucuronides.[102] Some studies also suggest that curcumin is first biotransformed to dihydrocurcumin, tetrahydrocurcumin and subsequently these compounds are converted to monoglucuronide conjugates.[103] All these reports offered evidence that systemic bioavailability of curcumin in its native form is low while curcumin metabolites are bio-absorbed at higher levels. According to recent reports the maximum blood levels that can be achieved after administering curcumin orally at 8 g/day is less than 1.5 μM.[104] Some of the curcumin metabolites such as tetrahydrocurcumin possess anti-inflammatory and antioxidant activities similar to that of curcumin thereby contributing to the overall biological effects of curcumin.[96]

1.6.2 Medicinal importance of curcumin

Turmeric has been used for thousands of years in Ayurvedic and Chinese medicine. In modern times, turmeric continues to be used as an alternative medicinal agent in many parts of Asia for the treatment of common ailments such as stomach upset, flatulence, jaundice, arthritis, sprains, wounds and infections.[95] Recent research has revealed that therapeutic effect of turmeric against multiple ailments is contributed by one of its active constituent curcumin. It possesses wide range of pharmacological

properties including anti-inflammatory, antioxidant, antineoplastic, antiangiogenic, cytotoxic, immunomodulatory and antimicrobial activities.[95,105,106] All these activities have been demonstrated both in cultured cells and in animal models. Additionally, curcumin has been shown to be effective against various skin diseases including psoriasis, scleroderma and dermatitis. Curcumin also enhances the wound healing process of the body.[107] Curcumin has been found to be a potent and selective inhibitor of the human immunodeficiency virus (HIV-1) long terminal repeat (LTR), which governs the transcription of HIV-1 genome and thus blocks the viral multiplication.[108] Curcumin has also been shown to play a protective role in diabetes mellitus type II by reducing the resistance to insulin. Curcumin prevents myocardial infarction and other cardiovascular diseases.[107] The cardioprotective effects of curcumin is due to its ability to (1) inhibit platelet aggregation, (2) inhibit inflammatory response, (3) lower (low density lipoprotein) LDL and elevate HDL (high density lipoprotein), (4) inhibit fibrinogen synthesis, and (5) inhibit oxidation of LDL. Curcumin also suppresses amyloid-induced inflammation; therefore it has been linked to the prevention of Alzheimer's disease.[109] All these medicinal properties of curcumin paved the way for its ongoing human clinical trials. Initial trials were emphasized on safety and pharmacokinetics in humans.[104,110] While, current trials are focused on exploring efficacy against neoplastic and preneoplastic diseases such as multiple myeloma, pancreatic cancer, myelodysplastic syndromes and colon cancer and conditions linked to inflammation such as psoriasis and Alzheimer's disease.[105,110,111]

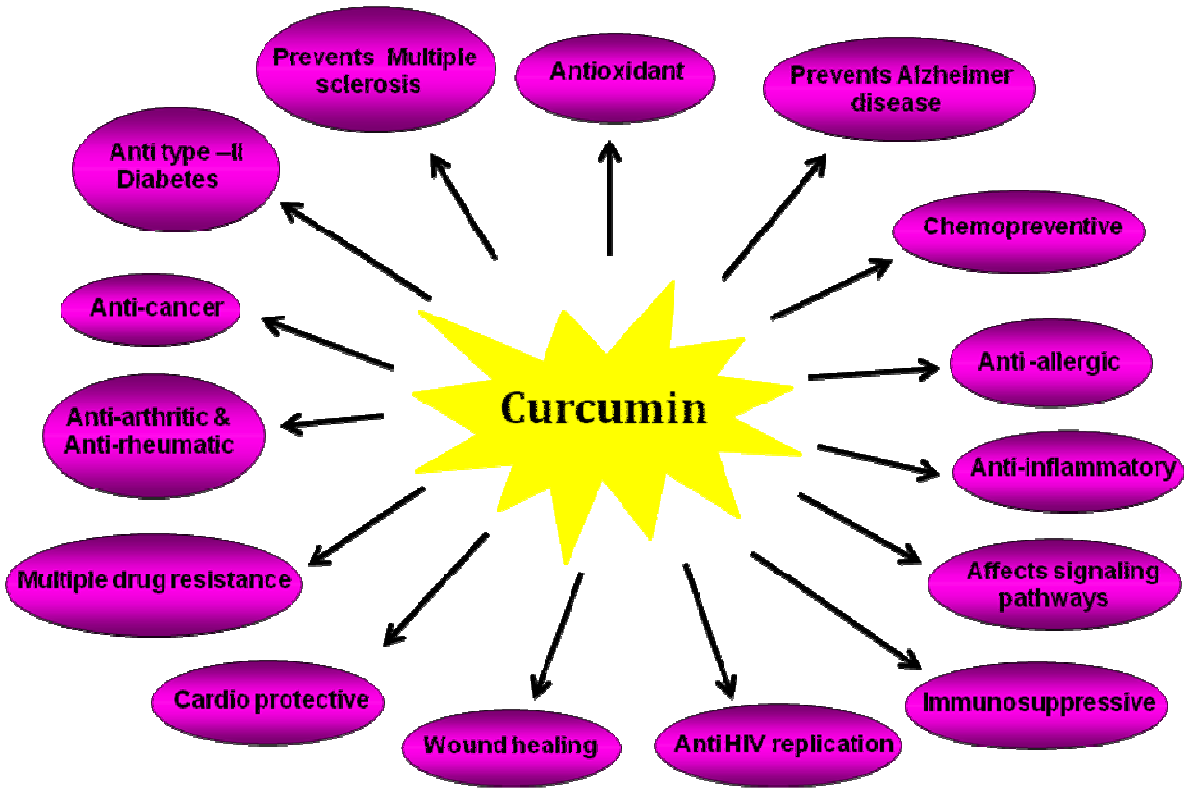

Scheme1.8: *Medicinal uses of curcumin*

At present 17 worldwide clinical trials (one phase I, eight phase II and eight phase I) are in progress, out of which, one involving the study of gemcitabine, curcumin and celecoxib for the treatment of metastatic colorectal cancer has entered phase III level.[96,110] In scheme 1.8, some of the important therapeutic properties of curcumin are listed with regard to human diseases.[107]

1.6.3 Factors involved in curcumin's anticancer activity

Curcumin acts as both chemopreventive and chemotherapeutic agent against cancer.[96,112] Carcinogenesis is the complex process by which normal cells develop into a malignant tumor.[113] It involves three stages (1) initiation during which normal cells become transformed (2) promotion in which transformed cells become preneoplastic and (3) progression which is the final irreversible step when the preneoplastic cell becomes

neoplastic. Curcumin can interfere in carcinogenesis process by inhibiting the initiation step or suppressing the promotion and progression stages.[96,111] Recent studies in numerous experimental carcinogenesis models and more recently clinical trials performed in patients with familial adenomatous polyposis have also confirmed that curcumin can ameliorate the progression to cancer in a variety of organ sites such as colon, duodenal, stomach, esophageal and oral, revealing its potential for chemoprevention.[96,112,114] Additionally, curcumin has been shown to induce apoptosis in a wide variety of cancer cells both in culture as well as animal model suggesting its chemotherapeutic effects.[96,107,112]

The identification of factors responsible for anticancer activity of curcumin has been a research area of immense interest over the years. The experimental results of all these investigations reveal that the ability of curcumin to lower cellular oxidative stress by scavenging ROS and to detoxify carcinogen by inducing phase II enzymes primarily mediate the cancer chemopreventive effects, while chemotherapeutic effects of curcumin are attributed to its ability to modulate many cellular and molecular pathways.[112] The cellular processes targeted by curcumin include gene expression, transcription factors, growth factors and their receptors, nuclear factors, hormones, and hormone receptors.[96,115,116] In human diseases such as cancer, such targets have been implicated at all stages of carcinogenesis (initiation, promotion, and progression). An example of a cellular target playing an important role in the pathogenesis of cancer is the cell survival signaling transcription factor, NF-κB.[117] It is activated by various stimuli such as carcinogens, oxidative stress, chronic inflammation, UV radiation, and abnormal hormonal stimulation and cytokine like TNF. Under normal condition NF-κB is

sequestered and bound in the cytoplasm by inhibitory proteins called I-κB. The stimuli activates the I-κB kinase (IKK), which mediates the phosphorylation and degradation of I-κB so that NF-κB is released and may translocate to the nucleus, where it induces the transcription of many of the key genes responsible for the inflammation, proliferation, invasion, metastasis and inhibition of apoptosis.[117] An important feature of the pathogenesis of malignant conditions is the activation of NF-κB. Curcumin is an inhibitor of NF-κB activation.[118] It actually inhibits the activity of IKK and thus prevents the phosphorylation of I-κB and the subsequent translocation of NF-κB to the nucleus.[117] Curcumin has also been reported to alter the expression of early growth response -1 (erg-1), cellular myelocytomatosis (c-Myc), TNF, interleukin-6 (IL-6), interleukin-8 (IL-8), adhesion molecules, inducible nitric oxide synthase (iNOS), matrix metalloproteinase-9 (MMP-9), cyclooxygenase-2 (COX-2), 5-lipoxygenase (5-LOX), cyclin D1, β catenin, B-cell lymphoma 2 (Bcl-2) and B-cell lymphoma xL (Bcl-xL) proteins in various cancer cell lines *in vitro*.[115,116,119,120] It is well known that p53 is a key gene for tumor suppression and induction of apoptosis. Under normal conditions, p53 inhibits the proliferation and growth of the cells with abnormal or damaged DNA, as seen in cancer and ageing. It is suggested that curcumin may inhibit p53 induced apoptosis by impairing the folding of p53 into the conformation required for its phosphorylation, its binding to DNA and its transactivation of genes that execute its tumor suppression function.[121] However, several reports also indicate that curcumin induces cell death or apoptosis in cancer cells through p53-dependent Bcl-2-associated X protein (BAX) induction.[122] In a separate study, curcumin also appeared to inhibit the Akt/PI3K pathway, which transmits signals received by epidermal growth factor receptors (EGFR) tyrosine kinase in A431

cells.[123] Protein kinase C (PKC) activation by exogenous and endogenous oxidants influences tumor promotion, cellular growth, differentiation and apoptosis. Curcumin inactivates PKC by reacting with it.[124] Hence, curcumin inhibits cancer development and progression, targeting multiple steps in the pathway to malignancy.

1.6.4 Curcumin: a potent antioxidant

Curcumin, with proven antitumor and anti-inflammatory activities exhibits potent antioxidant activity. It has been shown to be an excellent scavenger of ROS such as superoxide anion radicals, lipid peroxyl radicals, hydroxyl radicals and nitrogen dioxide radicals, whose production is implicated in the induction of oxidative stress.[125-129] Its free radical scavenging ability is comparable to well known antioxidants like vitamins C and E.[130] It has been shown to inhibit lipid peroxidation in a variety of *in vitro* models such as rat brain homogenates, rat liver microsomes, erythrocytes, liposomes, and macrophages, where peroxidation is induced by Fenton reagent, H_2O_2, and 2,2-azo-bis(2-amidinopropane) hydrochloride (AAPH).[131,132] It has been reported to inhibit singlet oxygen-stimulated DNA cleavage in plasmid pBR322 DNA, H_2O_2 and AAPH induced hemolysis of erythrocytes.[96,129] In epithelial cells, curcumin has been shown to increase GSH levels which, led to lowered ROS production.[133] Curcumin also mediates its antioxidative effects by elevating the levels of phase II enzymes such as NAD(P)H:quinone reductase (QR) and HO.[124,134] For example, *in vitro* incubation of bovine aortic endothelial cells and human proximal renal tubular cells with curcumin has been reported to result in dose and time dependent increase of *HO-1* mRNA, protein expression and enzymatic activity.[135] The postulated mechanism for these actions involves the activation of PKC pathways and antioxidant response element (ARE)

mediated transcriptional induction.[124,136] It was also shown to inhibit oxidative damage in different animal models. For example, curcumin inhibited lipid degradation and decreased ischemia-induced biochemical changes in heart in the feline model.[137] In a focal cerebral ischemia model of rats, it offered significant neuroprotection through inhibition of lipid peroxidation, increase in endogenous antioxidant defense enzymes and reduction in peroxynitrite formation.[138] Further, studies on the mechanistic aspects of antioxidant activity revealed that phenolic hydroxyl groups of curcumin play a significant role in its diverse antioxidant activity.[128,139,140] However, some reports suggested that both hydroxyl and diketone groups exert antioxidant properties. The phenolic hydroxyl groups give free radical scavenging ability and the diketone structure is considered to be responsible for its ability to bind to metals.[141] The ability of curcumin to act as an antioxidant in the presence of metals arises mainly by preventing the Fenton chemistry within cells through chelation of free metal ions such as Cu^{+2}, Fe^{+2}, etc.[142] Additionally, there are also some reports which indicate that stable metal complexes of curcumin exhibit higher antioxidant activity as compared to native curcumin molecule. The manganese complexes of curcumin and its diacetyl derivative were found to show greater SOD activity, hydroxyl radical scavenging activity, and nitric oxide radical scavenging activity than the parent molecules.[55,141] The copper complex of curcumin also has been found to exhibit antioxidant, superoxide-scavenging and SOD enzyme mimicking activities superior to those of curcumin itself.[55,141] Thus, curcumin exhibits a variety of beneficial effects and appears to have a significant potential in the treatment of multiple diseases that are mediated through oxidative stress.

1.7 Selenium: A micronutrient

Selenium is an element belonging to the 16th group in the periodic table. Its atomic weight is 78.96 and atomic number is 34. The element selenium was discovery in 1817 by Joens Berzelius and named after the Greek goddess of the moon, Selen. About 140 years later, Schwarz and Foltz, (1957) discovered its role as micronutrient in animals.[143] The entry point of selenium in animals is via plants, which absorb the element in its inorganic form from the soil. In plants, selenium gets converted to organic forms such as methylated low-molecular-weight selenium compounds and the amino acids such as selenomethionine, selenocysteine, methylselenocysteine and γ-glutamyl-Se-methylcysteine.[144] Selenomethionine is incorporated into the proteins in place of methionine and it accounts for >50% of the total selenium content of the plants whereas, selenocystine, methylselenocysteine and γ-glutamyl-Se-methylcysteine are not significantly incorporated into plant proteins and are at relatively low levels.[144-146] Animals including humans obtain selenium primarily in the form of selenomethionine by consuming plant products. The selenomethionine obtained from these sources acts as a precursor for the synthesis of selenocysteine. Both selenomethionine and selenocysteine are viewed as the analogs of naturally occurring aminoacids, methionine and cysteine respectively.[147] Selenomethionine is nonspecifically incorporated in to proteins in place of methionine. However, selenocysteine is regarded as the 21st aminoacid and has specific genetic codon UGA and tRNA for its incorporation in to proteins.[148] The groups of proteins that contain selenocysteine as an integral part of their polypeptide chain are defined as selenoproteins and these proteins are responsible for most of the physiological functions mediated by selenium such as roles in cellular antioxidative protection, redox

regulation, male fertility, thyroid function and immune function.[147,149] Selenoproteins are present in all lineages of life (i.e., bacteria, archaea, and eukarya). In prokaryotes, formate dehydrogenase, hydrogenases and glycine reductase are important selenoproteins in which selenocysteine has been verified as the selenium moiety.[150] In eukaryotes at least 25 selenoproteins have been identified so far and some of them are listed in table 1.3.[147,151]

Table 1.3: *Important selenocysteine containing proteins in eukarya*

Selenoproteins	**Functions**	**Location**
Glutathione Peroxidase (GPx)		
Cellular GPx	Removal of hydroperoxides	Ubiquitous
Gastrointestinal GPx	Removal of hydroperoxides	Gastrointestinal tracts
Extracellular GPx	Removal of hydroperoxides	Plasma
Phospholipid hydroperoxide GPx	Removal of hydroperoxides	Ubiquitous, testis
Iodothyronine Deiodinases (ID)		
Type I ID	Conversion of T4 to T3	Thyroid, liver, kidney
Type II ID	Conversion of T4 to T3	Pituitary gland, CNS
Type III ID	Conversion of T4 to T3	Placenta
Thioredoxin Reductases (TrxR)		
TrxR-1	Reduction of thioredoxin	Ubiquitous - cytosol
TrxR-2	Reduction of thioredoxin	Ubiquitous-mitochondria
Selenoprotein P (SeP)	Antioxidant, transport	Plasma
Selenophosphate synthetase (SPS)	Selenophosphate synthesis	Ubiquitous
Selenoprotein W	Not known	Muscle

The most important and well studied selenoprotein in eukaryotes is GPx. It is an antioxidant enzyme that detoxifies peroxides from the cells and protects against oxidative stress.[23] It has been found to be essential for life in knockout mouse model. The details of

this enzyme have been discussed earlier in section 1.2.1.1 of this chapter. Selenocysteine is the active site of GPx enzyme and is directly involved in catalytic reactions.[152] For example during catalytic reaction of GPx the selenol (ESeH) of the selenocysteine in the active site of GPx undergoes a redox cycle involving the selenolate anion as the active form that reduces hydrogen peroxides.[152] The selenolate, which is oxidized to selenic acid, reacts with GSH to form a selenosulfide adduct (ESeSG). A second GSH then regenerates the active form of the enzyme by attacking the selenosulfide to form oxidized glutathione (GSSG). Thus two equivalents of GSH are oxidized to the disulfide and water, while the hydrogen peroxide is reduced to water.[153] The catalytic mechanism of GPx is shown in scheme 1.9.

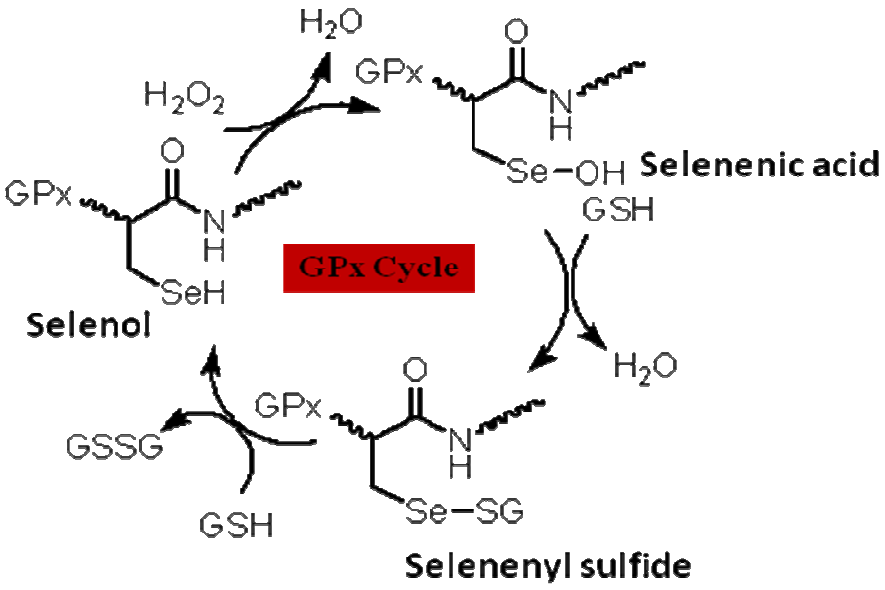

Scheme 1.9: *Catalytic mechanism of GPx*

Apart from selenoproteins, some low-molecular weight selenium compounds, such as methylselenic acid, methylselenol, methylselenocysteine, and selenomethionine synthesized in the body as byproduct of selenium metabolism also contribute to physiological functions through their antioxidant, antitumorigenic and chemopreventive

mechanisms.[145] In addition to that selenium metabolites have been shown to be very effective in the detoxification of heavy metals such as Cd, Hg, Pb, As, cis-Pt derivatives.[145,154] One of the mechanisms suggests the formation of biologically inactive selenides which accumulate as granules in some organs.[145]

1.7.1 Selenium deficiency and supplementation

Selenium is essential for life, and there is no doubt that adequate amounts of this element are required for optimal health. The recommended nutritional dose of selenium for normal humans is 50-60 µg/day.[155,156] Selenium intake less than 50 µg/day has been reported to cause several deficiency syndromes. For example Keshan disease a potentially fatal form of cardiomyopathy (disease of the heart muscle) in children has been found prevalent in parts of China with extremely low levels of selenium intake (< 25 µg/day).[157] Similarly, several epidemiological, cell and animal studies have shown a strong correlation between lower selenium intake and risks of some kinds of cancer.[158] Additionally, selenium deficiency has also been linked to pathological conditions, such as male infertility, decrease in immune and thyroid function, and several neurologic conditions, including Alzheimer's and Parkinson's disease.[159-163]

On the other side, selenium intake higher than the daily recommended nutritional dose is considered as selenium supplementation and its upper safe limit is about 200 µg/day.[156] The compounds available for selenium supplementation include the inorganic forms sodium selenite, sodium selenate and the organic forms, selenomethionine, methylselenocysteine and high selenium enriched yeast.[145] The foods rich in selenium like broccoli, mushrooms, cabbage, radishes, onions, garlic, fish (Tuna), whole grains, wheat and Brazil nuts act as dietary selenium supplements.[145,164] Selenium

supplementation has been reported to be beneficial for human health. For example it has been shown that supplementation of normal individuals with selenium enriched brewers's yeast containing predominantly selenomethionine decreases overall cancer morbidity by nearly 50%.[165] Similarly Keshan disease, a pathological condition of selenium deficiency, is preventable by selenium supplementation.[166] In another study, supplementation with selenium exhibited immunostimulant effects by enhancing the proliferation of T cells.[167] All these reports confirm that selenium is a trace element of fundamental importance to human health with a relatively narrow window of tolerance.

1.7.2 Selenium toxicity

At initial stages, selenium was mainly recognized for "selenosis" a condition of acute selenium poisoning in humans, which was characterized by loss of hair, nails and swelling at the fingertips. In the 1930's, several researchers identified selenium toxicity to be a direct cause of alkali disease and blind staggers, and then Nelson et al. (1943) classified selenium as a carcinogen[168-170] Since then a large number of reports on *in vivo* toxicology of selenium compounds has appeared in literature. However, all these studies emphasized that selenium becomes toxic only if its intake crosses the supplementation limit (> 200 µg/day).

The molecular mechanism underlying selenium toxicity is still not completely understood. Most of the current knowledge about selenium toxicity has been established by studying the toxicological effects of supplementation with inorganic selenite at supra nutritional doses in animal models. The toxicology of inorganic selenium has been related to the oxidation of thiols of biological importance. In fact, selenite (Se^{4+}) readily oxidizes sulfhydryl groups, producing disulfide and unstable intermediates like

selenotrisulfide that subsequently decomposes to elemental selenium.[171] Later, it was shown that selenite was a good catalyst for the oxidation of a variety of biologically significant thiols such as GSH, cysteine, dihydrolipoic acid, and coenzyme A producing superoxide and hydrogen peroxide.[172-174] Apart from this, selenium also exhibits toxicity due to its non specific incorporation in to proteins leading to loss of protein functions.[175] The toxicity of selenium compounds not only depends on the quantity of element consumed, but also on its chemical form. For example organoselenium compounds in general are less toxic compared to inorganic selenium compounds because of the slow release of elemental selenium.[156]

1.7.3 Need for organoselenium compounds

Interest in the use of organoselenium compounds for therapeutic studies started with the findings that organoselenium compounds are much less toxic compared to the inorganic selenium species. Since then, a lot of effort has been directed towards the development of stable organoselenium compounds that could be used as dietary supplement, antioxidant enzyme mimic, antitumor, anti-infective agents, cytokine inducers and immunomodulators.[176] However, among these the synthesis of organoselenium compounds exhibiting catalytic functions similar to that of GPx gained maximum importance.[153] Till date several organoselenium compounds have been developed that mimic the GPx activity *in vitro* and function as an antioxidant *in vivo*.[153,177] However, the most promising organoselenium compound exhibiting GPx activity is ebselen [2-phenyl-1,2-benzisoselenazol-3(2H)-one]. Ebselen was first synthesized in 1942 by Lesser and Weiss.[57] It is not only an established GPx mimic but also exhibits several other pharmacological activities like scavenging of ROS such as

peroxynitrate and anti-inflammatory effects. It was even tested in clinic for the treatment of cerebral ischaemia and showed positive results.[57] The discovery of ebselen as a GPx mimic provided an impetus trend among synthetic organometalic community to work on design and synthesis of organoselenium compounds with GPx mimetic activity for their application as antioxidant and therapeutic agent.[177] Indeed some alkyl and aryl compounds have been found to be more potent GPx mimic than ebselen and are in different stages of testing.

1.8 Objectives of the thesis

Recent focus on antioxidant research is to develop multifunctional compounds having antioxidant activity along with other important pharmacological activities such as radioprotective, antitumor and anti-inflammatory activities. Natural products derived from the plant sources are considered pharmacologically safe since they are consumed regularly as part of the diet. Therefore, such compounds are the first choice of researchers for the exploration of their antioxidant property. There has also been a growing interest among researchers for exploring new synthetic derivatives as novel class of drugs with multiple activities and target specificity. However, the main hurdle in developing such compounds as therapeutic agents is that they switch over from antioxidant to pro-oxidant behavior depending on the dosage and type of the target cell. This differential anti or pro-oxidative activity of a compound has its own significance like for example: the antioxidative property may be useful to protect the normal cells from oxidative stress while pro-oxidative property may confer the molecule a selective toxicity to tumor cells. It is therefore, necessary to identify the conditions under which such compounds show differential activities in order to take full advantage of their therapeutic potential. With

this aim, in the present thesis, curcumin a natural product from *Curcuma longa L*, its copper complex that acts as a SOD mimic, and a synthetic selenocystine derivative having GPx activity have been evaluated for antioxidant/pro-oxidant activity. Wherever possible, they have also been examined for their ability to offer protection against radiation induced oxidative stress (radioprotector) in different biological models (*in vivo* and *in vitro*).

CHAPTER 2

MATERIALS & METHODS

2.1 Chemicals

Curcumin, dimethyl sulphoxide (DMSO), thiobarbituric acid (TBA), butylated hydroxy toluene (BHT), Tris base, HEPES buffer, 2,2'-azobis(2-amidinopropane) hydrochloride (AAPH), ethylene diamine tetra acetic acid (EDTA), glutathione (GSH), N-acetyl cystine (NAC), 5,5'-dithiobis-2-nitrobenzoic acid (DTNB), diethyl pyrocarbonate (DEPC), dinitrophenylhyodrazine (DNPH), SYBR Green-II dye, sodiumdodecylsulphate (SDS), cumene hydroperoxide (CuOOH), 2-mercaptoethanol (2-ME), aspartate, glutamine, alanine, α-keto glutarate (α-KG), sodium sarcosinate, sodium orthovanadate (Na_3VO_4), phenylmethanesulphonylfluoride (PMSF), high melting point agarose, low melting point agarose, hydrogen peroxide, xanthine , NADPH, triton X-100, nonidet P - 40 (NP-40), propidium iodide (PI), ethidium bromide, 3-[4,5-dimethylthiazole-2-yl]-2,5-diphenyl tetrazolium bromide (MTT), 4'6-diamidino-2-phenylindol (DAPI), Dulbecco's modified essential medium (DMEM), Rosewell park memorial institute (RPMI) -1640 medium, protenase K, cytochrome c and RNAase were purchased from Sigma Chemical Company, USA. Xanthine oxidase was obtained from Calbiochem, U.S.A. Penicillin, streptomycin, fetal calf serum (FCS) and reverse transcription - polymerase chain reaction (RT-PCR) kit were procured from Invitrogen, USA. Total RNA isolation kit, BM chemiluminiscence western blotting kit, and secondary antibody (anti-rabbit or anti-sheep) was obtained from Roche Molecular Bio chemicals, Germany. Nitrocellulose membrane and primary antibody for western blotting were obtained from Amersham Pharmacia Biotech, UK and Cell Signaling Technologies USA respectively. Dichlorofluorescein diacetate (DCF-DA) was obtained from Molecular probes, USA. GPx activity kit (RS 504) was obtained from Randox

laboratories, UK. All other chemicals with maximum available purity were purchased from reputed local manufacturers/suppliers. The gene specific primers for RT-PCR were custom synthesized from the local agents. The reagent solutions were prepared in nanopure water from a Millipore Milli-Q system just before the use. Absorption spectra were recorded on a JASCO V-530 spectrophotometer and fluorescence intensity was recorded on a Hitachi F-4010 fluorimeter. PCR was performed on Techne thermocycler (Model no – TC512, UK).

2.2 Animals, isolation of cells, procurement of cell lines and cell culture

2.2.1 Animals

Eight to ten weeks old inbred Swiss albino male mice weighing approximately 20-25 g, reared in the animal house of Bhabha Atomic Research Centre (BARC), were used for *in vivo* studies. Animals were maintained on a standard laboratory diet with water *ad libitum* in polypropylene cages and air-conditioned (24 ± 2°C) rooms with a 12 hourly dark and light schedule. All animal experiments were conducted adhering to the guidelines from Institutional Animal Ethics Committee of BARC.

2.2.2 Isolation of murine spleen cells

For preparation of spleen cell suspension mice were sacrificed by cervical dislocation. Spleen was removed from the mice and single cell suspension from spleen was obtained by gently teasing the organ in to RPMI 1640 medium (containing 15 mM HEPES, 2 mM glutamine, 100 IU/ml penicillin, 100 µg/ml streptomycin and 20 µM 2-mercaptoethanol) using a sterile nylon mesh. Red blood cells were eliminated by treatment with 0.83% ammonium chloride solution. Lymphocyte rich cells were further washed with RPMI medium to remove traces of ammonium chloride and the viability

was assessed by trypan blue dye exclusion. This preparation is referred to as splenic lymphocytes.

2.2.3 Isolation of human RBCs

Blood samples were obtained by venipuncture from healthy volunteers with strict adherence to the ethical guidelines laid down by the Institutional Animal Ethics Committee of BARC. Blood was collected in heparinised tubes and centrifuged for 10 minutes (min) at 1000 x *g* and 4°C using a cold centrifuge (Remi compufuge, CPR-24). Samples were washed three times with a phosphate buffered saline (PBS: NaCl 150 mM, KH_2PO_4 0.58 mM and Na_2HPO_4 3.4 mM, pH 7.4). Plasma and buffy coat were carefully removed by aspiration after each washing. RBCs were finally suspended in the buffer solution to obtain a hematocrit of approximately 50%, stored at 4°C and were used within 6 hours.

2.2.4 Cell lines

The different cell lines such as RAW 264.7 (mouse macrophage cell line), MCF7 (breast cancer cells of human origin), EL4 (T cell lymphoma of murine origin) and NIH3T3 (mouse fibroblast cells), were obtained from National Centre for Cell Science, India.

2.2.5 Cell culture

EL4 cell line as suspension in RPMI medium, RAW 264.7 cells as suspension in DMEM medium, MCF7 cell line as adherent in DMEM medium, NIH3T3 cell line as adherent in RPMI medium and freshly isolated spleen lymphocytes as suspension in RPMI medium were cultured and supplemented with 10 % fetal bovine serum, 100 µg/ml

streptomycin and 100 units/ml penicillin. The incubation was carried out in a humified tissue culture incubator, at 37ºC with 5% CO_2 atmosphere.

2.3 Anti- hemolytic experiments

2.3.1 Free radical generation to induce hemolysis

AAPH is the most commonly used source for generating free radicals specifically peroxyl radicals in *in vitro* systems.[178] AAPH is a water-soluble crystalline di-azo compound. The chemical structure of AAPH is shown in scheme 2.1. The free radical reaction is initiated by the peroxyl radicals generated by thermal decomposition of AAPH in the presence of oxygen.

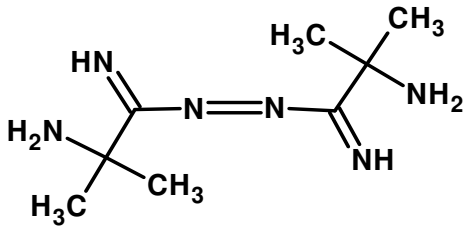

Scheme 2.1: *Chemical structure of AAPH* (*R' – N = N – R'*)

When AAPH is added as initiator, it decomposes at physiological temperature (37°C) in aqueous solutions to generate alkyl radical ($R'^{\bullet}$), which in presence of oxygen is converted to the corresponding peroxyl radicals ($R'OO^{\bullet}$) (equations 2.1 and 2.2).

$$R' - N = N - R' \longrightarrow 2R'^{\bullet} + N_2 \qquad (2.1)$$

$$R'^{\bullet} + O_2 \longrightarrow R'OO^{\bullet} \qquad (2.2)$$

Where, R′ is –C $(Me)_2$–C (NH_2)=NH_2^+

At 37°C in neutral water, the half life of AAPH is about 175 hours (h) and generates radicals at a rate of 1.3 x 10^{-6} [AAPH]/s.[178] These peroxyl radicals induce oxidation of polyunsaturated lipids (LH) in RBC membranes causing a chain reaction known as lipid

peroxidation (equations 2.3, 2.4 and 2.5). As a result of this, the RBC membrane undergoes quick damage and losses its integrity, leading to the release of hemoglobin (hemolysis), intracellular K^+ ions and depletion of glutathione level.[179] However, in presence of antioxidants (AH), the oxidative damage to RBCs can be inhibited due to scavenging of peroxyl radicals (equation 2.6).

$$R'OO^{\bullet} + LH \longrightarrow R'OOH + L^{\bullet} \quad (2.3)$$

$$L^{\bullet} + O_2 \longrightarrow LOO^{\bullet} \quad (2.4)$$

$$LH + LOO^{\bullet} \longrightarrow L^{\bullet} + LOOH \quad (2.5)$$

$$AH + LOO^{\bullet} \longrightarrow A^{\bullet} + LOOH \quad (2.6)$$

Therefore oxidation of RBCs membranes by AAPH provides a good approach for studying the free radical induced membrane damage and also to evaluate the antioxidant activity of external agents in terms of their ability to inhibit above processes.[179]

2.3.2 Measurement of hemolysis

Hemolysis of RBCs was carried out by mixing 5% suspension of RBCs in 10 mM PBS (pH 7.4) with AAPH solution (final concentration 50 mM) in a reaction volume of 1 ml. The concentration of AAPH to induce hemolysis was selected based on previous reports.[180] This reaction mixture was incubated for 3 h at 37°C with gentle shaking. The extent of hemolysis was determined spectrophotometrically by measuring the absorbance of hemolysate at 540 nm as described previously.[181] For reference, RBCs were treated with distilled water and the absorbance of the hemolysate at 540 nm was used as 100% hemolysis.

2.3.3 Measurement of K^+ ion loss

Pecked RBCs were suspended in 3 ml of 10 mM PBS (pH 7.4) to give 0.5% hematocrit. To AAPH (50 mM) was added and this system was incubated at room temperature for 3 h. After centrifugation at 1500 x *g* for 10 min, the concentration of K^+ ion in the supernatant was measured using flame photometry (Chemito, model no - AA 203, India).[182] For reference of 100% intracellular K^+ ion, a sample of RBCs was hemolysed in distilled water and the K^+ ion concentration was determined in the supernatant after centrifugation. Flame photometry uses the flame which, evaporates the solvent and also sublimates and atomizes the metal and then excites a valence electron to an upper energy state. Light is emitted at characteristic wavelength for each metal as the electron returns to the ground state and it makes qualitative determination possible. Flame photometers use optical filters to monitor for the selected emission wavelength produced by the analyte species. Comparison of emission intensities of unknowns to that of standard solutions (plotting calibration curve) allows quantitative analysis of the analyte metal in the sample solution. Because of the very narrow and characteristic emission lines from the gas-phase atoms in the flame plasma, the method is relatively free of interferences from other elements. Therefore, the flame photometry is very sensitive; measuring concentration of ppm magnitude (part per million).

2.3.4 Membrane lipid peroxidation

The most widely used method for measurement of lipid peroxidation is TBARS method. During lipid peroxidation membrane lipids break down into number of products such as hydro peroxides, alkadienal, malonaldehyde, 4- hydroxy nonenal (4HNE) etc as discussed earlier in section 1.1.2 of chapter 1. The TBARS method is based on the

principle that malondialdehyde forms a 1:2 adduct with thiobarbituric acid i.e. one molecule of malonaldehyde and two molecules of TBA to form a red malonaldehyde-TBA adduct as shown in scheme 2.2, which can be quantitatively estimated either by spectrophotometrically (532 nm) or by fluorimetry. The absorbance at 532 nm is not specific to TBA chromogen but some other products of lipid peroxidation like 2, 4 alkadienals also react with TBA to show strong absorption at 532 nm. In order to emphasis the lack of specificity, the values obtained in the test are commonly described as TBARS (TBA reactive substances)[183].

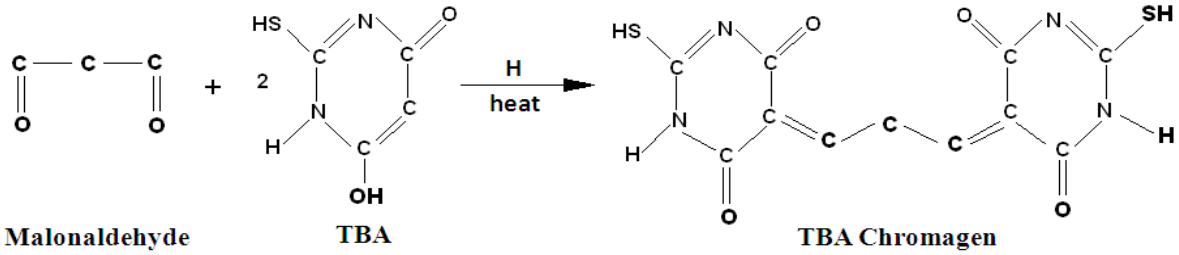

Scheme 2.2: *Reaction showing formation of TBA chromogen*

Hence AAPH induced lipid peroxidation in RBCs was assessed by measuring the TBARS. For this 5% suspension of RBCs in 10 mM PBS (pH 7.4) was incubated under air atmosphere with 50 mM AAPH at 37°C for 3 h to initiate membrane damage. After incubation, the system was centrifuged at 1500 x *g* for 10 min, the pellet was washed twice with cold PBS and resuspended in to 300 µl PBS (pH 7.4) to which 900 µl of TBA reagent (0.375% thiobarbituric acid, 0.25 M HCl, 15% trichloroacetic acid and 6 mM EDTA) was added. The reaction mixture was incubated at 85ºC for 20 min and cooled to ambient temperature. Samples were centrifuged at 12000 x *g* for 10 min at 25ºC and TBARS in the supernatant was estimated by measuring the absorbance at 532 nm (ε532 =

1.56 x 10^5 $M^{-1}cm^{-1}$). The results were expressed as nanomoles (nmoles) of TBARS per mg of hemoglobin.[184]

2.3.5 Glutathione (GSH) estimation

The standard method for the determination of GSH present in proteous samples is based on the reaction between sulfhydryl groups of GSH with DTNB or Ellman's reagent that produces a yellow-colored 5-thio-2-nitrobenzoic acid (TNB) as shown in the scheme 2.3.[185] The amount of TNB production is directly proportional to the concentration of GSH in the sample. Measurement of the absorbance of TNB at 405 or 412 nm provides an accurate estimation of GSH in the sample.[186] GSH is easily oxidized to the disulfide dimer GSSG in contact with oxygen (air). Therefore enough care is taken while handling the samples. Samples require de-proteination before estimation of glutathione. Deproteination is performed by precipitating the proteins and high molecular weight polypeptides with chilled TCA reagent. GSH being a tri-peptide does not get precipitated with TCA reagent. The supernatant obtained is free of proteins and contains GSH and GSSG.

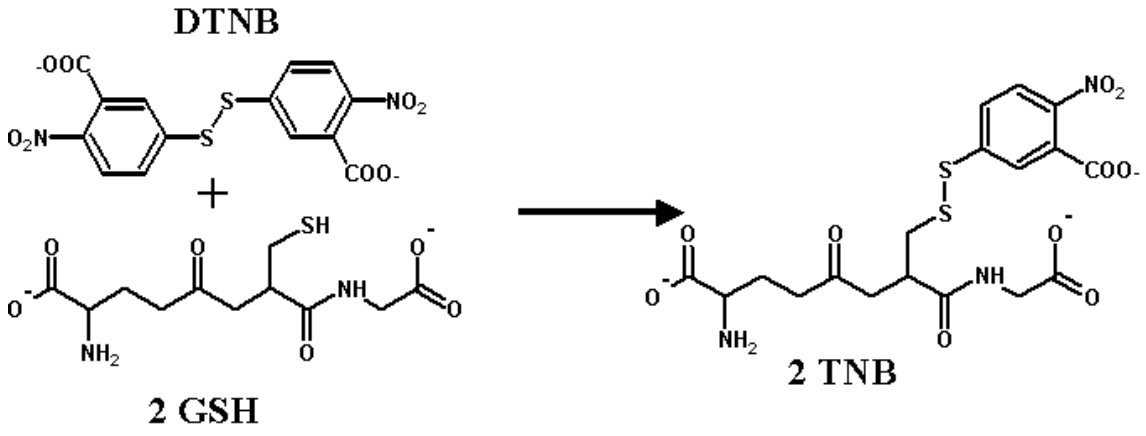

Scheme 2.3: *Reaction of Ellman's Reagent with reduced glutathione*

In a typical experiment, 5% suspension of RBCs in 10 mM PBS (pH 7.4) was subjected to hemolysis by treatment with AAPH for 3 h. After incubation, the system was centrifuged at 1500 x *g* for 10 min, the pellet was washed twice with cold PBS and lysed by adding 200 µl of nitrogen saturated autoclaved water. The lysate was precipitated using 10% TCA and about 50 µl of supernatant was mixed with 6 µM DTNB. The mixture was incubated for 10 min and absorbance was measured at 412 nm against appropriate control samples that were processed in parallel without adding the DTNB. Using the molecular extinction coefficient of $\varepsilon = 1.36 \times 10^4\ M^{-1}\ cm^{-1}$ at 412 nm, the concentration of GSH was estimated and expressed as nmoles GSH per mg of hemoglobin. Although GSH forms the majority of DTNB reactive thiols, the small-molecular-weight thiols other than GSH too react with DTNB. Therefore, the total DTNB reactive thiols were also addressed as non-protein thiols content.

2.4 Measurement of oxidative stress in cells and tissue

2.4.1 Preparation of cell and tissue homogenate

The tissue or cell homogenate was prepared by disrupting the tissue or cell mass in an appropriate volume of PBS buffer, pH 7.4 using a Branson sonifier (250, VWR Scientific, Danbury, CT, USA) and bioruptor (Cosmos Bio, Tokyo, Japan) respectively for 30 s each with cooling in ice-chilled water. The homogenates were centrifuged at 800 x *g* for 5 min at 4^{o}C to separate the nuclear debris. The supernatant so obtained was used for the estimation of antioxidant enzymes (SOD, catalase, and GPx) activity, thiobarbituric acid reactive substances (TBARS), protein carbonyls, glutathione (GSH) and total thiol contents. Protein content in the tissue or cell homogenate was determined

using bovine serum albumin as a standard protein and protein estimation kit (Bangalore Genei, India) as per the manufacturer's instruction.

2.4.2 Assays for antioxidant enzymes

SOD activity was determined by monitoring the inhibition of reduced cytochrome c (Fe^{2+}) formation from cytochrome c (Fe^{3+}) in presence of superoxide radical generating xanthin–xanthin oxidase system as described previously.[187] Briefly 25 µl of the tissue or cell homogenate was added to an assay mixture containing 10 mM Tris buffer (pH 8.0), 600 µM EDTA, xanthine (50 µM) and cytochrome c (Fe^{3+}) (9.5 µM) in a total volume of 1 ml. The reaction was initiated with xanthine oxidase (10 mU/ml) and the formation of reduced cytochrome c (Fe^{2+}) was monitored at 550 nm. The change in absorbance per unit time (ΔA/min) was monitored up to 300 seconds. Using the ΔA/min the pecent inhibition of cytochrome c reduction by the tissue or cell homogenate was estimated according to equation 2.7.

$$\%\ Inhibition = \frac{\Delta A(Uninhibited) - \Delta A(Inhibited)}{\Delta A(Uninhibited) - \Delta A(Blank)} \times 100 \qquad (2.7)$$

Here ΔA(uninhibited), ΔA(inhibited), and ΔA(blank), represent absorbance at 550 nm in solutions containing (xanthine + xanthine-oxidase+ cytochrome c), (xanthine + xanthine-oxidase + cytochrome c + tissue/cell homogenate) and (xanthine + cytochrome c) respectively.SOD activity was expressed as units/mg of protein where 1 unit is defined as the amount of enzyme present that inhibits cytochrome c reduction by 50%.

The catalase activity was determined by monitoring the enzyme–catalyzed decomposition of H_2O_2 at 240 nm as described earlier.[188] The reaction mixture contained 15 mM of H_2O_2 in 10 mM of Tris buffer, pH 7.4. The reaction was initiated by addition of 25 µl of the tissue or cell homogenate and the decrease in absorbance/min (ΔA/min)

was calculated from the initial linear portion of the curve using 3.9 x 10^4 M^{-1} cm^{-1} as the extinction coefficient of H_2O_2. Catalase activity was expressed as units/mg of protein where 1 unit is defined as the amount of enzyme consuming 1 µmole of H_2O_2 per min.

The GPx activity was estimated using Randox Kit, UK as per manufacturer's instruction. Enzyme activity was expressed as units/mg of protein where 1 unit is defined as the amount of enzyme oxidizing 1 µmole of NADPH per min.

2.4.3 Estimation of total thiol and GSH content

For the estimation of non-protein thiol content, 200 µl of the tissue or cell homogenate was precipitated with ice chilled 10% TCA and about 50 µl of the supernatant obtained, was mixed with 6 µM DTNB. For the estimation of total thiols about 50 µl of the tissue fraction, without precipitation of the proteins was mixed with 10 mM DTNB. The reaction mixture in both the cases was processed as explained in earlier section and total thiol and GSH content was evaluated by measuring the absorbance at 412 nm.[186] The results were expressed as nmoles of total thiol/ GSH per mg of protein.

2.4.4 Estimation of lipid peroxidation

Approximately 300 µl of tissue homogenate or 5 x 10^6 cells suspended in to 300 µl of 10 mM PBS buffer was mixed with 900 µl of TBA reagent and processed for the estimation of TBARS as described in earlier section.[184] The lipid peroxidation was expressed as nmoles of TBARS per mg of protein.

2.4.5 Protein oxidation

The tissue or cell homogenate containing approximately 1 mg soluble proteins in 10 mM PBS, pH 7.4 was taken and total proteins were precipitated with ice chilled 10% TCA. The pellet was suspended in 0.2% DNPH in 2N HCl and incubated at room

temperature for 2 hours. Proteins were reprecipitated with TCA and excess DNPH was removed with several washes of 50% ethyl acetate in ethanol. Decolorized protein pellet was dissolved in 6N guanidine hydrochloride and the optical density was measured at 370 nm. The amount of protein carbonyls were determined by using an extinction coefficient of 2.1 x 10^4 M^{-1} cm^{-1} and expressed as nmols of protein carbonyls/mg of protein.[189]

2.4.6 Estimation of intracellular ROS

Intracellular ROS levels were estimated using a cell permeable oxidation sensitive probe DCF-DA whose fluorescence intensity increases after being oxidized to dichlorofluorescein (DCF) by reactive oxygen species (ROS). For this 1 x 10^6 cells suspended in 1 ml of 10 mM PBS buffer were incubated with oxidation sensitive DCF-DA (a final concentration of 10 µM) for 30 min at 37º C.[190] After incubation cells were washed three times with cold PBS to remove the extracellular probe and lysed in PBS containing 1% Tween 20. The supernatant assayed for DCF fluorescence (excitation at 480 nm and emission at 530 nm). The representative values were expressed as mean fluorescence intensity at 530 nm.

2.5 Methods for molecular studies in cells and tissue

2.5.1 RNA isolation and RT-PCR analysis

Obtaining high quality, intact RNA is the first and often the most critical step in performing many fundamental molecular biology experiments, including Northern analysis, nuclease protection assays and RT-PCR. The major threat to the RNA extraction process is the contamination with RNAase enzyme. This enzyme is practically present everywhere. It degrades RNA immediately. Therefore all pipette tips, eppendorf tubes

and glassware were treated with DEPC to destroy ribonucleases. Total RNA from tissue or cell mass was isolated using RNA isolation kit (Roche Biochem, Germany) and was eluted in 50 µl deionised DEPC-treated water. The total RNA in sample was quantified by measuring the absorbance at 260 nm. Measuring absorbance ratio of 260 nm and 280 nm suggests the purity of RNA. The RNA free from protein and DNA contamination gives the ratio of A_{260}/A_{280} in between 1.6 to 2. About 2 µg of total RNA was used for the synthesis of complementary DNA (cDNA) by reverse transcription (cDNA synthesis kit, Invitrogen, USA) following the manufacturer's instructions. The cDNA was amplified using 2 µl of cDNA in 25 µl reaction system with 10 picomoles (pmoles) of the gene specific primers for 35 cycles. Each cycle consisted of 30 s of denaturation at 94ºC, 30 s of annealing at 57ºC and 60 s of extension at 72ºC. β-actin was used as internal control in all the reactions. The band intensity was quantified by gelquant software (version 2.7 DNR imaging systems Ltd. Israel). Fold changes were calculated after normalization to β-actin.

2.5.2 Western blotting

The tissue or cell lysate for western blotting was prepared by homogenizing the tissue or cell mass in buffer containing 10 mM Tris (pH 7.5), 150 mM NaCl, 1% NP-40, 1% Triton-X 100, 1% sodium deoxycholate, 0.1% SDS, 50 mM NaF, 1 mM Na3VO4, 20 mM sodium glycerophosphate, 1 mM EDTA, 2 mM PMSF, 1 mM benzamidine and 1X protease inhibitor cocktail (Sigma-Aldrich, USA). Proteins in the homogenate were estimated using bovine serum albumin (BSA) as a standard protein and protein estimation kit (Bangalore Genei, India) as per manufacturer's instruction. Approximately 50 µg protein was denatured at 95°C with sample buffer (0.125 M Tris buffer (pH 6.8), 4%

SDS, 20% glycerol, 2% 2-ME, 0.03 mM bromophenol blue) for 5 min and were separated by electrophoresis in 12% SDS– PAGE gels for low molecular weight proteins and on 8 % SDS–PAGE gels for middle and high range molecular weight proteins.[191] Proteins were transferred onto a nitrocellulose membrane (Amersham Pharmacia Biotech, Little Chalfont, UK), blocked overnight with a blocking solution (5% BSA in TBS containing 0.1% Tween 20) and exposed to the primary antibody raised in rabbit or sheep for 2 hours at room temperature. After washing, the membranes were incubated for 1 hour at room temperature with horseradish peroxidase (HRP) linked secondary antibody such as anti-rabbit (1:1500) or anti-sheep (1: 1500) (Roche Molecular Bio chemicals, Germany) and signals were detected using chemiluminiscence western blotting kit (Roche Molecular Bio chemicals, Germany) as per the manufacturer's instructions. For reprobing, membranes were stripped with 100 mM 2-ME, 2% SDS and 62.5 mM Tris–HCl (pH 6.9) for 20 min at 50°C followed by immunoblotting as mentioned above. Equivalent protein loading was demonstrated by staining the membranes in 1% Ponceau S. The band intensity was quantified by gelquant software. Fold changes were calculated after normalization to Ponceau S.

2.5.3 Isolation of nuclei for NF-κB measurement in cells

The nuclear extract from cells was isolated according to the procedure described earlier.[192] The cells were washed two times with 10 mM PBS, resuspended and incubated on ice for 15 min in hypotonic buffer A (10 mM HEPES, pH 7.9, 10 mM KCl, 0.1 mM EDTA, 0.1 mM EGTA, 1 mM DTT, 0.5 mM PMSF, and 0.6% NP-40). Cells were vortexed gently for lysis and nuclei were separated from the cytosol by centrifugation at 12,000 x *g* for 1 min. Nuclei resuspended in buffer B (20 mM HEPES, pH 7.9, 25%

glycerol, 0.4 M NaCl, 1 mM EDTA, 1 mM EGTA, 1 mM DTT, 0.5 mM PMSF) and were shaken for 30 min at 4°C. Nuclear extracts were obtained by centrifugation at 12,000 x *g* and protein concentration were estimated. Nuclear extract was fractionated on 12 % SDS-PAGE gel, transferred to nitrocellulose membrane, and probed with rabbit anti-NF-κB (p65) antibody using chemiluminiscence western blotting kit. Equivalent protein loading was demonstrated by staining membranes in 1% Ponceau S. Fold changes were calculated after normalization to Ponceau S.

2.6 Cytotoxicity studies in cells

2.6.1 Viability assay

The viability of cells was determined by trypan blue dye exclusion test using a hemocytometer or MTT dye conversion assay.[193,194] For trypan blue dye exclusion test about 2 x 10^4 cells of tumor physiology and 1 x 10^5 cells of normal physiology were added to each well of 24-well plates in 1 ml of tissue culture medium in triplicate. After 24 hours of addition floating cells in the medium of each well were transferred to centrifuge tubes. Adherent cells were detached and were added to the corresponding floating cells before centrifugation. The pellet was suspended and 0.14% trypan blue was mixed with the same volume of cell suspension and 5 min later the stained (dead) and unstained (viable) cells were counted in hemocytometer. The cell viability for each group was calculated as percentage (%) according to equation 2.8.

$$\%\ Viability = \frac{Number\ of\ living\ cells}{Total\ number\ of\ cells\ including\ living\ and\ dead} \times 100 \qquad (2.8)$$

For MTT assay briefly, 5 x 10^4 cells of tumor physiology and 4 x 10^4 cells of normal physiology were cultured in 100 µl volume of tissue culture medium in a 96 well plate for 24 hours, the cells were washed once and further incubated for 4 hours with MTT

dye. The blue formazan precipitate obtained was dissolved using solubilization buffer, kept overnight at 37ºC and the absorbance at 550 nm was measured using a scanning plate reader (Bio-Tek Instruments, USA).[194] The results were expressed as the mean absorbance ± SEM for three replicates.

2.6.2 Apoptosis assay

Apoptosis in cells was determined by fluorescence activated cell sorting (FACS) analysis or DNA fragmentation assay.[195,196] For the estimation of apoptosis, cells were cultured for 24 h at 37ºC in humified chamber with 5% CO_2 atmosphere. After 24 hours, cells were collected by centrifugation at 1,000 x *g* for 4 min, washed twice with 10 mM PBS, suspended in 1 ml of staining solution containing 50 µg/ml PI, 0.1% sodium citrate and 0.1% Triton X-100 and then analyzed by flow cytometry. PI binds to DNA and the intensity of fluorescence at 580 nm represents the total DNA content. Most of cells were in G1 phase of cell cycle (2n DNA content). The pre G1 phase population represented the apoptotic cells.

The DNA fragmentation assay was performed in cells or tissues by homogenizing 2 mg of tissue or 1 x 10^6 cells in 0.5 ml of 10 mM Tris-HCl (pH 8.0) buffer containing 150 mM NaCl, 2.5 mM EDTA, protenase K (200 µg/ml), 0.5% SDS, 0.2% Triton X –100 and incubated at 50^{o}C for 1 h in the dry bath. The mixture was treated with 25µl of RNAse (1 mg/ml) and incubated for another 1 h. Following this the DNA was precipitated with 2.5 volume ethanol in presence of 0.1 volume of 5 M ammonium acetate at –20^{o}C for overnight and dissolved in TE buffer. The amount of DNA was estimated spectrophotometrically by measuring the absorbance at 260 nm and equal amount of DNA from all the samples was electrophoresed on a 1.5% agarose gel. The

DNA fragments were visualized by gel documentation unit (U-genius, Syngene, Germany).

2.7 Methods for evaluating physiological parameters under *in vivo* radioprotection

2.7.1 Estimation of liver function

Blood samples were collected from animal on the appropriate day of post irradiation and serum was separated. The level of serum alanine aminotransferase (ALT) and aspartate aminotransferase (AST) levels were estimated by the methods of Reitman and Frankel, (1957).[197] In brief, 0.2 ml aliquot of serum with 1 ml of substrate (aspartate and α-KG for AST: alanine and α-KG for ALT) in phosphate buffer (pH 7.4) was incubated for 1 hour for AST and 30 min for ALT. 1 ml aliquot of DNPH solution was added to arrest the reaction and kept for 20 min at room temperature. After incubation, 1 ml of 0.4 N NaOH was added and the absorbance was measured at 540 nm. Activities are expressed as international units /liter (IU l^{-1}).

2.7.2 Endogenous spleen colony assay

Endogenous spleen colony assay is based on the fact that macroscopic colonies arise in the spleens of irradiated animals after a week time post irradiation. Therefore for spleen colony assay on the 11^{th} of day post-irradiation, animals were sacrificed by cervical dislocation and spleens were removed immediately, blotted free of blood, weighed immediately and spleen index was calculated (spleen index= (spleen weight/body weight) x 100). Later, they were fixed in Bouin's fixative (mixture of saturated picric acid - 71.4 ml, formalin (10%) - 23.8 ml, glacial acetic acid - 4.76 ml) and the spleen colony forming units (CFUs) were counted in the same spleen manually.[198]

2.7.3 Histopathological studies

The tissues were collected on the appropriate day of post irradiation. The tissues were fixed in 10% neutral buffered formalin, dehydrated by passing through a graded series of alcohol and embedded in to paraffin blocks. The sections of 5 µm thickness were cut using a rotary microtome (AO 820, USA). The sections of tissues were stained in eosin and Harris haematoxylin and examined using upright trinocular microscope attached to CCD camera.[199]

2.7.4 Estimation of DNA damage by alkaline single cell gel electrophoresis

The radiation induced DNA damage was checked in peripheral leukocytes by single cell gel electrophoresis (comet assay) as described previously.[200] For this about 50 µl of peripheral blood was collected from tail of animals at 30 min post irradiation. The fully frosted microscope slides were layered with 500 µl of 1% agarose in saline and a cover slip was placed over it and kept at 4°C for 10 min for solidification. The cover slip was then removed and the second layer of 300 µl of 0.8% low melting agarose (LMA) containing ~ 30 µl peripheral blood at 38ºC was added. Cover slip was placed immediately, and the slides were placed at 4ºC. After solidification of the LMA, the cover slips were removed and the slides were placed in the ice chilled lysis buffer containing 2.5 M NaCl, 100 mM EDTA, 10 mM Tris–HCl, pH 10.0 and 1% DMSO, 1% Triton X-100 and 1% sodium sarcosinate for 1 h at 4ºC. The slides were then removed from the lysis buffer and rinsed with alkaline solution placed on a horizontal electrophoresis tank filled with freshly prepared alkaline buffer (300 mM NaOH, 1 mM EDTA and 0.2% DMSO, pH >13.0). The slides were equilibrated in that buffer for 20 min and then electrophoresis was carried out at 22 V, 299 mA for 30 min. After

electrophoresis was completed the slides were washed gently with 0.4M Tris–HCl buffer, pH 7.5, to remove any alkali present. The slides were stained by 50 µl of 5 X SYBR Green-II dye and visualized using Carl Zeiss Axioplan fluorescent microscope. The images were captured using an imaging system. Fifty images were grabbed for each slide and these images were analyzed using CASP software by which % DNA in tail, tail length (TL), tail moment (TM) and olive tail moment (OTM) were obtained.

2.8 Irradiation source

Cobalt-60 (^{60}Co) is the most widely used source for γ irradiation. Cobalt-60 is made in reactor by irradiation of cobalt metal with neutron according to the equation 2.8 involving ^{59}Co (n, γ) ^{60}Co reaction.[69]

$$^{59}Co + n^{1} \longrightarrow {}^{60}Co + \gamma \qquad (2.8)$$

^{60}Co emits two γ-rays of 1.17 and 1.33 MeV per disintegration and it has half-life of 5.27 years.[61] For use of ^{60}Co as radiation source the ^{59}Co metal is irradiated in a nuclear reactor in the form of pellets, pencils or thin disks and these are placed in containers, which are then assembled into radiation source of a desired size like Gamma cell 220, Theratron etc. For the dose measurement of ^{60}Co γ source, Fricke dosimeter is used.[69] This dosimeter has linear response up to 500 Gy of dose and can also be used for dose rate up to 10^6 Gy/s. The principle involved is the radiation-induced oxidation of ferrous ion to ferric ion at low pH and in the presence of oxygen. The standard dosimeter solution contains 1 x 10^{-3} M ferrous ion, 1 x 1 0^{-3} M NaCl in 0.4 M H_2SO_4 (pH 0.46) and is saturated with air (the concentration of oxygen is about 2.5x10^{-4} M). Small variation in concentrations of the solutes does not affect the response of this dosimeter. The reactions involved are the following:

$$e_{aq}^{-} + H^{+} \longrightarrow H^{\bullet} \quad (2.10)$$

$$H^{\bullet} + O_2 \longrightarrow HO_2^{\bullet} \quad (2.11)$$

$$Fe^{2+} + HO_2^{\bullet} \xrightarrow{H^{+}} Fe^{3+} + H_2O_2 \quad (2.12)$$

$$Fe^{2+} + H_2O_2 \longrightarrow Fe^{3+} + {}^{\bullet}OH + OH^{-} \quad (2.13)$$

$$Fe^{2+} + {}^{\bullet}OH \longrightarrow Fe^{3+} + OH^{-} \quad (2.14)$$

$$G(Fe^{3+}) = 3g(H^{\bullet} + e_{aq}^{-}) + g({}^{\bullet}OH) + 2g(H_2O_2) \quad (2.15)$$

Putting g-values of the primary radicals G (Fe^{3+}) becomes 15.5. The most common method for measuring the ferric ion formed is by spectrophotometry, comparing the absorbance of the irradiated and non-irradiated dosimeter solutions at the wavelength at which ferric ion shows maximum absorption (~ 304 nm). The absorbance measurement should be made soon after irradiation so that adventitious oxidation of the solutions is minimized. The mean absorbed dose (D) measured using this method is given by the following relation:

$$D = \frac{9.684 \times 10^{6} \Delta A}{\varepsilon l \rho G} Gy \quad (2.16)$$

where, ΔA is the change in absorbance of dosimeter solution before and after irradiation. G is yield (number of molecules per 100 eV) of ferric ions due to irradiation, ε is extinction coefficient (2201 $M^{-1}cm^{-1}$) of ferric ions at the measuring wavelength, ρ (1.024) is the density (gcm^{-3}) of dosimeter solution, *l* is the path length in cm.

CHAPTER 3

STUDIES ON BIOCHEMICAL EFFECTS OF CURCUMIN IN CELLS

Section I: Differential antioxidant and pro-oxidant activities of curcumin in cells

3.1 Introduction

As discussed in chapter 1, curcumin has been shown to exhibit antioxidant activity both *in vitro* and *in vivo*.[96] In addition to that, it also exhibits anti-inflammatory and anti-cancer properties following oral or topical administration.[105,106] Although most of the studies indicated positive benefits, there are still some misconceptions about its usage as drug. Because few studies have suggested that in selected conditions, curcumin may not only be ineffective, but may have adverse activities. For example, curcumin induced DNA fragmentation and base damage in the presence of copper and isozymes of cytochrome p450 (CYP) that are present in lung, lymph, liver, and skin.[201] The authors hypothesized that the damage was the result of CYP-catalyzed O-demethylation of curcumin, leading to the formation of an O-demethyl curcumin radical, which, in the presence of copper, formed a DNA-damaging Cu(I)-hydroperoxo complex. DNA damage was attenuated when concentrations of curcumin exceeded those of copper, presumably due to the chelation of copper by curcumin. Copper dependent formation of 8-hydroxy-deoxyguanosine in response to curcumin was also reported by Yoshino et al. (2004) and further they linked the appearance of DNA damage to apoptotic cell death in HL60 cells.[202] Similarly, curcumin-mediated DNA damage was also reported in mouse lymphocytes using a comet assay.[203]

Additionally, several reports have emerged in the last one decade demonstrating pro-oxidative nature of curcumin, in view of its ability to promote oxidative stress in transformed cells in culture.[112,204] These effects have been correlated with enhanced ROS production, alteration of the cellular redox homeostasis (e.g., the depletion of

glutathione), and disruption of the mitochondrial functions e.g., dissipation of mitochondrial inner transmembrane potential.[205-209] The enhancement of oxidative stress by curcumin in transformed cells ultimately results in mitochondrial-mediated apoptosis, and this has been considered as one of the mechanisms responsible for the anticancer activity of curcumin.[112,190,210]

The mechanism by which curcumin mediates its pro-oxidant effects is not completely understood. However, some reports suggest that curcumin irreversibly binds to mitochondrial thioredoxin reductase, and modifies its activity in to NADPH oxidase through alkylation of cysteine residue present in the catalytically active site of the enzyme.[209] This leads to the production of ROS, which according to few others is due to the α,β-unsaturated carbonyl moiety of curcumin.[129] The pro-oxidant property is also believed to be due to the generation of phenoxyl radicals of curcumin by heme peroxidase-H_2O_2 system.[60] These phenoxyl radicals could be repaired by cellular GSH or NADH. In this process, the resulting $GS^{\bullet}$ radical forms $GSSG^{\bullet-}$ radical and this may further reduce O_2 to form $O_2^{\bullet-}$ radical leading to elevated ROS levels.[60]

In short, all these reports support that curcumin may switch from antioxidant to pro-oxidant depending on cell type, redox environment and dosage.[105] Considering the potential of curcumin as a therapeutic agent and the number of ongoing clinical trials, it is essential to understand its dual behaviour as antioxidant or pro-oxidant in different cellular system of the body. Oral usage of curcumin results in its systemic distribution to peripheral blood circulation.[96] The peripheral blood vascular system possesses different kinds of cells including erythrocytes or red blood cells (RBCs) and leukocytes such as monocytes and lymphocytes. These cells perform a number of physiologically important

functions for the body like oxygen transport, immune functions, etc. However the functional activities of these cells are highly sensitive to changes in intracellular redox environment induced by an antioxidant/pro-oxidant.[211] Therefore it is important to identify the conditions under which curcumin mediates antioxidant/pro-oxidant effects in such cells.

With this background, the differential antioxidant/pro-oxidant nature or redox modulating effects of curcumin in two different cellular systems including freshly isolated human RBCs and murine macrophage cell line (RAW 264.7) have been discussed in this section.

3.2 Results

3.2.1 Studies in human RBCs

The RBCs are the most important cells of peripheral blood vascular system of vertebrates.[212] The number of RBCs in a healthy human being ranges from 4.5 - 5.0 x 10^6/µl. RBCs circulate oxygen throughout the body and carry the waste metabolic products to the excretory and detoxifying organs such as kidney and liver respectively.[213] The damage to RBCs negatively affects the organism in several ways. Because, certain organs in the body require a continuous supply of oxygen in order to generate energy for their proper functioning, e.g. heart and brain. RBCs are enucleated cells enclosed by a lipid bilayer similar to the other nucleated cells in the body.[212] During the formation of RBCs from their progenitor cells i.e. the reticulocytes, the nucleus comes out and hemoglobin protein enters the cells. Thus RBCs contain hemoglobin as the major protein component within them.[212,213] Any damage to the RBCs membrane therefore will lead to leakage of hemoglobin from cells to outer matrix. This process is known as hemolysis.[179]

Membranes of RBCs are rich in polyunsaturated fatty acids, which are very susceptible to free radical mediated peroxidation leading to release of hemoglobin (hemolysis) and K^+ ions. Therefore, if any compound is capable of inhibiting the process of oxidative damage in RBCs, it can be considered as antioxidant, while the compound inducing it, is a pro-oxidant.[179,214,215]

With this background, the effect of treatment concentrations on the antioxidant action of curcumin in RBCs was evaluated by following the inhibition of hemolysis induced by an azo compound, AAPH.[179] However, the pro-oxidant effect of curcumin was evaluated by monitoring its own effect on inducing hemolysis or any other associated effects like lipid peroxidation, K^+ leakage and GSH depletion in RBCs. Earlier Deng et al. (2006) have also studied the ability of curcumin to inhibit AAPH induced oxidative hemolysis in RBCs.[180] In this study, authors monitored only one parameter that is the inhibition of hemoglobin leakage by curcumin and on this basis explained its antioxidant activity. However, in our study, in addition to hemoglobin release, several other critical parameters like membrane lipid peroxidation, K^+ leakage and intracellular GSH levels have also been estimated. This would help in understanding o antioxidant/pro-oxidant activity of curcumin unambiguously.

For these studies, RBCs suspension in phosphate saline buffer (PBS) were pre-incubated with varying concentration of curcumin at 37^{o}C for 30 min, washed twice with cold PBS and then subjected to AAPH induced hemolysis at 37^{o}C for 3 hours. The 30 min incubation time would ensure that curcumin is taken up by the RBCs. The curcumin stock solution was prepared in DMSO and diluted with the PBS buffer to get the desired

concentration. Appropriate DMSO controls were taken in all the experiments. Each experiment was done in triplicates and results are presented as means ± SEM, n = 3.

3.2.1.1 Inhibition of AAPH induced hemolysis and lipid peroxidation

In the absence of AAPH, RBCs in PBS were stable and the hemolysis was negligible. When aqueous suspension of RBCs was incubated with AAPH, about 53% of hemolysis was observed. It is evident from figure 3.1 that the percent hemolysis gradually decreased with increasing concentration of curcumin, from which the IC_{50} value, was found to be 43 ± 5 μM. Inset of figure 3.1 shows variation in TBARS level in RBCs after subjecting to AAPH induced damage in the presence and absence of different concentrations of curcumin.

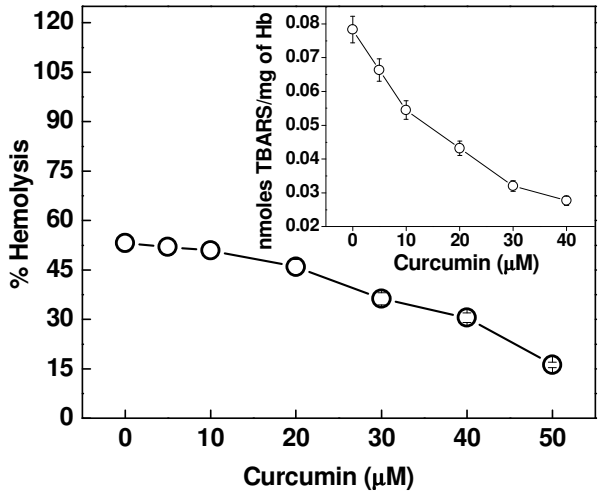

Figure 3.1 *Variation in percent hemolysis in human RBCs pre-incubated with different concentrations of curcumin and then subjected to hemolysis by 50 mM AAPH for 3 hours. Inset shows variation in TBARS levels as a function of curcumin concentration in the same system.*

The level of TBARS was significantly increased after incubation of RBCs with AAPH as compared to the control sample. In the presence of curcumin, there was gradual decrease

in TBARS formation and this inhibition increased with increasing curcumin concentration from 5 to 40 μM, from which the IC_{50} value, was found to be 23.2 ± 2.5 μM. The percent hemolysis in RBCs incubated with curcumin (5-50 μM) in the absence of AAPH was almost identical to that of control sample indicating curcumin itself could not induce hemolysis. The incubation of RBCs with curcumin in the absence of AAPH did not show any significant change in the level of TBARS as compared to control sample.

3.2.1.2 Inhibition of AAPH induced K^+ ion leakage

In the absence of AAPH, the K^+ ion leakage from RBCs was negligible. When aqueous suspension of RBCs was incubated with AAPH, about 79% of K^+ ion leakage was observed.

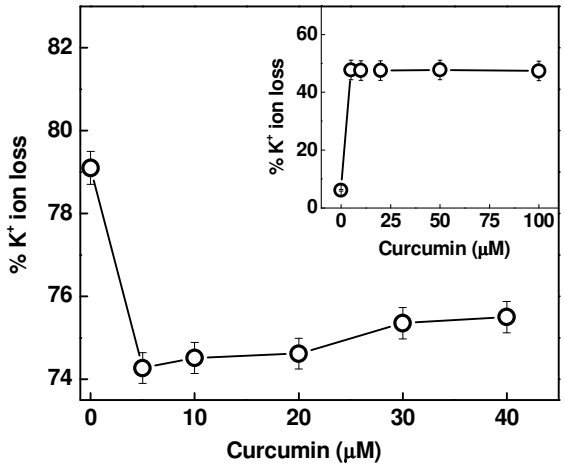

Figure 3.2 *Variation in percent K^+ ion loss in human RBCs incubated with 50 mM AAPH for 3 hours in presence of different concentrations of curcumin. Inset shows variation of percent K^+ ion loss in human RBCs incubated with different concentrations of curcumin without any added AAPH.*

Figure 3.2 shows the variation in % K^+ ion leakage from RBCs pre-incubated with increasing concentrations of curcumin (5-40 μM) for 30 min at 37^0C and then subjected

to hemolysis. It is evident from figure 3.2 that the percent K^+ ion leakage is lower in curcumin pretreated samples compared to AAPH treated sample, however in each case, the K^+ ion leakage increased with increasing concentration of curcumin. Inset of figure 3.2 shows variation in percent K^+ ion loss in RBCs after incubation with different concentrations of curcumin (5 to 100 μM) for 3 hours in the absence of AAPH. From the figure it is clear that the percent K^+ ion loss is significantly higher in curcumin treated samples as compared to control sample. The percent K^+ ion loss was almost identical nearly 47% at all the concentrations of curcumin (5 to 100 μM) tested in the present study.

3.2.1.3 Effect of curcumin on GSH levels in RBCs after hemolysis

Figure 3.3 shows change in GSH levels in RBCs after treatment with AAPH and also in presence of increasing concentration of curcumin (5 to 40 μM). The normal basal level of GSH in RBCs was found to be 2.74 ± 0.05 nmoles/mg of hemoglobin and after incubation with AAPH, the GSH level reduced to about 1.82 ± 0.03 nmoles/mg of hemoglobin. Addition of curcumin to this reaction system prevented the reduction in GSH content with increasing concentration up to 10 μM. However, curcumin treatment at concentrations >10 μM reduced GSH content in the concentration dependant manner. Inset of figure 3.3 shows variation in GSH level in RBCs after incubation with different concentrations of curcumin (5 to 40 μM) for 3 hours in the absence of AAPH. From the figure it is clear that the level of GSH in curcumin treated RBCs was almost constant up to treatment concentration of 10 μM, however beyond that a concentration dependant decrease in level of GSH was observed.

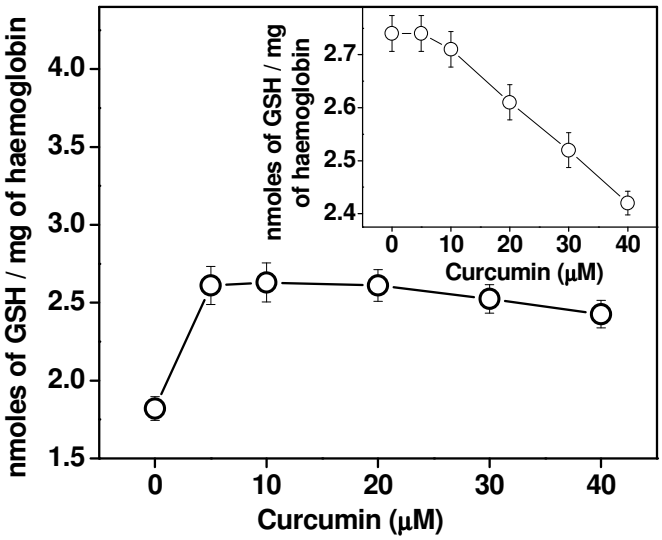

Figure 3.3 *Variation in GSH levels in human RBCs incubated with 50 mM AAPH for 3 hours in presence of different concentrations of curcumin. Inset shows variation in glutathione levels in human RBCs incubated with different concentrations of curcumin without any added AAPH.*

3.2.1.4 Reaction of curcumin with AAPH peroxyl radicals

Curcumin mediated protection of RBCs from AAPH induced hemolysis could be due to scavenging of AAPH peroxyl radicals as shown in the equation 3.1.

$$\text{AAPH} \rightarrow [\text{Peroxyl radical}] + \text{Curcumin} \rightarrow \text{Product} \qquad (3.1)$$

To test this, direct reaction of curcumin with AAPH was studied by following the time dependent changes in the absorbance of curcumin at 435 nm in presence of AAPH. Curcumin showed a broad absorption spectrum in PBS solution containing 1% DMSO with maximum absorption at ~ 435 nm, while that of 50 mM AAPH at pH 7 showed absorption maximum at 350 nm, with no absorption at wavelength > 400 nm (Fig. 3.4a and 3.4b).

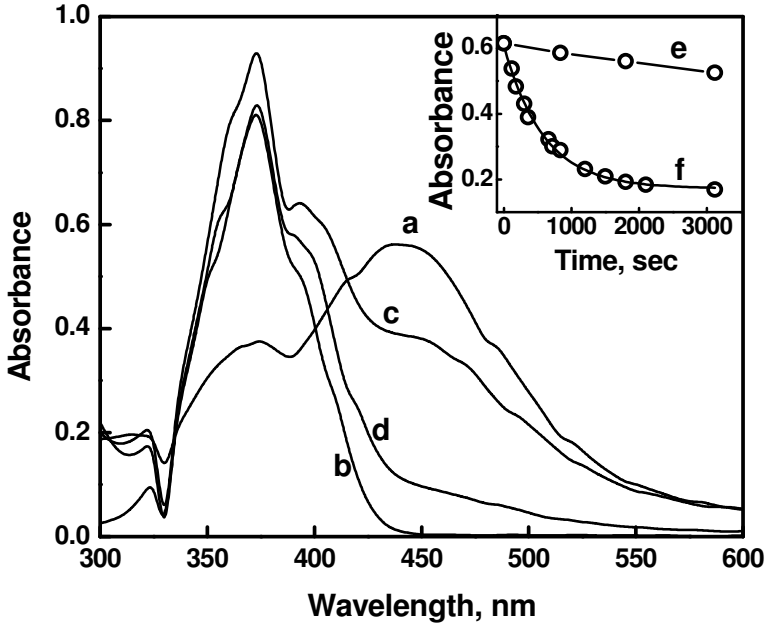

Figure 3.4 *Absorption spectra of (a) 25 μM curcumin, (b) 50 mM AAPH in PBS buffer containing 1% DMSO. (c) and (d) correspond to the spectra obtained on mixing 25 μM curcumin with 50 mM AAPH after 5 min and 30 min respectively. Inset shows the change in absorbance of 30 μM curcumin at 435 nm as a function of time in (e) the absence and (f) in presence of 50 mM AAPH at pH 7.*

On addition of AAPH, the absorption spectrum of curcumin changed significantly and the absorbance due to curcumin decreased completely in a time dependant manner. Figure 3.4c and 3.4d, show spectra recorded at two different times of 5 and 30 minutes after incubation with AAPH. Curcumin in aqueous medium is unstable and decays with the half-life of 96.7 min (Fig. 3.4e). Fig. 3.4f shows the decay of the parent curcumin (30 μM) absorbance at 435 nm after mixing with AAPH. As seen in the figure the decay of curcumin becomes faster in the presence of AAPH with the half-life of 4.5 min. This is much faster than the self decay of curcumin, therefore the self decay of curcumin can be ignored under these conditions. The rate constant of the reaction (3.1) was calculated by

fitting the absorption-time plot to first order exponential function according to equation 3.2.

$$A_t = A_o e^{-(k_{obs} t)} \qquad (3.2)$$

Here A_o and A_t represent the respective initial absorbance and absorbance at given time "t" at 435 nm. k_{obs} is the observed first order decay rate constant.

The k_{obs} was estimated at four different curcumin concentrations (10 – 50 μM) and the average value of k_{obs} divided by curcumin concentration was considered as the bimolecular rate constant for the reaction of AAPH with curcumin. The bimolecular rate constant for the reaction between curcumin and AAPH was estimated to be 63.4 ± 12.7 M^{-1} s^{-1}. This value may not be a true representation of the rate constant for the overall reaction (3.1), because the decomposition of AAPH being the slowest becomes rate limiting. This however, confirms that curcumin reacts directly with radicals derived from AAPH.

Encouraged by these results, further studies on antioxidant/pro-oxidant action of curcumin were carried out in macrophage cells.

3.2.2 Studies in murine macrophage cells (RAW264.7)

Macrophages are white blood cells, produced by the extravasation and division of circulating monocytes within tissues. These cells play a very important role in non-specific defense or innate immunity as well as in specific defense mechanisms or adaptive immunity of vertebrates. Their role is to phagocytose (engulf and then digest) cellular debris and pathogens, and to stimulate lymphocytes and other immune cells to respond to the pathogen.[216] These cells are inherently exposed to higher ROS production or oxidative stress during their normal immune functions and are capable of restoring

redox homeostasis through induction of intracellular antioxidants including non protein thiols and antioxidant enzymes such as SOD family (e.g. cytoplasmic Cu,Zn-SOD and mitochondrial Mn-SOD), catalase, glutathione peroxidase (GPx) and heme oxygenase (HO-1). Therefore, the antioxidant/pro-oxidant activity of curcumin in these cells is expected to depend on its ability to modulate the levels of intracellular ROS, non-protein thiols and antioxidant enzymes. With this background, the effects of treatment concentration and incubation time of curcumin on intracellular ROS generation, non protein thiols level and mRNA expression of antioxidant enzymes was investigated in murine macrophage cell line (RAW 264.7).

Since recent approach of antioxidant therapy is to use a combination of antioxidants to achieve desired therapeutic potential, the effects of water soluble thiol antioxidants such as GSH or N-acetyl cysteine (NAC) on curcumin mediated cellular modifications were also studied by pre-treating the cells with GSH or NAC.[217] Further, the ability of curcumin to modulate γ-radiation induced oxidative stress and cell death was also investigated in these cells. Based on these studies, the concentration and time dependant differential action of curcumin as a pro-oxidant or antioxidant in macrophage cells have been discussed.

RAW 264.7cells in DMEM medium were seeded (1 x 10^6 cells/ml) in six-well culture plates, kept overnight for attachment and then treated with curcumin. The reducing agents like GSH or NAC added to the cells 2 h prior to addition of curcumin. The stock solution of curcumin was prepared in DMSO and diluted with the culture medium to get the desired concentration. The maximum concentration of DMSO was within permissible limits of toxicity (≤ 0.1%). Appropriate DMSO controls were taken in

all the experiments. The experimental parameters like ROS generation, non-protein thiol levels and mRNA expression of antioxidant enzymes were estimated at 2, 6 and 18 hours (h) after curcumin addition to monitor its early and delayed effects on cellular redox environment. The expression of different antioxidant and antiapoptotic genes at mRNA level was checked by reverse transcription–polymerase chain reaction (RT-PCR). β-actin mRNA expression was used as an internal control. The primers used for RT-PCR (forward and reverse respectively) are listed in table 3.1. The results are presented as mean ± S.E.M. for two independent experiments run in triplicates. Data were analyzed by one-way and two-way ANOVA of SPSS software (version 8.0.0) to confirm the variability of data and for multiple comparisons of means. P values ≤ 0.05 were considered as statistically significant.

Table 3.1: *Gene specific RT-PCR primers*

Genes	**Primer sequence**	
Mn-SOD	Forward	5'-GCACATTAACGCGCAGATCA-3'
	Reverse	5'-AGCCTCCAGCAACTCTCCTT-3'
Cu,Zn-SOD	Forward	5'-AAGGCCGTGTGCGTGCTGAA-3'
	Reverse	5'-CAGGTCTCCAACATGCCTCT-3'
Catalase	Forward	5'-GCAG ATACCTGTGAACTGTC-3'
	Reverse	5'-GTAGAATGTCCGCACCTGAG-3'
GPx	Forward	5'-CCTCAAGTACGTCCGACCTG-3'
	Reverse	5'-GTAGAATGTCCGCACCTGAG-3'
HO-1	Forward	5'-AACAAGCAGAACCCAGTC-3'
	Reverse	5'-TGTCATCTCCAGAGTGTTC-3'
β-actin	Forward	5'-TGGAATCCTGTGGCATCCATGAAAC-3'
	Reverse	5'-TAAAACGCAGCTCAGTAACAGTCCG-3'
Bcl-2	Forward	5'-TGCACCTGACGCCCTTCAC-3'
	Reverse	5'-TAGCTGATTCGACCATTTGCCTGA-3'
Bcl-XL	Forward	5'-TGGTCGACTTTCTCTCCTAC-3'
	Reverse	5'-GAGATCCACAAAAGTGTCCC-3'

3.2.2.1 Biphasic effects of curcumin on ROS levels and non-protein thiol content

Intracellular ROS levels were estimated using a cell permeable oxidation sensitive probe dichlorofluorescein diacetate (DCF-DA), which on oxidation produces fluorescent DCF.[190] Figure 3.5A and 3.5B show the representative fluorescence intensities of DCF indicating ROS levels at 2 and 18 h after curcumin (1-25 μM) addition to cells. Curcumin increased ROS levels steadily up to 25 μM concentration at 2 h after addition to cells. However, the ROS levels dropped below the control levels at 18 h after addition. The levels of non-protein thiols content were measured at the same time points using 5,5'-dithiobis-2-nitrobenzoic acid (DTNB) after curcumin addition and it indicated that the basal levels of non-protein thiols content (0.251 ± 0.015 nmoles/μg of protein) decreased at 2 h (Fig. 3.5C). Interestingly, at later time point (18 h) the levels of non-protein thiols increased significantly with increasing concentration (1-25 μM) of curcumin (Fig. 3.5D).

Taken together these results suggest that curcumin could modify the redox environment within cells in a concentration and time dependent manner. Further to know whether curcumin mediated redox changes in cells could be restored by the addition of water soluble antioxidants like GSH or NAC, the cells were treated with 1 mM concentration of NAC or GSH for 2 h prior to addition of curcumin (1-25 μM). The ROS levels and non-protein thiols were measured at 2 and 18 h respectively. Exogenous addition of GSH or NAC prior to curcumin addition significantly decreased the ROS generation at 2 h (Fig. 3.5A). NAC was more effective than GSH in this respect. At later time point (18 h), NAC and curcumin treated cells showed lower ROS levels than the cells treated with curcumin alone (Fig. 3.5B). Similarly, pretreatment with NAC or GSH abrogated curcumin mediated decrease in the levels of non-protein thiols at early time

point (2 h) (Fig. 3.5C). However, at a later time point (18 h), NAC potentiated the curcumin mediated increase in non-protein thiol levels while GSH decreased it (Fig. 3.5D). Thus NAC and GSH had an opposing effect on curcumin-mediated changes in levels of non-protein thiols at 18 h. The group treated with GSH alone did not bring down basal ROS levels.

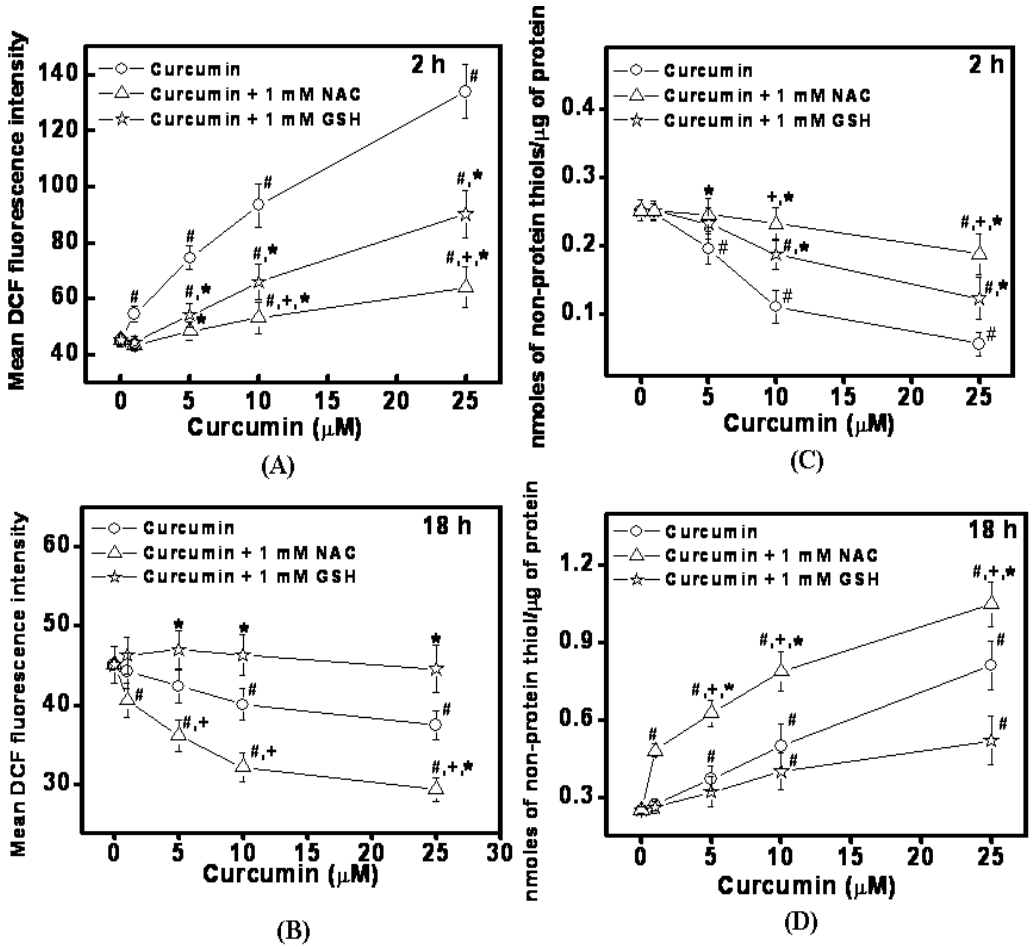

Figure 3.5 *Effect of curcumin (1 –25 μM) on ROS levels and non-protein thiols content at two different timepoints 2 h (A & C) and 18 h (B & D) after its addition and modulation by NAC (1 mM) or GSH (1 mM).* $^{\#}$ *P<0.05 as compared to ROS or non-protein thiols levels of control cells.*P<0.05 as compared to ROS or non-protein thiols levels of cells treated with curcumin at a particular concentration.* $^{+}$*P<0.05 as compared to ROS or non-protein thiols levels of cells treated with curcumin at a particular concentration in presence of GSH.*

However, non-protein thiol content increased marginally from basal levels of 0.251 ± 0.015 nmoles/μg of protein to 0.264 ± 0.018 nmoles/μg of protein at 18 h. Interestingly, addition of NAC alone reduced basal levels of ROS by 11% at 2 h and by 25% at 18 h, while non-protein thiols content increased to 0.371 ± 0.049 nmoles/μg of protein at 2 h and 0.568 ± 0.085 nmoles/μg of protein at 18 h compared to basal levels.

3.2.2.2 Effects of curcumin on the expression of antioxidant genes

Experiments were carried out to monitor the effects of low (5 μM) and high (25 μM) concentrations of curcumin on cellular antioxidant mechanisms. Antioxidant enzymes such as Mn-SOD, Cu,Zn-SOD, catalase, GPx and HO-1 play an important role in maintaining the redox homeostasis within the cells.[23] Therefore expression of these enzymes at mRNA level was monitored in the cells at 6 and 18 h after curcumin addition. Curcumin upregulated the mRNA levels of *GPx*, *catalase* and *Cu,Zn-SOD* genes over the control in a concentration and time dependent manner with peak levels observed at 18 h after addition (Fig. 3.6A, 3.6B, 3.7A and 3.7B). The relative increase in the expression of *GPx* gene upon treatment with 5 & 25 μM curcumin was significantly higher as compared to increase in the expression of *catalase* and *Cu,Zn-SOD* genes. Although *HO-1* gene also showed an increase in the levels of mRNA with increase in concentration of curcumin from 5 to 25 μM, the peak level was observed at 6 h instead of 18 h. In contrast, the *Mn-SOD* gene showed time dependent decrease upon treatment with 5 and 25 μM curcumin (Fig. 3.6A, 3.6B, 3.7A and 3.7B). Pretreatment of cells with 1 mM GSH or NAC for 2 h modulated the curcumin's effect on gene expression. Pretreatment with GSH reduced the magnitude of induction in the expression of *GPx*, *catalase*, *Cu,Zn-SOD* and *HO-1* genes at both the time points (Fig. 3.6A, 3.6B, 3.7A and 3.7B).

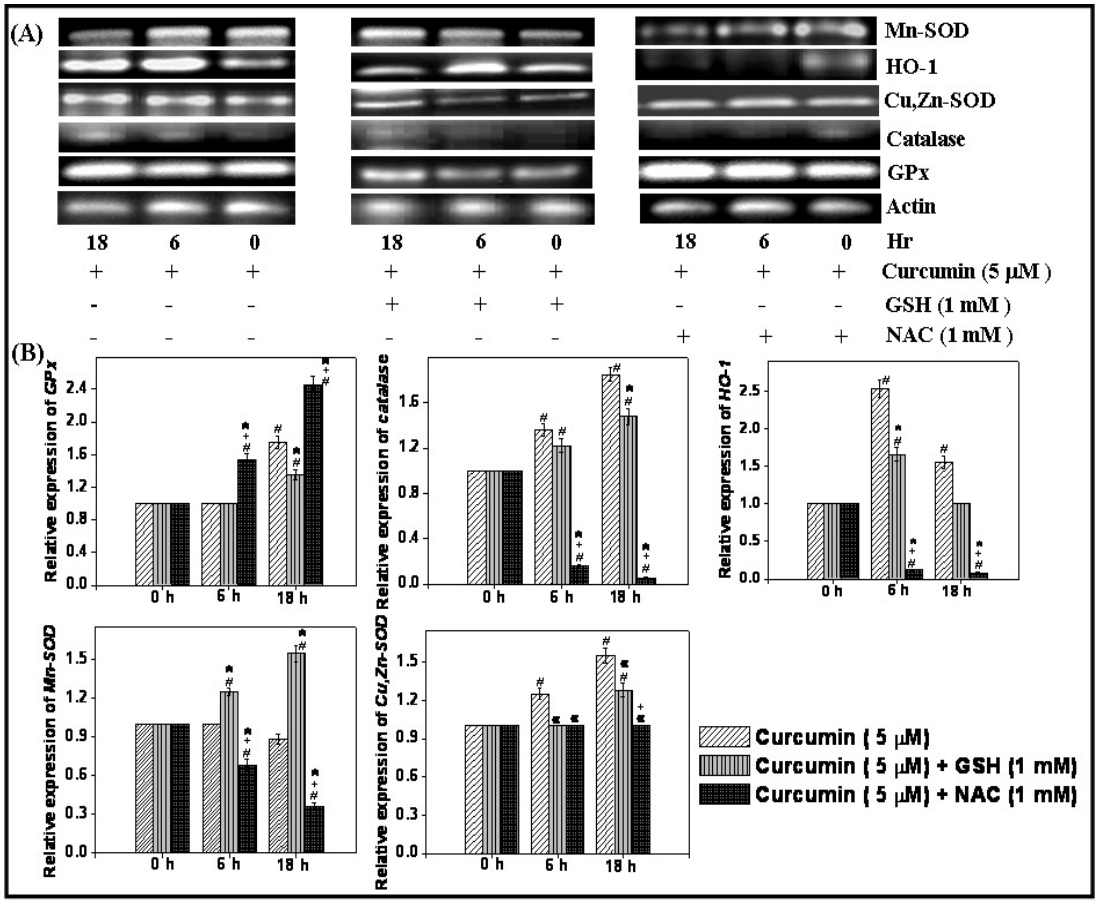

Figure 3.6 *Effect of 5 μM curcumin on the mRNA expression of antioxidant genes (GPx, catalase, HO-1, Cu,Zn-SOD and Mn-SOD) at 6 and 18 h after its addition and modulation by NAC (1 mM) or GSH (1 mM). (A) RT-PCR analysis (B) Bar graph showing time dependant variation in the relative expression of the genes.* $^{\#}$ *P<0.05 as compared control cells. *P<0.05 as compared to cells treated with curcumin at a particular timepoint.* $^{+}$*P<0.05 as compared to cells treated with curcumin and GSH at any time point.*

Interestingly, GSH also restored the suppression of *Mn-SOD* gene expression after treatment with curcumin (5 & 25 μM). On the other hand cells pretreated with NAC showed an increase in the expression of *GPx* gene and decrease in the expression of *catalase, Cu,Zn-SOD, HO-1* and *Mn-SOD* genes at 6 and 18 h as compared to curcumin treatment alone (Fig. 3.6A, 3.6B, 3.7A and 3.7B). These results indicated a differential effect of GSH and NAC on curcumin induced gene expression in RAW cells.

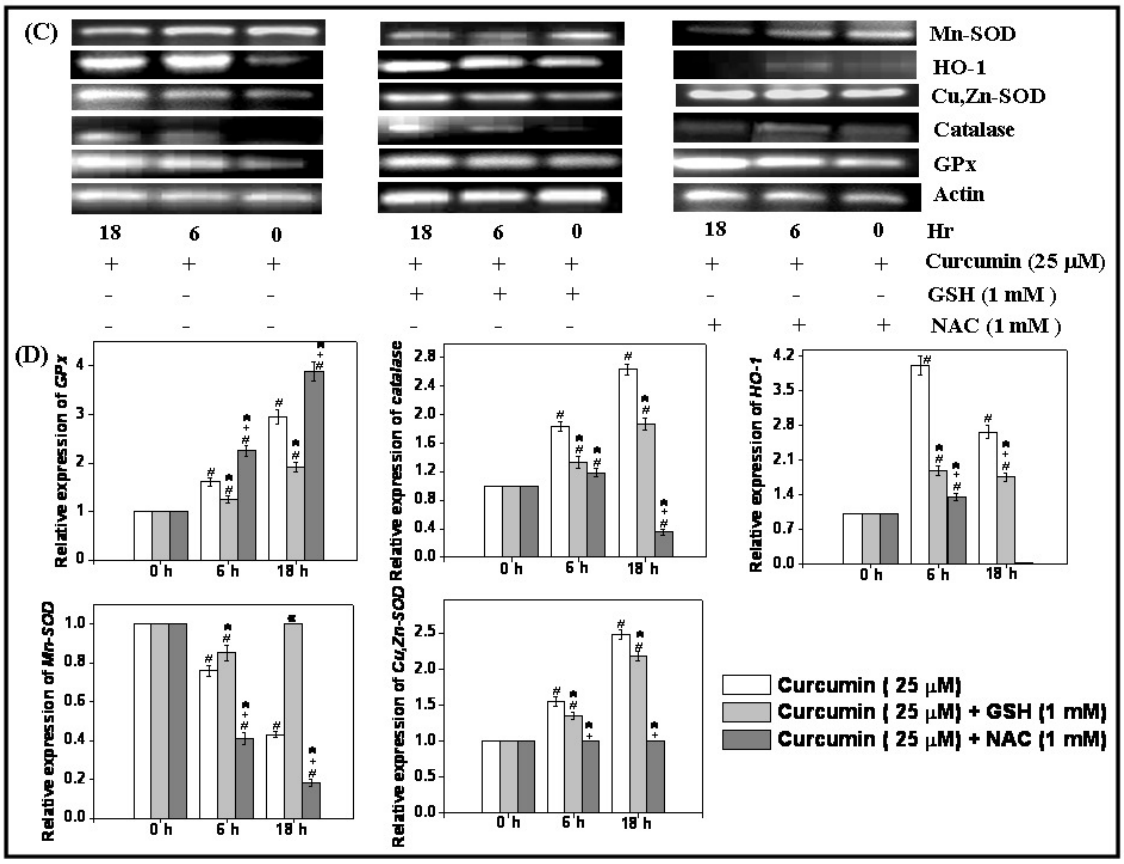

Figure 3.7 *Effect of 25 μM curcumin on the mRNA expression of antioxidant genes (GPx, catalase, HO-1, Cu,Zn-SOD and Mn-SOD) at 6 and 18 h after its addition and modulation by NAC (1 mM) or GSH (1 mM). (A) RT-PCR analysis (B) Bar graph showing time dependant variation in the relative expression of the genes.* $^{\#}$ *P<0.05 as compared to mRNA expression levels of control cells. *P<0.05 as compared to mRNA expression levels of cells treated with curcumin at a particular time point.* $^{+}$*P<0.05 as compared to mRNA expression levels of cells treated with curcumin at any time point in presence of GSH.*

The group treated with GSH alone did not show changes in the expression of all the five antioxidant genes at 6 and 18 h compared to control levels (Fig. 3.8). However, the group treated with NAC showed significant upregulation of *GPx* at 18 h, repression of *Mn-SOD* and *HO-1* at both time points. However, the expression of *catalase* and *Cu,Zn-SOD* was comparable to that of control (Fig. 3.8).

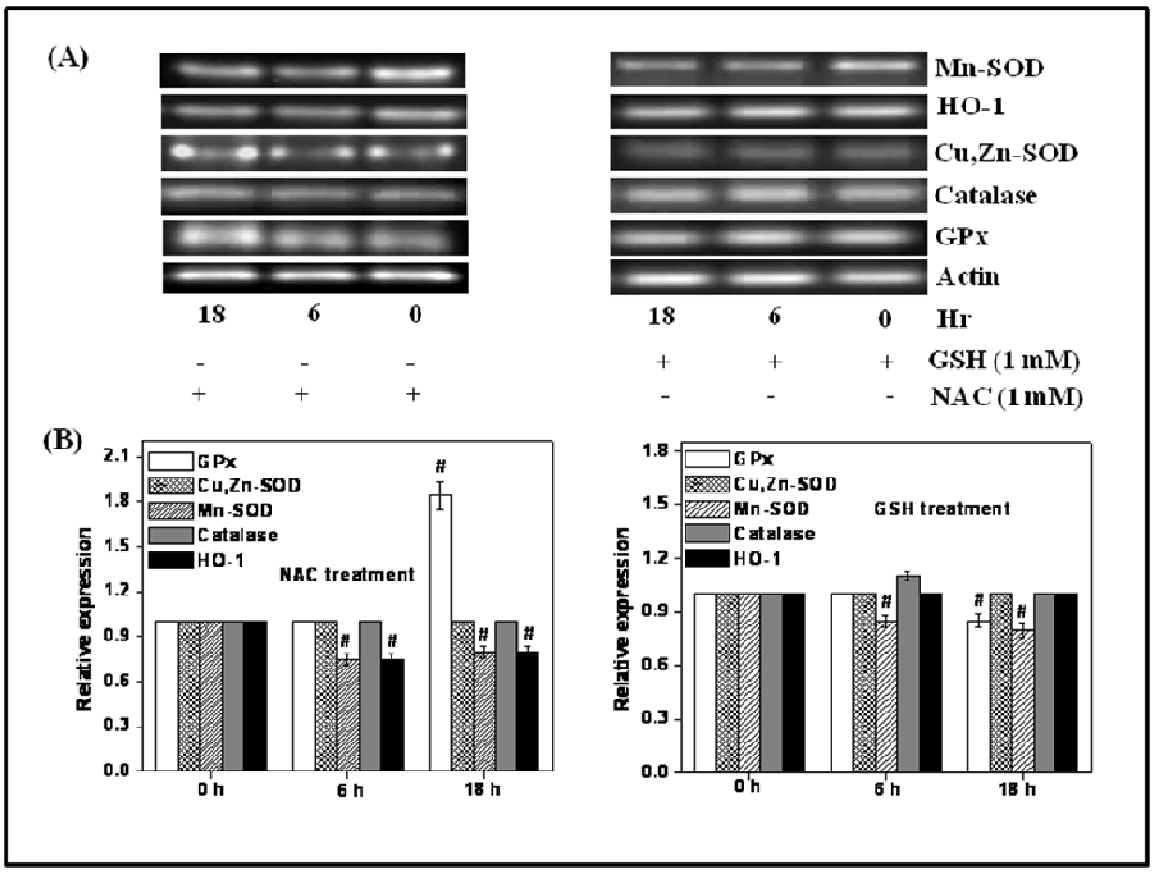

Figure 3.8 *(A) Effect of 1 mM NAC or GSH on the mRNA expression of antioxidant genes (GPx, catalase, HO-1, Cu,Zn-SOD and Mn-SOD mRNA) (B) Bar graph showing time dependant variation in the relative expression of above genes after treatment with 1 mM NAC or GSH.* $^{\#}$ *P<0.05 as compared to mRNA expression levels of control cells.*

3.2.2.3 Effect of curcumin on cell viability

To investigate, how changes in the redox environment induced by curcumin affect the cell viability, cells were incubated with curcumin (5 and 25 μM) for 24 h and the % cell viability under different treatment conditions was determined by trypan blue dye exclusion test and has been shown as bar graph in figure 3.9A. The figure clearly reveals that treatment at 5 μM curcumin resulted in marginal decrease in cell viability while that at 25 μM showed significant reduction. Addition of GSH or NAC resulted in the

complete recovery of viability in cells treated with 5 μM of curcumin. However, at 25 μM of curcumin, NAC offered better protection than GSH. Treatment with NAC or GSH alone did not induce loss of cell viability. Further mRNA expression levels of antiapoptotic genes such as *Bcl-2* and *Bcl-XL* were measured at 18 h after curcumin addition**.** The results showed that significant decrease in the mRNA expression levels of *Bcl-2* and *Bcl-XL* genes was seen only at 25 μM curcumin (Fig. 3.9B and 3.9C).

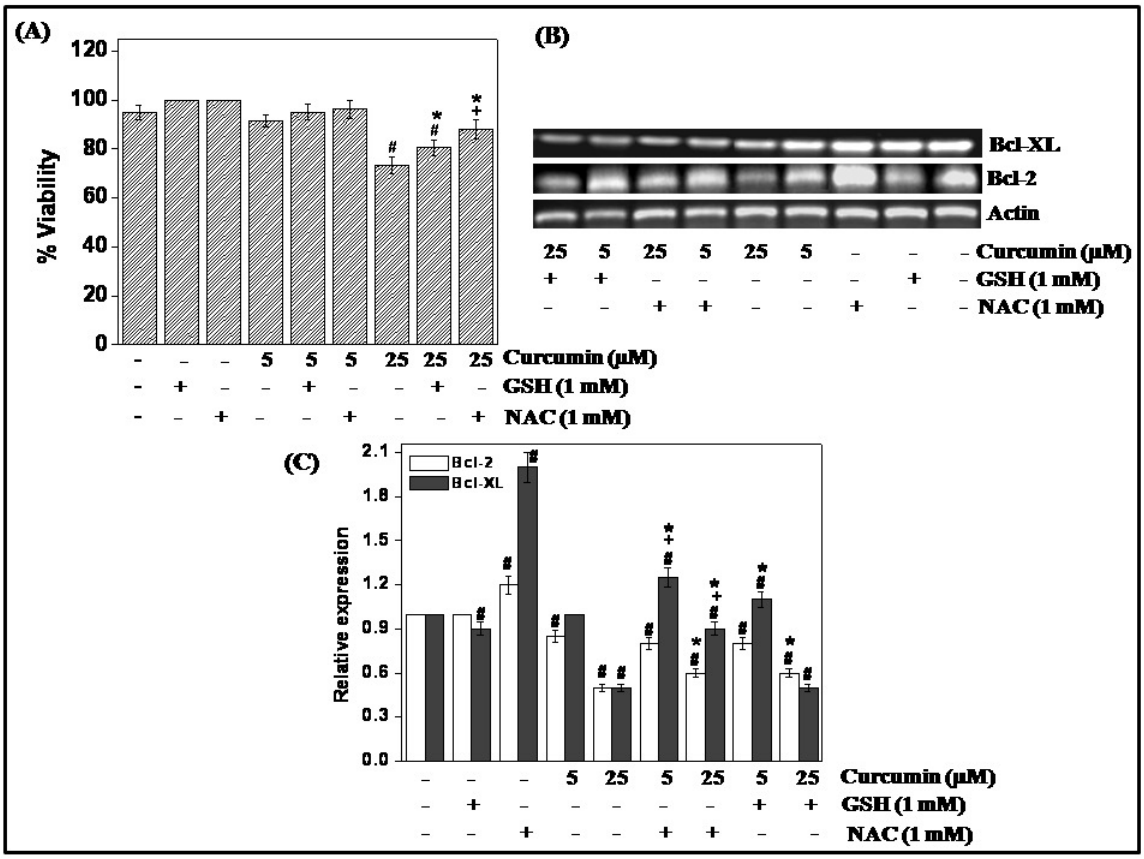

Figure 3.9 *Effect of curcumin (5 or 25 μM) in combination with NAC (1 mM) or GSH (1 mM) on cell viability. (A) Bar graph showing variation in the cell viability. (B) RT-PCR analysis showing comparative expression of antiapoptotic genes Bcl-2 and Bcl-XL in cells. (D) Analysis of the relative expression of above genes under different treatment conditions.* $^{\#}$ *P<0.05 as compared to control cells. *P<0.05 as compared to cells treated with curcumin.* $^{+}$*P<0.05 as compared to cells treated with curcumin in presence of GSH.*

However, treatment with 1 mM NAC or GSH prior to curcumin (5 and 25 μM) addition abrogated curcumin mediated decrease in expression of antiapoptotic genes and NAC was better than GSH in its action (Fig. 3.9B and 3.9C). The group treated with GSH alone did not change the mRNA expression levels of *Bcl-2* and *Bcl-XL*, while NAC showed significant upregulation of these genes (Fig. 3.9B and 3.9C).

3.2.2.4 Effect of GSH or NAC on cellular uptake of curcumin

In order to understand the mechanism responsible for differential effects of NAC or GSH on curcumin induced redox changes, uptake of curcumin in cells in presence of GSH or NAC was estimated. The cells were incubated with 20 μM of curcumin in presence or absence of 1 mM GSH or NAC for 4 h.

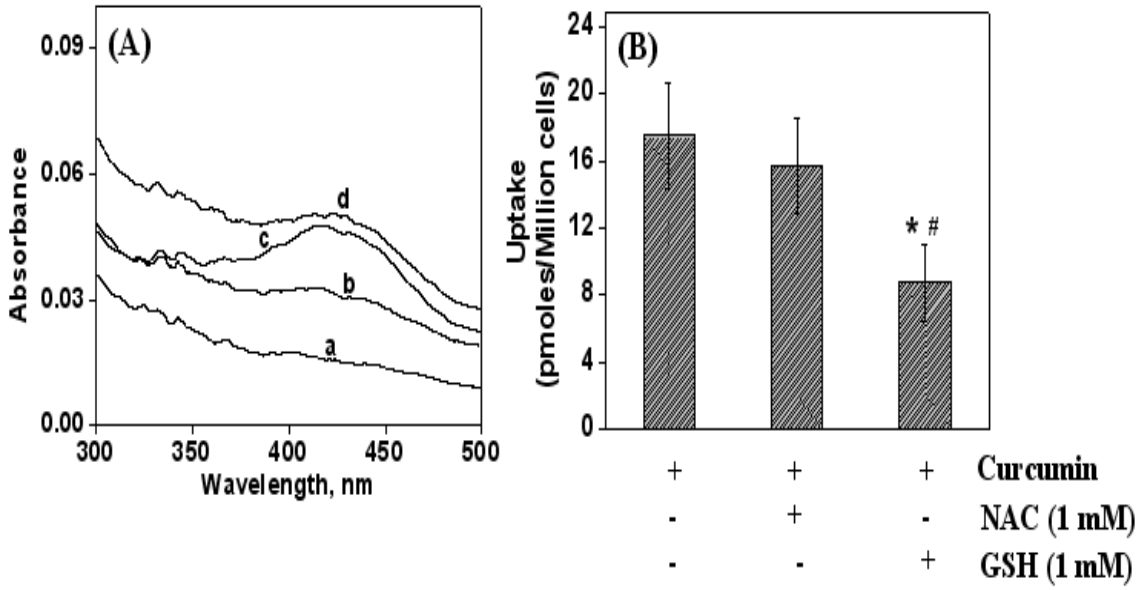

Figure 3.10 *Effect of NAC (1 mM) or GSH (1 mM) on cellular uptake of curcumin: (A) Absorption spectra of methanolic curcumin from cells (a) control cells (b) cells treated with 20 μM curcumin and GSH (c) cells treated with 20 μM curcumin and NAC (d) cells treated with 20 μM curcumin only. (B) Bar graph showing relative cellular uptake under various treatment conditions as mentioned above in pmoles/million cells after normalization to 1 nmol of curcumin added/million cells/ml. *P<0.05 as compared to curcumin treated group. # P<0.05 as compared to curcumin and NAC treated group.*

The concentration of curcumin entered in to the cell was calculated by following absorption spectrum of curcumin extracted in to methanol from cell lysate and using the molar absorption coefficient at 428 nm as 48000 $M^{-1}cm^{-1}$. The detailed methodology for the estimation of intracellular curcumin will be discussed in section III. Figure 3.10A shows the absorption spectrum of intracellular curcumin and figure 3.10B shows relative uptakes in pmoles/million cells under different treatment conditions. The basal level of cellular uptake of curcumin was about 17.5 ± 3.1 pmoles/million cells. In the presence of NAC, the uptake marginally decreased to 14.7 ± 2.8 pmoles/million cells. However, in the presence of GSH, it significantly reduced to 8.75 ± 2.3 pmoles/million cells. These results suggest that pretreatment with GSH inhibited the cellular uptake of curcumin, while NAC was less effective.

3.2.2.5 Concentration dependent response of curcumin to γ-irradiation

To investigate the concentration dependant differential antioxidant and pro-oxidant activity, against γ-radiation induced oxidative stress, the cells after treatment with curcumin (5 and 25 μM) for 30 min were exposed to γ-radiation to an absorbed dose of 2 Gy using a ^{60}Co γ-source at a dose rate of 4 Gy min^{-1} [69]. After irradiation, ROS levels, expression of anti-apoptotic markers such as *Bcl-2* and *Bcl-XL* and cell viability were examined at 2, 18 and 24 h respectively. Figure 3.11A shows the intracellular ROS levels under different treatment conditions. Exposure of cells to γ-radiation elevated ROS levels, which was marginally lowered in presence of 5 μM curcumin, while at 25 μM curcumin, the ROS levels significantly increased. However, when cells were treated with curcumin (5 and 25 μM) in combination with 1 mM GSH or NAC, the radiation induced ROS levels decreased significantly. NAC was again more effective than GSH. Further,

the mRNA levels of *Bcl-2* and *Bcl-XL* and cell viability, assessed under the same conditions showed that γ-radiation suppressed the expression of antiapoptotic genes and reduced the cell viability (Fig. 3.11B, 3.11C and 3.11D). Curcumin at 5 μM partially inhibited the radiation-mediated repression of *Bcl-2* and *Bcl-XL* genes while 25 μM of curcumin further suppressed radiation induced abrogation of these genes (Fig. 3.11B and 3.11C).

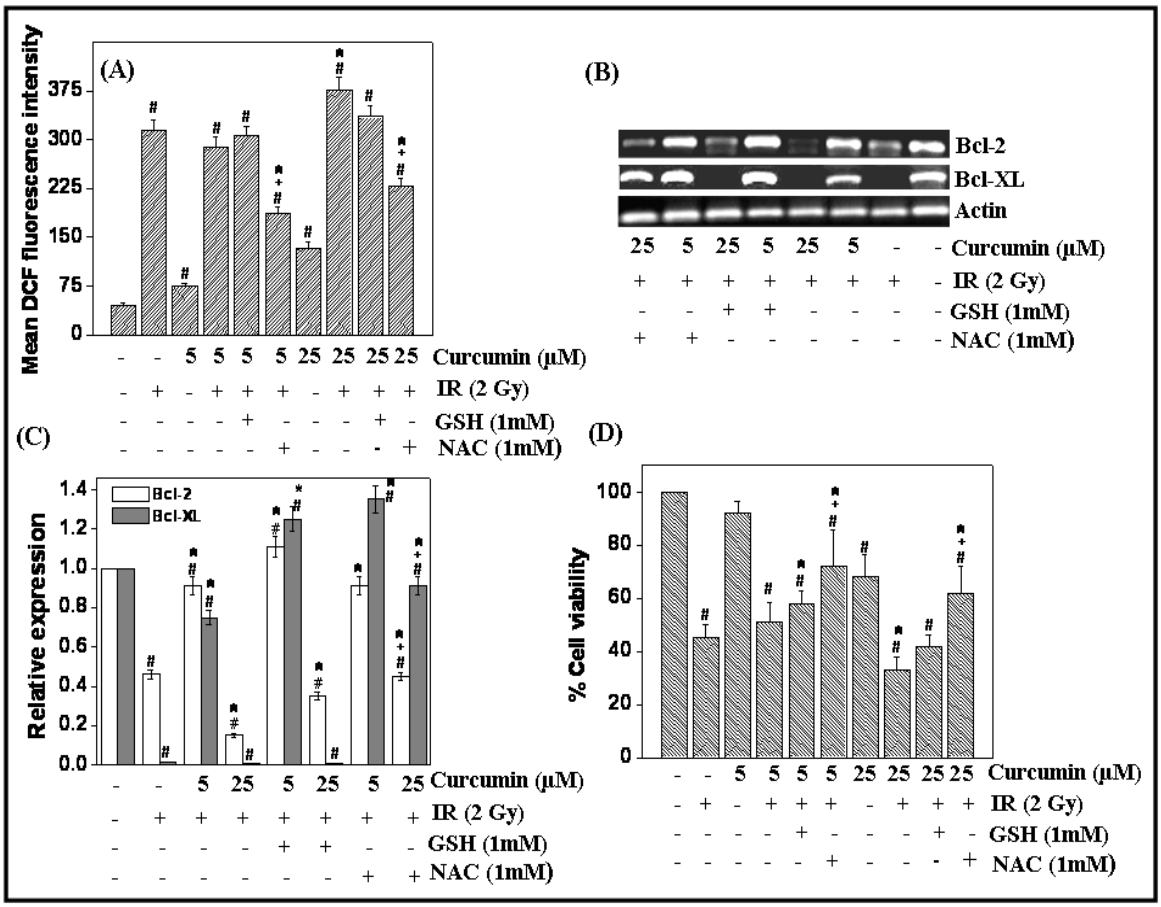

Figure 3.11 *Effect of curcumin pretreatment at 5 or 25 μM concentration in combination with NAC (1 mM) or GSH (1 mM) on γ-radiation (absorbed dose, 2Gy) induced oxidative stress in cells. (A) ROS levels. (B) RT-PCR analysis showing comparative expression of antiapoptotic genes Bcl-2 and Bcl-XL. (C) Analysis of the relative expression of the above genes under different treatment conditions. (D) Bar graph showing variation in the cell viability.* $^{\#}$ *P<0.05 as compared to control cells. *P<0.05 as compared cells treated with curcumin.* $^{+}$*P<0.05 as compared to cells treated with curcumin in presence of GSH.*

Similar changes in cell viability were observed when cells treated with curcumin (5 and 25 μM) were exposed to radiation (Fig. 3.11D). Treatment with either NAC or GSH prior to curcumin addition and exposure to γ-radiation partially, inhibited the radiation–mediated decrease in expression of antiapoptotic genes and loss of viability in cells and between the two NAC was better than GSH.

3.3 Discussion

Curcumin a yellow pigment from *curcuma longa* is a potent antioxidant and exhibits multiple pharmacological activities and is now being considered for therapeutic application for the treatment of various cancers and inflammatory diseases.[105,106] However, recent publications on pro-oxidant activity of curcumin in transformed cells as well as cell free system suggest a need for the careful examination of its antioxidant and pro-oxidative activity in vital cells of body before considering it for therapeutic application.[105,112] Additionally, there is need to enhance the antioxidant effect of curcumin in normal cells and one of the strategies for this is to apply it in combination with reducing agents or water soluble antioxidants like thiols.[217] Considering the importance of RBCs and macrophages in the functioning of human body, present investigation was carried in these two cellular systems.[211]

The effect of curcumin on membrane lipid peroxidation, loss of hemoglobin and release of intracellular K^+ ions have been estimated in human RBCs treated with AAPH to explore its antioxidant/pro-oxidant activity.[179] The results obtained from these studies indicate that curcumin by itself did not cause either lipid peroxidation or hemolysis to RBCs, and showed significant protection from AAPH induced lipid peroxidation and hemolysis. Like in lipid peroxidation and hemolysis assays, curcumin did not show

progressive inhibition of K^+ ion loss and GSH depletion under AAPH treated condition thus making us unable to estimate their IC_{50} values. Curcumin treated samples showed lower percent of K^+ ion loss as compared to AAPH treated samples. However in each case, the percent K^+ ion loss increased with increasing concentrations of curcumin. Therefore to know whether curcumin itself has any effect on K^+ ion loss, we looked at the loss of K^+ ion in only curcumin treated samples. The results clearly suggest that curcumin at concentration as low as 5 μM drastically increased the loss of K^+ ions (47%) from RBCs. With the increasing curcumin concentration the percent of K^+ ion loss remained almost the same suggesting the saturation effect of curcumin on K^+ ion loss. The ability of curcumin to induce the K^+ ion loss may be because of its effect on Na^+/K^+ ion channels present on RBC membranes. This indicates that curcumin may not be acting as a simple antioxidant but probably has a pro-oxidant effect.

GSH is the most abundant of the thiols present in mammalian cells.[218] It performs a number of vital cell functions including maintaining the essential thiol status of proteins by preventing oxidation of sulfahydryl groups or by reducing disulphide bonds induced by oxidative stress, or by scavenging free radicals. During oxidative stress, the cellular pool of GSH is depleted. Exogenously applied antioxidants protect GSH levels in cells by preventing them from being consumed in reaction with free radicals.[219] Our results indicate that the GSH levels come down significantly in RBCs after AAPH incubation, but treatment with curcumin in the concentration range from 5 to 10 μM significantly prevented the decrease in GSH level. However, further increase in concentration of curcumin showed decrease in GSH level in a concentration dependant manner. Like in case of K^+ ion loss, curcumin treatment alone in a concentration range up to 10 μM level

did not show much effect on GSH level however further increase in curcumin concentration resulted in significant decrease of GSH levels, probably due to the reaction of curcumin with GSH.[220] Some reports suggest that curcumin reacts with free radicals and generates less reactive phenoxyl radicals which are repaired by the cellular GSH pool.[60] Therefore, the observed decrease in GSH level in curcumin (>10 μM) pretreated samples after exposure to AAPH could also be due to the excess accumulation of phenoxyl radicals produced from the reaction between curcumin and AAPH. Hence this observation indicates pro-oxidant behavior of curcumin at higher concentrations.

To find out more about the possible mechanisms responsible for the overall protective effect of curcumin against AAPH induced oxidative damage to RBCs, reactions of curcumin with AAPH peroxyl radicals was studied. The results revealed that curcumin reacts with the peroxyl radicals generated from AAPH with a bimolecular rate constant of 63.4 ± 12.7 $M^{-1}s^{-1}$. Earlier using pulse radiolysis technique, it has been reported that curcumin reacts with trichloromethyl peroxyl radical and lineolic peroxyl radical with rate constant of 5 x 10^8 $M^{-1}s^{-1}$ and 5.3 x 10^5 $M^{-1}s^{-1}$ respectively.[128] The low rate constant (1.3 x 10^{-6} s^{-1}) with AAPH may be due to slow release of peroxyl radicals from AAPH decomposition, which is rate determining step.[178] Thus scavenging of peroxyl radicals generated from AAPH by intracellular curcumin may be contributing to the overall protection as shown in scheme 3.1.

The studies in RBCs indicated that curcumin exhibits antioxidant effects at lower concentrations (≤10 μM) and pro-oxidant activity at higher concentrations (> 10 μM). This prompted us to study the effect of curcumin on cellular redox environment in RAW 264.7 cells in the concentration range from 0 to 25 μM.

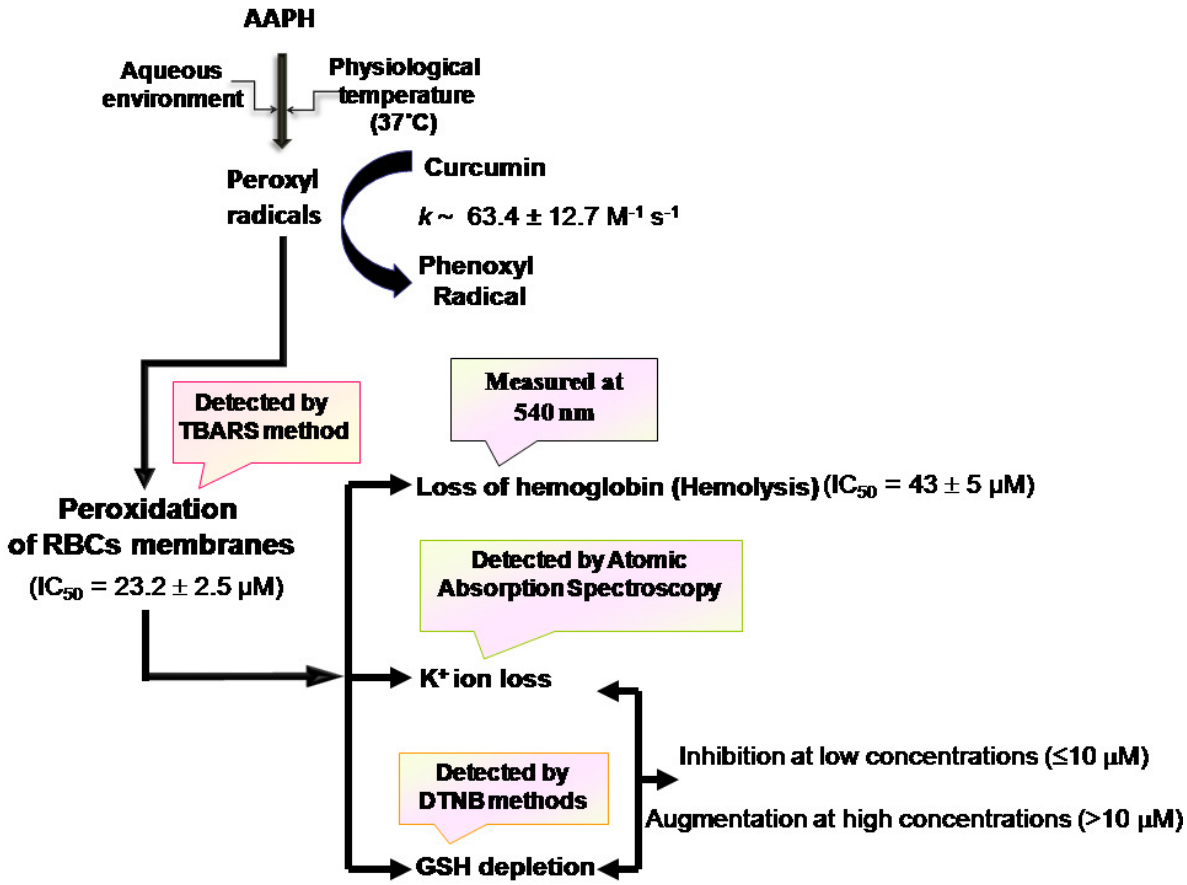

Scheme 3.1: *Schematic representation of the AAPH induced oxidative hemolysis in RBCs and its inhibition by curcumin*

We also made an attempt to investigate the influence of exogenous GSH at concentration similar to intracellular levels on the redox modulating ability of curcumin. For this, the cells were treated with 1 mM concentration of GSH prior to curcumin addition. Since NAC is permeable to cell and exerts antioxidant effects by increasing intracellular GSH contents, the effect of NAC on curcumin induced modifications was also investigated at equimolar concentration.[221]

Treatment of cells with curcumin (1 – 25 µM) elevated the DCF fluorescence (ROS levels) at 2 h in a concentration dependent manner, similar to the earlier observations.[210] This increase in ROS levels at 2 h was also accompanied by decrease in

the levels of intracellular non-protein thiols indicating that curcumin provoked oxidative stress early after its addition. Interestingly, we observed that ROS levels decreased below basal levels at 18 h after curcumin addition suggesting that the pro-oxidant activity of curcumin was only transient. The mechanism by which curcumin induces ROS is not clear. However, it has been proposed that curcumin binds to thioredoxin reductase, thereby converting its activity to NADPH oxidase, which leads to the production of ROS.[209] The most important intracellular antioxidant GSH constitutes major non-protein thiols in cells.[218,222] The decreased levels of non-protein thiols at early time point (2 h) after curcumin addition may be due to oxidation of GSH to GSSG by ROS or due to formation of Michael adduct between GSH and curcumin. However when low concentration of curcumin is available within cells due to poor cellular uptake, reactions of curcumin with GSH are not likely to play a prominent role in lowering non-protein thiols content. The incubation of cells with curcumin for 18 h led to significant increase in levels of non-protein thiols in a concentration dependent manner. This observation also ruled out the possibility of formation of Michael adduct of curcumin with GSH in cells. One of the reasons responsible for these observations appears to be the oxidative stress mediated depletion of GSH leading to induction of its intracellular synthesis.[222] Additionally, curcumin is also reported to increase the biosynthesis of GSH by stimulating the γ-glutamate–cysteine ligase activity.[124,133,223]

Our investigations on the expression of antioxidant enzymes at 6 and 18 h after treatment with 5 or 25 μM curcumin, showed induction of *GPx*, *catalase*, *HO-1* and *Cu,Zn–SOD* genes with increasing time and concentration. Although the exact mechanism(s) by which curcumin activates the expression of these genes is not clearly

understood, the observed increase in expression of some of the antioxidant genes like *GPx* and *HO-1* after curcumin addition to cells may be attributed to activation of transcription factor Nrf-2.[136] These time course studies reveal that antioxidant effects precede pro-oxidant effects of curcumin. These studies also indicate that the reduced ROS levels at 18 h after curcumin addition to cells may be due to elevated *GPx*, *Cu,Zn–SOD* expressions and non-protein thiols levels in the present study. A striking observation of the present study is that curcumin reduced the *Mn-SOD* gene expression. The transcription factor NF-κB regulates the expression of *Mn-SOD* gene.[224] and curcumin is a known suppressor of basal and induced NF-κB level.[225] Therefore the observed decrease in the *Mn-SOD* expression upon curcumin treatment can directly be attributed to inhibition of NF-κB.

The assessment of cell viability at 24 h revealed that curcumin did not induce loss of viability at 5 μM, however lower but significant loss of viability was observed at 25 μM. These results indicate that despite increased expression of antioxidant genes at 25 μM of curcumin, the cells did not survive. The loss of cell viability after treatment of 25 μM curcumin was also evident in terms of the decrease in the expression of antiapototic genes such as *Bcl-2* and *Bcl-XL*, which are required for cell survival.[208] This observed loss of viability may be due to irreversible damage caused by increased production of ROS at early time point (2 h), decreased *Mn-SOD* expression and induction of apoptosis. Earlier reports on apoptosis induction support this argument that increased ROS levels leads to cell death and Mn-SOD is essential to protect the cells from mitochondrial oxidative stress.[226]

Further the effects of exogenously added reducing agents on curcumin-mediated cellular modifications were studied by pre-treating the cells with GSH or NAC. GSH inhibited curcumin induced oxidative stress and antioxidant effects at 2 and 18 h respectively. However, NAC inhibited the pro-oxidant effects of curcumin at early time point (2 h) and augmented the non-protein thiol levels at 18 h. NAC is a cell permeable reducing agent and acts as a precursor for the synthesis of intracellular GSH.[221] This may be the reason for the additive effect of NAC on curcumin-mediated increase in non-protein thiols levels at 18 h. GSH also lowered the curcumin induced expressions of *GPx*, *Cu,Zn-SOD* and *HO-1* genes and increased the expression of *Mn-SOD* gene. While, NAC increased the curcumin induced expression of *GPx* and reduced the expression of all the other genes examined. The enhanced expression of *GPx* in the presence of NAC may be due to increased intracellular synthesis of GSH.[219] Pretreatment with equimolar (1mM) concentration of GSH or NAC inhibited curcumin induced cell death, however NAC was more effective than GSH. This differential action could be due to their ability to inhibit cellular uptake of curcumin as GSH is impermeable to cells.[28] Our experiments indeed showed that GSH significantly inhibited the cellular uptake of curcumin. Under similar condition, pretreatment with NAC did not affect curcumin uptake by the cells. The mechanism(s) by which exogenously added GSH prevents the cellular uptake of curcumin is not known. Probably, Michael addition in the cell culture medium, as discussed before may be responsible for this observation.[220,227]

Studies on the effects of curcumin in combinations with GSH or NAC against γ-radiation induced oxidative stress in RAW cells showed interesting results. At 5 μM, curcumin decreased radiation induced ROS production at 2 h and inhibited the loss of cell

viability at 24 h only marginally. However, at 25 μM, curcumin significantly enhanced both radiation induced ROS production and loss of cell viability. The protective effects at 5 μM were in correlation with the restoration of γ-irradiation induced decrease in *Bcl-2* & *Bcl-XL* expressions, while at 25 μM it completely abolished their expression. As expected, both GSH and NAC enhanced the radioprotective action of curcumin at 5 μM and inhibited the sensitizing activity at 25 μM. These studies thus suggest that curcumin induces concentration and time dependent differential changes in oxidative stress and antioxidant gene expression levels leading to inhibition or promotion of cell death in RAW 264.7 cells.

3.4 Conclusions

Based on the studies performed in two different cellular systems, namely RBCs and macrophages, it has been concluded that curcumin exhibits both antioxidant and pro-oxidant activity and at higher concentration, it is the latter one, which predominates over the former. In RBCs the antioxidant activity was evidenced by the protection against AAPH induced oxidative damage and pro-oxidant activity by the induction of intracellular K^+ ion leakage and GSH depletion. Similarly in macrophage cells, even though curcumin increased the expression of antioxidant genes with increasing concentration, it induced ROS generation, contributing to the cytotoxicity at higher concentration. In this respect, it is worth mentioning that most of the *in vivo* studies dealing with curcumin as an anti-tumor agent discuss about its poor bioavailabilty as low blood levels are achieved after excessive oral administration. Our results thus compliment these studies and suggest that low blood levels of curcumin will have antioxidant activity on RBCs and macrophages, which is desired along with its anti-tumor activity.

Additionally, the exogenous treatment with cell permeable thiol (NAC) inhibited the curcumin induced expression of most of the antioxidant genes; however the cell impermeable thiol (GSH) lowered the magnitude of induction of the genes indicating differential modulation by thiols to curcumin action in cells. These effects are attributed to differential cellular uptake of curcumin in presence of thiols suggesting that thiols can be employed to modulate desired therapeutic applications of curcumin.

Apart from the additive approach as studied in the present section, it is also possible to improve the antioxidant activity of curcumin by exploiting its structural changes. In this respect development of curcumin – transition metal complex as SOD mimetic drugs is of current priority among researchers. In the next section we compared the antioxidant activity of curcumin with its copper complex synthesized in our laboratory in terms of their ability to prevent radiation induced oxidative stress in spleen lymphocytes.

Section II: Radioprotection studies of copper (II) chelates of curcumin in cells

3.5 Introduction

One of the mechanisms responsible for the antioxidant action of curcumin is the ability to chelate transition metal ions.[228] Such chelation not only reduced the toxicity induced by the free ions but also helped in the design of new superoxide dismutase (SOD) mimics.[55,229-231] SOD is an endogenous enzymatic antioxidant that converts superoxide radical to hydrogen peroxide which is then converted to water by catalase enzyme.[23] Although, a superoxide radical itself is not so reactive towards bio-molecules, it plays a very important role in disease development by helping in generation of more powerful hydroxyl radicals ($^{\bullet}OH$) through the Haber-Weiss reaction.[1] Therefore, native SOD had been used as a therapeutic agent to attenuate ROS induced diseases like hyperoxia, reperfusion injury, immune deficiency disease, ulceractive colitis and inflammation associated diseases.[232] The native enzyme however, has several limitations such as short shelf life, low lipid solubility, low penetration into cells, etc and in order to overcome these difficulties new SOD mimics are being developed.[233]

Most of the SOD mimics are designed with a redox active metal centre, like copper, manganese etc. similar to the active metal site of the native SOD.[55,234-239] The metal centre in the active site of native SOD enzyme undergoes stepwise reduction and oxidation by superoxide radical during catalytic cycle as shown in scheme 3.2. For example, in Cu,Zn-SOD enzyme, the superoxide radical reduces Cu (II) to Cu (I) and produces oxygen. The reduced Cu (I) is oxidized to Cu (II) by another molecule of superoxide radical thereby producing hydrogen peroxide and regenerating back the enzyme.[9]

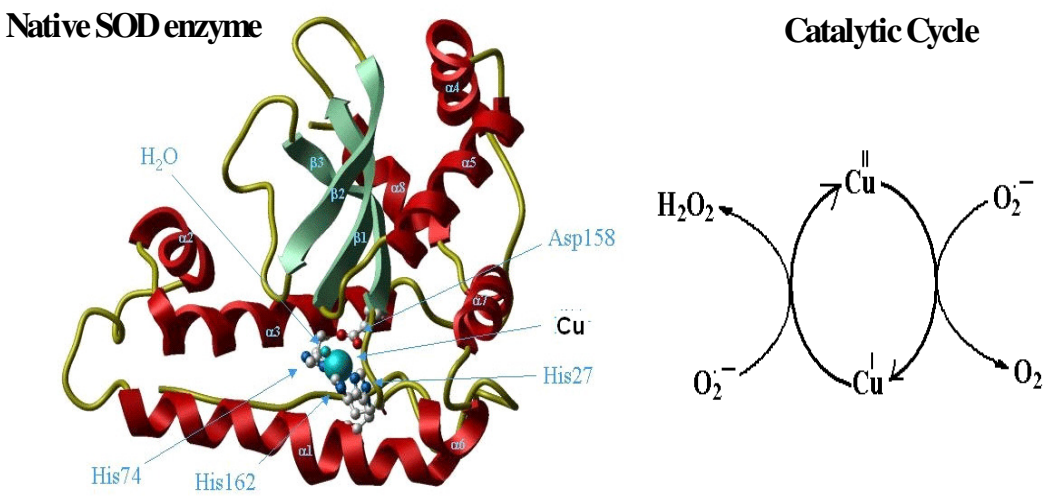

Scheme 3.2: *Structure of native SOD enzyme and its catalytic mechanism*

Aqua complex of transition metals have also been shown to exhibit the ability to efficiently catalyze superoxide dismutation, but such complexes induce Fenton type reaction in the biological system generating potentially damaging hydroxyl radicals.[1] Therefore, SOD mimics made by complexation of metals with functional ligands like antioxidants are preferred as they avoid the participation of free metal ions in Fenton chemistry as well as show additive antioxidant effects.[238]

One of the interests of our group has been to develop new transition metal-curcumin complexes as SOD mimics. Curcumin through the α, β-unsaturated β-diketone (heptadiene-dione) moiety, can form chelates of the type 1:1 and 1:2 with copper, iron, manganese and other transition metals (scheme 3.3). With this background, two different copper (II)-curcumin complexes with the stoichiometry of 1:1 and 1:2 were synthesized by the reaction of copper acetate and copper chloride with curcumin. The complexes were characterised by elemental analysis and different spectroscopic techniques. Details of the synthesis and characterisation of this complex have been reported by Barik et al

(2005 & 2007).[141,187] The chemical structure of 1:1 and 1:2 copper-curcumin complexes are given in scheme 3.3.

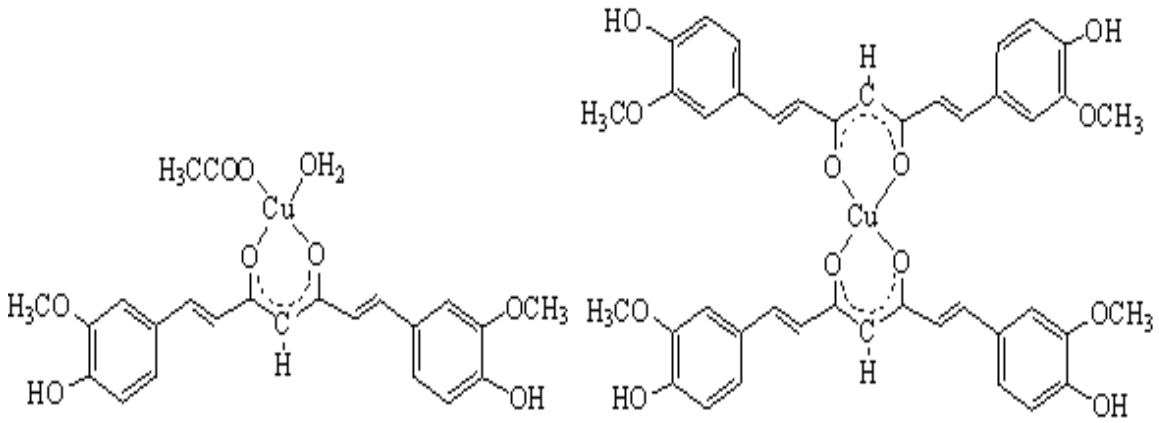

1:1 complex **1:2 complex**

Scheme 3.3: *Molecular structures of Cu(II)-curcumin complexes (1:1 and 1:2)*

EPR studies confirmed the structures of 1:1 and 1:2 complexes as distorted orthorhombic and symmetric square planar respectively. Both the complexes had high stability constant (log K_f = ~14) in DMSO medium. SOD activity of the complexes studied by xanthine and xanthine oxidase assay indicated that the 1:1 complex is nearly ten times more potent as SOD mimic than the 1:2 complex. Similarly the rate constant for the scavenging of superoxide radical of the 1:1 complex was found to be seven times higher than that of the 1:2 complex. Cyclic voltammetry measurement showed reversible redox potential of the Cu^{+2}/Cu^{+} couple for both the complexes as ~0.4 V vs. NHE, which is within the range responsible for superoxide dismutation reaction. The comparative physiochemical properties of 1:1 and 1:2 complexes are listed in table 3.2.[141,187] The complexes were also tested for their ability to inhibit radiation induced lipid peroxidation in liposomes, where the 1:1 complex was found to exhibit inhibition of lipid peroxidation to a greater extent

than the 1:2 complex.[141,187] From all these studies, it is evident that 1:1 complex is a better antioxidant, an efficient superoxide scavenger and also a more potent SOD mimic. Therefore 1:1 complex was further examined for antioxidant activity in cells and hereafter it will be referred as only complex.

Table 3.2: *Comparative properties of Cu(II)-curcumin complexes (1:1and 1:2)*

Physico-chemical properties	**1:1 Cu(II)-curcumin**	**1:2 Cu(II)-curcumin**
Absorption Maximum (DMSO)	426 nm ($\varepsilon = 97000 \pm 200$ $M^{-1}cm^{-1}$)	370 nm ($\varepsilon = 22125 \pm 100$ $M^{-1}cm^{-1}$)
Cu (II)/Cu (I) reduction potential	0.38 ± 0.03 V vs. NHE	0.42 ± 0.04 V vs. NHE
Formation constant (K_f) (M^{-1})	3.7×10^{14}	3.9×10^{15}
Superoxide radical rate constant	$7.1 \pm 0.1 \times 10^5$ $M^{-1}s^{-1}$	$1.04 \pm 0.17 \times 10^5$ $M^{-1}s^{-1}$
IC_{50} value of superoxide radical scavenging (Xantin / Xanthin oxidase assay)	6.7 μM	68.0 μM
Inhibition of Lipid peroxidation (In liposomes, 10 μM, Dose 210 Gy)	98%	15%

As discussed in chapter 1, the exposure of ionizing radiation induces production of ROS which initiate damage to bio-molecules leading to cell death. In past several compounds with antioxidant (ROS scavenging) activities have been explored as radioprotectant.[76] Accordingly, treatment of cells with exogenous antioxidants in form of SOD mimic prior to irradiation is expected to prevent the radiation induced oxidative stress and this will have implications in developing new radioprotector.[56]

Therefore, the aim of the present study is to investigate the modulation of γ-radiation induced oxidative stress by the complex in freshly isolated spleen lymphocytes

and to compare these results with those for curcumin. The spleen lymphocytes were freshly isolated from Swiss albino mice and the viability was assessed by trypan blue dye exclusion test using hemocytometer.[195] Curcumin and the complex are insoluble in water, but show fairly good solubility in alkaline water. Therefore, a stock solution of curcumin and the complex were prepared in nitrogen saturated aqueous solutions with 0.2 M NaOH. Nitrogen was used to prevent oxidation and the stability of the solutions during the experimental period was monitored by following the absorption spectra from time to time. Splenic lymphocytes suspended in serum free RPMI 1640 medium were seeded at 2.5 x 10^6 cells/ml to which stock solution of either curcumin or the complex was added to get final concentration of 10 μM. The pH of the culture medium after the addition of these agents was found to be 7.5. The lymphocytes were incubated with curcumin or the complex for 30 min followed by γ-irradiation using a ^{60}Co γ-source with a dose rate of 4 Gy min^{-1}. After irradiation, fetal bovine serum was added at a concentration of 5% v/v and incubation was done at 37°C in humified incubator with 5% CO_2 in air for different times (0-60 min) as desired in the study and then processed for different experiments. The oxidative stress parameters like lipid peroxidation, protein carbonylation and intracellular antioxidant levels were estimated at one hour (h) post irradiation to check the ability of the complex to prevent the initial radiochemical events through free radical scavenging mechanisms. In order to identify the molecular mechanisms, the kinetics of activation of protein kinase Cδ (PKCδ) and nuclear factor - kappa B (NF-κB) after irradiation in presence or absence of these compounds was also studied by western blotting.[191,192] The primary antibodies for western blotting included rabbit monoclonal anti-IκBα (1:1000), rabbit monoclonal anti-phospho (Ser40) PKCδ (1:1000) and rabbit

anti-NF-κB (p65) from Cell Signalling, U.S.A and sheep monoclonal anti-Mn-SOD (1:1000) (Calbiochem, U.S.A). Each experiment was performed at least in triplicate using a single splenic lymphocyte preparation. The entire experiment was repeated twice. Results are presented as means ± SEM, n = 6. Data were analyzed with student's "t" test and P values ≤ 0.05 were considered as a significant. The control in each experiment represents splenic lymphocytes treated with culture medium containing 0.2 M NaOH.

3.6 Results

3.6.1 Effect of curcumin and the complex on antioxidant enzymes status

The activities of the different antioxidant enzymes (SOD, GPx and catalase) in lymphocytes estimated at 1h after treatment with either curcumin or the complex under irradiated and unirradiated conditions are shown in figure 3.12. Treatment with the complex or curcumin alone resulted in significant (P<0.05) increase in GPx and catalase activities however, SOD activity was reduced after treatment with curcumin or the complex.

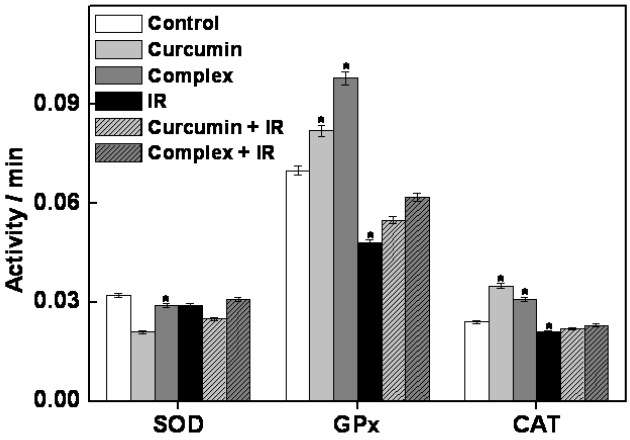

Figure 3.12 *Effect of curcumin and the complex on antioxidant enzymes activities of γ-irradiated and unirradiated splenic lymphocytes. *P<0.05 as compared to control. IR – Irradiation (2 Gy)*

The GPx and catalase activities were increased by 17% and 46% respectively in curcumin treated cells however, by 40% and 29% respectively in the complex treated cells. The decrease in SOD activity was observed to be a lesser extent in the complex treated cells compared to curcumin treated cells. The results also indicated that irradiation alone led to a significant ($P<0.05$) decrease in activities of all the antioxidant enzymes, which was reversed by pretreatment with curcumin or the complex. The complex was more effective in this respect.

3.6.2 Effect of curcumin and the complex on protein oxidation and lipid peroxidation

The relative TBARS formation, indicative of lipid peroxidation at 1 h post irradiation (2 to 8 Gy) in curcumin or the complex pretreated and untreated lymphocytes is shown in figure 3.13. Lipid peroxidation in cells increased with increase in absorbed dose of radiation. Pretreatment with either curcumin or the complex led to reduction in the extent of lipid peroxidation at all the doses. The complex was found to be more effective in reducing the formation of TBARS at all doses compared to curcumin. The percentage inhibition of lipid peroxidation by the complex at different dose of 2, 4, 6 and 8 Gy was 75%, 70%, 28% and 20% respectively, while that for curcumin under similar conditions was 50%, 40%, 20% and 15% respectively. Inset of figure 3.13 shows the relative carbonyl formation due to protein oxidation induced by γ-radiation from 2 to 8 Gy both in the absence or presence of either curcumin or the complex at identical time point. The results indicated inhibition of the radiation-induced cellular protein oxidation by these compounds, with the complex showing much stronger inhibition. The percentage reduction in protein carbonyl formation by the complex at different doses of 2, 4, 6 and 8

Gy was 48%, 40%, 24% and 3% respectively while the values under similar experiments with curcumin were found to be 28%, 19%, 15% and 2% respectively.

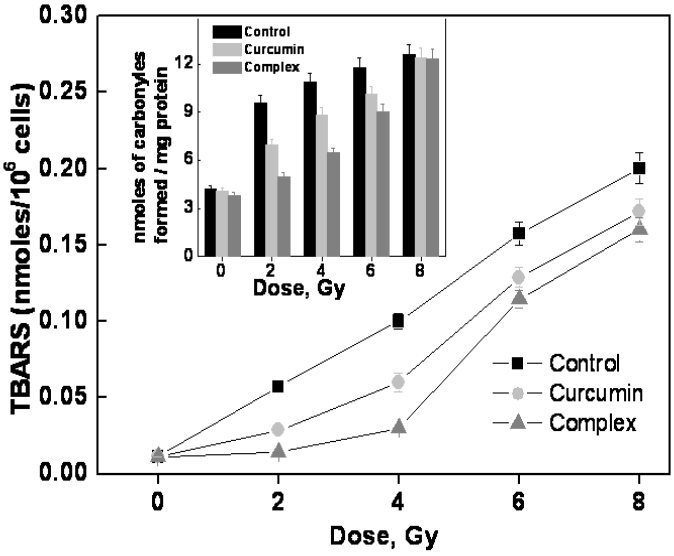

Figure 3.13 *Line graph showing inhibition of lipid peroxidation estimated in terms of TBARS in splenic lymphocytes ($5x10^6$) treated with curcumin and the complex, and exposed to varying dose of γ-radiation (2-8 Gy). Inset shows bar graph indicating inhibition of protein oxidation estimated in terms of protein carbonylation by compounds at different absorbed doses (2-8 Gy) of γ-radiation.*

In order to understand the factors responsible for the protection afforded by the complex in the above studies, the signaling pathways were checked.

3.6.3 Effect of curcumin and the complex on PKCδ phosphorylation

The phosphorylation at Ser 40 residue of PKCδ in lymphocytes was assessed at 5, 15, 30 and 60 min after irradiation alone or after irradiation along with pre-treatment with either curcumin or the complex. Western blots and relative intensities representing the level of phosphorylated PKCδ at the above four time points are shown in figure 3.14 (A,

B, C and D). Following γ-irradiation an increased phosphorylation of PKCδ was observed within 5 min, which reappeared at 60 min (Fig. 3.14 B & D).

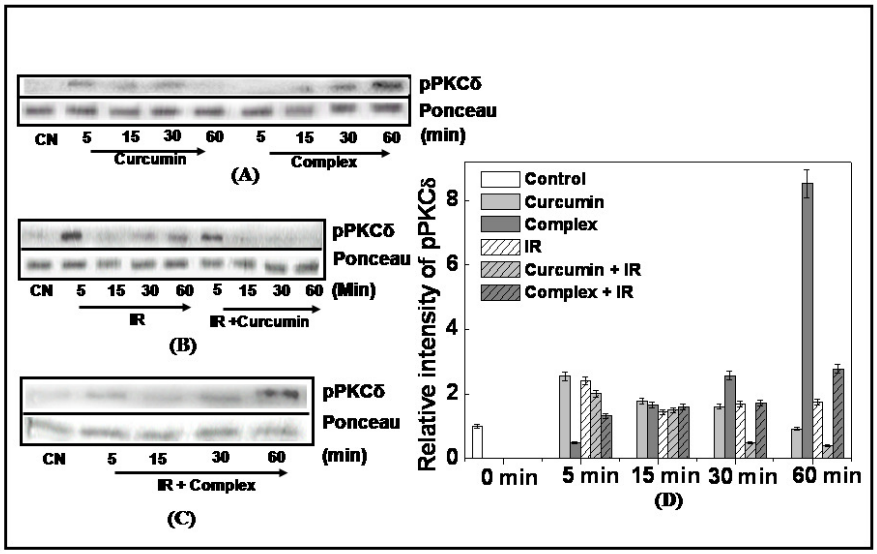

Figure 3.14 *Western blot analysis showing the comparative level of phospho PKCδ at different time points. (A) In lymphocytes after treatment with curcumin and the complex (B) In curcumin pretreated lymphocuytes after irradiation (C) In complex pretreated lymphocytes after irradiation (D) Bar graph showing relative intensities of phospho PKCδ. IR - Irradiation (2 Gy)*

When irradiation was preceded by curcumin or the complex treatment, the increased phosphorylation observed at 5 min was suppressed (Fig. 3.14 B, C & D). Here the complex showed stronger inhibition than curcumin. However, at 60 min, pretreatment with the complex resulted in increased phosphorylation of PKCδ, as compared to irradiation alone or pretreatment with curcumin (Fig. 3.15 C & D). Treatment with curcumin or the complex alone also resulted in increased phosphorylation of PKCδ but with different kinetics of activation. The complex showed time dependent increase, upto

eight folds at 60 min (Fig. 3.15 A & D). This indicates that the complex promotes growth in normal cells since increased expression of PKCδ could be anti-apoptotic.

3.6.4 Effect of curcumin and the complex on IκBα accumulation

The accumulation of IκBα in lymphocytes was checked at 5, 15, 30 and 60 min after irradiation alone or after pre-treatment with either curcumin or the complex. Western blot analysis and the relative intensities representing the level of IκBα at the above four time points are shown in figure 3.15.

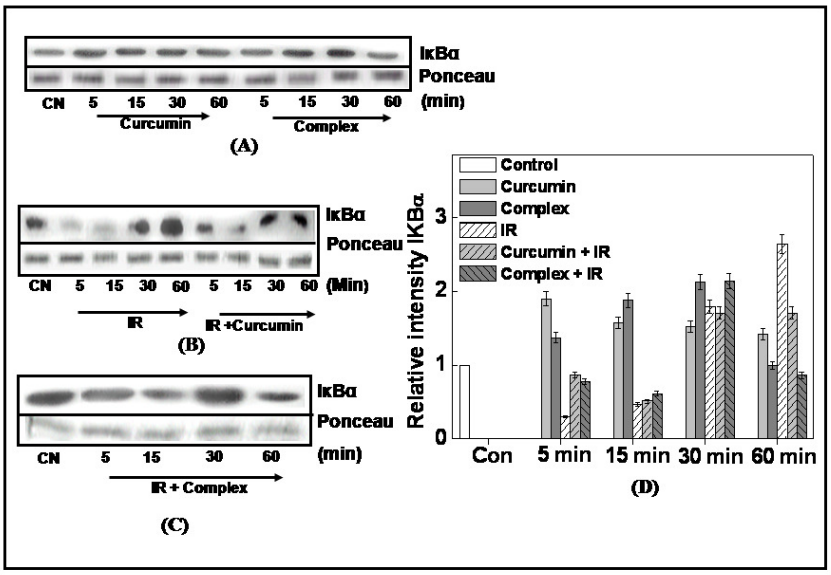

Figure 3.15 *Western blot analysis showing the comparative level of IκBα at different time points (A) In lymphocytes after treatment with curcumin and the complex (B) In curcumin pretreated lymphocuytes after irradiation (C) In complex pretreated lymphocytes after irradiation (D) Bar graph showing relative intensities of IκBα. IR - Irradiation (2 Gy)*

Following γ-irradiation the degradation of IκBα was observed within 5 min (Fig. 3.15 B & D). At 30 min there was a significant reappearance of IκBα and it continued to increase and reached up to ~3 folds at 60 min (Fig. 3.15 B & D). Pretreatment with

curcumin or the complex prevented the initial degradation of IκBα at 5 min (Fig. 3.15 B, C & D). Interestingly, the complex was also found to be effective in reversing the irradiation induced IκBα accumulation at 60 min (Fig. 3.15 C & D). Treatment with both the compounds alone reduced the levels of IκBα as compared to the control, however their kinetics was different (Fig. 3.15 A & D). The degradation of IκBα is known to release NF-κB, which transports to the nucleus where it acts as a transcription factor for many anti-apoptotic genes.

3.6.5 Effect of curcumin and the complex on nuclear transport of NF-κB and *Mn-SOD* expression

Figure 3.16 (A & B) show the expression levels of NF-κB in nuclear extract of lymphocytes at a time point of 60 min. Following irradiation, the level of NF-κB decreased in the nuclear extract of untreated lymphocytes.

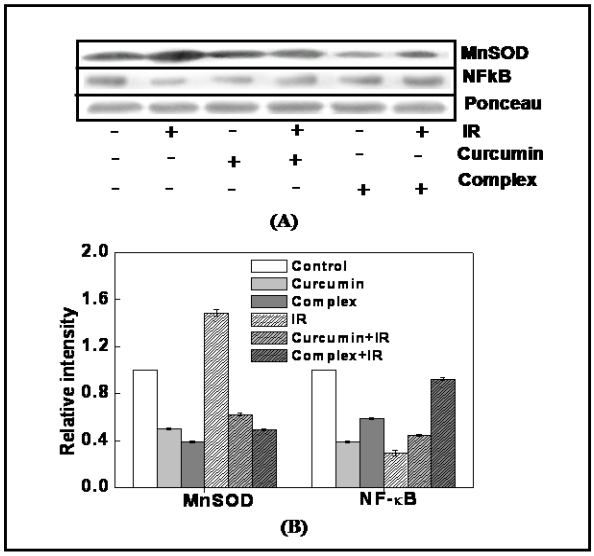

Figure 3.16 *Effects of curcumin and the complex on the nuclear transport of NF-κB and expression of Mn-SOD in γ-irradiated and unirradiated lymphocytes. (A) Western blot analysis showing the comparative level of NF-κB in nuclear extract and MnSOD in cytoplasmic extract after one hour of treatment with curcumin and the complex. (B) Bar graph representing relative intensities of NF-κB and Mn-SOD. IR - Irradiation (2 Gy)*

However, when irradiated lymphocytes were pre-treated with curcumin or the complex, the decrease in the level of NF-κB was reversed marginally by curcumin but very efficiently by the complex. Treatment with either curcumin or the complex alone also reduced the level of NF-κB in the nuclear extract. The reduction in the levels of NF-κB, following curcumin and the complex treatment was ~ 60 % and 40% respectively as compared to the control.

3.6.6 Effect of curcumin and the complex on γ-radiation induced apoptosis

Figure 3.17 shows percentage apoptosis in irradiated and unirradiated lymphocytes treated with curcumin and the complex for 24 h.

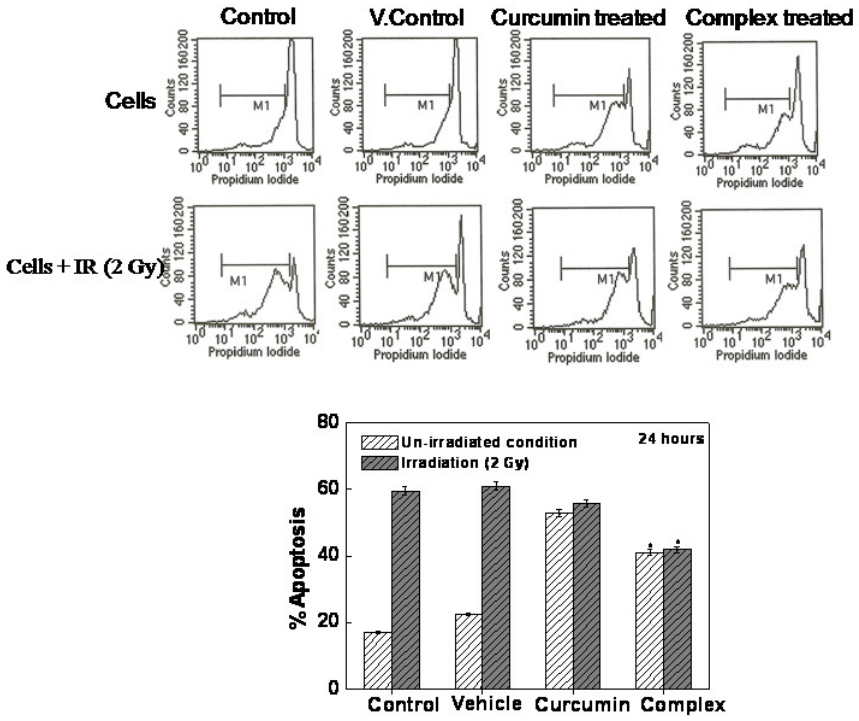

Figure 3.17 *Effects of curcumin and the complex on cellular cytotoxicity estimated in terms of apoptosis of spleen lymphocyte and modulation of γ-radiation induced apoptosis. The percentage apoptotic cells were calculated from pre G1 peak as estimated through Fluorescence Activated Cell Sorter (FACS). *P<0.05 as compared to curcumin treated lymphocytes. IR- Irradiation (2 Gy)*

Although both curcumin and the complex alone led to increase in apoptosis, as did the vehicle, they were able to confer protection to irradiated cells. Between the two compounds the percent apoptosis was found to be significantly lower in case of the complex treated cells under unirradiated condition. Irradiation alone led to substantial increase in apoptosis. However, pretreatment with the complex and curcumin decreased the percentage apoptosis observed in irradiated lymphocytes and the complex was more effective in this respect. The decrease in irradiation-induced apoptosis by the complex was 20%.

3.7 Discussion

Since ionizing radiation mediates cellular damage through ROS generation, compounds that regulate the fate of such species like antioxidants and antioxidant enzyme mimics are of great importance in the protection of cells against radiation-induced damage.[76] In the present study a 1:1 copper (II)-curcumin complex having superoxide radical scavenging ability along with SOD like activity has been evaluated for iradioprotective efficiency in splenic lymphocytes exposed to γ-radiation and the results have been compared with those of curcumin.

In agreement with the previous reports, γ-irradiation (2 Gy) induced increase in lipid peroxidation, and protein carbonyl levels and decrease in antioxidant enzymes activities.[195,240] Both curcumin and the complex prevented the decrease in GPx and catalase activities after irradiation. The complex showed significant reversal of irradiation induced decrease in GPx and SOD activities. The functional efficiency of GPx depends on the optimal supply of the redundant GSH.[219] Previously from our lab, it has been reported that the complex exhibits free radical scavenging activity. Therefore, complex

treatment is expected to prevent the intracellular depletion of GSH and thus maintains its cellular concentration needed for GPx activity. However the superior SOD activity under irradiated condition shown by the complex could be because of its acquiring the additional superoxide – dismutating copper (II) centre. Both curcumin and the complex also showed considerable reduction in TBARS levels (due to lipid peroxidation) and protein carbonyls formation up to an absorbed dose of 4 Gy. However, further increase in the radiation doses reduced the efficacy of these compounds**.** At all the absorbed doses employed in these studies, the complex provided better protection than curcumin.

Apart from free radical scavenging activities, compounds like curcumin are involved in activation or inhibition of various signaling pathways, such as PKCδ and NF-κB, which are crucial to the cell survival.[124,224] PKCδ is a signal transduction protein which in phosphorylated form leads to upregulation of cytoprotective gene like *HO-1*.[124] NF-κB is a redox sensitive transcription factor and is translocated to nucleus following degradation of its inhibitory protein (IκB) in cytoplasm. In the nucleus, NF-κB induces transcription of several genes related to cell survival and proliferation.[241] In order to understand how the complex could influence their activation in comparison with curcumin, studies were carried out on the phosphorylation of PKCδ and nuclear translocation of NF-κB. We followed the activation of PKCδ and NF-κB after irradiation in presence or absence of these compounds over a time period of 5 to 60 min. The inhibition of irradiation induced phosphorylation of PKCδ at 5 min was observed by both the complex and curcumin, with complex showing stronger inhibition. Since the early effects seen at 5 min could be stress responses, which occur due to the production of ROS, the complex therefore seems to be a better scavenger of ROS *ex vivo* due to its

ability to prevent radiation induced initial activation of PKCδ. Additionally, the reduction in irradiation-induced degradation of IκBα at 5 min with the complex strengthens the fact that the complex is more effective radical scavenger and hence prevents the immediate effects of irradiation. After the initial damage response, the cell assesses the damage and activates the signaling pathways, which then determine the fate of the cell. In this study, the activation of PKCδ, which is observed at 5 min, may be a stress response following which at later time periods (60 min) the signals that will protect the cells were initiated. The extensive phosphorylation of PKCδ at 60 minutes in the complex pretreated and irradiated spleenocytes indicates that the complex is more efficient than curcumin in activating cytoprotective pathways after the damage. Similarly after initial reduction observed at 5 min, there was an accumulation of IκBα at 30 min. At 60 min there was again a decrease in the level of IκBα in the complex treated irradiated lymphocytes indicating a degradation of IκBα. This would lead to excess of translocation of NF-κB to the nucleus and the expression of cytoprotective genes.[225] These results were further supported by the content of NF-κB in the nucleus which was found to be more in the complex pretreated irradiated spleenocytes at 60 min after irradiation. The delayed phosphorylation of PKCδ, in the complex treated lymphocytes along with the delayed degradation of IκBα (60 min) indicates a more prolonged action of the complex as compared to curcumin. The reason for this could be the delayed biological half-life of the complex and hence its higher effectiveness. The expression of *Mn-SOD*, a cytoprotective gene and a transcript of NF-κB was also looked at after 60 min of treatment with the compounds. Irradiation is known to induce the expression of *Mn-SOD* through ROS generation. Accordingly, we observed increased levels of *Mn-SOD* in irradiated

spleenocytes. Pretreatment with the complex or curcumin prevented this increase, further supporting the ROS scavenging capacity of the compounds, with complex again faring better than curcumin. Comparing the translocation of NF-κB and the expression of its downstream target gene *Mn-SOD*, it was observed that the complex did not inhibit the translocation of NF-κB to the nucleus as observed with curcumin, but surprisingly it inhibited the expression of *Mn-SOD* more than curcumin. The *Mn-SOD* gene contains binding motifs for a number of transcription factors including NF-κB, activator proteins 1 (AP1) and 2 (AP2), specificity protein 1 (Sp1) and adenosine 3', 5'-cyclic monophosphate-regulator element binding factor (CREB), however Sp1 and AP2 have been linked with the process of repression of *Mn-SOD* rather than its constitutive expression.[242-244] Therefore, the differential repression of *Mn-SOD* by curcumin or the complex may be due to their differential action on Sp1 and AP2.

The complex and curcumin have also been evaluated for their cytotoxicity on splenic lymphocytes and for their protective effect against γ-radiation (2 Gy) induced apoptosis. Curcumin is well known to induce cytotoxicity in tumor cell lines and in splenic lymphocytes.[192,245] When metal complexes are employed as antioxidants in cells, there is a possibility of their undergoing hydrolysis, thereby releasing free copper ions.[230] If this were the case, in the present study, the complex would have increased apoptosis more than that of curcumin. However, the extent of apoptosis caused by the complex was found to be significantly less than that of curcumin. This suggested that the complex was stable within the lymphocytes and did not undergo any hydrolysis. The complex also showed better overall protection against γ-irradiation by decreasing the radiation-induced apoptosis. Based on these studies we also initiated investigation on the *in vivo*

radioprotective effects of complex at Manipal College of Pharmacy. The primarily studies indicated that administration of complex at a dose of 50 mg/kg body weight in Swiss albino mice prior to γ-irradiation at an absorbed dose of 4.5 Gy was more effective in protecting the antioxidant enzymes 1 h post irradiation compared to curcumin treated group.

Thus all the above studies confirm the potential of transition metal-curcumin complexes as SOD mimics in the protection of radiation induced oxidative stress. However, a compound just by exhibiting the antioxidant activity in *ex vivo* and *in viro* models should not be considered pharmacologically active unless its *in vivo* efficacy is known. One of the limitations of drug development programme is the poor *in vivo* bioavailability. The most important factor affecting the bioavailability of a compound is its lipophilicity.[246] The compounds having either very high or very low lipophilicity are not considered good for therapeutic application as they are poorly bio-absorbed. In present study, by complexing copper with curcumin we have achieved SOD mimicking property but solubility of the compound has been reduced as compared to curcumin indicating it has become more lipophilic. Another important aspect is the metabolism and stability of such complexes *in vivo* as curcumin is known to metabolize very fast in the body. Therefore, it would be interesting in future to study the metabolism, pharmacokinetic behavior, stability and radioprotective efficacy of such complex using *in vivo* models before exploiting them to develop novel drugs. Our future studies will also be focused on evolving various strategies like functional group substitution to reduce the lipophilicity of such complexes.

3.8 Conclusion

In conclusion, the present study establishes that the complex has lesser cytotoxicity and better antioxidant or radioprotective activity at cellular level, which is reflected as maintenance of antioxidant enzymes, reduction in lipid and protein damage. The complex also scored better than curcumin in activation of various signaling pathways in temporally relevant manner i.e. PKCδ and NF-κB, which would then play a crucial role in determining fate of the cell. The radioprotective effect of the complex appears to be contributed by both SOD-like property and free radical scavenging. Overall, these studies give hope that perhaps the copper-curcumin complexes might be useful as radioprotector, once pharmacologically optimized. Therefore, synthesis of SOD mimic from antioxidants like curcumin appears to be a promising research area to look upon with an aim to use them for therapeutic application as radioprotector.

In addition to antioxidant property, anti-tumor and chemopreventive effects are the two other important pharmacological activities of curcumin which has been studied in great detail using tumor cell line and animal models. In spite of all the advancement on curcumin research, there are no studies addressing its cellular uptake and localization in the context of antitumor effects. In the next section we compared the uptake, localization and toxicity of curcumin in normal and tumor cells to explain its differential toxicity in these cells.

Section III: Quantitative cellular uptake, localization and cytotoxicity of curcumin in normal and tumor cells

3.9 Introduction

Therapeutic selectivity or preferential killing of cancer cells without significant toxicity to normal cells is one of the most desirable properties of an antitumor agent. It is encouraging to see that the current research has established that curcumin exhibits this selectivity.[112,116,247] For instance, Syng-ai et al., has shown that the percentage of apoptosis induced by curcumin (40 μM, 24 h) in three cancer cell lines (including HepG2 hepatocellular carcinoma cells) was approximately 90%, while it was lower than 3% in five different types of normal cells (including normal hepatocytes).[208] Similarly, curcumin (48 h treatment) induced apoptosis in chronic lymphocytic leukemia (B-CLL) cells from 14 patients at lower concentrations (EC_{50} = 5.5 μM) than in mononuclear cells (EC_{50} = 21.8 μM) from healthy donors.[248] In another study, the percentage of apoptotic cells induced by curcumin (40 μM, 24 h) was higher (46.65%) in the multidrug- resistant breast carcinoma cell line MCF-7/TH than that (1.80%) in the human mammary epithelial cell line MCF-10A.[249] The question thus arises is that what confers this selectivity? Several researchers are attempting to address this question. For example one of the mechanisms reported for its selectivity toxicity includes its ability to inhibit transcription factors like NF-kB and AP-1, which are constitutively expressed in tumor cells but not in normal cells.[112,116] Apart from this, another important finding in the last one decade is that curcumin has the ability to selectively increase the cellular levels of ROS or pro-oxidant effect in tumor cells leading to toxicity.[190,207-210]

Our previous studies (section I) suggested that the differential antioxidant to pro-oxidant activity of curcumin is also influenced by its intracellular concentration. This

prompted us to hypothesize that the reasons for the selectivity of curcumin for tumor cells might be due to its higher uptake as well as differential localization in these cells as compared to normal cells. To address this, we have quantitatively estimated curcumin uptake in different normal and tumor cells.

Earlier researchers have employed sensitive techniques like high performance liquid chromatography (HPLC) and liquid chromatography-mass spectrometry (LC-MS) for the detection of extremely low serum levels (in micromolar range) of curcumin, after high amounts (several grams) of oral administration.[96] However, there are no methods available in the literature for the quantitative estimation of curcumin in the target cells. In order to address this issue, absorption and fluorescence based method for detection of intracellular curcumin have been developed and used for estimation of curcumin uptake in different types of cells.

Earlier several researchers including our group has reported that curcumin exhibits medium dependant photophysical properties.[99] Although the absorption properties of curcumin do not show significant change, its fluorescence spectrum, fluorescence maximum and the fluorescence quantum yield have been found to be very sensitive to the nature of the medium or environment.[99,228,250,251] For example it exhibits very low fluorescence in aqueous solutions, whereas in polar aprotic medium; its fluorescence intensity is increased substantially. Earlier this property has been used as a tool by our group to monitor its interaction with liposomes and proteins such as human serum albumin (HSA) and bovine serum albumin (BSA).[252-254] The photophysical properties of curcumin in liposomes, serum albumins and some of the organic solvents are listed in table 3.3.[99]

Table 3.3: *Photophysical properties of curcumin in different mediums*

Medium	**λ_{abs}, nm**	**Molar extinction coefficient (ε), $M^{-1}cm^{-1}$**	**λ_{fl}, nm**	**Fluorescence Quantum Yield (ϕ)**	**Binding constant (M^{-1})**
BSA	440		510	0.05	10^4 to 10^5
HSA	430	9.4×10^4	520-530	0.038	10^4 to 10^5
Liposomes	420	8.2×10^4	498	0.025	10^4 to 10^5
Methanol	428	4.8×10^4	546	0.028	
DMSO	432	5.5×10^4	535	0.050	
Acetonitrile	418		521	0.156	
SDS/ H_2O	426		492		
TX-100/H_2O	427		518	0.022	

These studies suggested that curcumin preferentially binds to the bio-molecules and its fluorescence is significantly enhanced on such binding. Therefore, these distinct changes in the absorption and fluorescence properties of curcumin on binding to different types of cells have been utilized to understand the nature of its interactions, localization and uptake in normal vs. tumor cells.

For the present studies, two tumor cell lines including MCF7 (breast cancer cells of human origin) and EL4 (T cell lymphoma of murine origin) cell lines and two normal cells like NIH3T3 (mouse fibroblast cells) and freshly isolated murine spleen lymphocytes have been selected. The characteristics of these cells are listed in table 3.4. Since spleen lymphocytes and EL4 cells are syngenic cells, they represent the ideal set of normal and tumor cells respectively for the comparative study. On the other hand, NIH3T3 and MCF7 cells belong to different lineages; however these have been selected

to represent the pair of normal and tumor cells respectively due to limitations of cell lines availability at our institute.

Table 3.4: *Description of cell lines*

Cells	**Type**	**Morphology**	**Origin**	**Properties**
Spleenocytes	Primary culture	Lymphoid growing as Suspension	Swiss albino mouse maintained at BARC	Exhibit normal properties of lymphocytes
EL4	Lymphoma cell line	Lymphoid growing as suspension	Established from ascetic fluid of a C57BL/6N mouse lymphoma	Interferon production, IL-1 production, Resistant to cortisol and dexamethasone, tumorigenicity Doubling time – 40 hours
NIH3T3	Fibroblast cell line	Fibroblasts growing adherently as monolayer	Established from Swiss NIH mouse embryos	Highly contact inhibited and are sensitive to sarcoma virus focus formation and leukaemia virus propagation
MCF7	Human breast adenocarcinoma cell line	Epithelial-like cells growing as monolayers	Established from the pleural effusion of Caucasian woman with metastatic mammary	Cytokeratin (+), Desmin (-) , Vimentin (-) Doubling time – 50 hours

The EL4 and NIH3T3 cells were cultured in RPMI medium whereas MCF7 cells were cultured in DMEM medium. The culture medium was supplemented with 10 % fetal bovine serum. The spleen lymphocytes were freshly isolated from Swiss albino mice and

cultured in RPMI medium supplemented with 10 % fetal bovine serum. The stock solution of curcumin was prepared in DMSO and diluted with the culture medium to get the desired concentration. The maximum concentration of DMSO employed in all these studies was within permissible limits of toxicity (≤ 0.1%). Following treatment with curcumin, its toxicity and uptake was monitored to establish a correlation between these two. Further intracellular localization of curcumin was studied in great detail in MCF7 cells and spleen lymphocytes employing subcellular fractionation and confocal microscopy. Each experiment was performed in triplicates and results are presented as mean ± S.E.M. The statistical analysis between different groups for significance was done using students't' test. A value of $P < 0.05$ was considered as statistically significant.

3.10 Results

3.10.1 Uptake measurements

For estimating uptake of curcumin, the cells suspended in culture medium were plated at ~$1x10^6$ cells/ml in culture discs, incubated with curcumin (at a concentration of 5 - 80 nmoles/ml) for 4 hours. The treated cells were spinned down at 2,000 x *g* in Beckman centrifuge for 5 min and washed thrice with cold phosphate buffered saline (PBS). The pellet was dried and suspended in 1 ml of methanol and sonicated till curcumin is completely extracted into the methanol fraction. The lysate was centrifuged at 8,000 x *g* for 5 min and absorption spectra of supernatant containing methanolic curcumin were recorded. From the absorbance at 428 nm and using the extinction coefficient of 48,000 $M^{-1}cm^{-1}$ for curcumin in methanol at 428 nm, total cellular uptake was estimated according to equation 3.3.

$$Total\ cellular\ uptake\ (pmoles/million) = \frac{OD_{428} \times Vol(ml)\ of\ cell\ lysate \times 10^{12}}{\varepsilon_{428} \times l \times 1000 \times Cell\ number\ in\ millions} \qquad (3.3)$$

Treatment at each concentration was done in triplicate and the estimated uptake at each concentration was normalized to one nmole/ml of curcumin treatment according to equation 3.4. The uptake values represented as pmoles/million cells were the average of six different normalized estimations at two different treatment concentrations of curcumin (10 and 20 nmoles/ml).

$$Normalized\ cellular\ uptake\ (pmoles/millions) = \frac{Total\ cellular\ uptake}{Treatment\ concentration\ (nmoles/ml\ culture\ medium/million\ cells)} \qquad (3.4)$$

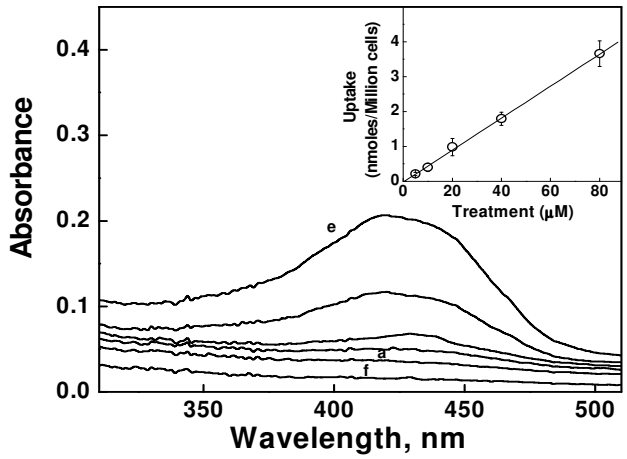

Figure 3.18 *Absorption spectra (a-e) of curcumin extracted in to 1 ml of methanol from MCF7 cells (2 x 10^6) after treatment with curcumin (at a concentration of 5 to 80 nmoles/ml in aqueous-DMSO) for 4 hours. Spectrum (f) represents the control MCF7 cells (2 x 10^6) treated with aqueous-DMSO without any curcumin. Inset shows variation in the total cellular uptake (without normalization with curcumin treatment) as a function of curcumin treatment.*

Figure 3.18 shows representative absorption spectra (a-e) of methanolic curcumin extracted from MCF7 cells, after treatment with different concentrations (5 to 80 nmoles/ml) of curcumin and the inset shows linear plot for the variation of cellular uptake

as a function of curcumin treatment concentration. Similarly cellular uptake of curcumin by the other two cell lines (EL4 and NIH3T3) and spleen lymphocytes were calculated at different curcumin treatment concentrations of 10 and 20 nmoles/ml. The results indicated that the uptake increased with increasing concentration of curcumin treatment in all the different cells and nearly doubled when treatment concentration was doubled. After normalization, cellular uptake was calculated and the average values of six different normalized estimations at two different treatment concentration of curcumin (10 and 20 nmoles/ml) are listed in table 3.5. It can be seen that the tumour cells (EL4 and MCF7) showed significantly (~ 1.5 to 2 folds) higher uptake as compared to normal cells (NIH3T3 and lymphocytes).

Table 3.5: *Cellular uptake, fluorescence spectral properties, and intensity variations of curcumin in different cells*

Cell lines	**λ_{fl}, nm** (λ_{ex}=420 nm)	**Average normalized cellular uptake** (pmoles/10^6 cells)	**Fl.intensity / pmole of curcumin uptake**(λ_{ex} = 420 nm)
Spleen lymphocytes	504	23.2 ± 4.3	0.023 ± 0.004
EL4	500	34.5 ± 6.4 [a, b]	0.064 ± 0.01 [a, b]
NIH3T3	535	22.6 ± 6.8	0.007 ± 0.002 [a]
MCF7	520	44.2 ± 7.2 [a, b]	0.067 ±0.01 [a, b]

[a] - Significant against spleen lymphocytes at $P < 0.05$

[b] - Significant against NIH3T3 cell line at $P < 0.05$

3.10.2 Fluorescence spectroscopic studies of intracellular curcumin

In order to explore difference in microenvironment experienced by curcumin molecule inside cells, spleen lymphocytes, EL4, NIH3T3 and MCF7 were treated with curcumin as described earlier , washed thrice with PBS, re-suspended in 1 ml of PBS and subjected to steady state fluorescence measurement. Figure 3.19 gives the fluorescence

spectra of curcumin-loaded cells (spectra c-f), after excitation at 420 nm. The fluorescence spectrum of curcumin in lymphocytes and EL4 cells is sharp and the maximum is at 500 to 505 nm, while those in MCF7 and NIH3T3 cells are broad with maximum at 520 to 535 nm respectively.

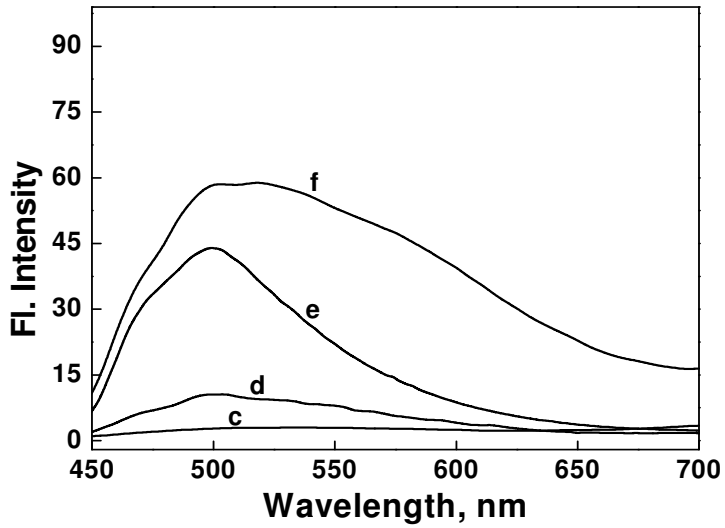

Figure 3.19 *The Spectra (c), (d), (e) and (f) are the fluorescence spectra of curcumin in NIH3T3, spleen lymphocytes, EL4 and MCF7 cells respectively after treatment with 20 nmoles/ml aqueous-DMSO solution of curcumin. Excitation wavelength 420 nm*

The fluorescence intensity, when compared in these four sets of cells, showed higher intensity in the two tumour cell lines. One of the reasons for such increase in fluorescence could be due to its increased uptake. To verify this, we calculated the fluorescence intensity to the same level of uptake and compared the fluorescence per unit uptake and the results are listed in table 3.5. It is clear that the fluorescence is at least 3-8 times more intense in the tumour cells than that in normal cells. The shift in fluorescence spectra and intensity variations clearly indicate that curcumin experiences different hydrophobic environments inside the tumour cells and interacts with them differently.

3.10.3 Fluorescence microscopy studies

The above observed fluorescence changes of curcumin in cells, prompted us to understand its intracellular localization by fluorescence imaging using an Olympus Fluoview 500 confocal laser-scanning microscope (Olympus, Tokyo, Japan) equipped with a multi-Argon laser for excitation at 458, 488 and 515 nm (Foldes-Papp et al., 2003). Slides for confocal microscopy of suspension cells were prepared by fixing curcumin-loaded cells in 1 % paraformaldehyde (PFA) in PBS for 15 min at 4ºC. 50 µl of cell suspension in PBS was spread on to confocal slide using cytocentrifuge, air dried and sealed with cover slip using mounting medium. For adherent cells, similar procedure was adopted except that these cells were first adhered to sterile coverslip and then processed for fixation. The images of cells were acquired either with 20X or a 60X water immersion objective after excitation at 458 nm using barrier filter. Although, the absorption maximum of curcumin is at ~ 420 nm , at the excitation wavelength of 458 nm, it has considerable absorption (45 to 70 % of the maximum absorption in different cells). Figure 3.20A, 3.20B, 3.22A and 3.22B give the confocal fluorescence images of curcumin treated lymphocytes, EL4, NIH3T3 and MCF7 cells respectively along with their corresponding phase contrast images and a few magnified images. At least five monochrome images were accumulated from five different microscopic fields of the same slide. The desired region on each fluorescent cell was selected and the mean fluorescence intensity/area for the region was determined using the fluoview software and the average values of 15 different regions are presented in table 3.6. From the table, it was observed that cells without curcumin treatment also showed some background fluorescence.

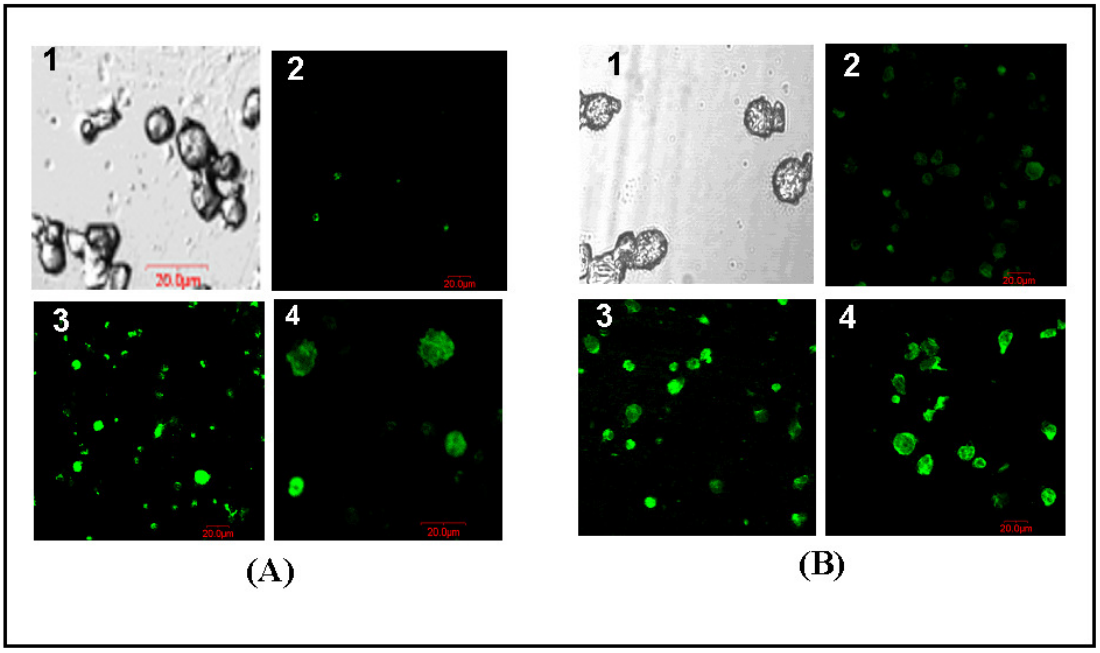

Figure 3.20 *Confocal micrographs of cells after treating with curcumin at concentration of 10 nmoles/ml. (A) Spleen lymphocytes (20 X Objective); 1- Phase contrast image, 2-Cells without curcumin treatment, 3- Cells treated with curcumin (2X zoom), 4- Cells treated with curcumin (6X zoom). (B) EL4 cells (20 X Objective); 1- Phase contrast image, 2-Cells without curcumin treatment, 3- Cells treated with curcumin (2X zoom), 4-Cells treated with curcumin (3X zoom) Excitation wavelength 458 nm.*

This could be due to fluorescence emission from intracellular bio-molecules like NAD and flavoproteins after non-specific excitation at 458 nm.[255] The difference in fluorescence intensities of curcumin treated and untreated cells supported our earlier observation that curcumin exhibits more fluorescence in tumor cell lines. Curcumin, being a lipophilic molecule, is expected to be localized in the membrane. However, the images of EL4 and lymphocytes show emission from the entire cells. Since in these cells, majority of the cell volume is occupied by the nucleus with very little cytoplasm, the emission could be from both the membrane and the nucleus. In case of MCF7 and NIH3T3 cells, due to their distinct morphology, fluorescence images indicate selective localization of curcumin in the cell membrane and the nucleus.

Table 3.6: *Confocal image analysis of curcumin treated MCF7 cells*

Cell lines	**Confocal imaging data Fl. intensity / area of cell**(λ_{ex} = 458 nm)		
	Control (Untreated)	**Treated (10 µM)**	**Difference (Treated – Control)**
Spleen lymphocytes	69 ± 12	125 ± 35	56 ± 23
EL4	106 ± 8	212 ± 23	106 ± 15 [(a, b]
NIH3T3	220 ± 27	259 ± 32	39 ± 5 [(a]
MCF7	208 ± 66	382 ± 91	174 ± 25 [(a, b]

[a] - Significant against spleen lymphocytes at $P < 0.05$

[b] - Significant against NIH3T3 cell line at $P < 0.05$

To confirm its nuclear localization, these cells were subjected to dual staining for which the cells treated with curcumin were thoroughly washed, fixed in 1 % PFA, stained with 4'6-diamidino-2-phenylindol (DAPI) (1mg/ml in PBS containing 0.1% Triton-X 100), a DNA selective fluorescent probe and mounted on the confocal slide.[256] The images of cells were acquired after exciting it with Coherent Mira 900F Titanium: Saphire infrared laser (Coherent Verdi-V5, Santa Clara, CA, USA) tuned to 720 nm and the fluorescence in the wavelength range of 400-470 nm was collected. This two-photon imaging avoids the photobleaching of cellular background fluorescence that could happen due to excitation by UV laser. To quantify the co-localization of curcumin and DAPI, images acquired separately for each of the probe were merged using the software. The fluorescence from curcumin was pseudo colored as green and that from DAPI as red (Image 3, & 5 of figure 3.22A and 3.22B respectively).

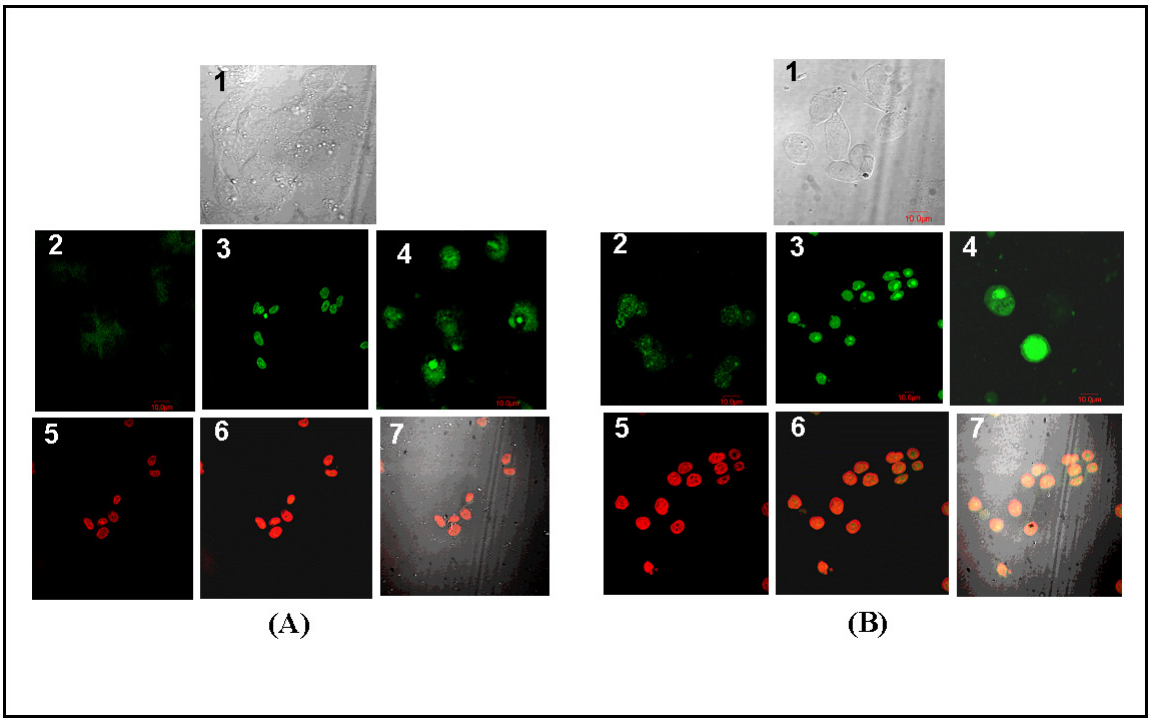

Figure 3.21 *Confocal micrographs of cells after treating with curcumin at concentration of 10 nmoles/ml.*
(A) NIH3T3 cells (60X objective); 1- Phase contrast image, 2-Cells without curcumin treatment, 3- cells treated with curcumin (1X zoom), 4- Cells treated with curcumin (2X zoom), 5 Cells stained with DAPI (1X zoom), 6 –Images 4 and 5 merged together (1X zoom), 7- Image 4 and 5 merged with image 1 (1X zoom).
(B) MCF7 cells (60X objective); 1- Phase contrast image, 2-Cells without curcumin treatment, 3- Cells treated with curcumin (1X zoom), 4- Cells treated with curcumin (2X zoom), 5 Cells stained with DAPI (1X zoom), 6 –images 4 and 5 merged together (1X zoom), 7- image 4 and 5 merged with image 1 (1X zoom).
For curcumin, λ_{ex}– 458 nm and DAPI, λ_{ex}–720 nm, two photon

The superimposed images as shown in images 6 & 7 of figure 3.22A and 3.22B respectively for NIH3T3 and MCF7 cells, clearly indicate green and red areas overlapping, confirming the co-localization of curcumin and DAPI in the nucleus. The cellular localization of curcumin as a function of time was also studied in MCF7 cells. In the absence of live cell imaging technique this was done by treating the cells with curcumin for different time periods (0.5 to 8 hrs), and after treatment, the confocal

fluorescence images were captured. Figure 3.22A and 3.22B respectively show the confocal micrographs and the plot of mean fluorescence intensity/area of MCF7 cells at different treatment times.

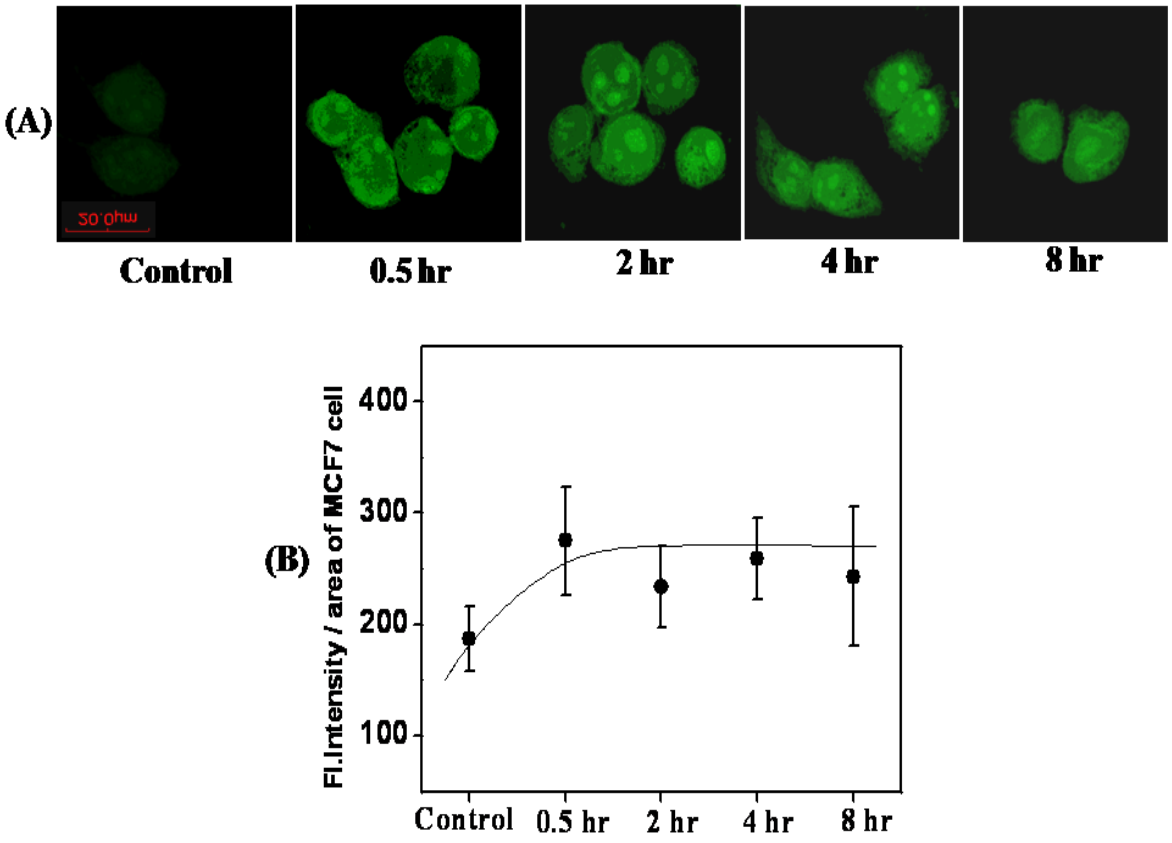

Figure 3.22 *(A) Confocal micrographs of MCF7 cells (60 X objective, 2X Zoom) at different time points (0.5 hr to 8 hr) after treatment with curcumin at concentration of 10 nmoles/ml. (B) Line graph showing variation in fluorescence intensity/area at different time points. Excitation wavelength 458 nm.*

From the figure it is clear that the fluorescence of curcumin could be observed as early as 0.5 hr within the cell and at this time point the intensity was maximum and observed uniformly from the entire cell. With progress of time (2 to 8 hr), the fluorescence

intensity appears to be localized into various compartments and over all intensity remained constant even up to 8 hours.

3.10.4 Subcellular distribution of curcumin

Since MCF7 cell line showed maximum uptake of curcumin, further studies were carried out to estimate the different subcellular distribution of curcumin. For this, ~ 2x 10^6 cells were incubated with curcumin (at a concentration of 20 nmoles/ml) for 4 hours. Following treatment, the subcellular fractionation was performed using differential centrifugation protocol described earlier with certain modifications.[257] In brief, the treated cells were suspended in to 0.5 ml of hypotonic lysis buffer (PBS with 10 mM KCl), allowed to swell on ice for 15 min, and then NP-40 (0.6%) was added. The sample was homogenized and subjected to varying centrifugal speed of 2,000 x *g* for 10 min, 10,000 x *g* for 15 min and 1,00,000 x *g* for 45 min respectively to collect the nuclear, mitochondrial and membrane fractions in the form of pellets and the cytosolic fraction as supernatant. All the pellet fractions were washed thrice with cold PBS, air-dried, and suspended in to 0.5 ml of methanol, sonicated, to extract the curcumin completely in methanol. The cytosolic fraction was vacuum dried and suspended in to 0.5 ml of methanol. Absorption spectra of methanolic curcumin from all the fractions were recorded as described above. The absorption spectra of methanolic curcumin from different subcelluar fractions of MCF7 is shown in figure 3.23 and by comparing the absorbance at 428 nm under identical volume conditions, the percentage distribution of curcumin in different cellular compartments was calculated and shown as inset of figure 3.23.

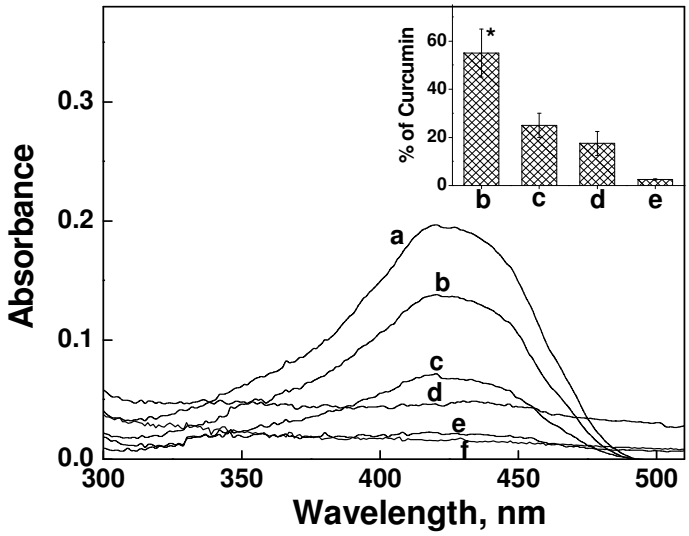

Figure 3.23 *Absorption spectra of curcumin extracted in methanol from different subcellular fractions of MCF7 cells (2 x 10^6) after treatment with 20 nmoles/ml of curcumin in aqueous-DMSO for 4 hours: a-total cellular fraction, b-membrane fraction, c-cytoplasmic fraction, d-nuclear fraction, e-mitochondrial fraction, f-control. Inset shows variation in percent curcumin in different subcellular fractions. Control represents cells (2 x 10^6) treated with aqueous-DMSO. * Significant against cytoplasmic, nuclear and mitochondrial fractions at P < 0.05*

The figure 3.23 confirms that the membrane fraction showed highest percentage of curcumin and the differential uptake in sub-cellular components is in the order membrane > cytoplasm > nucleus > mitochondria. Although these studies are too preliminary and need more confirmative studies, they support the previous reports that the cell membrane is the preferred site of localization for curcumin and curcumin is localised in the nucleus too.

3.10.5 Cytotoxicity measurements

The cytotoxic activity of curcumin in different cell lines and spleen cells was assessed by the MTT dye conversion assay.[194] Table 3.7 shows the cytotoxic effect of curcumin at concentrations of 20 to 40 nmoles/ml in different cell lines. The results

indicate that there is an increase in the cytotoxicity in individual cell line with increasing concentration of curcumin treatment. Tumor cells EL4 and MCF7 showed significantly higher sensitivity towards the cytotoxic activity of curcumin compared to normal fibroblast cells NIH3T3.

Table 3.7: *Effect of curcumin on the viability of different cell lines assayed by MTT reduction measured at 550 nm*

Treatment (Curcumin)	**MCF-7** λ_{abs} 550 nm	**EL4** λ_{abs} 550 nm	**NIH3T3** λ_{abs} 550 nm
Control	0.83 ± 0.01	0.79 ± 0.02	0.44 ± 0.01
20 nmoles/ml	0.65 ± 0.02 [c]	0.56 ± 0.01 [c,d]	0.37 ± 0.01
Cytotoxicity (%)	22 %	30 %	16 %
40 nmoles/ml	0.50 ± 0.01 [c]	0.30 ± 0.01 [c,d]	0.29 ± 0.01
Cytotoxicity (%)	41 %	63 %	35 %

[c] - Significant against NIH3T3 cell line at $P < 0.05$

[d] - Significant against MCF7 cell line at $P < 0.05$

Between the tumor cells, EL4 showed significantly higher toxicity compared to MCF7 even at lesser uptake, indicating that the cells of lymphoid origin experience more toxicity of curcumin. The above observations have been represented in figure 3.24, as percentage change in cytotoxicity against total cellular uptake for these three different cells at different treatment conditions. The treatment of the cell lines with curcumin at a concentration of 10 nmoles/ml showed only little toxicity. This experiment with normal spleen lymphocytes has not been reported as large fluctuations were observed in their viability in 24 h time period.

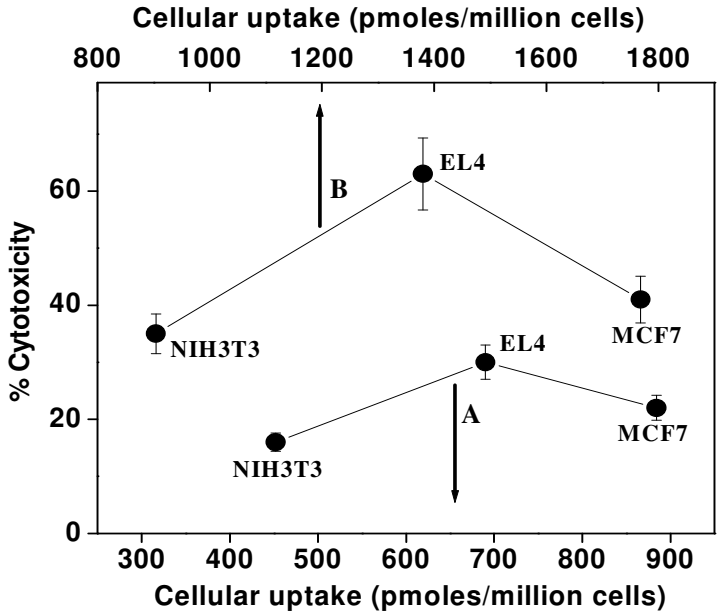

Figure 3.24 *Change in cytotoxicity of curcumin, assayed by MTT, against cellular uptake for different cells at two different treatment conditions. (A) 20 nmoles curcumin/ml and (B) 40 nmoles curcumin/ml.*

3.11 Discussion

In the present study, the absorption and unique fluorescence spectral properties of curcumin, were used to measure quantitative uptake and intracellular localization of curcumin in four different cell types and these parameters were correlated with its cytotoxicity.

Our results clearly indicate that tumor cells show preferential uptake of curcumin compared to normal cells. Curcumin being a lipophilic molecule interacts with cellular membrane and is subsequently transported inside the cell. Among various factors that are responsible for higher curcumin uptake in tumor cells against normal cells could be their differences in membrane structure, protein composition and bigger size.[258,259]

The fluorescence spectra of cellular curcumin showed two interesting factors. The fluorescence intensity was always higher in tumor cells compared to normal cells and the fluorescence maximum of curcumin in suspension cells was more blue shifted as compared to that in adherent cells. In the earlier studies it has been shown that curcumin exhibits weak fluorescence with featureless and broad maximum ~550 nm in aqueous methanol solution, however in presence of phosphatidylcholine (PC) liposome or human serum albumin (HSA) protein its fluorescence intensity is significantly enhanced along with large blue shift in the fluorescence maximum with their respective values at 498 nm and 515 nm for liposomes and HSA protein.[252-254] These reports thus suggest that the fluorescence maximum and fluorescence quantum yield of curcumin are highly sensitive to the medium polarity and availability of the hydrophobic pockets such as protein and lipid.[99] Since living cells are rich, and differ in lipid and protein content, change in fluorescence spectral behavior of curcumin is expected upon interaction with living cells and accordingly present observations indicated that curcumin interacts differently with different cells. Although there are no reports available in literature on differential polarity of these different cells, the observed fluorescence spectral changes however suggest differences in the protein and lipid composition of these cells. The more polar environment in the adherent cells could be due to adhering proteins (cadherins) and several cell-cell junction (gap junction, tight junction and adherent junction) proteins.[260-263] However, in tumor cells of adherent type such as MCF7 other factors like differential pool of cytoplasmic proteins (resulting from altered gene expression) and the difference in the composition of membrane lipids can also contribute towards the intracellular microenvironment or hydrophobicity.[264-266] These significantly prominent fluorescence

changes of curcumin also indicate that curcumin can be used as a new probe to understand the behavior of different cell types.

The fluorescence imaging studies revealed very encouraging results and clearly showed localization of curcumin inside the cells. In all the cells, curcumin fluorescence could be seen in the membrane but in MCF7 and NIH3T3 cells, due to their distinct morphology, localization inside the nucleus was also observed. Studies on isolation of curcumin from sub-cellular fractions also confirmed the differential localization of curcumin in the membrane, cytoplasm and nuclear compartments of the cell with preferred localization in the membrane. The localization of curcumin in the nucleus was a new and unexpected observation, which needs to be addressed. To understand this, more detailed experiments are needed with special emphasis on identification of the cellular proteins that specifically interact with curcumin and helping its transport to nucleus. We propose to address these issues in future. The cytotoxicity studies indicated a linear relationship between uptake and cytotoxicity in each cell type. However, the cells of lymphoid origin appeared to be more sensitive to curcumin than the non-lymphoid cells even when these cells showed lesser uptake. In addition to this, our studies also indicated selective toxicity of curcumin in tumor cells as compared to normal cells. This is in correlation with our studies that curcumin acts as a pro-oxidant at higher concentration and therefore higher uptake in tumor cells may be responsible for its preferential toxicity.

3.12 Conclusions

In conclusion, our present studies gave a method to estimate quantitative uptake of curcumin and the results provided confirmation that tumor cells preferentially take up more curcumin which may be one of the mechanisms responsible for its selective

toxicity. The preliminary studies on fluorescence spectrum of curcumin in cells indicated that the fluorescence maximum and intensity of curcumin are dependent on the cell type. Since tumor cells and normal cells differ in their lipid and protein composition, future studies may be explored to monitor changes in fluorescence properties of curcumin to evaluate the membrane microenvironment in different cells and to examine its ability to act as a probe for selective imaging of tumor cells. Another important finding of present studies is the fluorescence imaging of curcumin inside cells. These studies confirmed the intracellular localization of curcumin and a surprising observation of its nuclear localization. Therefore, it would be interesting in future to study the interactions of curcumin with different nuclear factors or target proteins and nucleic acids like DNA or RNA and such studies would be useful in understanding its selective toxicity in more detail.

CHAPTER 4

ANTIOXIDANT & RADIOPROTECTIVE STUDIES ON 3,3'-DISELENODIPROPIONIC ACID, A GPx MIMIC: *IN VITRO* & *IN VIVO* STUDIES

4.1 Introduction

Radioprotectors are employed to minimize the short and long term effects of radiation damage to living cells.[74,267] Most of the compounds such as amifostine, cysteine, N-acetylcysteine, cysteamine, cystamine, aminoethylisothiourea dihydrobromide and mercaptoethyl guanidine examined for radioprotection till today, belong to the class of sulphur compounds.[76] Out of these, amifostine is the only clinically acceptable radioprotector.[84] Although, these agents exhibit very effective radioprotection, they have their limitations of inherent toxicity and slow action to become ideal radioprotectors.[76] Therefore, there is a need to design and develop new compounds with lower toxicity and improved efficacy.

Selenium an essential trace element for both animals and humans belongs to the same group in periodic table as sulfur.[146,162] Selenium and sulfur have many similar properties like electronegativity, oxidation states, atomic size, etc and selenium undergoes easy oxidation as compared to sulfur. Therefore, selenium compounds are expected to exhibit better free radical scavenging activity.[145] Another markedly important difference between the two is that selenium induces the expression of a variety of selenoproteins including one of the most important antioxidant enzymes, glutathione peroxidase (GPx), a property which is not seen with sulfur.[149,268] All these differences suggest that selenium compounds may possess better antioxidant activity than sulfur compounds. Considering these differential anti-oxidative properties of selenium, it is expected that selenium compounds could be explored as alternate radioprotectors. With this view, the screening of selenium compounds for radioprotection has been initiated.

Sodium selenite (Na_2SeO_3) was the first selenium compound tested for radioprotection in mice. In this study, selenite (0.8 and 1.6 mg/kg body weight) administered intraperitoneally (i.p.) before or shortly after irradiation increased the whole body survival.[269,270] In another study, selenite (0.1 mg /kg body weight) in combination with vitamin E (200 mg/kg body weight) administered through i.p for 10 days in rats before γ-irradiation prevented the radiation induced reduction in levels of antioxidant enzymes.[271] Additionally, a recent study showed that selenite exhibited radioprotection in normal fibroblast cells, but not in head and neck carcinoma cells.[272] Based on these studies, selenite was even tested in clinic to reduce the side effects of radiochemotherapy in head and neck cancer patients. In this clinical study, selenite administered at a dosage of 500 µg per day increased the activity of serum GPx and also reduced the therapy induced production of free radicals.[273] Although, these studies established selenite as a potential radioprotector in animals and cells, it was also reported to exhibit behavioral toxicity in animal models.[269,270]

Unlike inorganic selenium compounds, organoselenium compounds are considerably less toxic, therefore researchers also examined such compounds for radioprotection. In the past, organoselenium compounds like selenourea, selenocystine, selenoxanthene and selenoxanthone have been examined for radioprotection using *in vitro* models, however these agents did not show promising activity.[274] Further, selenomethionine was tested for radioprotection in animals and when administerd i.p. at dosages of 0.8, 1.6 and 4 mg/kg body weight, significantly increased the survival of irradiated mice.[269,270] It was equally protective when administered at 24 h, 1 h and 15 min prior to γ-irradiation. However, due to its similarity with naturally occurring aminoacid,

methionine, it nonspecifically gets incorporated in to cellular proteins resulting in unwanted side effects and this property restricted its further exploration as radioprotector.[270,275] Recently a synthetic organoselenium compound ebselen, a well studied GPx mimic has been tested for radioprotection in mice and U937 monocytic cells.[276] The results of this study indicated that ebselen administration for 14 days at a daily dosage of 10 mg/kg body weight in mice before whole body irradiation provided substantial protection against killing and oxidative damage. It also prevented the radiation induced oxidative stress and apoptosis in U937 cells.

With an aim to develop a radioprotector, our research group had also initiated work on design, synthesis and development of GPx active selenium compounds. One of the constraints in the development of selenium compounds is their stability and poor water solubility. Several synthetic groups have been working on development of GPx active selenium compounds.[153] and in this regard both aliphatic and aromatic compounds have been examined as GPx mimics. In one such study, Back and Moussa (2003) showed that certain aliphatic seleno-ethers and diselenides depending on the substitution on the aliphatic chain showed higher GPx activity as well as better water solubility than ebselen.[277] Considering this, 3,3'-diselenodipropionic acid (DSePA), a water soluble diselenide, was synthesized in our laboratory according to the literature reported method.[278] The compound is structurally related to the diselenide amino acid selenocystine, and it was characterized by NMR, mass and IR spectroscopy. The chemical structure of DSePA is shown in scheme 4.1.

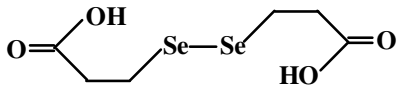

Scheme 4.1: *3,3'-Diselenodipropionic acid (DSePA)*

^{1}H NMR (CD_3OD) δ: 2.81 (t, $SeCH_2$); 3.10 (t, CH_2CO) (COOH proton exchanged with CD_3OD). ^{13}C {^{1}H} NMR (CD_3OD) δ: 23.4 (s, $SeCH_2$); 35.4 (s, CH_2CO); 174.3 (s, CO). ^{77}Se {^{1}H} NMR (CD3OD) δ: 322 (s). IR spectra: ν(C=O) = 1694 cm^{-1}; Mass spectra: m/z = 306 (molecular ion); 288 (M-H_2O). The m/z value given here is based on ^{78}Se isotope with natural abundance of 49.82%.

Further, DSePA was examined for GPx mimetic, antioxidant and radioprotective activities, which have been discussed in this chapter.

4.2 Results

4.2.1 GPx-mimetic studies in cell free system

The GPx like catalytic activity of DSePA was determined by following the decay of NADPH at 340 nm in the reaction system consisting of NADPH (0.34 mM), glutathione reductase (0.5 mU/ml), glutathione (GSH), cumene hydroperoxide (CuOOH) and DSePA. In this reaction, DSePA would catalyze the reduction of CuOOH using GSH as reducing agent and during this process GSH is oxidized to GSSH (equation 4.1).

$$CuOOH + 2GSH \xrightarrow{DSePA} CuOH + GSSG + H_2O \quad (4.1)$$

In order to continue the catalytic cycle, GSSG is converted back to GSH by utilizing NADPH in glutathione reductase catalyzed reaction as shown in equation 4.2.

$$NADPH + GSSG + H^+ \xrightarrow[reductase]{Glutathione-} 2GSH + NADP^+ \quad (4.2)$$

Therefore, the decay of NADPH can be used to estimate the GPx catalytic activity by monitoring the initial rate (*v*), which was calculated from the initial portion of the

NADPH decay trace using the extinction coefficient as 6220 $M^{-1}cm^{-1}$, at 340 nm.[57] In the first step, the concentrations of GSH and CuOOH were kept constant and that of DSePA was varied from 47 to 140 μM. The *v* value obtained at each concentration of DSePA was plotted against DSePA concentration to ensure linearity in the given range as shown in figure 4.1. The plot is linear in the concentration range and did not reach saturation. From this linear plot, the molar concentration of DSePA required to oxidize 1 μmol of NADPH in one minute was calculated to be 12.84 mM. According to standard definition, one unit of GPx enzyme is defined as the amount of enzyme that catalyses the oxidation of 1 μmol of NADPH in one minute, therefore 12.84 mM concentration of DSePA represents the mass equivalent for one unit of GPx.

The GPx activity of DSePA may be either due to its affinity for GSH or CuOOH. To further understand this, Lineweaver-Burk (L-B) plots for GSH and CuOOH were made separately. For these experiments, concentration of DSePA was kept constant and *v* was determined at different concentrations of either GSH or CuOOH by keeping the other substrate constant. The L-B plot was obtained by fitting of the data according to equation 4.3 and from the slope and intercept of the L-B plot the respective V_{max} and K_m values were estimated.

$$\frac{1}{\nu} = \frac{K_m}{V_{max}}\frac{1}{[S]} + \frac{1}{V_{max}} \tag{4.3}$$

Here V_{max} is the maximum rate of the enzymatic reaction, and K_m is the Michaelis-Menten constant. Inset (a) of the figure 4.1 shows the L-B plot for thiol obtained by keeping the concentration of DSePA (100 μM) and CuOOH (180 μM) fixed and varying the concentration of GSH (4 mM – 17 mM). From this, the K_m and V_{max} values for GSH

were estimated to be 10.2 mM and 4.8 μM/min respectively. Similarly L-B plot for affinity for hydroperoxide was obtained (inset (b) of Fig. 4.1) at different concentration of CuOOH (0.9 – 1.44 mM) keeping the concentration of DSePA (100 μM) and GSH (4 mM) fixed. From this, the K_m and V_{max} values for CuOOH were estimated to be 0.14 mM and 2.24 μM/min respectively. Inverse of K_m is related to the binding of the substrate to the enzyme, i.e. higher the value of K_m, lower is the binding of the substrate to the enzyme.

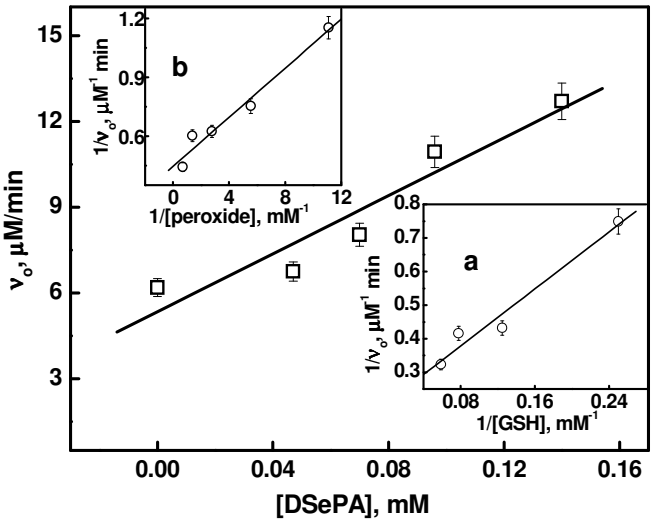

Figure 4.1 *Variation in the initial rate of decay of NADPH at 340 nm as a function of the concentration of DSePA. Inset (a) and (b) show L–B plots obtained on varying the concentration of GSH and cumene hydroperoxide (CuOOH) respectively. Results are presented as mean ± SEM (n =3).*

Thus lower value of K_m for CuOOH in comparison with GSH indicates that DSePA has higher affinity or binding to the peroxide than GSH. To understand the significance of this in GPx catalytic mechanisms, we tried to relate different steps involved in the GPx cycle of DSePA. A diselenide can show its GPx activity through two mechanisms. (1) Reduction pathway in which diselenide is first reduced to a selenol (RSeH) in presence of

GSH. The selenol then reacts with hydroperoxides and gests oxidized to selenenic acid (RSeOH). This selenenic acid on two-step reactions with two moles of GSH is converted back to the selenol.[279] (2) Oxidation pathway in which diselenide can directly react with a hydroperoixde to form RSeOH, which can either be regenerated back to selenol by the thiols as observed in most selenium GPx mimics. However some recent reports indicated that aliphatic selenoacids (like DSePA) in presence of excess hydroperoxide may also undergo further oxidation to form seleninic acid (RSeOOH), which may finally be converted into smaller products that do not cause recycling of the enzyme.[277] Since DSePA showed higher affinity for peroxide it can be inferred that the GPx activity of DSePA may arise through the oxidation pathway as shown in scheme - 4.2.

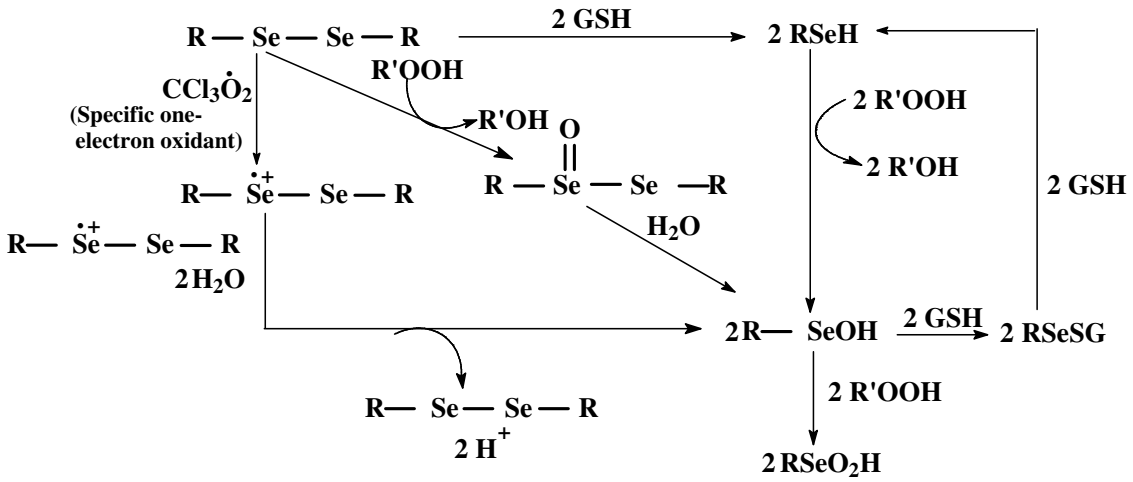

where R= -CH_2CH_2COOH

R′= alkyl/aryl group

Scheme 4.2: *Catalytic mechanism of DSePA*

4.2.2 Free radical scavenging ability of DSePA

The free radicals scavenging ability of DSePA was evaluated by studying the reaction of peroxyl radicals with DSePA using pulse radiolysis technique. Pulse radiolysis experiments were performed on a 7 MeV linear electron accelerator, using 50

ns electron pulse with an absorbed dose of 8-12 Gy and the transients were detected by absorption spectrometry.[280] Trichloromethyl peroxyl ($CCl_3O_2^{\bullet}$) radicals are model peroxyl radicals, which can be conveniently produced by the radiolysis of aqueous solutions containing 48% 2-propanol and 4% CCl_4.[281] The reactions leading to the generation of peroxyl radicals are shown in scheme 4.3.

$$H_2O \xrightarrow{e^- beam} {}^{\bullet}OH + {}^{\bullet}H + e_{aq}^- \quad (4.4)$$

$${}^{\bullet}OH / H^{\bullet} + (CH_3)_2CHOH \rightarrow (CH_3)_2C^{\bullet}OH + H_2O / H_2 \quad (4.5)$$

$$(CH_3)_2C^{\bullet}OH + CCl_4 \rightarrow (CH_3)_2CO + {}^{\bullet}CCl_3 + H^+ + Cl^- \quad (4.6)$$

$$CCl_4 + e_{aq}^- \rightarrow {}^{\bullet}CCl_3 + Cl^- \quad (4.7)$$

$${}^{\bullet}CCl_3 + O_2 \rightarrow CCl_3O_2^{\bullet} \quad (4.8)$$

Scheme 4.3: *Reactions showing generation of peroxyl radicals*

The reaction kinetics was quantified by following the time dependent changes in the concentration of radicals during the course of their reaction with DSePA. The reaction of DSePA (1 mM) with $CCl_3O_2^{\bullet}$ at physiological pH (~7) produced a transient radical species having absorption spectrum in the wavelength range from 300 to 600 nm, with maximum at 560 nm (Fig. 4.2 (a)). $CCl_3O_2^{\bullet}$ radicals can react with DSePA either by electron transfer or by H-atom abstraction. To understand this, independent experiments on reaction of DSePA with specific one-electron oxidant, $N_3^{\bullet}$ was carried out and the results showed formation of similar transient absorption spectrum (Fig. 4.2 (b)).[282] This confirmed that DSePA reacts with $CCl_3O_2^{\bullet}$ preferentially by electron transfer, forming a selenium centered radical cation ($DSePA^{\bullet+}$) as observed in several other organoselenium compounds.[283]

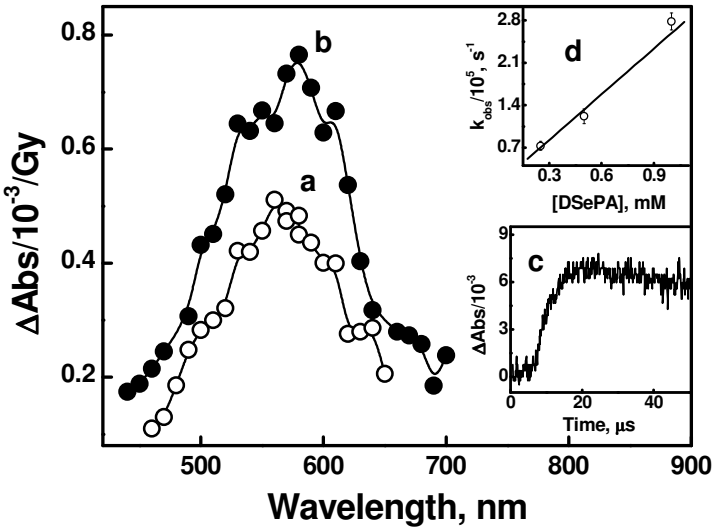

Figure 4.2 *Differential absorption spectrum of the transient species produced on reaction of DSePA (1 mM) with (a) $CCl_3O_2^{\bullet}$ and (b) $N^{\bullet}_3$ radicals at pH 7. Inset (c) shows absorption-time plot for the formation DSePA radical cation at 560 nm. Inset (d) shows variation in the observed pseudo first order rate constant at 560 nm, as a function of DSePA.*

The reactions of DSePA with $CCl_3O_2^{\bullet}$ radicals and one-electron oxidant, $N_3^{\bullet}$ are shown in scheme 4.4.

$$CCl_3O_2^{\bullet} + DSePA \rightarrow DSePA^{+\bullet} + CCl_3O_2^{-} \quad (4.9)$$

$$N_3^{\bullet} + DSePA \rightarrow DSePA^{+\bullet} + N_3^{\bullet} \quad (4.10)$$

Scheme 4.4: *Reactions between DSePA and oxidizing radicals*

In compounds like, DSePA the selenium centre undergoes one-electron oxidation, and due to the presence of electron donating carboxylate groups, the electron density on the selenium atom is increased. This is also responsible for the subsequent stability of the radical cation on the two selenium atoms.[283] Such easy oxidation makes DSePA a very efficient scavenger of oxidizing free radicals. The bimolecular rate constant for the reaction of DSePA with $CCl_3O_2^{\bullet}$ was determined by following the buildup kinetics of the

transient at 560 nm (Fig.4.2, inset (c)) in presence of different concentration of DSePA and from the slope of the linear plot as given in the inset (d) of figure 4.2, the rate constant was determined to be 2.7 x 10^8 $M^{-1}s^{-1}$. Generally rate constants for the reaction of $CCl_3O_2^{\bullet}$ radicals with chain breaking antioxidants like, vitamin E, curcumin, etc are in the same range.[128] Therefore, the peroxyl radical scavenging ability along with GPx mimicking activity of DSePA may contribute to its antioxidant activity. This prompted us to investigate its antioxidant activity using biological models such as red blood cells (RBCs).

4.2.3 Antioxidant activity in human RBCs

The antioxidant activity of DSePA was evaluated in terms of its ability to inhibit (AAPH) induced oxidative damage in human red blood cells (RBCs). For these studies, RBCs suspension in phosphate saline buffer (PBS) were pre-incubated with varying concentration of DSePA at 37^{o}C for 30 min, washed twice with cold PBS and then subjected to AAPH (50 mM) treatment. The 30 min incubation would ensure that DSePA is taken up by the RBCs.

RBC membranes are highly susceptible to AAPH induced lipid peroxidation. Figure 4.3(a) shows the variation in lipid peroxidation estimated as TBARS in RBCs after subjecting to AAPH induced damage in the presence and absence of different concentrations of DSePA. The level of TBARS in RBCs was significantly increased after incubation with AAPH as compared to the control sample. In the presence of DSePA, there was a significant decrease in TBARS formation and this inhibition increased with increasing DSePA concentration from 12.5 to 125 μM, from which the IC_{50} value, i.e. the

concentration of DSePA required to inhibit TBARS formation by 50%, was found to be 45 ± 5 μM.

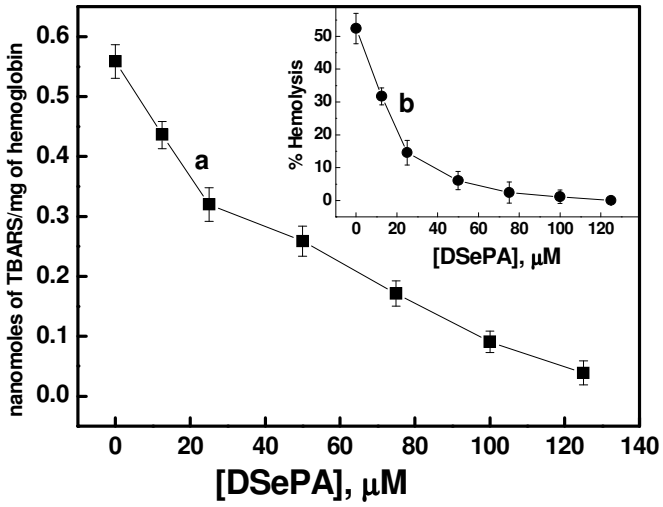

Figure 4.3 *Variation of lipid peroxidation (a) and percent hemolysis (b) in human RBCs induced by 50 mM AAPH after incubation for 3 hours at different concentrations of DSePA. Results are presented as mean ± SEM (n =3).*

Subsequent to membrane damage RBCs undergo leakage of hemoglobin (hemolysis) and K^+ ions from within. Accordingly, when aqueous suspension of RBCs was incubated with AAPH, about 52% of hemolysis was observed. The percent hemolysis progressively decreased with increasing concentration (12.5 to 125 μM) of DSePA and at 125 μM of DSePA there was no hemolysis. From this, the IC_{50} value was estimated to be 20 ± 2 μM.

Similarly the percent K^+ ion loss in RBCs after incubation with AAPH and its inhibition by increasing concentrations of DSePA are shown in figure 4.4(a). Incubation of RBCs with AAPH resulted in about 90% loss of intracellular K^+. This process was inhibited in a progressive manner when DSePA was added to the reaction system in

increasing concentrations (12.5 to 125 μM). The IC_{50} value for this was estimated to be 75 ± 8 μM.

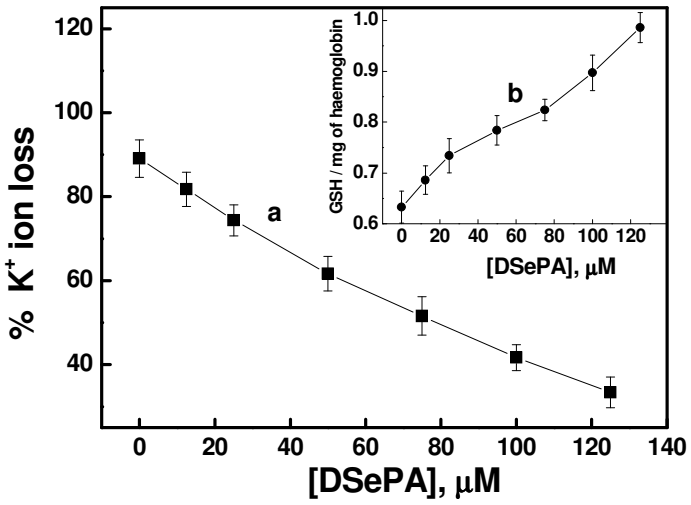

Figure 4.4 *Variation of K^+ ion loss (a) and GSH levels (b) in human RBCs incubated with 50 mM AAPH for 3 hours in presence of different concentrations of DSePA. Results are presented as mean ± SEM (n =3).*

One of the important markers of oxidative damage in RBCs is the depletion of intracellular GSH due to its utilization for the scavenging of free radicals. Therefore GSH levels were also monitored in RBCs after AAPH induced hemolysis. Inset (b) of figure 4.4 shows change in GSH levels in RBCs after treatment with AAPH and also in presence of increasing concentration of DSePA (12.5 to 125 μM). The normal basal level of GSH in RBCs was found to be 1.07±0.05 nmoles/mg of hemoglobin and after incubation with AAPH, the GSH level reduced to about 0.63±0.03 nmoles/mg of hemoglobin. Addition of DSePA to this reaction system prevented the reduction in GSH content in a concentration dependent manner.

The incubation of RBCs with DSePA in the absence of AAPH did not show any significant change in the level of TBARS, hemolysis, percent K^+ ion and GSH content as compared to control sample indicating DSePA itself could not induce oxidative damage to RBCs. All these results confirmed antioxidant activity of DSePA. After ensuring its antioxidant activity DSePA was examined for toxicity in cells and in mice model.

4.2.4 *In vitro* cytotoxicity studies

The cytotoxic effect of DSePA was studied in normal quiescent splenic lymphocytes and their syngenic constitutively proliferating EL4 cells (T cell lymphoma of murine origin) by the MTT dye conversion assay.[194]

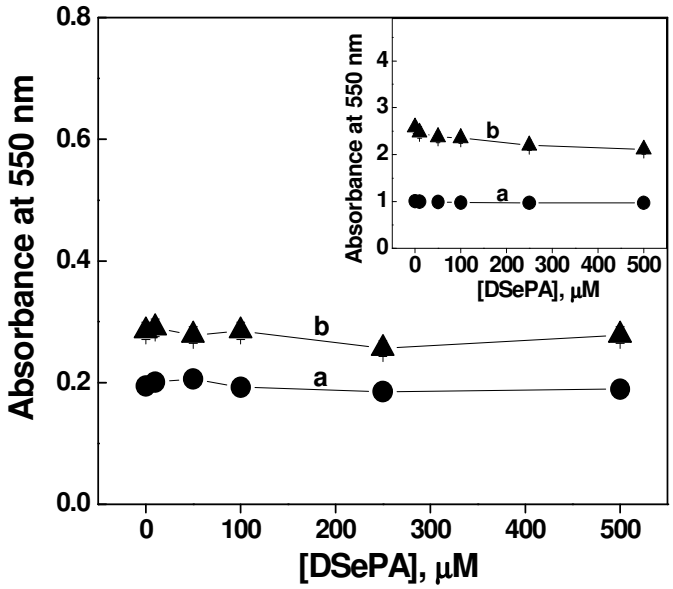

Figure 4.5 *Effect of DSePA concentration on the viability of freshly isolated spleen lymphocytes for (a) 24 hr and (b) 48 hr assayed by MTT. Inset shows the effect of DSePA concentration on the viability of tumor cell line EL4 for (a) 24 hr and (b) 48 hr assayed by MTT. Results are presented as mean ± SEM (n =3).*

Figure 4.5 and the inset show viability of lymphocytes and EL4 cells, respectively cultured for 24 (curve a) and 48 h (curve b) in presence of different concentrations of DSePA. It can been seen from figure 4.5 that there was no effect of DSePA in the concentration range of 10 to 500 μM on the viability of either lymphocytes or EL4 cells, confirming that DSePA is non-toxic to these cells under *in vitro* conditions.

4.2.5 *In vivo* acute toxicity studies

The antioxidative properties of DSePA as explained in earlier sections encouraged us to evaluate it for radioprotection in animal models. However, before proceeding for the *in vivo* studies it is essential to understand its behavioural toxicity. Therefore, acute toxicity of DSePA was studied in Swiss albino mice. For this, animals were divided into groups of 10 each and were injected with DSePA (i.p.) in the dosage range of 0.25 to 120 mg/kg body weight, observed continuously for 2 h, then, frequently up to 6 h, and daily thereafter for 30 days, and mortality if any was recorded. The control group was injected i.p. with saline solution. Administration of DSePA at a dose of 0.25 – 40 mg/kg body weight did not produce any noticeable signs of toxicity within 30 days. However, administration of 120 mg/kg resulted in the death of mice within 24 h. Hence, effect of graded doses in the range between 40 to 120 mg/kg on the survival of the mice was studied. The average percent mortality (n = 10) was converted into probit values by referring to appropriate table according to the previously reported procedure.[284,285] The LD_{50} dosage was estimated to be 88.6 mg/kg body weight from the plot of probit values against logarithmic dose of DSePA for i.p. mode of administration in the mice (Fig. 4.6).

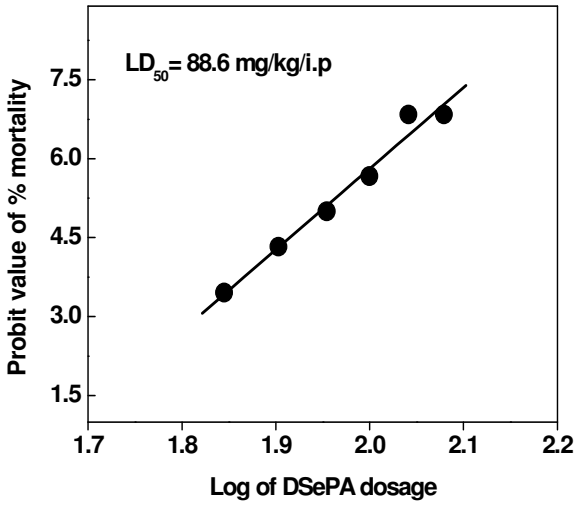

Figure 4.6 *Determination of LD_{50} dosage of DSePA in Swiss albino mice (n = 10).*

Further as per standard definition, $1/10^{th}$ of the LD_{50} dosage is considered as maximum tolerable dose (MTD), which is equivalent to 8.6 mg/kg body weight (i.p.). Therefore, for present radioprotection studies in the mice, a completely safe and nontoxic dosage of 2.0 mg/kg was selected.

4.2.6 *In vivo* radioprotection studies

Earlier reports suggested that selenium compounds exhibit biological effect only when they are administered as supplement, in the present study it was planned to investigate the radioprotective effects of DSePA by administering it at a non toxic dosage for 5 consecutive days prior to irradiation.[276] For this, mice were divided into four groups with 5 animals in each group. Group I was injected i.p. with saline solution for 5 consecutive days and served as sham control group. Group II was γ-irradiated (radiation control). Group III was injected with DSePA (2 mg/ Kg body weight i.p.) for 5 consecutive days (DSePA control). Group IV received a daily injection of DSePA (2 mg/Kg body weight i.p.) for 5 consecutive days and 1 h after the last dose, mice were γ-

irradiated (DSePA pretreatment). For irradiation, mice were randomized, placed in ventilated perspex containers and subjected to whole body γ-irradiation from ^{60}Co Theratron –780 (Atomic Energy of Canada Ltd, Canada) at a dose rate of 0.52Gy/min and an SSD of 100 cm at BARC centre and from ^{60}Co Theratron teletherapy unit (Siemens, Germany) at a dose rate of 1.66Gy/min and an SSD of 55.1 cm at Manipal College of Pharmacy, India. The absorbed radiation dose for each experiment was decided as per the previous standardizations, in such a way that significant damage in irradiated group as compared to control group is observed.[198] After irradiation, animals were maintained under normal laboratory conditions and sacrificed by cervical dislocation to study the protection of different organs like hepatic, hematopoietic and gastrointestinal (GI) systems. All the experimental data were analyzed by one-way ANOVA using Origin (version 6.1) software and P values ≤ 0.05 was considered as a significant.

4.2.6.1 Hepatoprotection

The hepatoprotective effect was evaluated by estimating the levels of enzymatic and nonenzymatic antioxidants, hepatic architecture and liver functions. The effect of DSePA on intracellular antioxidant status at both enzymatic and non-enzymatic levels was investigated at 24 h after exposure to an absorbed dose of 3 Gy. Irradiation led to the decrease in the activities of antioxidant enzymes like GPx, catalase and superoxide dismutase (SOD) by 29, 22 and 48 % respectively with respect to the sham control. The experimental data in form of bar graph is shown in figure 4.7 (A-C). DSePA pretreatment ameliorated the effect of radiation exposure and resulted in significant increase in the activities of GPx, catalase and SOD enzymes by 62, 15 and 44 % respectively compared

to the radiation control group. The DSePA control group showed negligible change in the activities of SOD and catalase enzymes; however there was a significant increase (1.5 folds) in the GPx activity compared to sham control group.

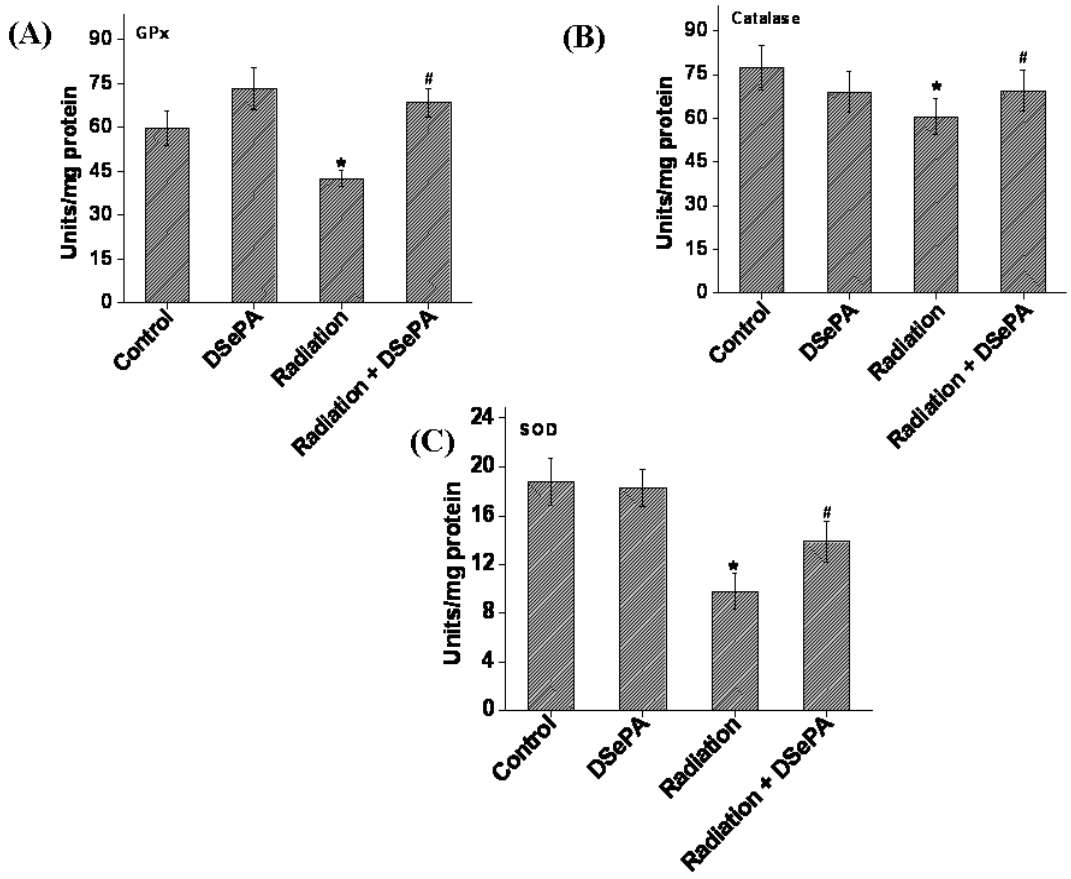

Figure 4.7 *Effect of DSePA pre-administration on γ-radiation (3 Gy) induced changes in the levels of antioxidant enzymes namely (A) GPx (B) catalase (C) SOD in hepatic tissues. The enzymes activities were determined at 24 h post irradiation. Results are presented as mean ± SEM (n =5). *P<0.05 as compared to control group, #P<0.05 as compared to irradiated group.*

Figures 4.8A and 4.8B show levels of total thiols and GSH in the hepatic tissue of different treatment groups. It can be seen that irradiation led to the significant decrease in total thiols and GSH levels, however DSePA pretreatment prevented this. The DSePA control group showed negligible changes in total thiols and GSH levels compared to the sham control group.

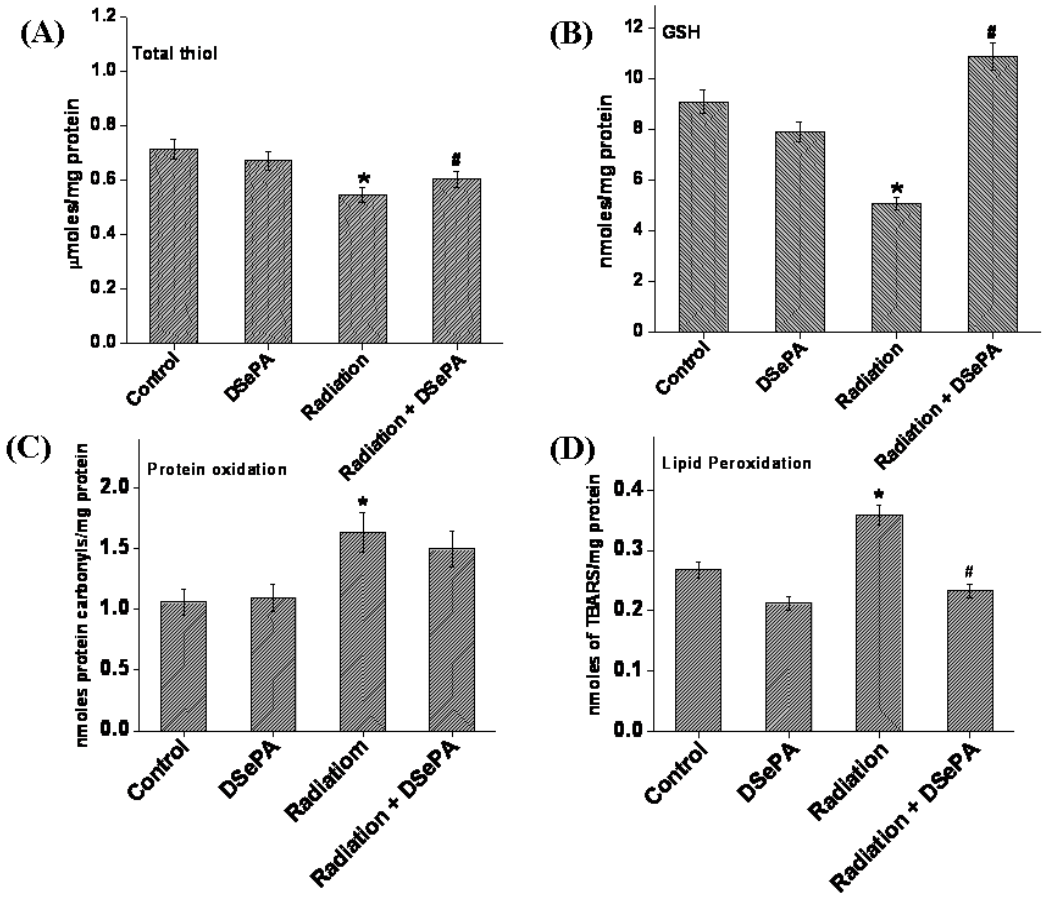

Figure 4.8 *Effect of DSePA pre-administration on the on γ-radiation (3 Gy) induced (A) GSH level (B) total thiol (C) lipid peroxidation and (D) protein carbonyls estimated at 24 h post irradiation. Results are presented as mean ± SEM (n=5). *P<0.05 as compared to control group, #P<0.05 as compared to irradiated group.*

The radiation induced hepatic damage was also confirmed by increase in the levels of protein carbonyls and TBARS in hepatic tissues of irradiated mice as compared to the sham control group. The results in the form of bar graph are shown in figures 4.8C and 4.8D. DSePA pretreatment reduced the lipid peroxidation and protein carbonyls respectively by 34 and 14 % compared to the radiation control group. The DSePA control group did not show induction of lipid peroxidation and protein oxidation as the TBARS and protein carbonyl levels were on par with those of the sham control values.

The effect of DSePA and γ-radiation on liver function was evaluated by estimating the levels of hepatic enzymes like alanine aminotransferase (ALT) and aspartate aminotransferase (AST) in serum of mice collected on 7th day post irradiation (3 Gy) and the results are shown in figure 4.9.

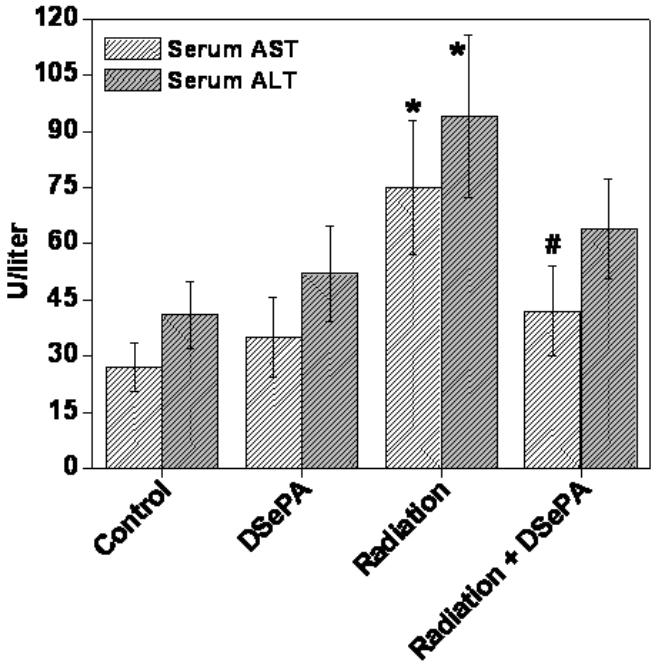

Figure 4.9 *Effect of DSePA pre-administration on the γ-radiation (3 Gy) induced changes in the levels of serum ALT and AST activities estimated on 7th day post irradiation. Results are presented as mean ± SEM (n=5). *P<0.05 as compared to control group, $^{\#}$P<0.05 as compared to irradiated group.*

Exposure to γ-radiation led to a significant increase in the levels of both serum ALT (130%) and AST (179%). DSePA pretreatment ameliorated irradiation induced elevations in ALT and AST serum levels. However, the levels were still higher by 58% and 55% for ALT and AST respectively over that of the sham control levels. The DSePA control group did not show any noticeable increase in the levels of ALT and AST.

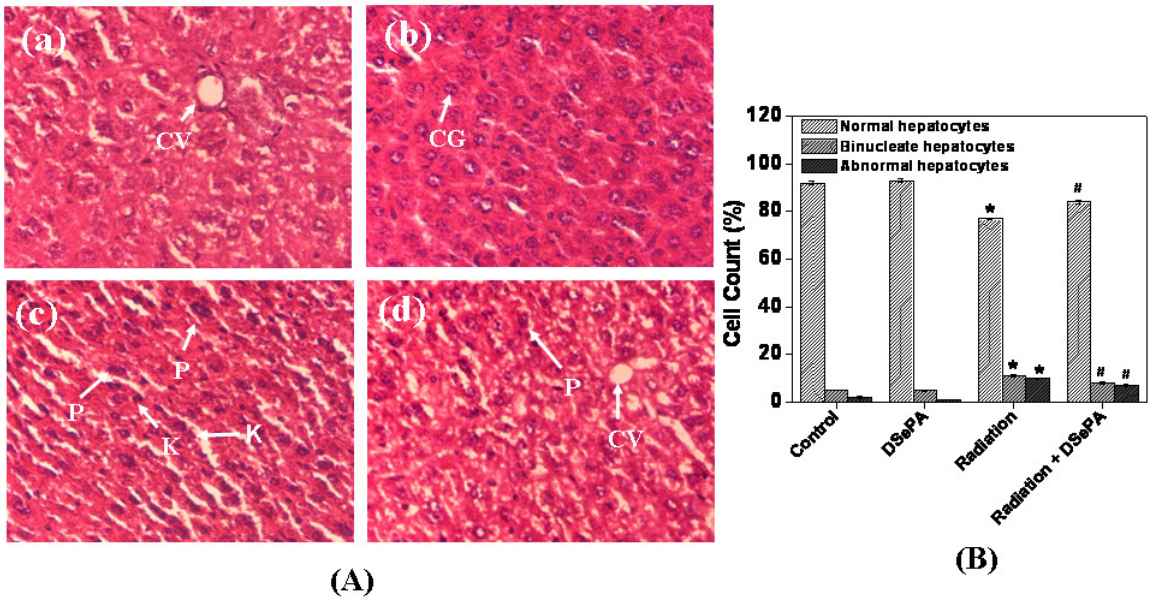

Figure 4.10 *Histopathological analysis of liver tissues performed on 7th day post irradiation. (A)(a) Normal control; (b) Mice administered with DSePA; (c) Mice exposed to 5 Gy of γ-radiation; (d) Mice administered with DSePA and exposed to 5 Gy of γ-radiation. (B) Bar graph showing percent variation in the count of normal, binucleate and abnormal hepatic cells under different treatment conditions. The tissue sections were stained with Eosin and Harris Haematoxylin and observed at 400 X magnification. Results are presented as mean ± SEM (n=5). Central vain - CV, Kuffer cell – K, Chromatin granule – CG, Pyknotic nuclei – P. *P<0.05 as compared to control group, #P<0.05 as compared to irradiated group.*

Further, effect of DSePA and γ-radiation on hepatic architecture was studied on 3rd day after exposure to an absorbed dose of 5 Gy. The histopathological analysis of hepatic tissues from radiation control groups indicated fragmentation of hepatic cells along with presence of many pyknotic and inflammatory kuffer cells as shown in figure 4.10A(c) and 4.10B. Hepatic tissues from DSePA control group showed normal appearance of hepatocytes (Fig. 4.10A(b) & B). However, the irradiated group receiving prior treatment of DSePA displayed normal appearance of hepatocytes along with decrease in the number of pyknotic and kuffer cells (Fig. 4.10A(d) & B). Therefore, the

results indicate prophylactic action of DSePA against γ-radiation induced hepatic damage.

4.2.6.2 Hematopoietic protection

The hematopoietic protection was assessed by calculating spleen index (spleen weight/total body weight), spleen cellularity and endogenous spleen colony formation. Effect of DSePA on spleen index, spleen cellularity and spleen colony formation was studied on 11th day after exposure to an absorbed dose of 7.5 Gy and the results are shown in figures 4.11A, 4.11B and 4.11C respectively.

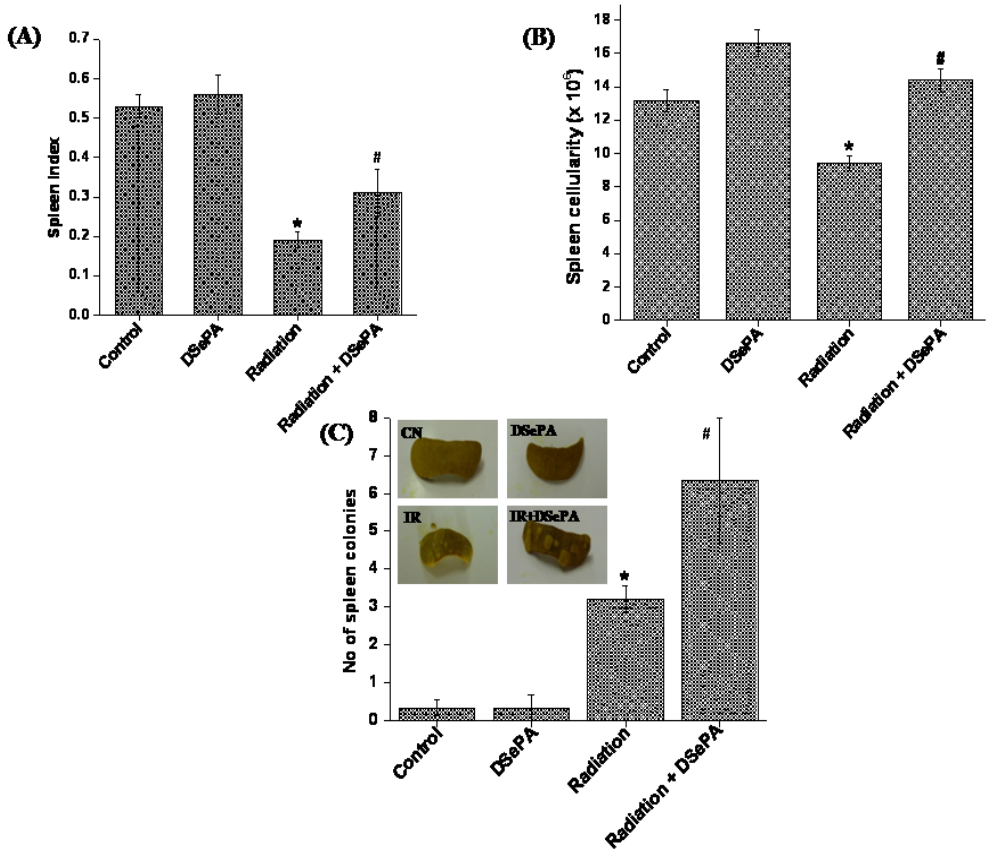

Figure 4.11 *Bar graphs showing effect of DSePA on spleen parameters excised 11 days after 7.5 Gy irradiation in mice (A) spleen index (B) spleen cellularity (C) spleen colonies, Inset shows the photographs of spleen tissue. Results are presented as mean ± SEM (n=5). IR – Irradiation. *P<0.05 as compared to control group, $^{\#}$P<0.05 as compared to irradiated group.*

Effect of DSePA on spleen index, spleen cellularity and spleen colony formation was studied on 11th day after exposure to an absorbed dose of 7.5 Gy and the results are shown in figures 4.11A, 4.11B and 4.11C respectively. Irradiation led to significant reduction in the spleen index (0.19 ± 0.01) as compared to the sham control (0.53 ± 0.03). DSePA pretreatment improved the spleen index to 0.36 ± 0.06 in comparison to radiation control. The spleen cellularity in different treatment groups were checked by counting the number of viable cells using trypan blue dye exclusion test. The results indicated that irradiation decreased the spleen cellularity by 32% as compared to sham control and DSePA pretreatment improved it by 60%. Apart from these data, another important parameter of hematopoietic protection is the evaluation of macroscopic colonies that arise in the spleens of irradiated animal. DSePA pretreatment induced the formation of colonies measured in terms of colony forming units (CFU) by 2.5 folds (8.50 ± 1.18), as compared to the radiation control (3.20 ± 0.37). No significant change in spleen index, spleen weight and CFU was observed in DSePA control group.

4.2.6.3 GI protection

It is known that exposure of animals to high doses of radiation (5–12Gy) causes acute death by inducing GI syndrome. GI syndrome is characterized by death of crypt cells, endothelial cell (villi) decrease in villus height and infiltration of inflammatory cells.[73] These parameters can be visibly scored by microscopic observation of villi height, number of villi and crypt cells in the histopathological grade sections made from intestinal tissue. The effect of DSePA against γ-radiation induced GI damage was checked on 3rd day after exposure to an absorbed dose of 7.5 Gy and the results are presented in figure 4.12.

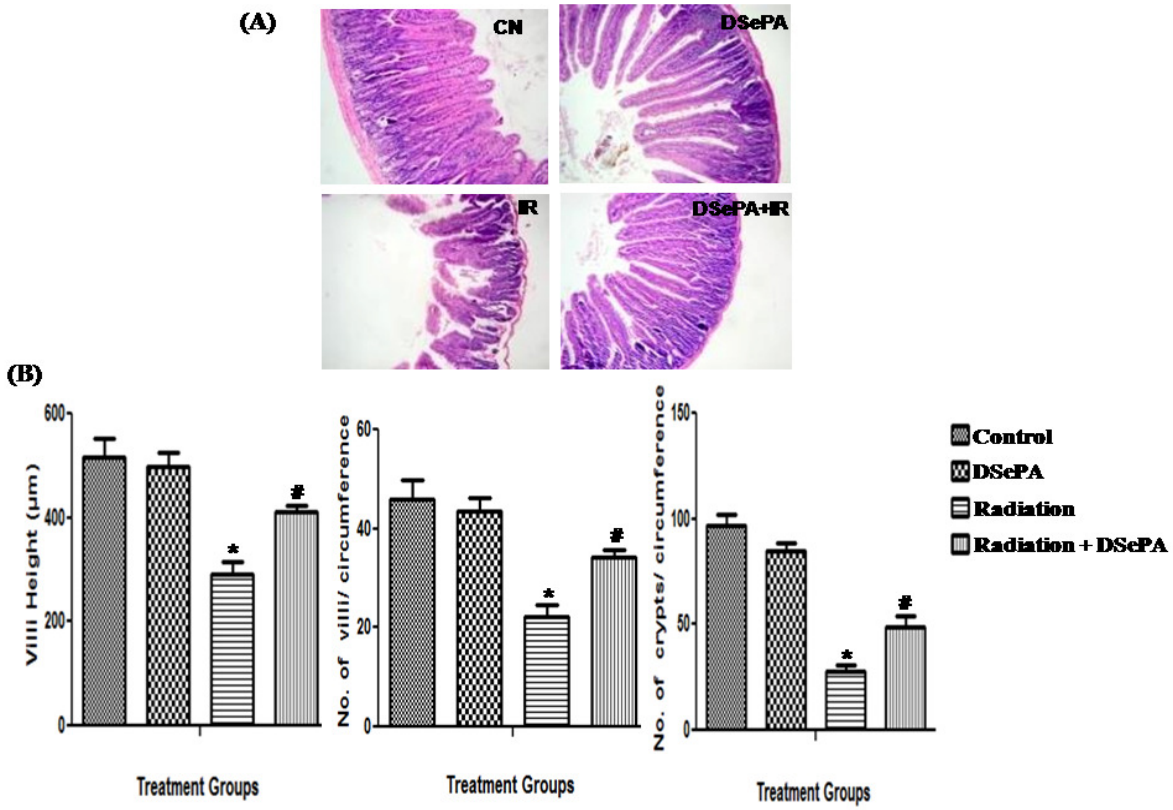

Figure 4.12 *Effect on DSePA on GI (jejunum) parameters excised 3 days post irradiation (7.5 Gy). (A) Histopathology of jejunum excised from animals of different groups. (B) Bar graph showing average villi height, no of villi and no of crypts obtained by analyzing 10 sections/mouse (n=5). CN – Control. IR – Irradiation. *P<0.05 as compared to control group, #P<0.05 as compared to irradiated group.*

Significant decrease in the number of villi, villus height, crypts and goblet cells per crypt was observed in the radiation control group compared to the sham control group. Also, increase in the number of dead cells, inflammatory cells, infiltration of fibroblasts was noticed in intestinal (jejunum) tissue of the radiation control group. DSePA pretreatment protected the crypts, villi and maintained villus height from radiation damage while there was no noticeable change in goblet and dead cells on post-irradiation (Fig. 4.12A and 4.12B). The overall improvement was evident from the gross anatomy of the intestinal sections. No anatomical changes were observed in DSePA control group.

4.2.6.4 Inhibition of DNA damage

One of the important targets of radiation is the DNA, which is also responsible for permanent radiation induced changes in the cells.[200] The ability of DSePA to protect from γ-irradiation induced DNA damage was checked in peripheral leukocytes by single cell gel electrophoresis (comet assay) at 30 min after exposure to an absorbed dose of 3 Gy. Typically, nucleoids of cells from sham control group were observed to be circular in shape while those from radiation control group looked like comets with maximum fluorescent intensity in the head region and diminishing towards the tail region, indicating higher magnitude of DNA damage. Figure 4.13A shows the frequency distribution histograms of tail length (TL), tail moment (TM), olive moment (OM) and percentage of DNA in the tail of blood leukocytes isolated from animals of different treatment groups. It can be observed from the figure that the levels of TL, TM, OM and the percentage of DNA in the tail was higher in the radiation control group as compared to sham control. However, cells from the irradiated group receiving prior treatment of DSePA showed significant decrease in the levels of TL, TM, OM and percentage of DNA and the levels were close to those of the sham control group. All the comet parameters in DSePA control group showed similar trend as that of the sham control indicating that DSePA by itself did not induce any DNA damage.

The DNA damage in hepatic tissue under similar treatment conditions was evaluated by examining the intactness of genomic DNA through agarose gel electrophoresis. The electrophoretic pattern of genomic DNA isolated from the hepatic tissue of different groups is shown in figure 4.13B. The radiation control group showed smear of DNA fragments along with generation of a few low molecular weight

fragments, indicating DNA damage. The group treated with DSePA prior to irradiation showed reduction in shearing of the DNA as compared to the radiation control. The DSePA control group showed intact DNA indicating no induction of DNA damage.

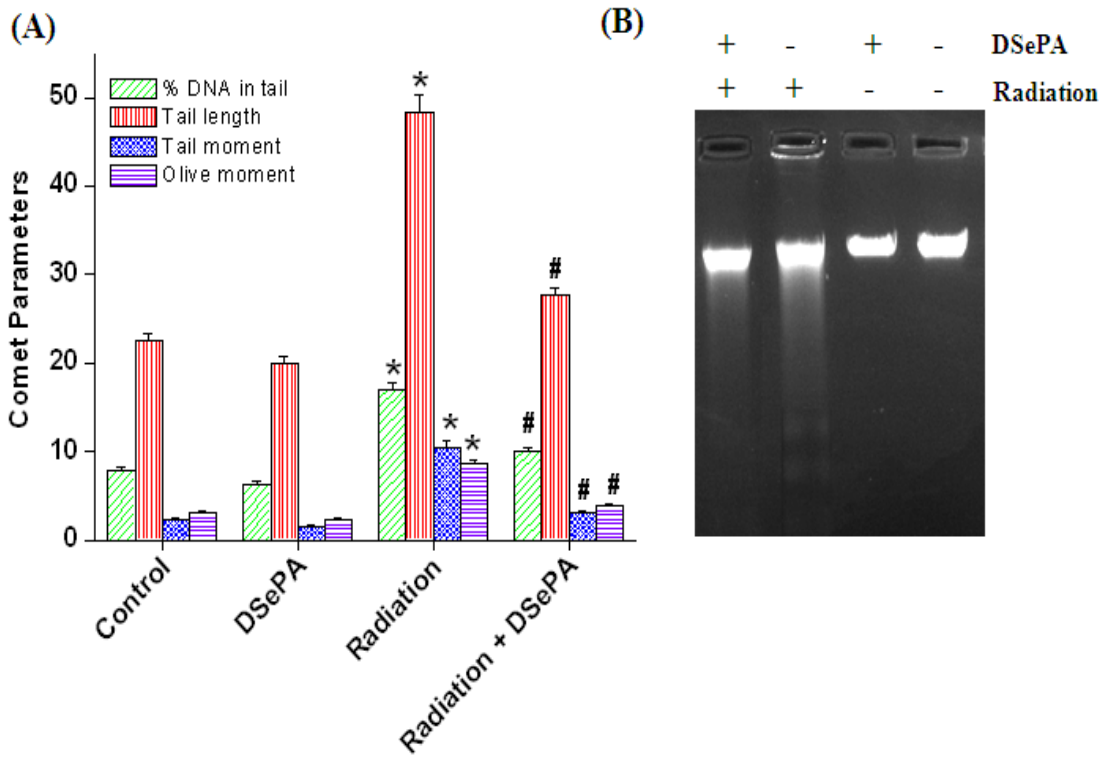

Figure 4.13 *Effect of DSePA on γ-radiation induced DNA damageat 30 min post irradiation (3 Gy) (A) In peripheral leukocytes by Comet assay (A) DNA Fragmentation in mice liver tissue. Bar graph represents means mean ± SEM obtained by analyzing 50 cells/mouse (n=5). *P<0.05 as compared to control group, #P<0.05 as compared to irradiated group.*

4.2.6.5 mRNA expression analysis of anti-apoptotic and DNA repair genes

The molecular mechanism responsible for radioprotective effect of DSePA was elucidated by studying its effect on the expression of anti-apoptotic and DNA repair genes at mRNA level by reverse transcription–polymerase chain reaction (RT-PCR) in spleen and hepatic tissue. The primers used for RT-PCR are listed in table 4.1.

Table 4.1: *Gene specific RT-PCR primers*

Genes	**Primer Sequence**	
GAPDH	Forward	5'-AATGTGTCCGTCGTGGATCTGA-3'
	Reverse	5'-GATGCCTGCTTCACCACCTTCT-3'
p21	Forward	5'-ATGTCCAATCCTGGTGATGT-3'
	Reverse	5'-TGCAGCAGGGCAGAGGAAGT-3'
GADD45α	Forward	5'-TGGTGACGAACCCACATTCAT-3'
	Reverse	5'-ACCCACTGATCCATGTAGCGAC-3'
Bcl-2	Forward	5'-TTCGCAGCGATGTCCAGTCAGCT-3'
	Reverse	5'-TGAAGAGTTCTTCCAACCACCGT-3'
BAX	Forward	5'-ATGCGTCCACCAAAGAAGCTGA-3'
	Reverse	5'-AGCAATCATCCTCTGCAGCTCC-3'

The oxidative damage caused to cellular components soon after irradiation forces cell to undergo apoptosis and hence for a chemical agent to be an effective radioprotectant, it must inhibit apoptosis. To study the effect of DSePA on γ-radiation induced apoptosis, the mRNA expression levels of *Bcl-2* and *BAX* genes in spleen and hepatic tissue at 24 h after exposure to an absorbed dose of 3 Gy was monitored. The RT-PCR analysis of these two genes and their relative expression levels are shown in figure 4.14. The results indicate that the level of *Bcl-2* expression decreased, along with notable increase in the level of *BAX* expression in both spleen and hepatic tissues of radiation control group as compared to the sham control group. DSePA pretreatment, increased the expression of *Bcl-2* gene, while, the expression of *BAX* gene reduced. The DSePA control group showed no significant changes in the expression levels of *Bcl-2* and *BAX* genes as compared to the sham control. The above observed protection from apoptosis rendered by DSePA could be due to induction of DNA repair genes.

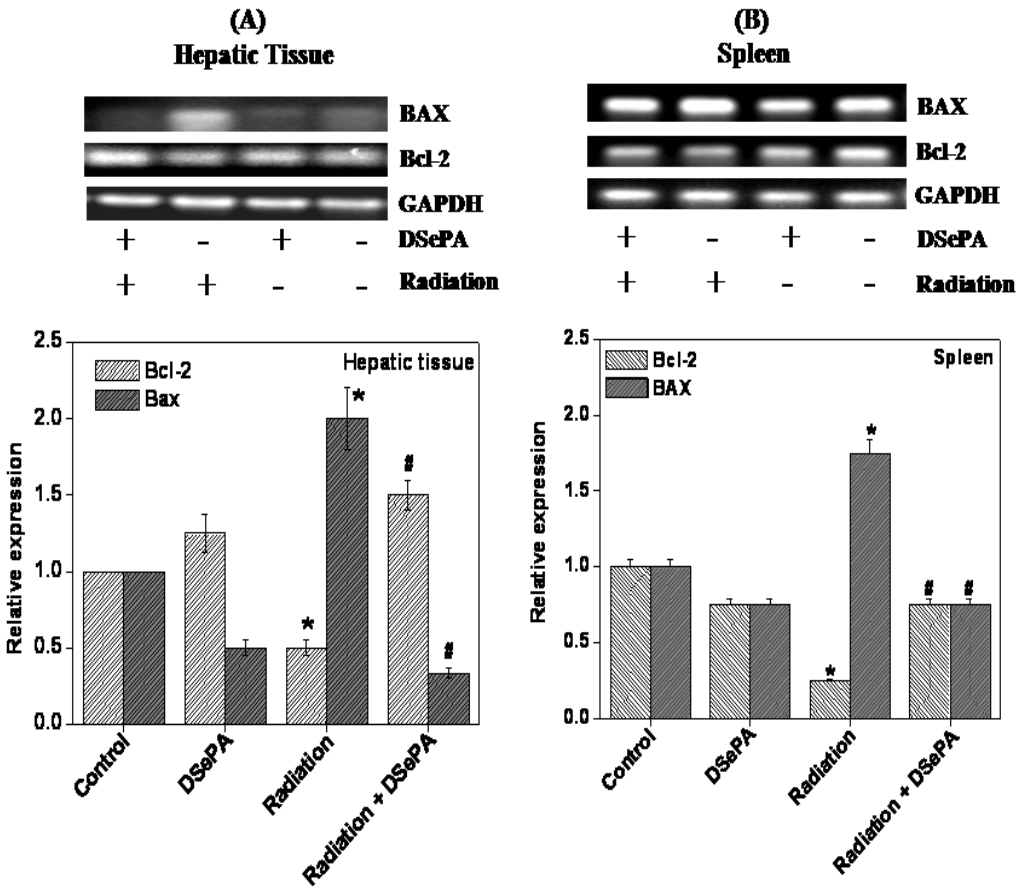

Figure 4.14 *Effect of DSePA on the mRNA expression of Bcl-2 and BAX genes at 3 h post irradiation (3 Gy) as monitored by RT-PCR analysis. (A) hepatic tissue. (B) spleen. Results are presented as mean ± SEM (n=5). *P<0.05 as compared to control group, #P<0.05 as compared to irradiated group.*

To establish this, mRNA expression levels of *p21* and *GADD45α* genes in both spleen and hepatic tissue at 3 h post irradiation were followed. The RT-PCR analysis of these genes and their relative expression levels are shown in figure 4.15. The results indicated that irradiation causes substantial increase in the levels of *p21* and *GADD45α* expression in both the tissues compared to the sham control group. However, the magnitudes of induction of both the genes were lower in the spleen as compared to the

hepatic tissue resulting in the sensitivity of spleenocytes to radiation. DSePA pretreatment significantly reduced the induction of *p21* gene in both the tissues, however its expression level was still higher compared to the sham control group. Additionally, DSePA augmented the expression level of *GADD45α* in both the tissues post irradiation. The DSePA control group showed negligible change in the expression of *p21* and *GADD45α* genes in the spleen as compared to the sham control. However in the hepatic tissue the DSePA treatment led to significant decrease in the expression of *p21* but no change in the expression of *GADD45α* was observed as compared to the sham control.

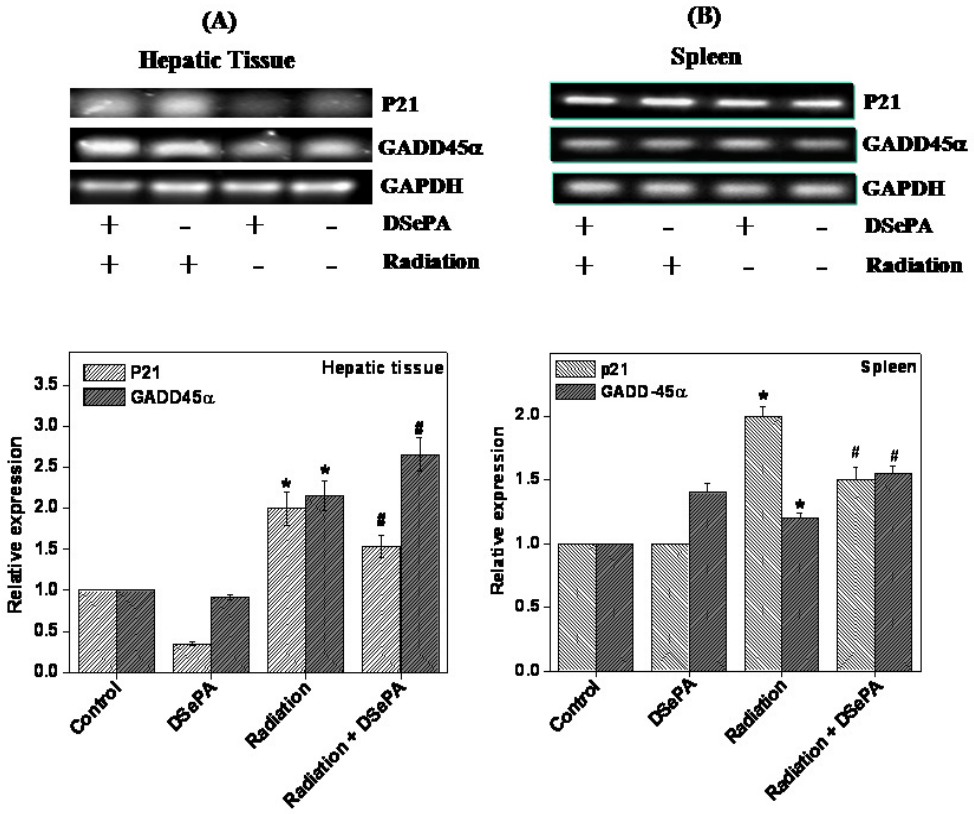

Figure 4.15 *Effect of DSePA on the mRNA expression of p21 and GADD45α genes at 3 h post irradiation (3 Gy) as monitored by RT-PCR analysis (A) hepatic tissue. (B) spleen. Results are presented as mean ± SEM (n=5). *P<0.05 as compared to control group, #P<0.05 as compared to irradiated group.*

4.2.6.6 Survival studies

The ability of DSePA to inhibit radiation-induced mortality was checked by survival studies. For this, animals were divided into four groups of 10 each and treated as described previously. The animals were monitored daily for 30 days after irradiation, and mortality was recorded. Survival curves were drawn by plotting percentage survival as a function of post-irradiation day. The effect of DSePA on survival of mice after whole body γ-irradiation at a lethal dose of 10 Gy is shown in figure 4.16A. The radiation control group exhibited signs of radiation sickness such as reduced intake of food and water, irritability, lethargy, ruffling of hair, weight loss, diarrhea, emaciation and epilation with median survival of only 11.5 days. DSePA pretreatment lowered the radiation sickness characteristics and increased the median survival time to 15.5 days. In DSePA pretreated group, the survival of animals at the end of 30 days after irradiation, increased by 30 %. DSePA control group did not show any toxic effects during the study period.

For estimating DMF, radiation dose-response curve was made by plotting the percentage survival of animals at the end of 30 days against the radiation doses (7–11Gy). From this curve the radiation $LD_{50/30}$ dose was estimated to 9.31 Gy.

$$DMF = \frac{Radiation\ LD_{50/30} in\ presence\ of\ drug}{Radiation\ LD_{50/30} in\ absence\ of\ drug} \qquad 4.11$$

DSePA pretreatment increased the radiation $LD_{50/30}$ of 9.31 to 10.29 Gy resulting in a DMF of 1.10 according to equation 4.11. Figure 4.16B shows the radiation dose curve.

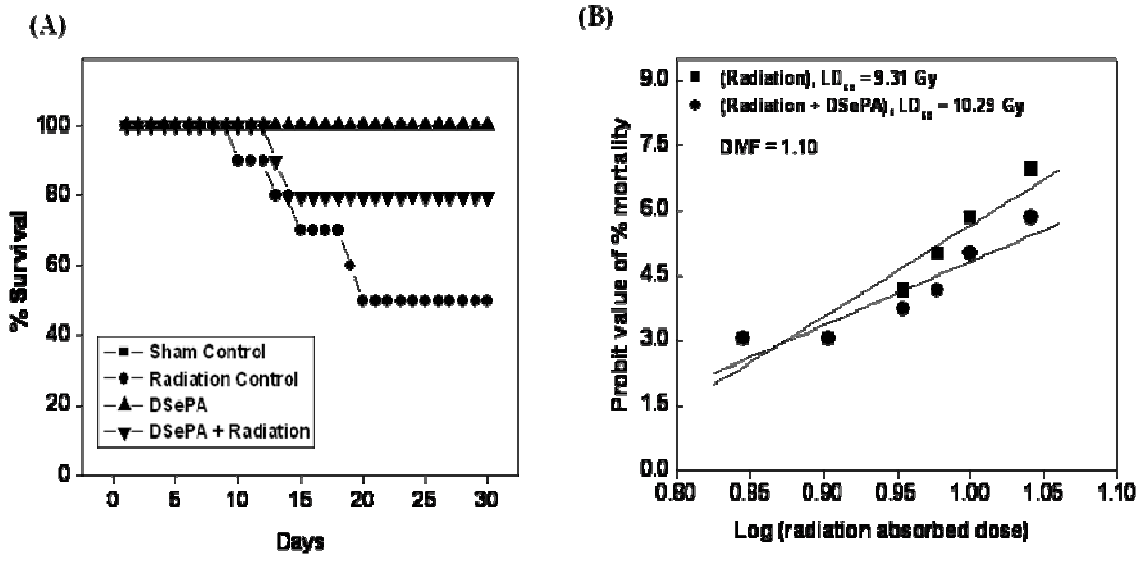

Figure 4.16 *(A) Kaplan-Meier estimate of 30 day survival of whole body 10 Gy γ-irradiated mice pre-administered with DSePA in comparison to other groups (B) Radiation dose response of DSePA against 7, 8, 9, 9.5, 10 and 11 Gy. Results are presented as mean ± S.E.M (n = 10).*

4.3 Discussion

Organoselenium compounds are being considered as new class of GPx active antioxidants because of their greater bioavailability, less toxicity and anti-inflammatory activity.[153,176] With our recent interest in the design of water-soluble bioactive selenium compounds, we have synthesized a simple, stable and water-soluble organoselenium compound, 3,3'-diselenodipropionic acid (DSePA). In the present study we tested the GPx like catalytic activity, free radical scavenging, antioxidant activity and radioprotective capability of DSePA. The GPx activity of the compound was evaluated by estimating its mass equivalent for one GPx unit and kinetic parameter such as K_m values for peroxide and thiol separately using the L-B plots. The results indicated that DSePA has more affinity towards the peroxide than the thiol and 12.84 mM of DSePA is equivalent to one unit of GPx. The GPx activity of DSePA in terms of mass equivalent

indicates that it has lower activity than the reported value for well known standards like ebselen.[57] The reason for this could be the higher affinity of DSePA for peroxides leading to oxidation of DSePA in to seleninic acid (RSeOOH) which is not recycled efficiently.[277] In addition to the GPx activity, DSePA was also observed to be a good scavenger of peroxyl radicals and the rate constant is comparable to well known GPx mimic ebselen and chain breaking antioxidants like vitamin E.[286]

With this background, the antioxidant activity of DSePA was evaluated by studying its ability to inhibit lipid peroxidation of the membrane fatty acids, loss of hemoglobin and release of intracellular K^+ ions in human RBCs treated with AAPH.[179] The results obtained from these studies indicated that DSePA protects RBCs from AAPH induced free radical damage. However, their IC_{50} values were not the same and followed the order as, K^+ ion loss > lipid peroxidation> hemolysis. This is probably because hemoglobin molecule with big size is difficult to be released from the damaged membranes, while K^+ ions, being smaller in size can be leaked even with slight disturbance in the membrane structure. Thus at a concentration of DSePA, where it shows little protection to membrane damage (assessed in terms of lipid peroxidation) can have a significant impact on the prevention of hemoglobin loss from RBCs, while to prevent the loss of intracellular K^+ ions, a much higher concentration of DSePA is required. GSH, a tripeptide containing cysteine, is the most abundant antioxidant present in mammalian cells.[28] During oxidative stress the exogenously applied antioxidants protect GSH levels in cells by preventing them from being consumed in reaction with free radicals.[219] Accordingly, our results indicated that the GSH levels reduced significantly in RBCs after AAPH incubation, but pretreatment with DSePA in the

concentration range (5-100 μM) prevented the decrease in GSH level. This observed antioxidant effect is likely due to both its ability to scavenge peroxyl radicals and its ability to act as a GPx mimic.

All these results prompted us to investigate the *in vivo* efficacy of DSePA to act as a radioprotector against γ-radiation induced oxidative stress. However, the necessary parameter to be evaluated before performing *in vivo* experiments is its acute toxicity. The *in vitro* toxicity of DSePA was studied using splenic lymphocytes and a tumor cell line of T cell (EL4). The results indicated that DSePA is non-toxic to both normal and tumor cells in the concentration range, where potent antioxidant activity was observed. The acute toxicity study of DSePA in Swiss Albino mice revealed its MTD as 8 mg/kg/i.p and thus any dosage below this would be safer for animal studies. Therefore in the present study a non toxic and safe dose of 2 mg/kg/i.p was employed and protection to various radiosensitive organs against γ-radiation was examined.

In line with the previous reports, irradiation induced increase in lipid peroxidation and protein carbonyl levels, and decrease in antioxidant enzymes activities, depletion of GSH/total thiol levels and shearing of DNA in hepatic tissue.[198,287] The histological appearance also diagnosed hepatic damage after γ-irradiation. Although the above studied parameters of oxidative stress provided indication about liver injury, an obvious sign of hepatic injury is the leakage of hepatic enzymes into plasma.[288] Accordingly, increase in the serum AST and ALT levels by γ-radiation indicated hepatic structural damage because these enzymes are localized in cytoplasm and are released in to circulation after cellular damage has occurred. DSePA pretreatment attenuated radiation induced hepatic damage by reversing all these parameters, suggesting its hepatoprotective effects. The

ability of DSePA to regain the normal hepatic architecture indicated its prophylactic action.

Other most sensitive organs to irradiation are the hematopoietic system and GI tract, both of which are critically important for survival.[73] Spleen index is an important marker to monitor damage to hematopoietic system. In the present study, DSePA pretreatment protected the mice from hematopoietic injury as seen from the increase in spleen index, number of spleen colonies and cellularity with respect to radiation control. Additionally, DSePA prevented DNA damage in peripheral leukocytes as shown by the decrease in the comet parameters.[200] Similarly, radiation induced damage to the GI tract is characterized by death of crypt cell, endothelial cell (villi), decrease in villus height and infiltration of inflammatory cells.[73] Excellent radioprotection to GI tract by DSePA was evident from the inhibition of the damage to the crypts, villi cells and maintenance of the height of villi. DSePA also prevented the infiltration of inflammatory cells, dead cells, mitotic cells and hypertrophy of the muscularis mucosa further confirming its ability to protect the GI tract.

We also made an attempt to understand the mechanisms responsible for the above observed radioprotection. Important molecular mechanisms responsible for radioprotection are free radicals scavenging, repair of free radicals induced damage and inhibition of free radicals initiated apoptosis.[65,289] Earlier we showed that DSePA effectively scavenged hydroxyl radicals ($^{\bullet}OH$) with rate constants of 18 x 10^9 $M^{-1}s^{-1}$ and in present study we have observed that it scavenges trichloromethyl peroxyl ($CCl_3O_2^{\bullet}$) with rate constant of 2.7 x 10^8 $M^{-1}s^{-1}$.[290] Therefore this radical scavenging power of DSePA may be involved in the inhibition of lipid peroxidation, protein carbonylation,

DNA damage and also for the maintenance of the antioxidant status (levels of antioxidant enzymes, GSH and total thiol) within the tissue. Additionally, increase in the activities of ROS scavenging enzymes (SOD, catalase, GPx) can also lead to free radical scavenging and subsequent reduction of tissue damage. DSePA itself had no effect on the activity of SOD and catalase enzymes. However, being a selenium compound, DSePA by itself was able to increase the levels of GPx enzymes.[268,149]

In response to radiation induced DNA damage, cells activate *p21* and *GADD45α* genes that regulate the cell arrest (G1/S and G2/M respectively) and DNA repair.[34,291-294] GADD45α is specifically associated with the nucleotide excision repair pathway (NER), which is responsible for DNA repair from genotoxic insults like radiation.[293] If the DNA repair is not successful, cells undergo apoptosis by the activation of mitochondrial dependant intrinsic pathway involving induction of pro-apoptotic gene *BAX* and suppression of anti-apoptotic gene *Bcl-2*.[295] Therefore studying the effect of DSePA on the expression of above genes post-irradiation would provide information on which of the above pathways is involved in the radioprotection. Accordingly, we observed that irradiation led to upregulation of the mRNA expression levels of *p21* and *GADD45α* genes at 3 h post irradiation in spleen and hepatic tissues. While, DSePA pretreatment caused augmentation and inhibition of radiation induced increase in expression of *GADD45α* and *p21* respectively. The decrease in *p21* expression could be due to the inhibition of radiation induced initial DNA damage by DSePA. However, the augmentation of *GADD45α* indicated its probable role in post irradiation G2/M cell arrest and DNA repair. Since, in present study both cell arrest and DNA repair activities have not been examined directly, the definite role of DSePA in these cellular processes

cannot be established at this stage and it would be interesting to explore this aspect in future. Also in accordance with the results on induction of the DNA repair genes, pre-administration of DSePA significantly reduced the γ-radiation induced increase in expression of *BAX* levels and simultaneously increased the expression of *Bcl-2*. This suggested that DSePA is able to inhibit apoptosis. Previous reports also suggest that proliferating cells like lymphocytes are more sensitive to radiation induced apoptosis which could be due to inefficient DNA repair.[295,296] In agreement with this, we observed slightly lesser induction of *GADD45α* gene and a much higher *BAX*/*Bcl-2* ratio (detriment of apoptotic potential of a cell) in spleen as compared to hepatic tissue. The administration of DSePA itself showed marginal induction of *GAD45α* gene, while the expression of *p21* was differentially modulated in spleen and hepatic tissues.

Finally, the above observations on the protection of different radiosensitive organs by DSePA should manifest as the improvement in the survival of animals from radiation induced mortality. Indeed our experiments showed 30% increase in the survival of the mice exposed to a lethal whole body dose of 10 Gy. We also estimated the DMF of this compound by studying the radiation-dose response against 7-11 Gy and was found to be 1.10. Considering that the MTD for DSePA is nearly 8.9 mg/kg, one can expect increase in survival at slightly higher and safe doses. In addition, DSePA was supplemented only for five days prior to irradiation. Therefore increasing the supplementation time also is another alternative for improving the radioprotective efficacy of DSePA.

From the above observations, it is clear that DSePA is a potent antioxidant with GPx activity and showed radioprotective action in mice model. The protective mechanisms of DSePA involved free radical scavenging, maintenance of antioxidant enzymes,

prophylactic action, lowering of DNA damage, induction of DNA repair genes and inhibition of apoptosis.

4.4 Conclusion

3,3'-diselenodipropionic acid (DSePA), a water soluble selenocystine derivative having GPx like activity showed protection to RBCs against free radical induced hemolysis, lipid peroxidation, and K^+ ions leakage indicating its antioxidant activity at cellular level. It was not toxic to normal spleen lymphocytes and EL4 tumor cells up to concentration of 500μM. When administered in to mice at a non-toxic dose of 2 mg/kg/i.p. for five consecutive days prior to γ-irradiation, DSePA showed overall radioprotection. It prevented irradiation induced lipid peroxidation, decreased expression of antioxidant enzymes and inhibited DNA damage. It showed excellent protection to organs that are sensitive to radiation like hematopoietic and gastrointestinal (GI) systems. At the same dosage, DSePA improved the 30 day survival of mice after whole body γ-irradiation at a lethal absorbed dose of 10 Gy by 30% and the dose modification factor is about 1.10. The studies thus confirm that DSePA could be considered as a non-toxic radioprotective agent in planned exposures such as radiotherapy and may be considered as a model compound in the design and synthesis of more stable, active and potent selenium antioxidants having high free radical scavenging ability, good GPx activity, low cytotoxicity, water solubility and radioprotective capability.

CHAPTER 5

SUMMARY

The major findings of the present thesis can be summarized as follows:

1) Curcumin, a natural polyphenol from turmeric has been examined for antioxidant and pro-oxidant effects in human RBC and macrophage model systems.

2) Curcumin treatment protected RBCs from AAPH induced hemolysis and lipid peroxidation in the entire concentration range studied from 1 to 50 μM, however it induced depletion of intracellular GSH levels and leakage of K^+ ions from RBCs even at concentration > 10 μM. These results indicated that curcumin exhibited both antioxidant and pro-oxidant effects in RBCs.

3) The dual antioxidant and pro-oxidant effects of curcumin were reconfirmed in macrophage cells. In these cells, curcumin exhibited time and concentration dependent dual effect of pro-oxidant or antioxidant through mediating changes in levels of cellular ROS, non-protein thiols and expression of antioxidant enzymes such as *GPx*, *catalase*, *Mn-SOD*, *Cu,Zn-SOD* and *HO-1*.

4) In the same macrophage cells, two thiols viz., cell impermeable GSH and cell permeable NAC modulated the antioxidant activity of curcumin. While GSH inhibited the expression of antioxidant genes and ROS production, NAC increased the expression of antioxidant genes and thereby reducing ROS. The opposing effects of GSH and NAC have been attributed to their modulation in curcumin uptake.

5) A 1:1 copper complex of curcumin, which exhibits SOD mimicking activity showed antioxidant effects in lymphocytes after exposure to γ-radiation, as seen by the activation of cytoprotective pathways, reduction of oxidative stress parameters and decrease in apoptosis. Under similar experimental conditions, when compared with curcumin, the complex was found

to be more effective. The studies can be explored to develop such compounds as radioprotectors in future.

6) Curcumin copper complex also appeared better than curcumin in activation of cytoprotective signaling pathways such as protein kinase C delta (PKCδ) and nuclear factor-κB (NF-κB) in temporally relevant manner, which play a crucial role in determining fate of the cell towards survival.

7) Employing absorption and fluorescence spectroscopy, it was possible to quantitatively estimate the uptake of curcumin in two different types of normal cells (lymphocytes, NIH3T3) and two different types of tumor cells (EL4 and MCF7). In general tumor cells exhibited much higher uptake of curcumin compared to the normal cells. Cytotoxicity studies in different cell lines indicated that the toxicity of curcumin increased with increasing uptake.

8) In MCF7 cells, curcumin was found to be localized in different subcellular compartments with maximum localization in the cell membrane followed by cytoplasm and nucleus. The nuclear localization of curcumin indicates its probable direct interaction with genomic DNA, which is of use to understand the molecular actions of curcumin inside the cells.

9) In a cell free system, 3,3'-Diselenodipropionic acid (DSePA) exhibited GPx like activity with higher substrate specificity towards peroxides than thiols.

10) DSePA showed protection to RBCs against AAPH induced oxidative damage indicating its antioxidant activity at cellular level.

11) The *in vivo* toxicity studies of DSePA in Swiss albino mice revealed its LD_{50} value as ~8 mg/kg body weight for i.p mode of administration.

12) Administration of DSePA at a non-toxic dose of 2 mg/kg body weight, i.p., for 5 consecutive days in Swiss albino mice increased GPx activity by 1.5 folds and prevented the radiation (3 Gy)

induced decrease in antioxidant enzymes and thiol levels in the liver. It also showed excellent protection to organs sensitive to radiation like hematopoietic and gastrointestinal systems.

13) DSePA also protected from γ-radiation induced DNA damage and positively modulated the expression of cell cycle and DNA repair genes like *p21* and *GADD45α* respectively to favor survival.

14) Finally, DSePA at the same dosage of 2 mg/kg body weight, i.p., improved the 30 day survival after whole body γ-irradiation at a lethal absorbed dose of 9.2 Gy by 30% and the dose reduction factor is about 1.10.

REFERENCES

1. Halliwell, B.; Gutteridge, J. M. C. Free Radicals in Biology and Medicine, Clarendon Press, Oxford, **1993**.
2. Nelson. D. L.; Cox, M. M. Lehninger Principles of Biochemistry (5th ed), Freeman, W. H. & company, San Francisco, **2008**.
3. Cadenas, E.; Davies, K. J. A. *Free Radic. Biol. Med.* **2000**, 29, 222–230.
4. Kovacic, P.; Pozos, R. S.; Somanathan, R.; Shangari, N.; O'Brien, P. J. *Curr. Med. Chem.* **2005**, 12, 2601–2623.
5. Muller, F. L.; Liu, Y.; Van Remmen, H. *J. Biol. Chem.* **2004**, 279, 49064–49073.
6. Valko, M.; Leibfritz, D.; Moncol, J.; Cronin, M. T. D.; Mazur, M.; Telser, J. *The International Journal of Biochemistry & Cell Biology* **2007**, 39, 44–84.
7. Kohen, R.; Nyska, A. *Toxicol. Pathol.* **2002**, 30, 620-630.
8. DeCoursey, T. E.; Ligeti, E. *Cell. Mol. Life Sci.* **2005**, 62, 2173–2193.
9. Fridovich, I. *Annl. NY Acad. Sci.* **1999**, 893, 13.
10. Fenton, H. J. H.; Jackson, H. *Chem. Soc. Trans.* **1899**, 75, 1.
11. Haber, F.; Weiss, J. *Proc. Roy. Soc. (Lond.)* **1934**, 147, 332.
12. Remacle, J.; Raes, M.; Toussaint, O.; Renard, P.; Rao, G. *Mutat. Res.* **1995**, 316, 103–122.
13. Droge, W. *Physiol. Rev.* **2002**, 82, 47–95.
14. Schreck , R.; Baeuerle, P. A. *Trends Cell Biol.* **1991**, 1, 39–42.
15. Finkel, T. *Curr. Opin. Cell Biol.* **1998**, 10, 248–53.
16. de Magalhaes, J. P.; Church, G. M. *Exp. Gerontol.* **2006**, 41, 1–10.
17. Davis, K. J. *J. Biol. Chem.* **1987**, 262, 9895–9901.
18. Grune, T.; Reinheckei, T.; Davies, K. J. A. *FASEB J.* **1997**, 11, 526–534.

19. Levine, R. L.; Stadtman, E. R. *Exp. Gerontol.* **2001**, 36, 1495–1502.

20. Beckman, K. B.; Ames, B. N. *J. Biol. Chem.* **1997**, 272, 19633–19636.

21. Dizdaroglu, M.; Jaruga, P.; Birincioglu, M.; Rodriguez, H. *Free Radic. Biol. Med.* **2002**, 32, 1102–1115.

22. Valko, M.; Rhodes, C. J.; Moncol, J.; Izakovic, M.; Mazur, M. *Chem. Biol. Interact.* **2006**, *160*, 1–40.

23. Mates, J. M. *Toxicology* **2000**, 153, 83-104.

24. McCord, J. M.; Fridovich, I. *J. Biol. Chem.* **1969**, 244, 6049.

25. Sumner, J. B.; Dounce, A. L. *J. Biol. Chem.* **1937**, 121, 417.

26. Sies, H. *Free Radic. Biol. Med.* **1999,** 27, 916–921.

27. Wendel, A.; Pilz, W.; Ladenstein, R.; Sawatzki, G.; Weser, U. *Biochim. Biophys. Acta* **1975**, 377, 211.

28. Schafer, F. Q.; Buettner, G. R. *Free Radic. Biol. Med.* **2001**, 30, 1191-1212.

29. Masella, R.; Di Benedetto, R.; Vari, R.; Filesi, C.; Giovannini, C. *J. Nutr. Biochem.* **2005***,* 16, 577–586.

30. Li, C.; Stocker, R. *Redox Rep.* **2009**, 14, 95-101.

31. Pae, H. O.; Kim, E. C.; Chung, H. T. *J. Clin. Biochem. Nutr.* **2008**, 42, 197–203.

32. Wallace, S. S. *Environ. Mol. Mutagen.* **1988**, 12, 431–477.

33. Coates, P. J.; Lorimore, S. A.; Wright, E. G. *Mutat. Res.* **2004**, 568, 5-20.

34. Amanullah, A.; Azam, N.; Balliet, A.; Hollander, C.; Hoffman, B.; Fornace, A.; Liebermann, D. *Nature* **2003**, 424, 741-742.

35. Zhang, Y.; Rohde, L. H.; Emami, K.; Hammond, D.; Casey, R.; Mehta, S. K.; Jeevarajan, A.; Pierson, D. L..; Wu, H. *DNA Repair* **2008**, 7, 1835-1845.

36. Seifried, H. E.; Anderson, D. E.; Fishera, I.; Milner, J. A. *Journal of Nutritional Biochemistry* **2007**, 18, 567–579.

37. Cameron, E.; Pauling, L. *Proc. Natl. Acad. Sci. USA* **1976**, 73, 3685–3689.

38. Willett, W. C.; MacMahon, B. *N. Engl. J. Med.* **1984**, 310, 697–703.

39. Radimer, K. L.; Bindewald, B.; Hughes, J.; Ervin, B.; Swanson, C.; Picciano, M. F. *Am. J. Epidemiol.* **2004**, 160, 339–349.

40. Bors, W.; Heller, W.; Michel, C.; Stettmaier, K. "Flavonoids and Polyphenols: chemistry and biology" *In Handbook of Antioxidants*. New York, **1996,** 409.

41. Kamal-Eldin, A.; Appelqvist, L. A. *Lipids* **1996**, 31, 671-701.

42. Scartezzini, P.; Speroni, E. *J. Ethnopharmacol.* **2000,** 71, 23–43.

43. Joshi, R.; Adhikari, S.; Patro, B. S.; Chattopadhyay, S.; Mukherjee, T. *Free Radic. Biol. Med.* **2001**, 30, 1390–1399.

44. Heim, K. E.; Tagliaferro, A. R.; Bobilya, D. J. *J. Nutr. Biochem.* **2002**, 13, 572–584.

45. Devasagayam, T. P. A.; Tilak, J. C.; Boloor, K. K.; Sane, K. S.; Ghaskadbi, S. S.; Lele, R. D. *J. Assoc. Physicians India* **2004**, 52, 794-804.

46. Bendich, A.; Olson, J. A. *FASEB J*. **1989,** 3, 1927-32.

47. Goldman, A. *Brit. J. Clin. Pharma.* **1995**, 19, 258-260.

48. Chung, J. G . *Toxicological sciences* **1999**, 51, 202-210.

49. Manach, C.; Scalbert, A.; Morand, C.; Rémésy, C.; Jiménez, L. *Am. J. Clin. Nutr.* **2004**, 79, 727-747.

50. Van der Kraaij, A. M.; van Eijk, H. G.; Koster, J. F. *Circulation* **1989**, 80, 158-164.

51. Fox, R. B. *J. Clin. Invest.* **1984**, 74, 1456-1464.

52. Bernard, G. R.; Lucht, W. D.; Niedermeyer, M. E.; Snapper, J. R.; Ogletree, M. L.; Brigham, K. L. *J. Clin. Invest.* **1984**, 73, 1772-1784.

53. Mitsos, S. E.; Askew, T. E.; Fantone, J. C. *Circulation* **1986**, 73, 1077-1086.

54. Vander Heide, R. S.; Sobotka, P. A.; Ganote, C. E. *J. Mol. Cell Cardiol.* **1987**, 19, 615-625.

55. Vajragupta, O.; Boonchoong, P.; Watanabe, H.; Tohida, M.; Kummasud, H.; Sumonont, Y. *Free Radic. Biol. Med.* **2003**, 35, 1632-1644.

56. Pollard, J. M.; Reboucas, J. S.; Durazo, A.; Kos, I.; Fike, F.; Panni, M.; Gralla, E. B.; Valentine, J. S.; Batinic-Haberle, I.; Gatti, R. A. *Free Radic. Biol. Med.* **2009**, 473, 250-260.

57. Parnham, M. J.; Sies, H. *Exp. Opin. Invest. Drugs* **2000**, 9, 607-619.

58. Seifried, H. E.; Anderson, D. E.; Milner, J. A.; Greenwald, P. New developments in antioxidant research, Nova Science Publishers Inc., Hauppauge (NY), **2006**.

59. Herbert, V. *Am. J. Clin. Nutr.* **1994**, 60, 157–168.

60. Galati, G.; Sabzevari, O.; Wilson, J. X.; O'Brien, P. J. *Toxicology* **2002**, 177, 91–104.

61. Von Sonntag, C. The chemical basis of radiation biology, Taylor and Francis, New York, **1987**.

62. Kogelnik, H. D. *Int. J. Radiat. Oncol. Biol. Phys.* **1996**, 35, 219–226.

63. Walker R. I.; Cerveny, R. J. Medical Consequences of Nuclear Warfare, Falls Church, VA: Office of the Surgeon General, **1989**.

64. Buxton, G. V.; Greenstock, C. L.; Helman, W. P.; Ross, A. B. *J. Phys. Chem. Ref. Data* **1988,** 17, 513–886.

65. Riley, P. A. *Int. J. Radiat. Biol.* **1994**, 65**,** 27-33.

66. Symons M. C. R.; Gutteridge, Free Radicals and Ion, Chemistry Biology and Medicine. Oxford University Press, Oxford, **1998**.

67. Ainsworth, E. J.; Afzal, S. M.; Crouse, D. A.; Hanson, W. R.; Fry, R. J. *Adv. Space Res.* **1989**, 9, 299-313.

68. Barabanova, A. V. The Medical Basis for Radiation Accident Preparedness, The Clinical Care of Victims, NewYork: Parthenon, **2002**.

69. Spinks, J. W. T.; Woods, R. J. An introduction to radiation chemistry, Weily Interscience Publication, New York, **1990**.

70. Pryor, W. A. *Basic Life Sci.* **1986**, 39, 45–59.

71. MacVittie, T. J.; Weiss, J. F.; Browne, D. Advances in the Treatment of Radiation Injuries. Pergamon press, Oxford, **1996**.

72. Weiss, J. F.; *Environ. Health Perspect.* **1997**, 105, 1473-1478.

73. Weiss, J. F.; Landauer, M. R.; Hogan, J. B.; Gunter-Smith, P. J.; Benson, K. A.; Neta, R.; Hanson, W. R. *Adv. Exp. Med. Biol.* **1997**, 400B, 865- 872.

74. Weiss, J. F.; Simic, M. G. *Pharmacol. Ther.* **1988**, 39, 1-414.

75. Maisin, J. R. *Int. J. Radiat. Biol.* **1998**, 73, 443–450.

76. Weiss, J. F.; Landauer, M. R. *Toxicology* **2003**, 189**,** 1- 20.

77. Patt, H. M.; Tyree, E. B.; Straube, R. L.; Smith, D. E. *Science* **1949**, 110, 213–214.

78. Bacq, Z.M.; Herve, A.; Lecomte, J.; Fischer, P.; Blavier, J.; Dechamps, G.; Le Bihan, H.; Rayet, P. *Arch. Int. Physiol.* **1951**, 59, 442-447.

79. Weiss, J. F.: Srinivasan, V.; Jacobs, A. J.; Rankin, W. A. *Proc. Am. Assoc. Cancer Res.* **1984**, 25, 235.

80. Landauer, M. R.; Davis, H. D.; Dominitz, J. A.; Weiss, J. F. *Pharmacol. Ther.* **1988**, 39, 97-100.

81. Sweeney, T. R. Survey of Compounds from the Antiradiation Drug Development Program of the U.S. Army Medical Research and Development Command. Washington, DC: U.S.Government Printing Office, **1979**.

82. Malaker, K. Radioprotectors: Chemical, Biological and Clinical Perspective. CRC Press, Boca Raton, **1998**.

83. Capizzi, R. L.; Oster, W. *Int. J. Hematol.* **2000**, 72, 425-435.

84. Andreassen, C. N.; Grau, C.; Lindegaard, J. C. *Seminars in Radiation Oncology* **2008,** 13, 62-72.

85. Brown, P. E. *Nature* **1967**, 213, 363-364.

86. Weiss, J. F.; Landauer, M. R. *Ann. New York Acad. Sci.* **2000**, 899, 44-60.

87. Srinivasan, V.; Jacobs, A. J.; Simpson, S. A.; Weiss, J. F. Modulation and Mediation of cancer by Vitamins. Karger press, Basel, **1983**.

88. Srinivasan, V.; Weiss, J. F. *Int. J. Radiat.Oncol. Biol. Phys.* **1992**, 23, 841-845.

89. Friedenthal, E.; Mendecki, J.; Davis, L.; Seifter, E. Vitamins and Minerals in the Prevention and Treatment of Cancer. CRC Press, Boca Raton, **1991**.

90. Okunieff, P. *Am. J. Clin. Nutr.* **1991**, 54, 1281S-1283S.

91. Farooqui, Z.; Kesavan, P. C. *Mutat. Res.* **1992**, 269, 225-230.

92. Uma Devi, P.; Ganasoundari, A.; Vrinda, B.; Srinivasan, K. K.; Unnikrishnan, M. K. *Radiat. Res.* **2000**, 154, 455-460.

93. Araujo, M. C.; Dias, F. L.; Takahashi, C. S. *Teratog. Carcinog. Mutag.* **1999**, 19, 9-18.

94. Gong, Y. F.; Huang, Z. J.; Qiang, M. Y.; Lan, F. X.; Bai, G. A.; Mao, Y. X.; Ma, X. P. Zhang, F. G. *Biomed. Environ. Sci.* **1991**, 4, 273-282.

95. Chattopadhyay, I.; Biswas, K.; Bandyopadhyay, U.; Banerjee, R. K. *Curr. Sci.* **2004**, 87, 44-53.

96. Strimpakos, A. S.; Sharma R. A. *Antioxidants Redox Signaling* **2008**, 10, 512-534.

97. Felter, H. W. L. J. *King's Am. Dispensatory* **1898,** 2.

98. Milobedzka, J. K. V. L. V. *Chem. Ber.* **1910**, 43, 2163.

99. Priyadarsini, K. I. *J. Photochem. Photobiol. C Photochem. Rev.* **2009**, 10, 81–95.

100. Wahlstrom, B.; Blennow, G. *Acta Pharmacol. Toxicol.* **1978**, 43, 86–92.

101. Ravindranath, V.; Chandrasekhara, N. *Toxicology* **1980**, 16, 259–265.

102. Ravindranath, V.; Chandrasekhara, N. *Toxicology* **1981**, 22, 337–344.

103. Pan, M. H.; Lin-Shiau, S. Y.; Lin, J. K. *Biochem. Pharmacol.* **2000**, 60, 1665–1676.

104. Cheng, A. L.; Hsu, C. H.; Lin, J. K.; Hsu, M. M.; Ho, Y. F;, Shen, T. S.; Ko, J. Y.; Lin, J. T.; Lin, B. R.; Ming-Shiang, W.; Yu, H. S.; Jee, S. H.; Chen, G. S.; Chen, T. M.; Chen, C. A.; Lai, M. K.; Pu, Y. S.; Pan, M. H.; Wang, Y. J.; Tsai, C. C.; Hsieh, C. Y. *Anticancer Res* **2001**, 21, 2895–2900.

105. Hatcher, H.; Planalp, R.; Cho, J.; Torti, F. M.; Torti, S. V. *Cell. Mol. Life Sci.* **2008**, 65, 1631–1652.

106. Aggarwal, B. B.; Harikumar, K. B. *The International Journal of Biochemistry & Cell Biology* **2009**, 41, 40–59.

107. Aggarwal, B. B.; Sundaram, C.; Malani, N.; Ichikawa, H. The Molecular Targets and Therapeutic Uses of Curcumin in Health and Disease, Springer, NY USA, **2007**.

108. Li, C. J.; Zhang, L. J.; Dezube, B. J.; Crumpacker, C. S.; Pardee, A. B. *Proc. Natl. Acad. Sci. USA* **1993**, 90, 1839-1842.

109. Ringman J. M.; Frautschy, S. A.; Cole, G. M.; Masterman, D. L.; Cummings, J. L. *Curr. Alzheimer Res.* **2005**, 2, 131–136.

110. Goel, A.; Kunnumakkara, A. B.; Aggarwal, B. B. Curcumin as ‘‘Curecumin’’: From kitchen to clinic. *Biochem. Pharmacol.* **2008**, 75, 787–809.

111. Aggarwal, B. B.; Kumar, A.; Bharti, A. C. *Anticancer Res.* **2003**, 23, 363-398.

112. Lopez-Lazaro, M. *Mol. Nutr. Food Res.* **2008**, 52, S103–S127.

113. Brennan, M. J. *Am. J. Clin. Pathol.* **1975**, 64, 797–809.

114. Rao, C. V.; Rivenson, A.; Simi, B.; Reddy, B. S. *Cancer Res.* **1995**, 55, 259–266.

115. Aggarwal, B. B.; Shishodia, S. *Biochem Pharmacol* **2006**, 71, 1397–1421.

116. Aggarwal, B. B.; Sung, B. *Trends in Pharmacological Sciences* **2008**, 30, 85-94.

117. Aggarwal, B. B. *Cancer Cell* **2004**, 6, 203–208.

118. Singh, S.; Aggarwal, B. B. *J. Biol. Chem.* **1995**, 270, 24995–25000.

119. Han, S. S.; Chung, S. T.; Robertson, D. A.; Ranjan, D.; Bondada, S. *Clin. Immunol.* **1999**, 93, 152–161.

120. Chen, A.; Xu, J.; Johnson, A. C. *Oncogene* **2006**, 25, 278–287.

121. Moos, P. J.; Edes, K.; Mullally, J. E.; Fitzpatrick, F. A. *Carcinogenesis* **2004**, 25, 1611–1617.

122. Choudhuri, T.; Pal, S.; Agwarwal, M. L.; Das, T.; Sa, G. *FEBS Lett.* **2002**, 512, 334–340.

123. Korutla, L.; Kumar, R. *Biochim. Biophys. Acta* **1994**, 1224, 597–600.

124. Rushworth, S. W.; Ogborne, R. M.; Charalambos, C. A.; O'Connell, M. A. *Biochem. Biophys. Res. Commun.* **2006**, 341, 1007-1016.

125. Sharma, O.P. *Biochem. Pharmacol.* **1976**, 25, 1811-1812.

126. Reddy, A. C.; Lokesh, B. R. *Molecular and Cellular Biochemistry* **1994**, 137, 1–8.

127. Unnikrishnan, M. K.; Rao, M. N. *Molecular and Cellular Biochemistry* **1995**, 146, 35–37.

128. Priyadarsini, K. I. *Free Radic. Biol. Med.* **1997**, 23, 838-844.

129. Anand, P.; Thomas, S. G.; Kunnumakkara, A. B.; Sundaram, C.; Harikumar, K. B.; Sung, B.; Tharakan, S. T.; Misra, K.; Priyadarsini, K. I.; Rajasekharan, K. N.; Aggarwal B. B. *Biochem. Pharmacol.* **2008**, 76, 1590–1611.

130. Toda, S.; Miyase, T.; Arichi, H.; Tanizawa, H.; Takino, Y. *Chemical and Pharmaceutical Bulletin* **1985**, 33, 1725–1728.

131. Reddy, A. C.; Lokesh, B. R.; *Molecular and Cellular Biochemistry* **1992**, 111, 117–124.

132. Sreejayan; Rao, M. N. *Journal of Pharmacy and Pharmacology* **1994**, 46, 1013–1016.

133. Biswas, S. K.; McClure, D.; Jimenez, L. A.; Megson, I. L.; Rahman, I. *Antioxid. Redox Signaling* **2005**, 7, 32–41.

134. Iqbal, M.; Sharma, S. D.; Okazaki, Y.; Fujisawa, M.; Okada, S. *Pharmacol. Toxicol.* **2003**, 92, 33-38.

135. Hill-Kapturczak, N.; Thamilselvan, V.; Liu, F.; Nick, H. S.; Agarwal, A. *Am. J. Physiol. Renal Physiol.* **2001**, 281, F851–F859.

136. Surh, Y. J.; Kundu, J. K.; Na, H. K. *Planta Med.* **2008**, 74, 1526-1539.

137. Dikshit, M.; Rastogi, L.; Shukla, R.; Srimal, R. C. *Indian Journal of Medical Research* **1995**, 101, 31–35.

138. Thiyagarajan, M.; Sharma, S. S. *Life Sciences* **2004**, 74, 969–985.

139. Priyadarsini, K. I.; Maity, D. K.; Naik, G. H.; Kumar, M. S.; Unnikrishnan, M. K.; Satav, J. G.; Mohan H. *Free Radic. Biol. Med.* **2003**, 35, 475-484.

140. Jovanovic, S. V.; Steenken, S.; Boone, C. W.; Simic, M. G. *J. Am. Chem. Soc.* **1999**, 121, 9677–9681.

141. Barik, A.; Mishra, B.; Shen, L.; Mohan, H.; Kadam, R. M.; Dutta, S.; Zhang, H-Y.; Priyadarsini, K. I. *Free Radic. Biol. Med.* **2005**, 39, 811-822.

142. Jiao, Y.; Wilkinson, J.; Christine Pietsch, E.; Buss, J. L.; Wang, W.; Planalp, R.; Torti, F. M.; Torti, S. V. *Free Radic. Biol. Med.* **2006**, 40, 1152-1160.

143. Schwarz, K.; Foltz C. M. *J. Am. Chem. Soc*. **1957**, 79, 3292.

144. Whanger, P. D. *J. Am. Coll. Nutr.* **2002**, 21, 223–232.

145. Tapiero, H.; Townsen, D. M.; Tew, K. D. *Biomed. Pharmacother.* **2003**, 57, 134-144.

146. Brenneisen, P.; Steinbrenner, H.; Sies, H. *Mol. Aspects Med.* **2005**, 26, 256-267.

147. Behne, D.; Kyriakopoulos, A. *Annu. Rev. Nutr.* **2001**, 21, 453–473.

148. Chambers, I.; Frampton, J.; Goldfarb, P.; Affara, N.; McBain, W.; Harrison, P. R. *EMBO J.* **1986**, 5, 1221–1227.

149. Papp, L. V.; Lu, J.; Holmgren, A.; Khanna, K. K. *Antioxid. Redox. Signal.* **2007**, 9, 775-806.

150. Kryukov, G. V.; Gladyshev, V. N. *EMBO Rep.* **2004**, 5, 538–543.

151. Kryukov, G. V.; Castellano, S.; Novoselov, S. V.; Lobanov, A. V.; Zehtab, O.; Guigo, R.; Gladyshev, V. N. *Science* **2003**, 300, 1439–1443.

152. Stadtman, T. C. *Annu. Rev. Biochem.* **1996**, 65, 83–100.

153. Mugesh, G.; du Mont, W-W. *Chem. Eur. J.* **2001**, 7, 1365-1370.

154. Issa, A. A.; Adam, M. S. *Folia Microbiologica*, **1999**, 44, 406-410.

155. Magee, R. J. *Main group Elements and Their Compounds*, Narosa publishing house, New Delhi, **1996**.

156. Zeng, H. *Molecules* **2009**, 14, 1263-1278.

157. Xia, Y.; Hill, K. E.; Byrne, D. W.; Xu, J.; Burk, R. F. *Am. J. Clin. Nutr.* **2005**, 81, 829–834.

158. Whanger, P. D. *Br. J. Nutr.* **2004**, 91, 11–28.

159. Sappey, C.; Legrand-Poels, S.; Best-Belpomme, M.; Favier, A.; Rentier ,B.; Piette , J. *AIDS Res. Hum. Retrovir.* **1994**, 10, 1451-1461.

160. Yu, S. Y.; Zhu, Y. J.; Li, W. G. *Biol. Trace Elem. Res.* **1997**, 56, 117-24.

161. Burk, R. F.; Early, D. S.; Hill, K. E.; Palmer, I. S.; Boeglin, M. E. *Hepatology* **1998**, 27, 794-798.

162. Rayman, M. P. *Lancet* **2000**, 356, 233-241.

163. Surai, P. Selenium in Nutrition and Health, Nottingham University Press, Nottingham, **2006**.

164. Block, E.; Birringer, M.; Jiang, W.; Nakahodo, T.; Thompson, H. J.; Toscano, P. J.; Uzar, H.; Zhang, X.; Zhu, Z. *J. Agric. Food Chem*. **2001**, 49, 458.

165. Clark, L. C.; Combs, G. F.; Turnbull, B. W.; Slate, E. H.; Chalker, D. K.; Chow, J.; Davis, L. S.; Glover, R. A.; Graham, G. F.; Gross, E. G.; Krongrad, A.; Lesher, J. L.; Park, H. K.; Sanders, B. B.; Smith, C. L.;Taylor, J. R. *JAMA* **1996,** 276, 1957–1963.

166. Duffield, A. J.; Thomson, C. D.; Hill, K. E.; Williams, S. *Am. J. Clin. Nutr.* **1999**, 70, 896–903.

167. Kiremidjian-Schumacher, L.; Roy, M.; Wishe, H. I.; Cohen, M .W.; Stotzky, G. *Biol. Trace Elem. Res.* **1994**, 41, 115-127.

168. Franke, K. W. *Journal of Nutrition* **1934**, 8, 597.

169. Moxon, A. L.; Rhian, M. *Physiol. Rev.* **1943**, 23, 305.

170. Nelson, A. A.; Fitzhugh, D. G.; Calvery, H. O. *Cancer Res*. **1943**, 3, 230.

171. Painter, E. P. *Chem. Rev*. **1941**, 28, 179.

172. Chaudiere, J.; Courtin, O.; Leclaire, J. *Arch. Biochem. Biophys*. **1992**, 296, 328.

173. Kitahara, J.; Seko, Y.; Imura, N. *Arch. Toxicol*. **1993**, 67, 497.

174. Spallholz, J. E. *Free Radic. Biol. Med*. **1994**, 17, 45.

175. Vinceti, M.; Wei, E. T.; Malagoli, C.; Bergomi, M.; Vivoli, G. *Rev. Environ. Health* **2001**, 16, 233–251.

176. Nogueira, C. W.; Zeni, G.; Rocha, J. B. *Chem. Rev.* **2004**, 104, 6255-6285.

177. Soriano-Garcia, M. *Curr. Med. Chem.* **2004,** 11, 1657-1669.

178. Niki, E. *Methods in Enzymology* **1990**, 186, 100-108.

179. Niki, E.; Komuro, E.; Takahashi, M.; Urano, S.; Ito, E.; Terao, K. *J. Biol. Chem.* **1988**, 263, 19809-19814.

180. Deng, S-L.; Cheng, W-F.; Zhou, B.; Yang, L.; Liu, Z-L. *Food Chem.* **2006**, 98, 112-119.

181. Kwak, C. S.; Mun, K. C.; Suh, S. I. *Transplant. Proc.* **2002**, 34, 2654-2655.

182. Ali, I.; Gatasheh, M. K. M.; Naseem, I. *Biochim. Biophys. Acta* **2000**, 1523, 225-229.

183. Pokorny, J.; Yanishlieva, N.; Gordon, M. Antioxidants in Food, CRC Press, New York, **2001**.

184. Sreejayan, N.; Rao, M. N. A.; Priyadarsini, K. I.; Devasagayam, T. P. A. *Int. J. Pharm.* **1997,** 151, 127-130.

185. Eyer, P.; Podhradsky, D. *Anal. Biochem.* **1986**, 153, 57-66.

186. Sedlak, J.; Lindsay, R. *Anal. Biochem.* **1968**, 25, 192-205.

187. Barik, A.; Mishra, B.; Kunwar, A.; Kadam, R. M.; Shen, L.; Dutta, S.; Padhye, S.; Satpati, A. K.; Zhang, H-Y.; Priyadarsini, K. I. *Eur. J. Med. Chem.* **2007**, 42, 431-439.

188. Abei, H. *Methods in Enzymology* **1984,** 105, 121-126.

189. Oliver, C. N.; Ahn, B.; Moerman, E. J.; Goldstein, S.; Stadtman, E. R. *J. Biol. Chem.* **1987**, 262, 5488-5491.

190. Hail Jr., N. *Free Radic. Biol. Med.* **2008**, 44, 1382-1393.

191. Kurrey, N. K.; Amit, K.; Bapat, S. A. *Gynecologic Oncology* **2005**, 97, 155-165.

192. Gao, X.; Kuo, J.; Jiang, H.; Deeb, D.; Liu, Y.; Divine, G.; Chapman, R. A.; Dulchavsky, S. A.; Gautam, S. C. *Biochem. Pharmacol.* **2004**, 68, 51-61.

193. Tolnai, S. *Methods in Cell Science* **1975**, 1, 37-38.

194. Mosmann, T. *J. Immunol. Methods* **1983**, *65,* 55-63.

195. Kumar, S. S.; Shankar, B.; Sainis, K. B. *Biochim. Biophys. Acta* **2004**, 1672, 100-111.

196. Zou, Y.; Niu, P.; Yang, J.; Yuan, J.; Wu, T.; Chen, X. *Cancer Biol. Ther.* **2008,** 5, 689-696.

197. Reitman, S.; Frankel, S. A. *Am. J. Clin. Pathol.* **1957**, 28, 56–63.

198. Prabhakar, K. R.; Veerapur, V. P.; Bansal, P.; Parihar, V. K.; Reddy, K. M.; Kumar, P. B.; Priyadarsini, K. I.; Unnikrishnan, M. K. *Chem. Biol. Interact.* **2007,** 165, 22-32.

199. Mallory, F. B. Animal Tissue Techniques, Freeman, W. H. & company, San Francisco, **1944**.

200. Sandhya, T.; Lathika, K. M.; Pandey, B. N.; Bhilwade, H. N.; Chaubey, R. C.; Priyadarsini, K. I.; Mishra, K. P. *Mutat. Res.* **2006,** 609, 17-25.

201. Sakano, K.; Kawanishi, S. *Arch. Biochem. Biophys.* **2002**, 405, 223–230.

202. Yoshino, M.; Haneda, M.; Naruse, M.; Htay, H. H.; Tsubouchi, R.; Qiao, S. L.; Li, W. H.; Murakami, K.; Yokochi, T. *Toxicol. In Vitro* **2004**, 18, 783–789.

203. Urbina-Cano, P.; Bobadilla-Morales, L.; Ramirez-Herrera, M. A.; Corona-Rivera, J. R.; Mendoza-Magana, M. L.; Troyo-Sanroman, R.; Corona-Rivera, A. *J. Appl. Genet.* **2006**, 47, 377–382.

204. Thayyullathil, F.; Chathoth, S.; Hago, A.; Patel, M.; Galadari, S. *Free Radic. Biol. Med.* **2008**, 45, 1403–1412.

205. Morin, D.; Barthelemy, S.; Zini, R.; Labidalle, S.; Tillement, J. P. *FEBS lett.* **2001**, 495, 131-136.

206. Sandur, S. K.; Ichikawa, H.; Pandey, M. K.; Kunnumakkara, A. B.; Sung, B.; Sethi, G.; Aggarwal, B. B. *Free Radic. Biol. Med.* **2007**, 43, 568-580.

207. Bhaumik, S.; Anjum, R.; Rangaraj, N.; Pardhasaradhi, B. V.; Khar, A. *FEBS Lett.* **1999**, 456, 311-314.

208. Syng-Ai, C.; Kumari, A. L.; Khar, A. *Mol. Cancer Ther.* **2004**, 3, 1101–1108.

209. Fang, J.; Lu, J.; Holmgren, A. *J. Biol. Chem.* **2005**, 280, 25284-25290.

210. Sandur, S. K.; Pandey, M. K.; Sung, B.; Ahn, K. S.; Murakami, A.; Sethi, G.; Limtrakul, P.; Badmaev, V.; Aggarwal, B. B. *Carcinogenesis* **2007**, 28, 1765-1773.

211. De la Fuente, M.; Victor, V. M. *Cell Biol.* **2000**, 78, 49-54.

212. Snyder, G. K.; Brandon, A. S. *American Zoologist* **1999**, 39, 189–198.

213. Beutler, E. Red Cell Metabolism. *A manual of biochemical methods* **1982**, 89, 137-140.

214. Vosters, O.; Nève, J. *Talanta* **2002**, 57, 595-600.

215. Chwalek, M.; Lalun, N.; Bobichon, H.; Plé, K.; Voutquenne-Nazabadioko, L. *Biochim. Biophys. Acta* **2006**, 1760, 1418-1427.

216. Gordon S.; Taylor, P. R. *Nature Reviews Immunology* **2005**, 5, 953-964.

217. Chen, J.; Wanming, D.; Zhang, D.; Liu, Q.; Kang, J. *Pharmazie* **2005**, 60, 57–61.

218. Dickinson, D. A.; Forman, H. J. *Biochem. Pharmacol.* **2002**, 64, 1019-1026.

219. Vivancos, M.; Moreno, J. J. *Free Radic. Biol. Med.* **2005**, 39, 91-97.

220. Awasthi, S.; Pandya, U.; Singhal, S.S.; Lin, J. T.; Thiviyanathan, V.; Seifert Jr., W. E.; Awasthi, Y. C.; Ansari, G. A. *Chem. Biol. Interact.* **2000**, 128, 19–38.

221. Hoffer, E. L.; Shenker, Y.; Baum, Y.; Tabak, A. *Free Radic. Biol. Med.* **1997**, 22, 567-572.

222. Sedlack, J.; L'Hanus, *Endocrinol. Exp.* **1982**, 16, 103-109.

223. Strasser, E. M.; Wessner, B.; Manhart, N.; Roth, E. *Biochem. Pharmacol.* **2005**, 70, 552-559.

224. Murley, J. S.; Kataoka, Y.; Weydert, C. Y.; Oberley, L. W.; Grdina, D. J. *Free Radic. Biol. Med.* **2006**, 40, 1004-1016.

225. Aggarwal, S.; Ichikawa, H.; Takada, Y.; Sandur, S. K.; Shishodia, S.; Aggarwal, B. B. *Mol. Pharmacol.* **2006**, 69, 195-206.

226. Lebovitz, R. M.; Zhang, H.; Vogel, H.; Cartwright, J.; Dionne, L.; Lu, N.; Huang, S.; Matzuk, M. M. *Proc. Natl. Acad. Sci. USA* **1996**, 93, 9782-9718.

227. Usta, M.; Wortelboer, H. M.; Vervoort, J.; Boersma, M. G.; Rietjens, I. M.; Van Bladeren, P. J.; Cnubben, N. H. *Chem. Res. Toxicol.* **2007**, 20, 1895-902.

228. Bong, P. H. *Bull. Korean Chem. Soc.* **2000,** 21, 81-86.

229. Dutta, S.; Murugkar, A.; Gandhe, N. P. *Metal Based Drugs* **2001**, 8, 183–187.

230. Vajragupta, O.; Boonchoong, P.; Berliner, L. J. *Free Radic. Res.* **2004**, 38, 303-314.

231. Annaraj, J. P.; Ponvel, K. M.; Athappan, P.; Srinivasan, S. *Transition Metal Chem.* **2004,** 29, 722–727.

232. Omar, B. A.; Flores, S. C.; McCord, J. M. *Adv. Pharmacol.* **1992**, 23, 109–161.

233. Cuzzocrea, S.; Riley, D. P.; Caputi, A. P.; Salvemini, D. *Pharmacol. Rev.* **2001**, 52, 135–159.

234. Faulkner, K. M.; Steven, R. D.; Fridovich, I. *Arch. Biochem. Biophys.* **1994,** 310, 341–346.

235. Weis, R. H.; Fretland, D.J.; Baron, D. A.; Ryan, U. S.; Riley, D. P. *J. Biol. Chem.* **1996**, 271, 26149–26156.

236. Durackova, Z.; Mendiola, A. M.; Sevilla, T. M.; Valent, A. *Bioelectrochem. Bioenerget.* **1999**, 48, 109–116.

237. Patel, M.; Day, B. J. *Trends. Pharmacol. Sci.* **1999**, 20, 359–364.

238. Riley, D. P. *Chem. Rev.* **1999**, 99, 2573– 2587.

239. Casolaro, M.; Chelli, M.; Ginanneschi, M.; Lachi, F.; Messori, L.; Muniz-Miranda, M.; Papini, A. M.; Kowalik-Jansowska, T.; Kozlowski, H. *J. Inorg. Biochem.* **2002**, 89, 181–190.

240. Han, Y.; Son, S-J.; Akhalaia, M.; Platonov, A.; Son, H-J.; Lee, K-H.; Yun, Y-S.; Song, J-Y. *eCAM* **2005**, 2, 529-536.

241. Yang, L.; Ross, K.; Qwarnstrom, E. V. *J. Biol. Chem.* **2003**, 278, 30881-30888.

242. Borrello, S.; Demple, B. *Arch. Biochem. Biophys.* **1997**, 348, 289-294.

243. Porntadavity, S.; Xu, Y.; Kiningham, K.; Rangnekar, V. M.; Prachayasitikul, V.; St. Clair, D. K. *DNA Cell Biol.* **2001**, 20, 473-481.

244. Xu, Y.; Porntadavity, S.; St. Clair, D. K. *Biochem. J.* **2002**, 362, 401-412.

245. Siwak, D. R.; Shishodia, S.; Aggarwal, B. B.; Kurzrock, R. *Cancer* **2005**, 104, 879-890.

246. Hamelin B. A.; Turgeon J. *Trends in Pharmacological Sciences* **1988**, 19, 26-37.

247. Choudhuri, T.; Pal, S.; Das, T.; Sa, G. *J. Biol. Chem.* **2005**, 280, 20059–20068.

248. Everett, P. C.; Meyers, J. A.; Makkinje, A.; Rabbi, M.; Lerner, A. *Am. J. Hematol.* **2007**, 82, 23–30.

249. Ramachandran, C.; You,W. *Breast Cancer Res. Treat.* **1999**, 54, 269–278.

250. Chignell, C. F.; Bilski, P.; Reszka, K. J.; Motten, A. N.; Sik, R. H.; Dhal, T. A. *Photochem. Photobiol.* **1994,** 59, 295-302.

251. Khopde, S. M.; Priyadarsini, K. I.; Palit, D. K.; Mukherjee, T. *Photochem. Photobiol.* **2000,** 72, 625-631.

252. Barik, A.; Priyadarsini, K. I.; Mohan, H. *Photochem. Photobiol.* **2003**, 77, 597-603.

253. Barik, A.; Mishra, B.; Kunwar, A.; Priyadarsini, K. I. *Chem. Phys. Lett.* **2007**, 436, 239-243.

254. Kunwar, A.; Barik, A.; Pandey, R.; Priyadarsini, K. I. *Biochim. Biophys. Acta* **2006**,1760, 1513-20.

255. Periasamy, N.; Verkman, A. S. *Anal. Biochem.* **1992**, 201, 107-113.

256. Suzuki, T.; Fujikura, K.; Higashiyama, T.; Takata, K. *The Journal of Histochemistry & Cytochemistry* **1997**, 45, 49–53.

257. Coda, L.; Salcini, A. E.; Confalonieri, S.; Pelicci, G.; Sorkina, T.; Sorkin, A.; Pelicci, P. G.; Di Fiore, P. P. *J. Biol. Chem.* **1998**, 273, 3003–3012.

258. Singer, S. J. *Ann. Rev. Biochem.* **1974**, 43, 805-833.

259. Singer, S. J. *Ann. Rev. Physiology* **2004**, 66, 1-27.

260. Troyanovsky, S. M. *Curr. Opin. Cell Biol.* **1999**, 11, 561-566.

261. Savagner, P. *BioEssays* **2001**, 23, 912–923.

262. Leckband Prakasam, D. A. *Ann. Rev. Biomed. Eng.* **2006**, 8, 259-287.

263. Suzuki, S.T. *Tanpakushitsu Kakusan Koso* **2006**, 51, 629-635.

264. Paweletz, C. P.; Gillespie, J. W.; Ornstein, D. K.; Simone, N. L.; Brown, M. R.; Cole, K. A.; Wang, O.; Huang, J.; Nan, Hu.; Yip, T.; Rich, W. E.; Kohn, E. C.; Linehan, M. W.; Weber, T.; Taylor, P.; Emmert-Buck, M. R.; Liotta, L. A.; Petricoin, E. F. *Drug Development Research* **2000**, 49, 34–42.

265. Sellers, T. A.; Yates, J. R. *Genetic Epidemiology* **2003**, 24, 83-98.

266. Glunde, K.; Chunfa, J.; Bhujwalla, Z. M. *Cancer Research* **2004**, 64, 4270-4276.

267. Weiss, J. F.; Kumar, K. S.; Walden, T. L.; Neta, R.; Landauer, M. R.; Clark, E. P. *Int. J. Radiat. Biol.* **1990**, 57, 709-722.

268. Venardos, K.; Harrison, G.; Headrick, J.; Perkins, A. *J. Trace Elem. Med. Biol.* **2004**, 18, 81-88.

269. Weiss, J. F.; Srinivasan, V.; Kumar, K. S.; Landauer, M. R. *Adv. Space Res.* **1992**, 12, 223-231.

270. Weiss, J. F.; Srinivasan, V.; Kumar, K. S.; Landauer, M. R.; Patchen, M. L. Trace Elements and Free Radicals in Oxidative Diseases. AOCS Press, Champaign, **1994**.

271. Noaman, E., Zahran, A. M.; Kamal, A. M.; Omran, M. F. *Biol. Trace Elem. Res.* **2002**, 86, 55-64.

272. Sagowski, C.; Wenzel, S.; Jenicke, L.; Metternich, F. U.; Jaehne, M. *Eur. Arch. Otorhinolaryngol* **2005**, 262, 459–464.

273. Buntzel, J.; Micke, O.; Mucke, R.; Glatzel, M.; Schonekaes, K. G.; Schafer, U.; Kisters, K.; Bruns, F. *Trace elements and electrolytes* **2005**, 22, 211-215.

274. Breccia, A.; Badiello, R.; Trenta A.; Mattii, M. *Radiat. Res.* **1969**, 38, 483.

275. Daniels, L. A. *Biol. Trace Elem. Res.* **1996**, 54, 185-199.

276. Tak, J. K.; Park, J. W. *Free Radic. Biol. Med.* **2009**, 46, 1177-1185.

277. Back, T. G.; Moussa, Z. *J. Am. Chem. Soc.* **2003**, 125, 13455-13460.

278. Arnold, A. P.; Tan, K. S.; Rabenstein, D. L. *Inorg. Chem.* **1986**, 25, 2433-2437.

279. Mishra, B.; Priyadarsini, K. I.; Mohan, H.; and Mugesh, G. *Bio-org. Med. Chem. Lett.* **2006,** 16, 5335-5338.

280. Guha, S. N.; Moorthy, P. N.; Kishore, K.; Naik. D. B.; Rao, K. N. *Proc. Indian Acad. Sci. (Chem. Sci.)* **1987**, 99, 261-271.

281. Alfassi, Z. B.; Mosseri, S.; Neta, P. *J. Phys. Chem.* **1987**, 91, 3383–3385.

282. Alfassi, Z. B.; Schuler, R. H. *J. Phys. Chem.* **1985**, 89, 3359-3363.

283. Mishra, B.; Priyadarsini, K. I.; Mohan, H. *J. Phys. Chem. A.* **2006,** 110, 1894-1900.

284. Samini, M.; Dehpour, A. R.; Hajinabi, K. *Acta Medica Iranica* **1997**, 35, 74-76.

285. Katzung, B. G. Basic and Clinical Pharmacology. Oxford press, **1988**.

286. Schöneich, C.; Narayanaswami, V.; Asmus, K. D.; Sies, H. *Arch. Biochem. Biophys*. **1990**, 282, 18-25.

287. Mansour, H. H.; Hafez, H. F.; Fahmy, N. M.; Hanafi, N. *Biochem. Pharmacol.* **2008**, 75, 773-780.

288. Ramadan, L. A.; Roushdy, H. M.; Abusenna, G. M.; Amin, N. E.; El-Deshw, O. A. *Pharmacological research* **2002**, 45, 447-454.

289. Maclachlan, T.; Narayanan, B.; Gerlach, V. L.; Smithson, G.; Gerwien, R. W.; Folkerts, O.; Fey, E. G.; Watkins, B.; Seed, T.; Alvarez, E. *Int. J. Radiat. Biol.* **2005**, 81, 567-579.

290. Mishra, B.; Kumbhare, L. B.; Jain, V. K.; Priyadarsini, K. I. *J. Phys. Chem. B* **2008**, 112, 4441-4446.

291. Fornace, A. J. Jr.; Nebert, D. W.; Hollander, M. C.; Luethy, J. D.; Papathanasiou, M.; Fargnoli, J.; Holbrook, N. J. *Mol. Cell. Biol.* **1991**, 11, 1009-1016.

292. Xiong, Y.; Hannon, G. J.; Zhang, H.; Casso, D.; Kobayashi, R.; Beach, D. p21 is a universal inhibitor of cyclin kinases. *Nature* **1993,** 366, 701-714.

293. Smith, M. L.; Kontny, H. U.; Zhan, Q.; Sreenath, A.; O'Connor, P. M.; Fornace, A. J. Jr. *Oncogene* **1996**, 13, 2255-63.

294. Smith, M. L.; Ford, J. M.; Hollander, M. C.; Bortnick, R. A.; Amundson, S. A.; Seo, Y. R.; Deng, C. X.; Hanawalt, P. C.; Fornace, A. J. Jr. *Mol. Cell. Biol.* **2000**, 20, 3705-14.

295. Radford, I. R. *Int. J. Radiat. Biol.* **1999**, 75, 521-528.

296. Mantena, S. K.; Unnikrishnan, S. K.; Joshi, R.; Radha, V.; Uma Devi, P.; Mukharjee, T. *Mutation Res.* **2008**, 650, 63-79.

List of journal publications included in the present thesis

1. **Kunwar, A.**; Barik, A.; Pandey, R.; Priyadarsini, K. I. Transport of liposomal and albumin loaded curcumin to living cells: an absorption and fluorescence spectroscopic study. *Biochim. Biophys. Acta.* **2006**, 1760, 1513-1520.

2. **Kunwar, A.**; Mishra, B.; Barik, A.; Kumbhare, L. B.; Pandey, R.; Jain, V. K.; Priyadarsini, K. I. 3,3'-diselenodipropionic acid, an efficient peroxyl radical scavenger and a GPx mimic, protects erythrocytes (RBCs) from AAPH-induced hemolysis. *Chem. Res. Toxicol.* **2007**, 20, 1482-1487.

3. **Kunwar, A.**; Narang, H.; Priyadarsini, K. I.; Krishna, M.; Pandey, R.; Sainis, K. B. Delayed activation of PKCdelta and NFkappaB and higher radioprotection in splenic lymphocytes by copper (II)-Curcumin (1:1) complex as compared to curcumin. J. *Cell. Biochem.* **2007**, 102, 1214-1224.

4. **Kunwar, A.**; Barik, A.; Mishra, B.; Rathinasamy, K.; Pandey, R.; Priyadarsini, K. I. Quantitative cellular uptake, localization and cytotoxicity of curcumin in normal and tumor cells. *Biochim. Biophys. Acta.* **2008**, 1780, 673-679.

5. Banerjee, A.; **Kunwar, A.**; Mishra, B.; Priyadarsini, K. I. Concentration dependent antioxidant/pro-oxidant activity of curcumin studies from AAPH induced hemolysis of RBCs. *Chem. Biol. Interact.* **2008**, 174, 134-139.

6. **Kunwar, A.**; Sandur, S. K.; Krishna, M.; Priyadarsini, K. I. Curcumin mediates time and concentration dependent regulation of redox homeostasis leading to cytotoxicity in macrophage cells. *Eur. J. Pharmacol.* **2009**, 611, 8-16.

7. **Kunwar, A.**; Bansal, P.; Jayakumar, S.; Bag, P. P.; Paul, P.; Reddy, N. D.; Kumbhare, L. B.; Jain, V. K.; Chaubay, R. C.; Unnikrishnan, M. K.; Priyadarsini, K. I. *In vivo* radioprotection studies of 3,3'-Diselenodipropionic acid (DSePA), a selenocystine derivative. *Free Radic. Biol. Med.* **2009** (Under revision)

Available online at www.sciencedirect.com
ScienceDirect
Biochimica et Biophysica Acta 1760 (2006) 1513–1520
BIOCHIMICA ET BIOPHYSICA ACTA
BBA
www.elsevier.com/locate/bbagen

Transport of liposomal and albumin loaded curcumin to living cells: An absorption and fluorescence spectroscopic study

Amit Kunwar [a], Atanu Barik [a], Ruchi Pandey [b], K. Indira Priyadarsini [a,*]

[a] Radiation and Photochemistry Division, Bhabha Atomic Research Centre, Trombay, Mumbai-400085, India
[b] Radiation Biology and Health Sciences Division, Bhabha Atomic Research Centre, Trombay, Mumbai-400085, India

Received 13 March 2006; received in revised form 27 June 2006; accepted 30 June 2006
Available online 8 July 2006

Abstract

Curcumin, a lipid soluble antioxidant, exhibits solvent and medium sensitive absorption and fluorescence properties. Using such changes, the average binding constants of curcumin to phosphatidylcholine (PC) liposomes and human serum albumin (HSA) were estimated to be 2.5×10^4 M^{-1} and 6.1×10^4 M^{-1} respectively. From the studies on temperature dependent fluorescence anisotropy of liposomal curcumin and its fluorescence quenching by acrylamide and iodide, it was concluded that curcumin is located in the gel phase of the liposomes. Similarly from the studies on quenching of tryptophan fluorescence in HSA by curcumin, it was found to be in the same domain as that of tryptophan. Both liposomal and HSA vehicles were examined for the transfer of curcumin to spleen lymphocyte cells, EL4 lymphoma cell line and compared with aqueous DMSO vehicles. From these studies it was found that liposomal vehicle is capable of loading more curcumin in to cells than HSA or aqueous-DMSO, and lymphoma cells show preferential uptake of curcumin to lymphocytes. The fluorescence of curcumin in EL4 lymphoma cells was found to be significantly higher as compared to the lymphocytes. The present study demonstrates a simple and quantitative method of estimation of curcumin delivered to cells by different vehicles using absorption and fluorescence spectroscopy.

Keywords: Curcumin; Liposomes; Human serum albumin; Absorption spectra; Fluorescence; Lymphocytes; EL4 lymphoma cells; Uptake

1. Introduction

Curcumin, a natural polyphenol, found in the rhizomes of *Curcuma longa* (turmeric), exhibits anti-inflammatory, anti-neoplastic, anti-oxidant and chemopreventive activities and has been shown to be pharmacologically safe even at high doses [1–3]. It is a hydrophobic molecule and is practically insoluble in aqueous solutions. Because of this hydrophobic nature, its bioavailability is poor after oral administration and therefore needs a carrier vehicle to transport to the desired targets. Curcumin has preferential interaction with serum albumins and lipid membranes [4–11]. Liposomes and serum albumins are some of the most commonly used transporting vehicles for drugs, proteins, hormones, diagnostic agents etc [12–15]. Liposomes are relatively easy to prepare, biodegradable, and have potential for high drug loading capacity. Serum albumin is the most abundant of the proteins, circulated several times in the blood [16]. Both liposomal and albumin delivery systems have been employed for intravenous administration of several hydrophobic drugs [17]. From *in vivo* studies, Li et al. showed that liposomal curcumin could suppress pancreatic carcinoma growth in murine xenograft models and inhibited tumor angiogenesis with equal or better efficiency as free curcumin [18]. In the literature, there are a few reports on the binding of curcumin to liposomes and albumins using spectroscopic methods [6–10]. However, there are no reports so far showing the quantitative estimation of transfer and delivery of curcumin from liposomes and albumins to cells. Here in this paper following absorption and fluorescence changes in curcumin in different systems, quantitative estimations were made on the loading of curcumin from phosphatidylcholine (PC) liposomes, and human serum albumin (HSA) to cellular systems. Curcumin exhibits solvent and medium sensitive excited state properties [19–21], which can be

* Corresponding author.
E-mail address: kindira@apsara.barc.ernet.in (K.I. Priyadarsini).

0304-4165/$ - see front matter © 2006 Elsevier B.V. All rights reserved.
doi:10.1016/j.bbagen.2006.06.012

easily monitored to follow its interaction with different systems [6–10,22–24]. Such changes in the fluorescence properties of curcumin have been utilized to evaluate the binding constants and the site of binding of curcumin to PC liposomes and HSA. Further cellular uptake of curcumin in mouse spleen lymphocytes and EL4 lymphoma cell line by these vehicles has also been studied.

2. Materials and Method

2.1. Reagents and equipments

HSA, curcumin (C.I. 75300), cholesterol, acrylamide, dipalmitoylphosphatidylcholine (DPPC), cell culture medium (RPMI 1640) and egg yolk phosphatidylcholine (PC) were from Sigma/Aldrich, USA and they have been procured from the local dealers. Potassium iodide (AR grade, BDH, India), spectro grade methanol and DMSO from Spectro Chem. India were purchased from the local market. The purity of curcumin was confirmed by TLC and HPLC [25]. Solutions were prepared in nanopure water from a Millipore Milli-Q system and the solutions were purged with nitrogen wherever required to minimize degradation. Mouse spleen lymphocytes were freshly isolated and EL4 cell line (Lymphoma of T cell of mouse origin) was obtained from ATCC, USA. Absorption spectra were recorded on a JASCO V-530 spectrophotometer and fluorescence spectra recorded on a Hitachi F-4010 fluorimeter. Fluorescence lifetimes were measured using a time-resolved spectrofluorimeter from IBH instrument, UK. The instrument works on the principle of time-correlated single-photon-counting (TCSPC). The details of the instrument have been described elsewhere [26]. All the experiments were repeated twice and each experiment was performed in duplicate.

2.2. Preparation of liposomes

Liposomes were prepared using the mixture of PC and cholesterol in the weight ratio of 2:1 respectively and solubilized in chloroform, the solvent was evaporated by rotavapour [27]. The resulting thin film was solubilized in 10 mM phosphate buffer (pH 7.4), and sonicated for 5 min using a bath type sonicator. The diameters of the liposomes ranged between 100 and 200 nm as estimated by light scattering measurements. The concentration of the phospholipids in liposomal solution was determined according to the method reported earlier [28].The fluorescence titrations of curcumin and PC liposome solutions were made as described earlier [29].

2.3. Encapsulation of curcumin in liposome

Curcumin containing liposomes were prepared by dissolving PC, cholesterol (in 2:1 ratio) and a known amount of curcumin (200 μM) in chloroform and the solvent was removed by evaporation [27,30]. The resulting thin film was solubilized in 10 mM phosphate buffer (pH 7.4), and sonicated for 5 min. The sample was centrifuged at 1000 rpm in Beckman centrifuge ($200\times g$) for 5 min and the supernatant containing curcumin loaded liposomes was separated from the pellet. The pellet contains unbound curcumin. The supernatant was recentrifuged two additional times. Each time the pellet was dried and dissolved in methanol. Finally these three fractions were pooled, volume was made up to 25 ml with methanol and absorption spectrum was recorded, using the molar absorption coefficient of curcumin in methanol at 428 nm as 48000 M^{-1} cm^{-1}, the amount of unbound curcumin was determined [21]. Subtracting this value from the initially added curcumin, the amount of curcumin actually loaded on liposomes was estimated. From this, a stock solution of 190 μM curcumin loaded in to 2.8 mM PC liposome was prepared. This stock solution after appropriate dilution was used for cell uptake studies. For fluorescence quenching studies, the liposomal curcumin solutions were incubated in quartz cells at 30 °C in the presence of iodide (I^-) and acrylamide as quenching agents in 10 mM phosphate buffer (pH 7) and the fluorescence intensity at 498 nm was monitored after excitation at 420 nm. The ionic strength of the solution was kept constant at 0.3 M using sodium chloride.

2.4. Preparation of HSA–curcumin complex

A stock solution of 10 mM curcumin in methanol was prepared and diluted with nitrogen saturated 5 mM aqueous Na_2HPO_4 solution to get a clear solution of 100 μM curcumin, and the methanol content in the solution did not exceed 1%. A stock solution of HSA was dissolved in 32.4 mM Na_2HPO_4 and 7.5 mM KH_2PO_4 buffer. These two solutions of HSA and curcumin were mixed very quickly to obtain the required concentration of HSA and curcumin. The stability of curcumin during the experiment was monitored by following the absorption spectrum of curcumin. The pH of the solution after mixing was 7.4. This system was used for fluorescence titration and estimation of the binding constant of curcumin with HSA. Curcumin was also solubilized by incubating solid curcumin with 30 μM HSA for half a day and then centrifuged to remove unbound curcumin and dialyzing the solution with aqueous buffer for 24 h. The clear supernatant contained 30 μM curcumin bound to HSA. This solution was found to be stable for a few days and therefore used for quantum yield estimation and cell uptake studies.

Fluorescence quantum yield (ϕ_F) of the HSA–curcumin and liposomal curcumin was determined using Coumarin-153 laser dye as a reference with a known ϕ_F of 0.56 in acetonitrile and the details are given in our earlier references [5,31,32]. Fluorescence anisotropy was measured in the same fluorimeter using parallel and perpendicular polarisers.

2.5. Estimation of binding constant between curcumin and liposomes and HSA by absorption and fluorescence measurements

The binding constants for the binding of curcumin to PC liposomes and HSA were determined by following the absorption spectra of solutions containing different concentrations of curcumin in liposomes and HSA. The process of binding of curcumin to the binding agent, BA (BA represents either PC liposomes or HSA) can be shown by the equations given below.

$$\text{Curcumin} + \text{BA} \rightleftharpoons \text{Complex} \tag{1}$$

The equilibrium constant K for the above equilibrium is given by equation

$$K = \frac{[\text{Complex}]}{[\text{BA}][\text{Curcumin}]} \tag{2}$$

For the above equilibrium, assuming 1:1 complex formation, the double reciprocal plot, also known as Benesi–Hildebrand plot [5] is made by following absorbance changes at a suitable wavelength, as a function of reciprocal concentration of PC or HSA or curcumin according to the Eq. (3) given below.

$$\frac{1}{\Delta A} = \frac{1}{K\Delta\varepsilon[\text{BA}]}\left(\frac{1}{[\text{Curcumin}]}\right) + \frac{1}{\Delta\varepsilon[\text{BA}]} \tag{3}$$

here ΔA and $\Delta\varepsilon$ correspond to the change in the absorbance and the molar extinction coefficient at the wavelength of the study respectively. [BA] and [Curcumin] correspond to the concentrations of binding agent (either liposome or HSA) and curcumin respectively. Using this equation, the values of K and $\Delta\varepsilon$ were estimated by following the absorbance changes in curcumin in the region 420 to 450 nm either as a function of different concentration of PC/HSA at a fixed concentration of curcumin or as a function of curcumin concentration fixing the concentration of either PC or HSA.

The binding constants were estimated by following the fluorescence changes also. Curcumin is non-fluorescent in neat aqueous solutions but its fluorescence intensity increases significantly in presence of PC or HSA. The changes in fluorescence intensity due to curcumin were followed as a function of concentration of PC or HSA according to Eq. (4) to estimate the binding constant [33].

$$F = \frac{F_0 + F_{\text{complex}}K[\text{BA}]}{1 + K[\text{BA}]} \tag{4}$$

here F_0 and F are the respective fluorescence intensity from curcumin at a suitable wavelength in the range from 490 to 520 nm in the absence and presence of either liposomes or HSA and F_{complex} is the saturation value.

2.6. Cell culture and uptake studies

For cell uptake studies, freshly isolated mouse spleen lymphocytes and EL4 cell line (T cell lymphoma of mouse origin) were used. Mouse spleen lymphocytes were isolated as described earlier [34]. Single cell suspension from spleen was obtained by gently teasing the organ in to RPMI 1640 medium (containing 15 mM HEPES, 2 mM L-glutamine, 100 IU/ml penicillin, 100 mg/ml streptomycin and 20 μM 2-mercaptoethanol) using a sterile nylon mesh. Red blood cells were eliminated by treatment with 0.83% ammonium chloride solution. Lymphocytes rich cells were further washed with medium to remove traces of ammonium chloride and the viability was assessed by trypan blue dye exclusion. This preparation was used for cell uptake studies. The EL4 cell line was cultured in suspension with RPMI 1640 medium containing 10% fetal bovine serum. For the cell uptake experiments spleenic lymphocytes and EL4 cell line were plated at $\sim 5\times10^6$ cells/ml using serum free RPMI 1640 medium with desired concentration of curcumin in liposomes, HSA or in aqueous-DMSO (for comparison) in 24 well plate. DMSO was added to aqueous solutions as curcumin is insoluble in water. For this, initially 10 mM stock solution of curcumin in DMSO was prepared and diluted with culture medium to get desired concentration of curcumin keeping final DMSO concentration less than 0.1%. The concentration of curcumin is expressed as nmol/million cells/ml. Vehicle controls were kept for each of the treatment condition. After incubation period of 4 h, cells were spinned down at 1000 rpm in Beckman centrifuge ($200\times g$) for 5 min and washed twice with cold phosphate buffered saline (PBS). Finally cells were resuspended in to 1 ml of aqueous PBS solution and absorption and fluorescence spectra of curcumin associated with cells was measured. The actual concentration of curcumin loaded into the cells was determined as given here. The curcumin loaded cells were spinned down, the pellet was dried and suspended in to 1 ml of methanol and sonicated for 5 min, so that curcumin is extracted into the methanol fraction. The lysate was centrifuged at 10000 rpm for 5 min and absorption spectra of supernatant containing methanolic curcumin was recorded. From the molar absorption coefficient of curcumin in methanol at 428 nm, the amount of curcumin loaded to cells was estimated. The results were normalized to 1 nmol of substrate added/million cells/ml and cell uptake has been expressed as pmol/million cells. The statistical significance of the difference in the uptake of curcumin by spleen lymphocytes and EL4 lymphoma cell line through different vehicles were assessed by students' t test. A value of $P<0.05$ was considered as statistically significant. Uptakes have been given as mean±SD, $n=4$.

3. Results

3.1. Binding of curcumin with PC liposomes

The absorption spectrum of curcumin is blue shifted from 425 nm to 420 nm in presence of liposomes (Figs. 1a and b respectively for 1% aqueous-methanol and PC liposomes). To estimate the binding constant of curcumin to PC liposomes, absorption changes at 420 nm were followed at pH 7.4 varying concentration of PC in liposome from 9.3 to 93 μM and keeping curcumin concentration at 5 μM and fitting the data to Eq. (3) the binding constant was estimated to be $(2.1\pm0.1)\times10^4\ M^{-1}$. From the same plot, the extinction coefficient of liposomal curcumin at 420 nm was estimated to be $82280\pm2000\ M^{-1}\ cm^{-1}$. This was also verified by varying the concentration of curcumin from 1.25 to 15 μM, keeping PC in liposomes at 93 μM.

Curcumin in aqueous buffer, containing 1% methanol exhibits weak fluorescence with featureless and broad maximum ~550 nm (inset a of Fig. 1). However with increasing addition of PC liposomes at a fixed amount of curcumin, the fluorescence intensity increased and there is a large blue shift (498 nm) in the fluorescence maximum on curcumin binding to PC liposomes (inset b of Fig. 1). The binding constant for the

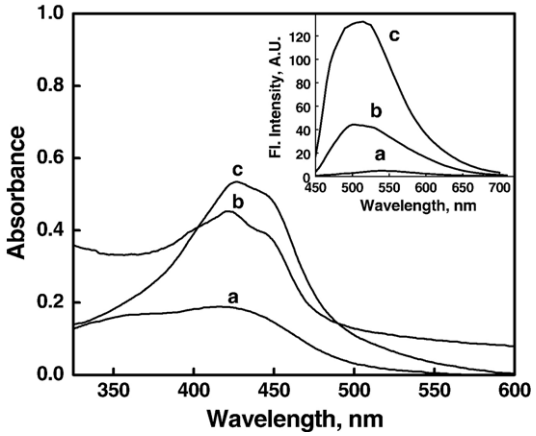

Fig. 1. Absorption spectra of curcumin at pH 7.4 (a) in aqueous solution containing 1% methanol, (b) in the presence of PC liposome and (c) in the presence of HSA. Inset shows relative fluorescence spectra of the same solutions, after excitation at 420 nm. For the reference spectra, corresponding blanks without curcumin were used.

binding of curcumin with liposomes was also estimated by following fluorescence intensity changes at 498 nm, after excitation at 420 nm for solutions containing 5 μM curcumin with varying liposome concentrations from 9.3 to 93 μM PC at pH 7.4. Fitting the data to Eq. (4), the binding constant K was estimated to be $(2.9\pm1.1)\times10^4\ M^{-1}$. The saturation concentration of PC liposome required for complete saturation of fluorescence intensity from 5 μM curcumin was 50 μM. Alternatively the fluorescence titrations were also done with fixed PC liposome concentration (93 μM) and varying curcumin concentration (1.25 to 15 μM). The concentration of curcumin required for complete saturation of liposome having 93 μM PC was 10 μM.

The fluorescence quantum yield of curcumin in liposome was estimated to be 0.025±0.003. The low value of fluorescence quantum yield in PC liposome indicates that most of the excited states of curcumin even in liposome undergo nonradiative decay by the presence of water molecules inside the liposomal bilayers. The blue shift in the fluorescence maximum and the increase in intensity with increasing liposome concentration suggest that curcumin in PC liposomes experiences nonpolar environment probably by binding to the hydrophobic regions of PC liposomes.

To understand the site of binding in liposomes, steady state fluorescence anisotropy measurements were performed on curcumin entrapped in PC liposomes. For these studies fluorescence anisotropy of curcumin in aqueous solutions containing 1% methanol was compared with that in presence of PC liposome. After excitation at 420 nm the fluorescence emission in both parallel and perpendicular directions was followed in the wavelength range of 460–600 nm, from which the anisotropy was calculated. The anisotropy significantly increased from 0.13±0.01 in aqueous methanol solution to 0.31±0.01 in the presence of PC liposome. This confirms that curcumin is well entrapped in the liposome gel phase, where it experiences a restricted motion. These measurements were also carried out at different temperatures varying from 25° to 50 °C,

which showed no significant change in anisotropy, indicating that curcumin remains well entrapped in liposome formulation within the temperature range. These parameters are listed in Table 1 for comparison with HSA. Since PC liposome is a mixture of lipids of different chain lengths and it is likely that some lipids may be in gel phase and some in fluid phase. We therefore verified this by studying temperature dependent fluorescence anisotropy of curcumin in DPPC liposomes (single chain lipid) both in the absence and presence of cholesterol and the studies indicated that in the absence of cholesterol, the anisotropy decreased by 20% above the phase transition temperature of 41 °C, but in presence of cholesterol the anisotropy remained constant. This study further confirmed our inference that curcumin is located in the gel phase of the liposomes [35].

To know more about the distribution of curcumin in different compartments of the PC liposome bilayer, experiments were carried out by following fluorescence quenching studies in presence of different quenchers at pH 7 [36,37]. Curcumin has two phenolic OH groups with first pK_a ~ 8.5. Therefore at pH 7, 90% of curcumin is in neutral form and ~ 10% is in anionic form [21]. The anionic form is less fluorescent (60%) than the neutral form in liposomes, but at pH 7 its contribution is very low therefore it is assumed that the anionic form does not significantly influence the fluorescence quenching experiments. Following the quenching of fluorescence from liposomal curcumin by using iodide and acrylamide [29] as quenchers, it is possible to evaluate the location of curcumin inside the membrane. Iodide is a hydrophilic quencher, which can access curcumin in the liposome surface, while acrylamide, being hydrophobic, can access curcumin only when inserted inside the liposome bilayer. The quencher concentrations were varied from 0 to 0.15 M keeping the ionic strength constant. The concentrations of the quenchers and salts were selected in such a way that they do not induce changes in the bilayer structure of liposomes. The fluorescence data were analyzed according to the Stern–Volmer Eq. (5)

$$\frac{F_0}{F} = 1 + K_D[Q] \quad (5)$$

here F_0 and F are the intensities of the fluorophore (liposomal curcumin) in the absence and presence of the quencher Q, respectively and K_D is the Stern–Volmer collision constant.

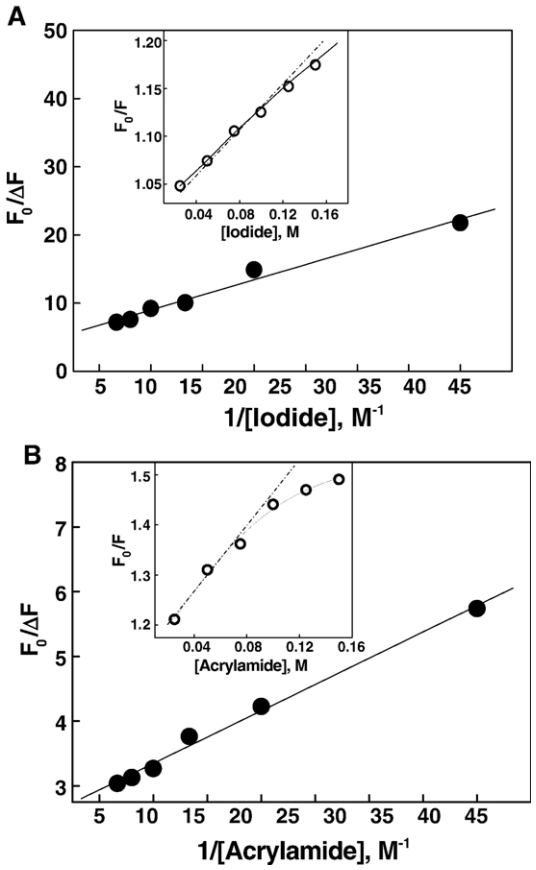

Fig. 2. Plots showing the fluorescence quenching of liposomal formulation (93 μM PC) containing 10 μM curcumin in phosphate buffer at pH 7 at constant ionic strength (0.3 M) (A) iodide as quencher and (B) acrylamide as quencher. Line shows fitting to Eq. (6). Insets of Fig. 2(A) and (B) respectively show the data for the quenching of curcumin fluorescence by iodide and acrylamide fitting to Eq. (5), dotted lines show linear fits for Eq. (5).

Insets of Figs. 2A and B show the fluorescence quenching data for iodide and acrylamide respectively and lines show fitting to Eq. (5). Here, deviation from linearity indicates presence of more than one class of fluorophore which are not equally accessible to the quencher [32]. The quenching process can be both static and dynamic. Static quenching occurs in the ground state by formation of non-fluorophoric complex in the presence of quencher and this has been analysed by following absorption spectra of curcumin in the presence of the quencher. The spectra

Table 1
Photophysical properties and cellular uptake of liposomal and HSA bound curcumin

Photophysical properties	PC Liposome	HSA
Absorption maximum	420 nm	430 nm
Fluorescence maximum	498 nm	515 nm
Fluorescence quantum yield	0.025±0.003	0.038±0.005
Fluorescence anisotropy	0.31±0.01	0.37±0.05
Binding constant (M^{-1})		
Absorption method	$(2.1\pm0.1)\times10^4$	$(1.2\pm0.1)\times10^4$
Fluorescence method	$(2.9\pm1.1)\times10^4$	$(1.1\pm0.2)\times10^5$
Molar extinction coefficient[a] (M^{-1} cm^{-1})	82280±2000 (420 nm)	94161±2000 (430 nm)
Cellular delivery (pmol/10^6 cells) after	Lymphocytes 30.9±1.6	Lymphocytes 25.8±0.8
treatment with 1 nmol curcumin/10^6 cells/ml	EL4 cells 42.0±4.3	EL4 cells 34.9±2.2

[a] Estimated by Benesi-Hildebrand plot for 1:1 complex.

showed decrease in the absorbance without any change in the nature of the spectrum in the presence of iodide and acrylamide (data not shown), indicating contribution from static quenching. Contribution from dynamic quenching was studied by following the fluorescence lifetime of curcumin in presence of the quenchers. Fluorescence decay profile of curcumin showed biexponential behavior in the absence of quenchers in liposomes with average lifetime of 322 ps. In the presence of iodide (0.15 M) and acrylamide (0.15 M) the average fluorescence lifetime decreased to 302 ps and 316 ps respectively, indicating that dynamic quenching is not very important. The detailed analysis of the contribution from static and dynamic quenching is not attempted in the present study. However, in order to understand the relative population of curcumin in different layers, the fluorescence intensity changes due to curcumin in presence of quenchers were treated with the modified Stern–Volmer Eq. (6) according to the procedure given in reference [27,32].

$$\frac{F_0}{\Delta F} = \left[\frac{1}{f_a K'_D[Q]}\right] + \left(\frac{1}{f_a}\right) \quad (6)$$

here ΔF is the difference between the fluorescence intensities from the fluorophore in the absence and presence of Q, f_a is the fraction of fluorophore that is accessible to the quencher and K'_D is the Stern–Volmer constant. Figs. 2A and B show fitting of the data to Eq. (6) for iodide and acrylamide respectively. The fitted parameters were found to be $f_a = 0.22 \pm 0.01$ and $K'_D = 10.3 \pm 1.7\ M^{-1}$ for iodide quenching and $f_a = 0.40 \pm 0.01$ and $K'_D = 31.6 \pm 2.1\ M^{-1}$ for acrylamide quenching. This confirms that curcumin is non-uniformly distributed into different compartments of the liposomal bilayer and is preferably located inside the hydrophobic interior, which is important for higher drug loading capacity of liposome formulation [38].

3.2. Binding of curcumin with HSA

Human serum contains albumin proteins, which help in carrying drug molecules to different targets [13,16]. Earlier we have studied the binding of curcumin to bovine serum albumin (BSA) in detail [5]. Here we briefly mention about the binding of curcumin to HSA. HSA is more physiologically relevant than BSA and the two mainly differ in tryptophan content [16].

The absorption spectra of curcumin were recorded in presence of HSA (30 μM) with varying concentration (2.5 to 30 μM) of curcumin in the wavelength range of 250 to 550 nm. The absorbance of curcumin at 430 nm increased in presence of HSA (Fig. 1c). Considering the complex formation between curcumin and HSA according to Eq. (3) the binding constant of curcumin and HSA was estimated as $(1.2 \pm 0.1) \times 10^4\ M^{-1}$ and the molar extinction coefficient of the bound complex at 430 nm was estimated to be $94161 \pm 2000\ M^{-1}\ cm^{-1}$. The same set of solution was used for estimation of binding constant by fluorescence titration method according to Eq. (4). From which the binding constant was estimated to be $(1.1 \pm 0.2) \times 10^5\ M^{-1}$. As observed with liposomes, when curcumin was bound to HSA solution, the fluorescence intensity increased significantly and the fluorescence maxima was blue shifted to 515 nm (inset c of Fig. 1). Fluorescence quantum yield of HSA bound curcumin was estimated to be 0.038 ± 0.005. The blue shift in the fluorescence maximum and increase in fluorescence quantum yield in HSA suggest that curcumin is located in the hydrophobic environment where quenching by water molecule is less probable. However the blue shift in fluorescence maximum in HSA is less than that in liposomes. This suggests that the hydrophobic pockets in HSA are more polar than the gel phase of liposomes, where curcumin is located. Fluorescence anisotropy of curcumin showed limiting value in HSA and no significant change in anisotropy was observed with temperature in the range from 30° to 50 °C. All these parameters of curcumin binding to HSA are listed in Table 1.

In order to understand the site of binding to HSA quenching of intrinsic fluorescence from HSA was followed in the presence of curcumin. HSA contains a tryptophan residue in 214 position in the peptide chain which is responsible for the intrinsic fluorescence of HSA. The tryptophan moiety in HSA can be excited at 280 nm, which emits fluorescence at 340 nm. As observed with BSA in our earlier studies [5], when curcumin (2.5 to 20 μM) was added to the HSA solution, the tryptophan fluorescence decreased due to quenching (figure not shown). For the quenching studies, the concentration of curcumin was such that, direct excitation of curcumin by 280 nm was minimum at the highest concentration of curcumin (~15% of the absorption by HSA). The quenching of tryptophan fluorescence by curcumin indicates that it is located in the vicinity of tryptophan.

3.3. Cellular uptake studies

Both liposomal and HSA formulations were subjected to cell uptake studies for their probable use as delivery vehicles of curcumin to cellular system. Such uptake studies will be useful to know which one of them is the most efficient carrier in comparison to fluid phase uptake of free curcumin (aqueous buffer containing 0.1% DMSO). To address this, we compared the uptake of curcumin using two different cell systems, normal mouse lymphocytes and mouse T lymphoma cell line EL4. The uptake was estimated by absorbance measurement of methanol extracted cell lysates as a function of the total amount of curcumin added in the incubation medium. Figs. 3 and 4 show absorption spectra of methanol extracted cell lysates and the absorbance is related to the amount of curcumin delivered. The cells were incubated with different concentrations of curcumin by different vehicles and the results represented by spectra “a to f” in Fig. 3 and spectra “a to e” in Fig. 4. Figs. 3g and 4f correspond to the cells treated with DMSO vehicle controls. Other vehicle controls (PC liposomes or HSA) showed similar spectra and therefore not included in the figure. The figure confirms concentration dependent uptake of curcumin by both the cell types. The average uptake of curcumin calculated from the absorption

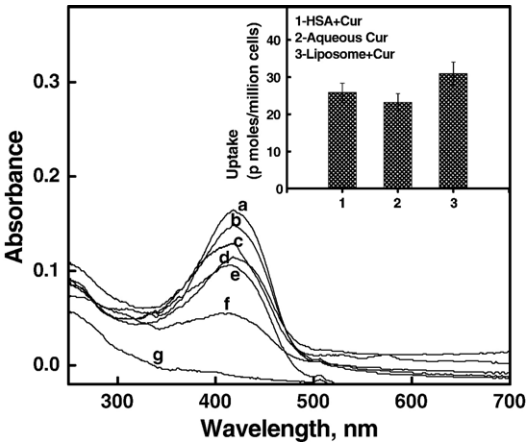

Fig. 3. Overlapped absorption spectra of methanol lysates of spleen cells treated with different concentrations of free, liposomal and HSA bound curcumin. Spectra a and b correspond to cells treated with liposomal curcumin at concentrations of 10 and 5 nmol/million cells/ml. Spectra c and d correspond to cells treated with aqueous-DMSO solutions of curcumin at concentrations of 10 and 5 nmol/million cells/ml. Spectra e and f correspond to cells treated with HSA bound curcumin at concentrations of 4 and 2 nmol/million cells/ml. Spectrum g corresponds to the aqueous-DMSO vehicle control. Inset shows uptake per 1 nmol of substrate added/million cells/ml within incubation period of 4 h by different vehicles.

spectra, expressed in pmol/million cells/ml, with different vehicles after normalization to 1 nmol of substrate added/million cells/ml for spleenic lymphocytes and EL4 lymphoma cell line are given in Table 1. Insets of Figs. 3 and 4 show bar graph indicating relative cell uptake by different vehicles. It can be seen that the uptake of curcumin is significantly higher in EL4 cells (nearly 1.5 times, $P<0.05$) with all the vehicles as compared to spleenic lymphocytes, indicating that tumor cells show preferential uptake of curcumin, which is in agreement with the literature reports [1,3]. The results further indicate that liposome mediated delivery is more efficient and is capable of loading more curcumin to both cell types as compared to either free curcumin or HSA bound curcumin. Between HSA bound curcumin and free curcumin, cellular delivery is almost similar.

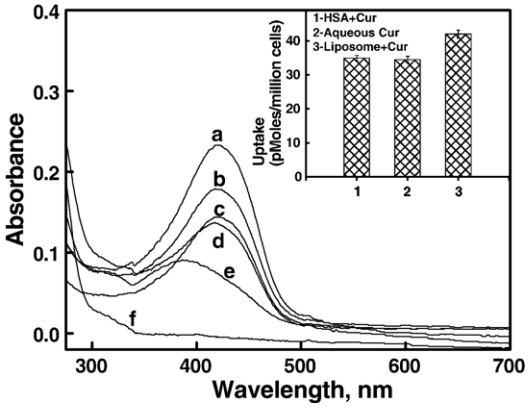

Fig. 4. Overlapped absorption spectra of methanol lysates of EL4 lymphoma cells treated with different concentrations of free, liposomal and HSA bound curcumin. Spectra a and b correspond to cells treated with liposomal curcumin at concentrations of 10 and 5 nmol/million cells/ml. Spectrum c corresponds to cells treated with aqueous-DMSO solution of curcumin at concentration of 5 nmol/million cells/ml. Spectra d and e correspond to cells treated with HSA bound curcumin at concentrations of 4 and 2 nmol/million cells/ml. Spectrum f corresponds to the aqueous-DMSO vehicle control. Inset shows uptake per 1 nmol of substrate added/million cells/ml within incubation period of 4 h by different vehicles.

Fluorescence spectra of curcumin in the above incubated spleenic lymphocytes and EL4 lymphoma cells were also recorded. For these studies, the cell suspensions were excited at 420 nm and fluorescence emission was followed in the wavelength range of 440 to 700 nm. Figs. 5a, b and c show fluorescence spectra of curcumin in spleenic lymphocytes treated with free, HSA and liposomal curcumin respectively. Figs. 5d, e and f show corresponding spectra in EL4 cells. The fluorescence from cells treated with vehicle controls showed no detectable fluorescence. Inset (A) of Fig. 5 gives the bar graph showing the comparative fluorescence intensity at fluorescence maximum at 498 nm in these systems. The results clearly support our previous observations that liposomal system could load more curcumin to both the cell types and EL4 cells show preferential uptake. Interestingly, for the same absorbance at the excitation wavelength, the relative fluorescence intensity was nearly three times more in EL4 cells as compared to lymphocytes suggesting higher fluorescence emission from curcumin in lymphoma cells. The nearly linear variation in the fluorescence intensity as a function of curcumin uptake in the two different cell systems, as shown in the inset (B) of Fig. 5 indicates that the fluorescence intensity is directly related to the uptake.

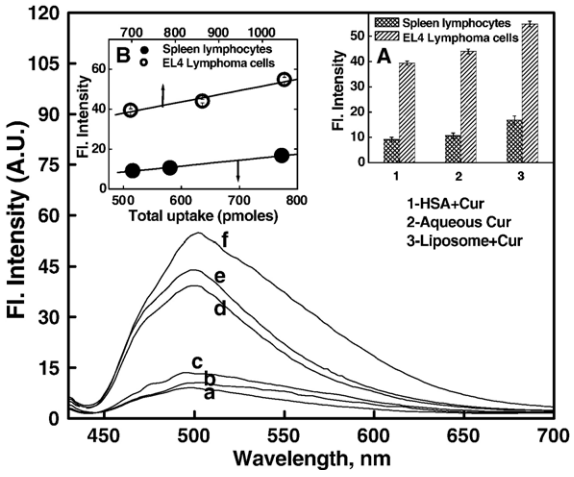

Fig. 5. Fluorescence spectra of curcumin in lymphocytes (a, b, c) and EL4 cells (d, e, f) after treating with aqueous-DMSO solution of curcumin, HSA and liposomal bound curcumin respectively in the culture medium for 4 h. Spectra c and f correspond to normal and tumor cells respectively treated with liposomal curcumin at concentration of 5 nmol/million cells/ml. Spectra b and e correspond to normal and tumor cells respectively treated with aqueous-DMSO solution of curcumin at concentration of 5 nmol/million cells/ml. Spectra a and d correspond to normal and tumor cells treated with HSA bound curcumin at concentration of 4 nmol/million cells/ ml. The excitation wavelength was 420 nm. Inset (A) shows bar graph representing comparative fluorescence intensities in EL4 cells and lymphocytes by different vehicles. Inset (B) shows linear plot for change in fluorescence intensity from curcumin in different cells with total cellular uptake.

4. Discussion

Curcumin, a natural pigment with remarkable pharmacological activity, is a hydrophobic compound and shows lipid solubility. Being hydrophobic, curcumin needs a carrier system to transport to different parts of the body. In the recent past several systems are being developed for selective drug delivery studies.

In this paper, we have studied interaction of curcumin with two important commonly used transport systems, liposomes and serum albumins. Curcumin is non-fluorescent in aqueous solutions. Its fluorescence quantum yield and fluorescence maximum are sensitive to solvent polarity and protic nature of the solvent. This property can be used as a tool to monitor its interaction with biomolecules and also its delivery to different targets. Following such fluorescence changes, we studied the binding of curcumin with liposomes and albumins. The results show high affinity of curcumin with these systems. We have also made an attempt to understand the site of binding of curcumin to these systems. In liposomes quenching of curcumin fluorescence by hydrophobic and hydrophilic quenchers was followed and from this, it was found that at neutral pH curcumin is loaded into the gel phase of liposomes. Similarly by following the quenching of intrinsic tryptophan fluorescence of HSA by curcumin, it was inferred that it is located in the vicinity of tryptophan. One of the drawbacks associated with the use of such formulations as drug delivery vehicles is their susceptibility to undergo leakage of entrapped drug during temperature increase [36]. The temperature dependent fluorescence anisotropy studies in these systems confirm that the binding is intact even up to 50 °C. Between liposomes and HSA, the average binding affinity of curcumin appears to be higher with HSA as compared to liposomes.

The two systems were employed for delivering curcumin to two different cells viz., normal spleen lymphocytes, and EL4 lymphoma cells. HSA is an endogenous vehicle for drug molecules, while liposomes are exogenously added carrier systems. They differ mainly in their mechanism of drug delivery. Albumin proteins release drug molecules to the target cells via fluid phase pinocytosis, while liposomes release drug molecules via membrane fusion [30]. The cells were incubated with these formulations for an identical time period, and the loaded curcumin was estimated quantitatively by absorption method. They were compared with aqueous DMSO vehicles. The results showed that there is a preferential loading of curcumin by liposomal system as compared to free and HSA bound form. This suggests that liposomal delivery is more efficient for hydrophobic drugs like curcumin and is therefore a preferred vehicle. The differential loading capacity of liposomes and HSA may also be due to their site of binding of curcumin in these systems, which needs to be addressed with more detailed experiments and calculations.

Another interesting observation, which cannot be ignored, is that the lymphoma cells show preferential uptake of curcumin and the fluorescence of curcumin is significantly higher in lymphoma cells as compared to normal cells. The enhanced uptake of curcumin by lymphoma cells could be either due to their high metabolic activity or larger size. The increase in fluorescence intensity in lymphoma cells indicates difference in microenvironment experienced by curcumin molecule inside these cells. Curcumin being a lipophilic molecule mainly gets located inside the membrane. Hence the fluorescence changes indicate difference in membrane composition of lymphoma cells compared to lymphocytes. Our future experiments are therefore directed to follow this more in detail to examine whether curcumin can be used for selective imaging of tumor cells. Detailed studies on cytotoxicity, metabolism and degradation of curcumin in different cells loaded by these different vehicles will also need to be addressed.

In conclusion the present study demonstrates the use of absorption and fluorescence methods for quantitative estimation and identification of the loading capacity of curcumin by different vehicles to normal and tumor cells. The absorption method is best suited for the quantitative estimation, while fluorescence method is useful in identifying the site of location. The results confirm that the most efficient means of delivering curcumin to cells is via incorporation in to liposomes, and also that curcumin is more readily taken up by lymphatic cancerous cells, than normal lymphocytes.

Acknowledgements

The authors are thankful to Dr. H. Pal for help in fluorescence studies and Dr. S. K. Sarkar, Head RPC Division, Dr. T. Mukherjee, Director, Chemistry Group and Dr. K. B. Sainis, Director, Bio-Medical Group for their constant encouragement and support.

References

[1] B.B. Aggarwal, A. Kumar, A.C. Bharti, Anticancer potential of curcumin: preclinical and clinical studies, Anticancer Res. 23 (2003) 363–398.
[2] R.A. Sharma, A.J. Gescher, W.P. Steward, Curcumin: the story so far, Eur. J. Cancer 41 (2005) 1955–1968.
[3] S. Shishodia, G. Sethi, B.B. Aggarwal, Curcumin: getting back to roots, Ann. N.Y. Acad. Sci. 1056 (2005) 206–217.
[4] K.I. Priyadarsini, Free radical reactions of curcumin in membrane models, Free Radical Biol. Med. 23 (1997) 838–843.
[5] A. Barik, K.I. Priyadarsini, H. Mohan, Photophysical studies on binding of curcumin to bovine serum albumin, Photochem. Photobiol. 77 (2003) 597–603.
[6] G. Began, E. Sudharshan, K. Udaya Sankar, A.G. Appu Rao, Interaction of curcumin with phosphatidylcholine: a spectrofluorometric study, J. Agric. Food Chem. 47 (1999) 4992–4997.
[7] S. Kapoor, K.I. Priyadarsini, Protection of radiation-induced protein damage by curcumin, Biophys. Chem. 92 (2001) 119–126.
[8] A. Ch. P. Reddy, E. Sudharshan, A.G.A. Rao, B.R. Lokesh, Interaction of curcumin with human serum albumin—a spectroscopic study, Lipids 34 (1999) 1025–1029.
[9] F. Zsila, Z. Bikadi, M. Simonyi, Unique, pH-dependant biphasic band shape of the visible circular dichroism of curcumin–serum albumin complex, Biochem. Biophys. Res. Commun. 301 (2003) 776–782.
[10] F. Zsila, Z. Bikadi, M. Simonyi, Molecular basis of the cotton effects induced by the binding of curcumin to human serum albumin, Tetrahedron: Assymetry 14 (2003) 2433–2444.
[11] M.O. Iwunze, Binding and distribution characteristics of curcumin solubilised in CTAB micelle, J. Mol. Liq. 111 (2004) 161–165.
[12] H. Brochu, A. Polidori, B. Pucci, P. Vermette, Drug delivery systems using immobilized intact liposomes: a comparative and critical review, Curr. Drug Deliv. 1 (3) (2004) 299–312.

[13] U. Kragh-Hansen, Molecular aspects of ligand binding to serum albumin, Pharmacol. Rev. 33 (1981) 17–53.
[14] I. Sjoholm, B. Ekman, A. Kober, I. Ljungstedt-Pahlman, B. Seiving, T. Sjodin, Binding of drugs to human serum albumin XI. The specificity of three binding sites as studied with albumin immobilized in microparticles, Mol. Pharmacol. 34 (1979) 160–171.
[15] R.H. Bisby, C. Mead, C.G. Morgan, Wavelength programmed solute release from photosensitive liposomes, Biochem. Biophys. Res. Commun. 276 (2000) 169–173.
[16] T. Peters, Serum albumin, Adv. Protein Chem. 37 (1985) 161–245.
[17] W.C. Zamboni, Liposomal, nanoparticle, and conjugated formulations of anticancer agents, Clin. Cancer Res. 11 (23) (2005) 8230–8234.
[18] L. Li, F.S. Braiteh, R. Kurzrock, Liposome encapsulated curcumin *in vitro* and *in vivo* effects on proliferation, apoptosis, signaling and angiogenesis, Cancer 104 (2005) 1322–1331.
[19] S.M. Khopde, K.I. Priyadarsini, D.K. Palit, T. Mukherjee, Effect of solvent on the excited state photophysical properties of curcumin, Photochem. Photobiol. 72 (2000) 625–631.
[20] C.F. Chignell, P. Bilski, K.J. Reszka, A.N. Motten, R.H. Sik, T.A. Dhal, Spectral and photochemical properties of curcumin, Photochem. Photobiol. 59 (1994) 295–302.
[21] P.H. Bong, Spectral and photophysical behaviours of curcumin and curcuminiods, Bull. Korean Chem. Soc. 21 (2000) 81–86.
[22] F. Cui, J. Fan, W. Li, Y. Fan, Z. Hu, Fluorescence spectroscopy studies on 5-aminosalicylic acid and zinc 5-aminosalylicylate interaction with human serum albumin, J. Pharm. Biomed. Anal. 34 (2004) 189–197.
[23] Y. Hu, Y. Liu, W. Jiang, R. Zhao, S. Qu, Fluorometric investigation of the interaction of bovine serum albumin with surfactants and 6-mercaptopurine, J. Photochem. Photobiol. 80 (2005) 235–242.
[24] H.A. Feldman, Mathematical theory of complex ligand-binding system at equilibrium: some methods for parameter fitting, Anal. Biochem. 48 (1972) 317–338.
[25] J. Taylor, I.J. McDowell, Determination of the curcuminoid pigments in turmeric (*Curcuma domestica* Val) by reversed-phase high-performance liquid chromatography, Chromatographia 34 (1992) 73–77.
[26] A. Barik, M. Kumbhakar, S. Nath, H. Pal, Evidence for the TICT mediated nonradiative deexcitation process for the excited coumarin-1 dye in high polarity protic solvents, Chem. Phys. 315 (2005) 277–285.
[27] N.L. Zalloum, D.N. Biloti, F.B.T. Pessine, Spectrofluorimetry and chemo metrics for investigation of norfloxacin distribution in multilamellar liposomes, Appl. Spectrosc. 59 (2005) 1032–1036.
[28] G.R. Bartlett, Phosphorus assay in column chromatography, J. Biol. Chem. 234 (1958) 466–468.
[29] A. Azzi, The use of fluorescent probes for the study of membranes, Methods Enzymol. 32 (1974) 234–246.
[30] K.-D. Lee, S. Nir, D. Papahadjopoulos, Quantitative analysis of liposome–cell interactions in vitro: rate constants of binding and endocytosis with suspension and adherent J774 cells and human monocytes, Biochemistry 32 (1993) 889–899.
[31] J. Guilford, R. Jacckson, C. Choi, W.R. Bergmark, Solvent effect on emission yield and lifetime of coumarin laser dyes: requirements for rotatory decay mechanism, J. Phys. Chem. 89 (1985) 294–300.
[32] J.R. Lakowicz, Principles of fluorescence spectroscopy, Kluwer Academic/Plenum Publishers, New York, 1999.
[33] M.K. Singh, H. Pal, A.S.R. Koti, A.V. Sapre, Photophysical properties and rotational relaxation dynamics of neutral red bound to β-cyclodextrin, J. Phys. Chem., A 108 (9) (2004) 1465–1474.
[34] S. Santosh Kumar, B. Shankar, K.B. Sainis, Effect of chlorophyllin against oxidative stress in splenic lymphocytes *in vitro* and *in vivo*, Biochim. Biophys. Acta 1672 (2004) 100–111.
[35] N.-W. Huh, N.A. Porter, T.J. McIntosh, S.A. Simon, The interaction of polyphenols with bilayers: conditions for increasing bilayer adhesion, Biophys. J. 71 (1996) 3261–3277.
[36] C. Bombelli, G. Caracciolo, P.D. Profio, M. Diociaiuti, P. Luciani, G. Mancini, C. Mazzuca, M. Marra, A. Molinari, D. Monti, L. Toccacieli, M. Venanzi, Inclusion of a photosensitizer in liposomes formed by DMPC/Gemini surfactant: correlation between physicochemical and biological features of the complexes, J. Med. Chem. 48 (2005) 4882–4891.
[37] T.G. Burke, T.R. Tritton, Location and dynamics of anthracyclines bound to unilamellar phosphatidylcholine vesicles, Biochemistry 24 (1985) 5972–5980.
[38] G. Costin, M. Trif, N. Nichita, R.A. Dwek, S.M. Petrescu, pH-sensitive liposomes are efficient carriers for endoplasmic reticulum-targeted drugs in mouse melanoma cells, Biochem. Biophys. Res. Commun. 293 (2002) 918–923.

JCB-07-0067(21348)

Journal of Cellular Biochemistry 9999:1–11 (2007)

Delayed Activation of PKCδ and NFκB and Higher Radioprotection in Splenic Lymphocytes by Copper (II)–Curcumin (1:1) Complex as Compared to Curcumin

Amit Kunwar,[1] H. Narang,[2] K. Indira Priyadarsini,[1] M. Krishna,[2]* R. Pandey,[2] and K.B. Sainis[2]

[1]Radiation & Photochemistry Division, Bhabha Atomic Research Centre, Mumbai 400085, India
[2]Radiation Biology & Health Sciences Division, Bhabha Atomic Research Centre, Mumbai 400085, India

Abstract A mononuclear 1:1 copper complex of curcumin had been found to be superior to curcumin in its anti-oxidant properties. This paper describes the radio-protective effects of the complex in splenic lymphocytes from swiss mice. The complex was found to be very effective in protecting the cells against radiation-induced suppression of glutathione peroxidase, catalase and superoxide dismutase (SOD) activities. Both curcumin and the complex protected radiation-induced protein carbonylation and lipid peroxidation in lymphocytes with the complex showing better protection than curcumin. It also showed better overall protection by decreasing the radiation-induced apoptosis. The kinetics of activation of PKCδ and NFκB after irradiation in presence or absence of these compounds was looked at to identify the molecular mechanism involved. The modulation of irradiation-induced activation of PKCδ and NFκB by curcumin and the complex was found different at later time periods although the initial response was similar. The early responses could be mere stress responses and the activation of crucial signaling factors at later time periods may be the determinants of the fate of the cell. In this study this delayed effect was observed in case of complex but not curcumin. The delayed effect of the complex along with the fact that it is a better free radical scavenger must be the reason for its better efficacy. The complex was also found to be less cytotoxic then curcumin at similar concentration. J. Cell. Biochem. 9999: 1–11, 2007.

Key words: curcumin; radioprotection; signaling; anti-oxidant; curcumin–copper complex

Radiotherapy is one of the treatment modalities for several kinds of malignancies. The major drawback in the treatment is that normal cells, in the vicinity of the tumor, also receive radiation doses similar to the tumor. This leads to undesirable side effects and increases the risk of secondary cancers. When ionizing radiation hits the cell various reactive oxygen species (ROS) are produced leading to the activation of signaling pathways that may be cytotoxic or cytoprotective [Riley, 1994]. There is, therefore, a need for prevention of such side effects. Natural agents that have low cytotoxicity and high anti-oxidant and anti-inflammatory activities are being studied for their efficacy in preventing radiation-induced side effects and killing of normal cells. Curcumin, an important natural phytochemical, found in the rhizomes of *Curcuma longa* or turmeric is an efficient free radical scavenger and reacts with most of the ROS such as superoxide, peroxyl, hydroxyl and nitrogen oxide radicals [Priyadarsini et al., 2003; Vajragupta et al., 2004] and has been studied in great detail. In addition to its anti-radical activity, curcumin has been shown in vivo to enhance the activities of anti-oxidant enzymes in liver and kidney [Iqbal et al., 2003]. It has also been reported to modulate the PKC and NF-κB signaling pathways [Siwak et al., 2005; Rushworth et al., 2006]. Activation of PKC pathway has been implicated in cell survival under oxidative stress, where it has

*Correspondence to: M. Krishna, xx[Q2]
E-mail: malini@barc.gov.in

Received 13 February 2007; Accepted 2 March 2007
DOI 10.1002/jcb.21348
Published online 00 Month 2007 in Wiley InterScience (www.interscience.wiley.com).

been reported to upregulate the transcription of several cytoprotective genes such as glutamyl cysteine ligase modulatory (GCLM) and homo-oxygenase-1 (HO-1) [Rushworth et al., 2006]. Activation of NF-κB by ionizing radiation has been found to protect cells from apoptosis and its inhibition enhanced radiation-induced apoptosis [Wang et al., 1996]. An additional mechanism has been said to be via upregulation of the transcription of ROS scavenging enzymes. One major class of these protective enzymes belongs to the mitochondrial superoxide dismutase (SOD) [Suresh et al., 1994], which is also the transcript of NF-κB [Murley et al., 2006]. Other important classes of anti-oxidant enzymes are glutathione peroxidase (GPx) and catalase [Matés, 2000].

Since copper chelates of anti-oxidants are well known as SOD mimics [Annaraj et al., 2004; Baum and Ng, 2004], a copper (II)–curcumin complex with the stoichiometry of 1:1 was synthesized and characterised in our laboratory [Barik et al., 2005, in press]. The complex had high stability constant ($\log(K_f) = 15$). Studies on the superoxide radical scavenging ability and the SOD mimicking activity of the complex, showed that the complex had higher SOD like activity as compared to curcumin. Based on these studies, it was felt that the complex might be more efficient in protecting against radiation-induced damage in cells. We, therefore, investigated the mechanism of action of the complex and compared it to curcumin. Radiation-induced damage to lipids and proteins, suppression of cellular anti-oxidant defense systems, apoptosis and activation of PKC and NF-κB signaling in splenic lymphocytes were looked at.

The structures of curcumin and the copper–curcumin complex are given in Scheme 1.

MATERIAL AND METHODS

Chemicals

Curcumin, thiobarbituric acid (TBA), butylated hydroxy toluene (BHT), components of cell culture medium (serum free RPMI 1640 medium), hydrogen peroxide, xanthine, NADPH, EDTA, EGTA, glycerol, PMSF, Triton X-100, NP-40, Tris base, HEPES buffer and propidium iodide (PI) were obtained from Sigma–Aldrich. Xanthine oxidase was obtained from Calbiochem. All other chemicals were locally procured and were with more than 98% purity. Solutions were always made in fresh nanopure water.

Synthesis

The complex was synthesized by refluxing equimolar mixture of copper acetate and curcumin in dry ethanol. The precipitated complex was washed several times by cold ethanol and water and dried in vacuum to get dry powder. This was characterised by elemental analysis and different spectroscopic techniques. Details of the synthesis and characterisation of this complex have been reported by Barik et al. [2005].

Animals

Eight to 10-week-old inbred swiss albino male mice weighing approximately 20–25 g and reared in the animal house of Bhabha Atomic Research Centre, were used. Animals were maintained on a standard laboratory diet with water ad libitum in polypropylene cages and air-conditioned ($24 \pm 2^{\circ}C$) rooms with a 12 hourly dark and light schedule. All experiments were conducted with strict adherence to the ethical guidelines laid down by the institutional animal ethics committee of Bhabha Atomic Research Centre.

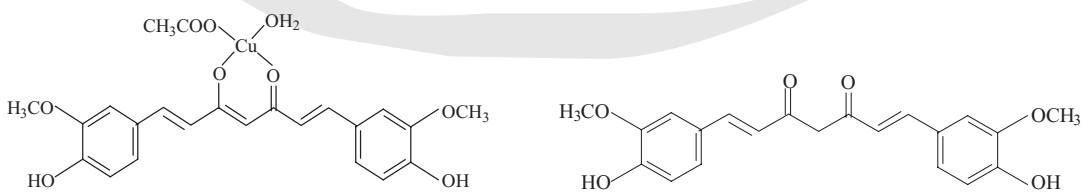

Cu-Curcumin Complex Curcumin

Scheme 1. xx[Q3]

Spleen Cell Suspension

For preparation of spleen cell suspension mice were sacrificed by cervical dislocation. Spleen was removed from the mice and single cell suspension from spleen was obtained by gently teasing the organ in to RPMI 1640 medium (containing 15 mM HEPES, 2 mM L-glutamine, 100 IU/ml penicillin, 100 μg/ml streptomycin and 20 μM 2-mercaptoethanol) using a sterile nylon mesh. Red blood cells were eliminated by treatment with 0.83% ammonium chloride solution. Lymphocyte rich cells were further washed with medium to remove traces of ammonium chloride and the viability was assessed by trypan blue dye exclusion. This preparation is referred to as splenic lymphocytes.

Drug Preparation and Treatment of Splenic Lymphocytes

Curcumin and the complex are insoluble in water, but show fairly good solubility in alkaline water. Therefore, a stock solution of curcumin and the complex were prepared in nitrogen saturated aqueous solutions with 0.2 M NaOH. Nitrogen was used to prevent oxidation and the stability of the solutions during the experimental period was monitored by following the absorption spectra from time to time. Splenic lymphocytes suspended in serum free RPMI 1640 medium were seeded at 2.5×10^6 cells/ml to which stock solution of either curcumin or the complex was added to get final concentration of 10 μM. The pH of the culture medium after the addition of these agents was found to be 7.5. Fetal bovine serum (FBS) was added at a concentration of 5% (v/v), 30 min after addition of compounds. The incubation of lymphocytes with compounds for 30 min prior to addition of FBS was referred to as treatment of cells. Further treatment incubation was done at 37°C in humified incubator with 5% CO_2 in air for different time points (0–60 min) desired in the study.

Irradiation Protocol

The lymphocytes were incubated with curcumin or the complex for 30 min as described in earlier section followed by γ-irradiation (2 Gy) using a ^{60}Co γ-source with a dose rate of 6 Gy min^{-1} as measured by standard Fricke dosimeter [Spinks and Woods, 1990]. Further irradiation, FBS was added at a concentration of 5% (v/v) and incubation was done at 37°C in humified incubator with 5% CO_2 in air for different times (0–60 min) as desired in the study.

Assays of Anti-oxidant Enzymes Activity

Cells were collected at a time point of 1 h by centrifugation at $900 \times g$ for 4 min from irradiated and unirradiated groups, washed twice with 10 mM phosphate buffered saline (PBS), were suspended in an appropriate volume of 10 mM Tris/HCl, pH 7.4, and disrupted twice by means of a bioruptor (Cosmos Bio, Tokyo, Japan) at 200 W for 30 s each. The supernatant was collected after centrifugation at $17{,}000 \times g$ for 15 min. Protein estimation in the supernatant was carried out by DC protein assay kit (Bio-Rad) following the manufacturer's instructions. Fifty micrograms of total protein was used for the enzyme assays. SOD activity was determined as described previously [Hodges et al., 2000]. Briefly, superoxide radicals were generated by enzymatic reaction of xanthine (50 μM) with xanthine oxidase (10 mU/ml) in presence of Tris buffer (pH 7.4) and 600 μM EDTA. The superoxide radicals generated by this method were allowed to react with cytochrome *c* (Fe^{3+}) (9.5 μM) to produce reduced cytochrome *c* (Fe^{2+}), absorbing at 550 nm. The change in absorbance per unit time (A/min) was monitored up to 300 s. The concentration of xanthine oxidase was adjusted such that △A/min is ~0.025. This system was used to determine SOD activity in whole cell homogenate. In the presence of whole cell homogenate the △A/min was found to be reduced. The average difference of △A/min recorded in the absence and presence of whole cell homogenate, respectively, was calculated and represented as activity. The catalase activity was determined as described earlier [Abei, 1984] by monitoring the enzyme-catalysed decomposition of H_2O_2 at 240 nm. Reaction mixture contained 15 mM of H_2O_2 in 50 mM of potassium phosphate buffer, pH 7.0. The reaction was initiated by addition of whole cell homogenate, and the decrease in absorbance/min was recorded. The average decrease in absorbance/min, calculated from the initial linear portion of curve was presented as activity. GPx activity was measured by the method as described previously [Tappel, 1978] in which GPx activity was coupled to the oxidation of (3 mM) NADPH by glutathione reductase. The oxidation of NADPH in the

presence of whole cell homogenate was followed as decrease in absorbance at 340 nm at 37°C for 20 min. The average decrease in absorbance/min was calculated from the most linear part of the curve and presented as activity.

Assessment of Lipid Peroxidation

Cells were collected at a time point of 1 h by centrifugation at $900 \times g$ for 4 min from irradiated and unirradiated groups, washed twice with 10 mM PBS and were finally suspended in 300 μl of 10 mM PBS. To this 900 μl of TBA reagent (100 μM BHT, 0.67% (w/v) TBA in a 10% (w/v) trichloroacetic acid solution and 0.25N HCl) [Kumar et al., 2004] was added. The reaction mixture was incubated at 85°C for 20 min and cooled to ambient temperature. Samples were centrifuged at $12{,}000 \times g$ for 10 min at 25°C and thiobarbituric acid reactive substances (TBARS) in the supernatant were estimated by measuring the absorbance at 532 nm ($\varepsilon 532 = 1.56 \times 105\ M^{-1}\ cm^{-1}$) [Sreejayan et al., 1997]. The results are expressed in terms of formation of TBARS/10^6 cells.

Protein Oxidation

Supernatants as obtained for enzyme activity at a time point of 1 h were used for measurement of protein carbonylation using the protocol described earlier [Oliver et al., 1987]. In brief, cell free extract containing approximately 100 μg soluble proteins in 10 mM PBS, pH 7.4 was taken and total proteins were precipitated with ice chilled 10% trichloroacetic acid (TCA). The pellet was suspended in 0.2% dinitrophenyl hydrazine (DNPH) in 2N HCl and incubated at room temperature for 2 h. Proteins were reprecipitated with TCA and excess DNPH was removed with several washes of 50% ethyl acetate in ethanol. Decolorized protein pellet was dissolved in 6N guanidine hydrochloride and the optical density was measured at 370 nm. Protein concentration was determined by DC protein assay kit (Bio-Rad) following the manufacturer's instructions.

Western Blotting

Cells were collected at different time points (0–60 min) from irradiated and unirradiated groups by centrifugation at $900 \times g$ for 4 min and washed twice with 10 mM PBS. Cells were lysed using lyses buffer as described earlier [Kurrey et al., 2005]. Proteins were estimated using DC protein assay kit (Bio-Rad) following the manufacturer's instructions. Protein samples were denatured at 95°C with sample buffer (0.125 M Tris buffer (pH 6.8), 4% SDS, 20% glycerol, 2% 2-ME, 0.03 mM bromophenol blue) for 5 min and were separated on 12% SDS-PAGE gel for MnSOD and 8% SDS-PAGE gels for IκBα and PKCδ. Proteins were transferred onto a nitrocellulose membrane (Amersham Pharmacia Biotech, Little Chalfont, UK), blocked overnight with a blocking solution (5% BSA in TBS containing 0.1% Tween 20) and were exposed to the primary Ab for 2 h at room temperature. Equivalent protein loading was demonstrated by staining the membranes in 1% Ponceau S. Primary antibodies included rabbit monoclonal anti-IκBα (1:1,000), rabbit monoclonal anti-phospho (Ser40) PKCδ (1:1,000) both from Cell Signalling, sheep monoclonal anti-MnSOD (1:1,000) (Calbiochem). After washing, the membranes were incubated for 1 h at room temperature with horseradish peroxidase (HRP) linked secondary Ab anti-rabbit (1:1,500), anti-sheep (1:15,00) (Roche Molecular Bio Chemicals, Germany) and signals were detected using BM chemiluminiscence western blotting kit (Roche Molecular Bio Chemicals, Germany) as per the manufacturer's instructions. For reprobing, membranes were stripped with 100 mM 2-ME, 2% SDS and 62.5 mM Tris–HCl (pH 6.9) for 20 min at 50°C followed by immunoblotting as mentioned above. The band intensity was quantified by gelquant software (version 2.7 DNR imaging systems Ltd., Israel). Fold changes were calculated after normalization to Ponceau S.

Isolation of Nuclei for NFκB Measurement

Nuclear extracts were prepared at a time point of 1 h from irradiated and unirradiated groups as described earlier [Gao et al., 2004]. In brief, cells were washed two times with 10 mM PBS, resuspended and incubated on ice for 15 min in hypotonic buffer A (10 mM HEPES, pH 7.9, 10 mM KCl, 0.1 mM EDTA, 0.1 mM EGTA, 1 mM DTT, 0.5 mM PMSF, and 0.6% NP-40). Cells were vortexed gently for lysis and nuclei were separated from the cytosol by centrifugation at $12{,}000 \times g$ for 1 min. Nuclei resuspended in buffer B (20 mM HEPES, pH 7.9, 25% glycerol, 0.4 M NaCl, 1 mM EDTA, 1 mM EGTA, 1 mM DTT, 0.5 mM PMSF) and were shaken for 30 min at 4°C. Nuclear extracts were obtained by centrifugation at $12{,}000 \times g$ and protein concentration was measured by DC

protein assay kit (Bio-Rad) following the manufacturer's instructions. Nuclear extract was fractionated on 12% SDS-PAGE gel, transferred to nitrocellulose membrane, and probed with rabbit anti-NF-κB (p65) antibody using BM chemiluminiscence western blotting kit (Roche Molecular Bio Chemicals, Germany) as per the manufacturer's instructions. Equivalent protein loading was demonstrated by staining membranes in 1% Ponceau S. Fold changes were calculated after normalization to Ponceau S.

Estimation of Apoptosis

For the estimation of apoptosis irradiated and unirradiated groups were cultured for 24 h at 37°C in humified chamber with 5% CO_2 atmosphere. After 24 h, cells were collected by centrifugation at $900 \times g$ for 4 min, washed twice with 10 mM PBS, suspended in 1 ml of staining solution containing 0.5 μg/ml PI, 0.1% sodium citrate and 0.1% Triton X-100 and then analyzed by flow cytometry. PI binds to DNA and the intensity of fluorescence at 580 nm represents the total DNA content. A majority of cells was in G1 phase of cell cycle (2n DNA content). The pre-G1 phase population represented the apoptotic cells.

Statistical Analysis

Each experiment was performed at least in triplicate using a single splenic lymphocyte preparation. The entire experiment was repeated twice. Results are presented as means ± SEM, n = 6. Data were analyzed with Student's *t*-test and *P* values ≤ 0.05 were considered as a significant.

RESULTS

Effect of Curcumin and the Complex on Anti-oxidant Enzymes Status in Spleenocytes With or Without Irradiation

The activities of the different anti-oxidant enzymes (SOD, GPx and catalase) in splenic lymphocytes estimated 1 h after treatment with either curcumin or the complex under irradiated (2 Gy) and unirradiated conditions are shown in Figure 1. Treatment with the complex and curcumin alone resulted in significant ($P < 0.05$) increase in glutathione peroxidase and catalase activities, SOD activity did not show any increase rather it was reduced. GPx and catalase activities increased by 17 and 46%,

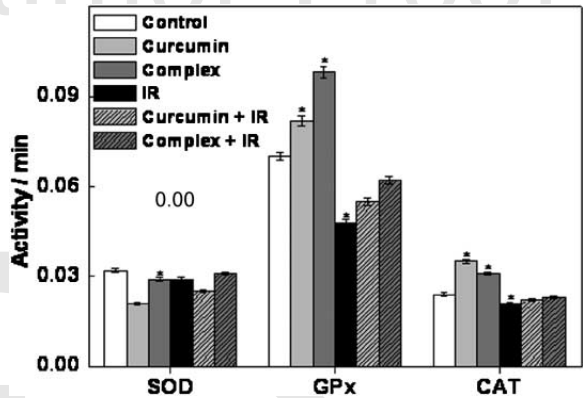

Fig. 1. Effect of curcumin and the complex on anti-oxidant enzymes activities of γ-irradiated and unirradiated (5×10^6) splenic lymphocytes. Enzymes activities were estimated using cell lysates prepared at a time point of 1 h from irradiated and unirradiated groups. Control represents splenic lymphocytes treated with only vehicle (0.2 M NaOH). *$P < 0.05$ as compared to control. IR—irradiation (2 Gy).

respectively, in curcumin treated cells and by 40 and 29%, respectively, in the complex treated cells. The decrease in SOD activity was observed to be lesser extent in the complex treated cells compared to curcumin treated cells. Irradiation alone led to a significant ($P < 0.05$) decrease in activities of all the anti-oxidant enzymes, which was reversed by pretreatment with curcumin or complex. The complex was more effective in this respect.

Effect of Curcumin and the Complex on Irradiation-Induced Protein Oxidation and Lipid Peroxidation in Spleenocytes

The relative TBARS formation, indicative of lipid peroxidation in spleenocytes at a time point of 1 h after irradiation alone (2–8 Gy) or after pretreatment with curcumin or the complex are shown in Figure 2. Lipid peroxidation in spleenocytes increased with increase in dose of irradiation. Pretreatment with either curcumin or the complex led to reduction in the extent of lipid peroxidation at all the doses. The complex was found to be more effective in reducing the formation of TBARS at all doses compared to curcumin. The percentage inhibition of lipid peroxidation by the complex at different doses of 2, 4, 6 and 8 Gy was 75, 70, 28 and 20%, respectively, while that for curcumin under similar conditions was 50, 40, 20 and 15%, respectively.

Inset of Figure 2 shows the relative carbonyl formation due to protein oxidation induced by

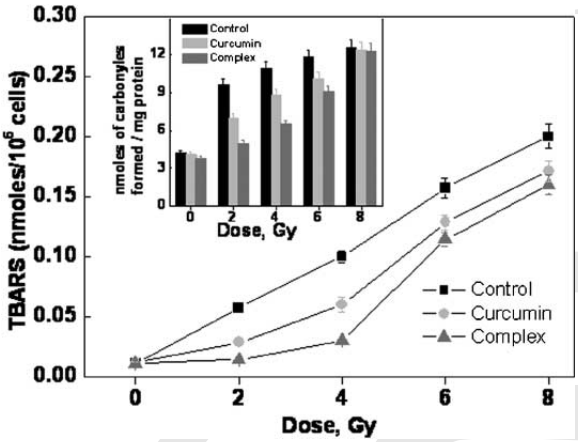

Fig. 2. Line graph showing inhibition of lipid peroxidation estimated in terms of TBARS at a time point of one hour in splenic lymphocytes (5×10^6) treated with curcumin and the complex, and exposed to varying dose of γ-radiation (2–8 Gy). Inset shows bar graph indicating inhibition of protein oxidation estimated in terms of protein carbonylation at a time point of 1 h by compounds at different absorbed doses (2–8 Gy) of γ-radiation.

γ-radiation from 2 to 8 Gy both in the absence or presence of either curcumin or the complex at identical time point. The results indicate inhibition of irradiation-induced increase in protein oxidation by these compounds, with the complex showing much stronger inhibition. The percentage reduction of carbonyl formation by the complex at different doses of 2, 4, 6 and 8 Gy was 48, 40, 24 and 3%, respectively, while with curcumin the percentage reduction was found to be 28, 19, 15 and 2%, respectively.

In order to understand the factors responsible for the protection afforded by the complex in the above studies, the signaling pathways were looked at.

Effect of Curcumin and the Complex on Protein Kinase Cδ Phosphorylation After Irradiation

The phosphorylation at Ser 40 residue of PKCδ in lymphocytes was assessed at 5, 15, 30 and 60 min after irradiation (2 Gy) alone or after pretreatment with either curcumin or the complex. Western blots and relative intensities representing the level of phosphorylated PKCδ at the above four time points are shown in Figure 3(A)–(D). Following γ-irradiation an increased phosphorylation of PKCδ was observed within 5 min, which reappeared at 60 min. When irradiation was preceded by curcumin or the complex treatment, the increased phosphorylation observed at 5 min was suppressed. Here the complex shows stronger inhibition than curcumin. However, at 60 min, pretreatment with the complex resulted in increased phosphorylation of PKCδ, as compared to irradiation alone or pretreatment with curcumin. Treatment with curcumin or the complex alone also resulted in increased phosphorylation of PKCδ but with different kinetics of activation. The

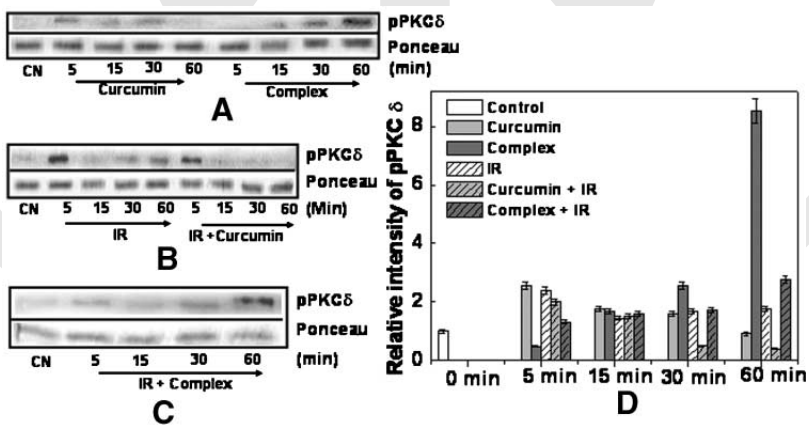

Fig. 3. Splenic lymphocytes (2.5×10^6) were treated with curcumin and the complex, irradiated with γ-radiation and then cultured. Whole cell extract was prepared at different times and western blotting was performed with phosphospecific (Ser40) antibody of PKCδ and IκBα antibody. **A**: Western blot analysis showing the comparative level of phospho PKCδ and IκBα in lymphocytes at different time points after treatment with curcumin and the complex. **B**: Western blot analysis showing the comparative level of phospho PKCδ and IκBα in curcumin pretreated lymphocytes at different time points after irradiation. **C**: Western blot analysis showing the comparative level of phospho PKCδ and IκBα in the complex pretreated lymphocytes at different time points after irradiation. **D**: Bar graph showing relative intensities of phospho PKCδ. Control represents splenic lymphocytes treated with only vehicle (0.2 M NaOH). Staining of the membrane with 1% Ponseau represents loading control. IR—irradiation (2 Gy).

complex showed time dependent increase, up to eightfold at 60 min, indicating that the complex promotes growth in normal cells since increased expression of PKCδ could be anti-apoptotic.

Effect of Curcumin and the Complex on IκBα Accumulation

The accumulation of IκBα in lymphocytes was checked at 5, 15, 30 and 60 min after irradiation (2 Gy) alone or after pretreatment with either curcumin or the complex. Western blot analysis and the relative intensities representing the level of IκBα at the above four time points are shown in Figure 4(A)–(D). Following γ-irradiation the degradation of IκBα was observed within 5 min. At 30 min there was a significant reappearance of IκBα and it accumulated to ~3 folds at 60 min. Pretreatment with curcumin or the complex prevented the initial degradation of IκBα at 5 min. The complex was also found to be more effective in significantly reversing the irradiation-induced IκBα accumulation at 60 min. Treatment with both the compounds alone reduced the levels of IκBα as compared to control although like PKCδ the kinetics of accumulation was different. IκBα after degradation is known to release NF-κB, which transports to the nucleus where it acts as a transcription factor for many anti-apoptotic genes.

Effect of Curcumin and the Complex on Nuclear Transport of NF-κB and *MnSOD* Expression

Figure 5 shows western blots (A) and relative intensities (B), respectively, of NF-κB in nuclear extract of same samples at a time point of 60 min. Following irradiation (2 Gy), the level of NF-κB decreased in the nuclear extract of untreated lymphocytes. However, when irradiated spleenocytes were pretreated with curcumin or the complex, the decrease in the level of NF-κB was reversed marginally by curcumin but very efficiently by the complex. Treatment with either curcumin or the complex alone also reduced the level of NF-κB in nuclear extract. The reduction after curcumin and the complex treatment was ~60 and 40%, respectively.

Western blot and relative intensities of MnSOD in untreated or treated lymphocytes are also shown in Figure 5. A marked increase in the level of MnSOD was observed after irradiation. Treatment with curcumin or the complex before irradiation inhibited this increase with the complex showing more profound effect than curcumin. The complex and curcumin treatment alone inhibited the expression of *MnSOD*.

Effect of Curcumin and the Complex on γ-Radiation-induced Apoptosis

Figure 6 shows percentage apoptosis in irradiated and unirradiated lymphocytes treated

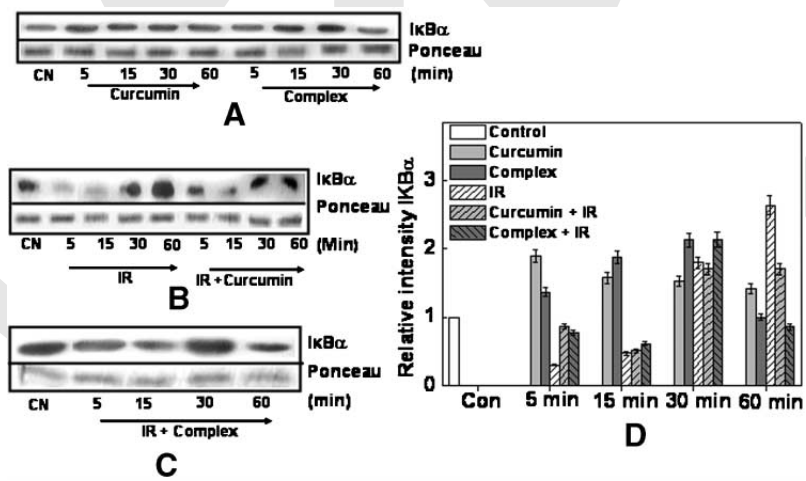

Fig. 4. Splenic lymphocytes (2.5×10^6) were treated with curcumin and the complex, irradiated with γ-radiation and then cultured. Whole cell extract was prepared at different times and western blotting was performed with IκBα antibody. **A**: Western blot analysis showing the comparative level of IκBα in lymphocytes at different time points after treatment with curcumin and the complex. **B**: Western blot analysis showing the comparative level of IκBα in curcumin pretreated lymphocytes at different time points after irradiation. **C**: Western blot analysis showing the comparative level of IκBα in the complex pretreated lymphocytes at different time points after irradiation. **D**: Bar graph showing relative intensities of IκBα. Control represents splenic lymphocytes treated with only vehicle (0.2 M NaOH). Staining of the membrane with 1% Ponseau represents loading control. IR—irradiation (2 Gy).

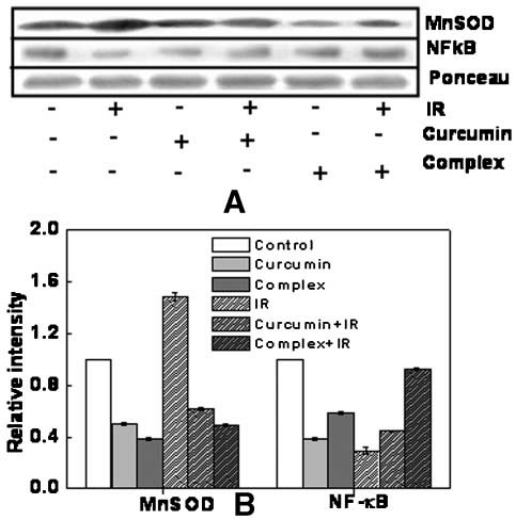

Fig. 5. Effects of curcumin and the complex on the nuclear transport of NF-κB and expression of *MnSOD* in γ-irradiated and unirradiated lymphocytes. **A**: Western blot analysis showing the comparative level of NF-κB in nuclear extract and MnSOD in cytoplasmic extract of (2.5×10^6) irradiated and unirradiated splenic lymphocytes after 1 h of treatment with curcumin and the complex. **B**: Bar graph representing relative intensities of NF-κB and MnSOD. Staining of the membrane with 1% Ponseau represents loading control. IR—irradiation (2 Gy).

with curcumin and the complex at 24 h. Although both curcumin and the complex alone led to increased apoptosis, as did the vehicle, they were able to confer protection in irradiated cells. Among the compounds the percent apoptosis was found to be significantly ($P < 0.05$) less in case of complex treated cells. Irradiation (2 Gy) alone led to substantial increase in apoptosis. The complex and curcumin were able to decrease the percentage apoptosis observed after irradiation and the complex was found to be more effective. The decrease in irradiation-induced apoptosis by the complex was 20%.

DISCUSSION

Favourable effects of curcumin on several parameters of oxidant–anti-oxidant balance have been reported by many investigators [Sharma, 1975; Strasser et al., 2005]. Its metal chelating ability has been utilized by several groups to further enhance its anti-oxidant activity [Afanas'ev et al., 2001; Vajragupta et al., 2003]. However, there are very few reports in the literature about the modulation of radiation-induced redox disturbances by curcumin [Chan et al., 2003; Krishnan et al.,

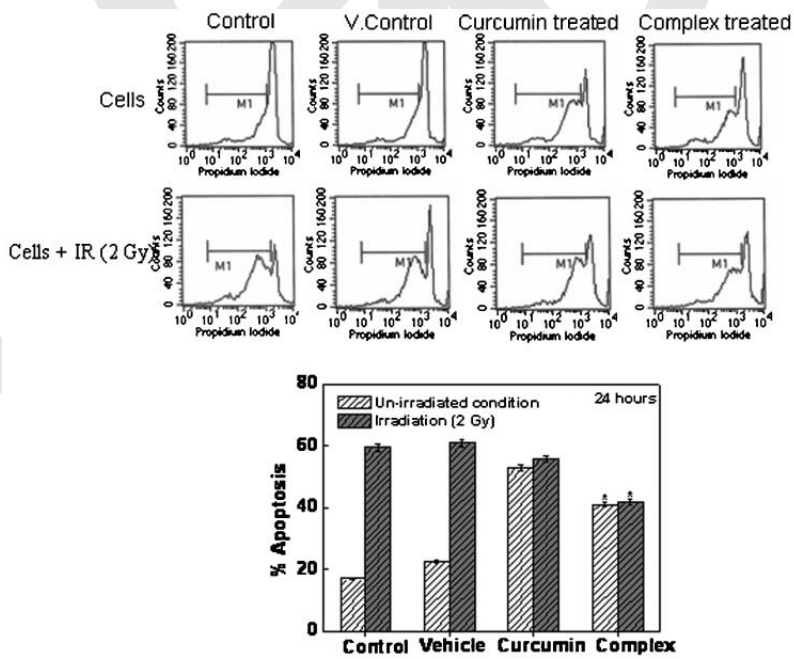

Fig. 6. Effects of curcumin and the complex on cellular cytotoxicity estimated in terms of apoptosis of spleen lymphocyte (2.5×10^6) after treatment with compounds and modulation of γ radiation-induced apoptosis. Lymphocytes were cultured for 24 h before staining with propidium iodide. The percentage apoptotic cells were calculated from pre-G1 peak as estimated through Fluorescence Activated Cell Sorter (FACS). Control represents spleen lymphocyte treated neither with any agent nor vehicle (0.2 M NaOH). $^*P < 0.05$ as compared to curcumin treated lymphocytes. IR—irradiation (2 Gy).

2006; Srinivasan et al., 2006] and in fact no reports on such changes by metal chelates of curcumin. The present study therefore deals with the modulation of γ-radiation activated signaling pathways as well as other radiation-induced disturbances such as change in anti-oxidant enzymes level, damage of cellular lipid, protein and apoptosis by a copper(II)–curcumin complex in splenic lymphocytes and the results have been compared with those of curcumin.

Treatment with either curcumin or the complex resulted in increased activities of anti-oxidant enzymes after 1 h in unirradiated lymphocytes. In agreement with the previous reports on suppression of anti-oxidant defences under elevated oxidative stress [Daniel et al., 1998; Bosch-Morell et al., 1999; Han et al., 2005], a decrease in activities of anti-oxidant enzymes after γ-irradiation (2 Gy) was observed. Both curcumin and the complex prevented the decrease in GPx and catalase activities after irradiation. The complex showed very significant reversal of irradiation-induced decrease in GPx and SOD activities. The functional efficiency of GPx depends on the optimal supply of the redundant GSH [Vivancos and Moreno, 2005]. The exogenously applied anti-oxidant prevents the depletion of GSH and thus maintains its cellular concentration needed for GPx activity. Therefore the superior GPx activity associated with the complex may be because of its enhanced anti-radical activity as reported in our previous studies [Barik et al., 2005]. However the superior SOD activity under irradiated condition shown by the complex could be because of its acquiring the additional superoxide-dismutating copper centre.

Both curcumin and the complex showed considerable reduction in TBARS and carbonyls formation in lymphocytes up to a dose of 4 Gy, further increase in the dose did not cause any further decrease. At all the absorbed doses employed in these studies, the complex provided better protection than curcumin.

Apart from free radical scavenging activities, the compounds like curcumin are involved in activation or inhibition of various signaling pathways, which are crucial to the cell. Some signaling components whose activation could be beneficial to the cell in terms of its survival were hence looked at; in the presence of both the compounds and their relative efficacies against irradiation-induced stress was compared. We followed the activation of PKCδ and NFκB after irradiation in presence or absence of these compounds over a time period of 5–60 min. The inhibition of irradiation-induced phosphorylation of PKCδ at 5 min was observed by both the complex and curcumin, with complex showing stronger inhibition. Since the early response seen at 5 min could be stress responses, which occurs due to the production of reactive oxygen species, the complex therefore seems to be a better scavenger of ROS in vivo and could prevent the initial activation of PKCδ observed with irradiation. Additionally, the reduction in irradiation-induced degradation of IκBα at 5 min with the complex strengthens the fact that the complex is more effective radical scavenger and hence prevents the immediate effects of irradiation. After the initial damage response, the cell assesses the damage and activates the signaling pathways, which then determines the fate of the cell. In this study the activation, which is observed at 5 min, may be a stress response following which at later time periods (60 min) the signals that will protect the cells were initiated. PKCδ has been shown previously to activate various cytoprotective genes [Rushworth et al., 2006], The extensive phosphorylation of PKCδ at 60 min in the complex pretreated and irradiated spleenocytes indicate that the complex is more efficient than curcumin in activating cytoprotective pathways after the damage. Likewise with IκBα, after initial reduction observed at 5 min, there was an accumulation at 30 min. At 60 min there was again a decrease in the level of IκBα in the complex treated irradiated lymphocytes indicating a degradation of IκBα. This would lead to excess of translocation of NF-κB to the nucleus and the expression of cytoprotective genes [Yang et al., 2003]. These results were further supported by the content of NF-κB in the nucleus which was found to be more in the complex pretreated irradiated spleenocytes 60 min after irradiation (Fig. 5). The delayed phosphorylation of PKCδ, in the complex treated lymphocytes along with the delayed degradation of IκBα (60 min) indicate a more prolonged action of the complex as compared to curcumin. The reason for this could be the delayed biological half-life of the complex and hence its higher effectiveness. The expression of *MnSOD*, a cytoprotective gene and a transcript of NF-κB was next looked at after 60 min of treatment with the compounds. ROS are known

to induce the expression of *MnSOD* in the cell. This has also been observed in our results with irradiated spleenocytes (Fig. 5). Pretreatment with the complex or curcumin prevented this increase indicating the strong scavenging capacity of the compounds, with complex again faring better than curcumin. Comparing the translocation of NF-κB and its downstream target gene *MnSOD*, it was observed that the complex did not inhibit the translocation of NF-κB to the nucleus as much as curcumin did. Inspite of increased translocation of NF-κB to the nucleus in the complex treated spleenocytes the expression of *MnSOD* was inhibited more by the complex. The reason for this may be that *MnSOD* gene contains binding motifs for a number of transcription factors including NF-κB, activator proteins 1 (AP1) and 2 (AP2), specificity protein 1 (Sp1) and adenosine 3′,5′-cyclic monophosphate-regulator element binding factor (CREB) [Borrello and Demple, 1997; Porntadavity et al., 2001; Xu et al., 2002], Sp1 and AP2 have been linked with the process of repression of *MnSOD* rather than its constitutive expression. The differential repression caused by curcumin or the complex may be because of the differential action of curcumin or the complex on Sp1 and AP2.

The complex and curcumin have also been evaluated for their cytotoxicity on splenic lymphocytes and for their protective effect against γ-radiation (2 Gy) induced apoptosis. Curcumin is well known to induce cytotoxicity in tumor cell lines and in splenic lymphocytes [Gao et al., 2004; Siwak et al., 2005; Aggarwal et al., 2006]. When metal complexes are employed as anti-oxidants in cells, there is a possibility of their undergoing hydrolysis, thereby releasing free copper(II) [Vajragupta et al., 2004]. If this was the case, in the present study, the complex would have increased apoptosis more than that of curcumin. However the extent of apoptosis caused by the complex was found to be significantly less than that of curcumin. This suggested that the complex was stable within the lymphocytes and did not undergo any hydrolysis.

Our results thus show that the complex has lesser cytotoxicity and better free radical scavenging capability, which is reflected as maintenance of anti-oxidant enzymes level, reduction in lipid and protein damage. Complex also scores better than curcumin in activation of various signaling pathways in temporally relevant manner, i.e. PKCδ and NFκB which would then play a crucial role in determining fate of the cell.

REFERENCES

Abei H. 1984. Catalase in vitro. Meth Enzymol 105:121–126.

Afanas'ev IB, Ostrakhovitch EA, Mikhal'chik EV, Ibragimova GA, Korkina LG. 2001. Enhancement of antioxidant and anti-inflammatory activities of bioflavonoids rutin by complexation with transition metals. Biochem Pharmacol 61:667–684.

Aggarwal S, Ichikawa H, Takada Y, Sandur SK, Shishodia S, Aggarwal BB. 2006. Curcumin (diferuloylmethane) down-regulates expression of cell proliferation and antiapoptotic and metastatic gene products through suppression of IkappaB alpha kinase and Akt activation. Mol Pharmacol 69:195–206.

Annaraj JP, Ponvel KM, Athappan P, Srinivasan S. 2004. Synthesis, spectra and redox behaviour of copper (II) complexes of curcumin diketimines as models for copper protein. Transition Metal Chem 29:722–727.

Barik A, Mishra B, Shen L, Mohan H, Kadam RM, Dutta S, Zhang H-Y, Priyadarsini KI. 2005. Evaluation of a new copper(II)-curcumin complexes as superoxide dismutase mimic and its free radical reactions. Free Radic Biol Med 39:811–822.

Barik[Q4] A, Mishra B, Kunwar A, Kadam RM, Shen L, Dutta S, Padhye S, Satpati AK, Zhang H-Y, Priyadarsini KI. in press. Comparative study of copper(II)-curcumin complexes as superoxide dismutase mimics and free radical scavengers. Eur J Med Chem.

Baum L, Ng A. 2004. Curcumin interaction with copper and iron suggest one possible mechanism of action in Alzheimer's disease animals models. J Alzh Dis 6:367–377.

Borrello S, Demple B. 1997. NfκB independent transcriptional induction of the human manganese superoxide dismutase gene. Arch Biochem Biophys 348:289–294.

Bosch-Morell F, Flohe L, Marin N, Romero FJ. 1999. 4-Hydroxy-nonenal inhibits glutathione peroxidase: Protection by glutathione. Free Radic Biol Med 26: 1383–1387.

Chan WH, Wu CC, Yu JS. 2003. Curcumin inhibits UV irradiation-induced oxidative stress and apoptotic biochemical changes in human epidermoid carcinoma A431 cells. J Cell Biochem 90:327–338.

Daniel RS, Mathew BC, Devi KS, Augusti KT. 1998. Antioxidant effect of two flavonoids from the bark of *Ficus bengalensis* Linn. in hyperlipidemic rats. Indian J Exp Biol 36:902–906.

Gao X, Kuo J, Jiang H, Deeb D, Liu Y, Divine G, Chapman RA, Dulchavsky SA, Gautam SC. 2004. Immonomodulatory activity of curcumin: Suppression of lymphocyte proliferation, development of cell-mediated cytotoxicity and cytokine production in vitro. Biochem Pharmacol 68: 51–61.

Han Y, Son S-J, Akhalaia M, Platonov A, Son H-J, Lee K-H, Yun Y-S, Song J-Y. 2005. Modulation of radiation induced disturbances of antioxidant defense systems by ginsan. eCAM 2:529–536.

Hodges GR, Young MJ, Paul T, Ingold KU. 2000. How should xanthine oxidase-generated superoxide yields be measured?. Free Radic Biol Med 29:434–441.

Iqbal M, Sharma SD, Okazaki Y, Fujisawa M, Okada S. 2003. Dietary supplementation of curcumin enhances antioxidant and phase II metabolising enzymes in ddY male mice: Possible role in protection against chemical carcinogenesis and toxicity. Pharmacol Toxicol 92: 33–38.

Krishnan S, Sandur SK, Shentu S, Aggarwal BB. 2006. Curcumin enhances colorectal cancer cell radiosensitivity by suppressing the radiation-induced nuclear factor-kappaB (NF-kB) pathway. Int J Radiat Oncol Biol Phys 66:S547.

Kumar SS, Shankar B, Sainis KB. 2004. Effect of chlorophyllin against oxidative stress in splenic lymphocytes in vitro and in vivo. Biochim Biophys Acta 1672: 100–111.

Kurrey NK, Amit K, Bapat SA. 2005. Snail and Slug are major determinants of ovarian cancer invasiveness at the transcription level. Gynecol Oncol 97:155–165.

Matés JM. 2000. Effects of antioxidant enzymes in the molecular control of reactive oxygen species toxicology. Toxicology 153:83–104.

Murley JS, Kataoka Y, Weydert CY, Oberley LW, Grdina DJ. 2006. Delayed radioprotection by nuclear transcription factor κB-mediated induction of manganese superoxide dismutase in human microvascular endothelial cells after exposure to the free radical scavenger WR1065. Free Radic Biol Med 40:1004–1016.

Oliver CN, Ahn B, Moerman EJ, Goldstein S, Stadtman ER. 1987. Age-related changes in oxidized proteins. J Biol Chem 262:5488–5491.

Porntadavity S, Xu Y, Kiningham K, Rangnekar VM, Prachayasitikul V, St. Clair DK. 2001. TPA-activated transcription of the human MNSOD gene: Role of transcription factors SP1 And Egr1. DNA Cell Biol 20: 473–481.

Priyadarsini KI, Maity DK, Naik GH, Sudheer Kumar M, Unnikrishan MK, Satav JG, Mohan H. 2003. Role of phenolic O–H and methylene hydrogen on the free radical reactions and antioxidant activity of curcumin. Free Radic Biol Med 35:475–484.

Riley PA. 1994. Free radicals in biology: Oxidative stress and the effects of ionizing radiation. Int J Radiat Biol 65:27–33.

Rushworth SW, Ogborne RM, Charalambos CA, O'Connell MA. 2006. Role of protein kinase C δ in curcumin-induced antioxidant response element-mediated gene expression in human monocytes. Biochem Biophys Res Commun 341:1007–1016.

Sharma OP. 1975. Antioxidant activity of curcumin and related compounds. Biochem Pharmacol 25:1811–1812.

Siwak DR, Shishodia S, Aggarwal BB, Kurzrock R. 2005. Curcumin-induced antiproliferative and proapoptotic effects in melanoma cells are associated with suppression of IkappaB kinase and nuclear factor kappaB activity and are independent of the B-Raf/mitogen-activated/extracellular signal-regulated protein kinase pathway and the Akt pathway. Cancer 104:879–890.

Spinks JWT, Woods RJ. 1990. An introduction to radiation chemistry. 3rd edition. Wiley Interscience Publication. pp 95–101.

Sreejayan N, Rao MNA, Priyadarsini KI, Devasagayam TPA. 1997. Inhibition of radiation induced lipid peroxidation by curcumin. Int. J. Pharm. 151:127–130.

Srinivasan M, Rajendra Prasad N, Menon VP. 2006. Protective effect of curcumin on γ-radiation induced DNA damage and lipid peroxidation in cultured human lymphocytes. Mutat Res 611:96–103.

Strasser E-M, Wessner B, Manhart N, Roth E. 2005. The relationship between the anti-inflammatory effects of curcumin and cellular glutathione content in myelomonocytic cells. Biochem Pharmacol 70:552–559.

Suresh A, Tung F, Moreb J, Zucali JR. 1994. Role of manganese superoxide dismutase in radioprotection using gene transfer studies. Cancer Gene Ther 1:85–90.

Tappel AL. 1978. Glutathione peroxidase and hydroperoxides. Meth Enzymol 52:506–508.

Vajragupta O, Boonchoong P, Berliner LJ. 2004. Manganese complexes of curcumin analogues: Evaluation of hydroxyl radical scavenging ability, superoxide dismutase activity and stability towards hydrolysis. Free Radic Res 38:303–314.

Vajragupta O, Boonchoong P, Watanabe H, Tohida M, Kummasud H, Sumonont Y. 2003. Manganese complexes of curcumin and its derivatives: Evaluation for the radical scavenging ability and neuroprotective activity. Free Radic Biol Med 35:1632–1644.

Vivancos M, Moreno JJ. 2005. β-Sitosterol modulates antioxidant enzyme response in RAW 264.7 macrophages. Free Radic Biol Med 39:91–97.

Wang CY, Mayo MW, Baldwin AS Jr. 1996. TNF- and cancer therapy-induced apoptosis: Protection by inhibition of NFκB. Science 274:784–787.

Xu Y, Porntadavity S, St. Clair DK. 2002. Transcriptional regulation of the human manganese superoxide dismutase gene: The role of specificity protein 1 (SP1) and activating protein-2 (AP2). Biochem J 362:401–412.

Yang L, Ross K, Qwarnstrom EV. 2003. RelA control of IκBα phosphorylation A positive feedback loop for high affinity NF-κB complexes. J Biol Chem 278:30881–30888.

Q1: Please check the suitability of the suggested short title.

Q2: Please provide address for correspondence.

Q3: Please provide caption for scheme 1.

Q4: Please update Ref. Barik et al. (in press) in list as well in text.

C1

REPRINT BILLING DEPARTMENT · 111 RIVER STREET, HOBOKEN, NJ 07030
FAX: (201) 748-7670
E-MAIL: reprints@wiley.com

PREPUBLICATION REPRINT ORDER FORM

Please complete this form even if you are not ordering reprints. This form **MUST** be returned with your corrected proofs and original manuscript. Your reprints will be shipped approximately 4 weeks after publication. Reprints ordered after printing will be substantially more expensive.

JOURNAL ***JOURNAL OF CELLULAR BIOCHEMISTRY (JCB)*** VOLUME _____ ISSUE _____
TITLE OF MANUSCRIPT _____
MS. NO. _____ NO. OF PAGES _____ AUTHOR(S) _____

No. of Pages	100 Reprints	200 Reprints	300 Reprints	400 Reprints	500 Reprints
	$	$	$	$	$
1-4	**336**	**501**	**694**	**890**	**1052**
5-8	**469**	**703**	**987**	**1251**	**1477**
9-12	**594**	**923**	**1234**	**1565**	**1850**
13-16	**714**	**1156**	**1527**	**1901**	**2273**
17-20	**794**	**1340**	**1775**	**2212**	**2648**
21-24	**911**	**1529**	**2031**	**2536**	**3037**
25-28	**1004**	**1707**	**2267**	**2828**	**3388**
29-32	**1108**	**1894**	**2515**	**3135**	**3755**
33-36	**1219**	**2092**	**2773**	**3456**	**4143**
37-40	**1329**	**2290**	**3033**	**3776**	**4528**

**REPRINTS ARE ONLY AVAILABLE IN LOTS OF 100. IF YOU WISH TO ORDER MORE THAN 500 REPRINTS, PLEASE CONTACT OUR REPRINTS DEPARTMENT AT (201) 748-5971 FOR A PRICE QUOTE.

☐ Please send me _____ reprints of the above article at $ _____

Please add appropriate State and Local Tax for United States orders only. (Tax Exempt No._____) $ _____

Please add 5% Postage and Handling $ _____

TOTAL AMOUNT OF ORDER** $ _____

***International orders must be paid in currency and drawn on a U.S. bank*

Please check one: ☐ Check enclosed ☐ Bill me ☐ Credit Card
If credit card order, charge to: ☐ American Express ☐ Visa ☐ MasterCard

Credit Card No _____ Signature _____ Exp. Date _____

BILL TO:
Name _____
Institution _____
Address _____
_____
Purchase Order No. _____

SHIP TO: (Please, no P.O. Box numbers)
Name _____
Institution _____
Address _____
_____
Phone _____ Fax _____
E-mail _____

111 River Street, 8th Floor
Hoboken, NJ 07030, USA
FAX: 201-748-7670

WILEY
Publishers Since 1807

COPYRIGHT TRANSFER AGREEMENT

Date:

To:

Production/Contribution ID#_____ Publisher/Editorial office use only

Re: Manuscript entitled_____
_____ (the "Contribution")
for publication in _____ (the "Journal")
published by Wiley-Liss, Inc., a subsidiary of John Wiley & Sons, Inc. ("Wiley").

Dear Contributor(s):

Thank you for submitting your Contribution for publication. In order to expedite the publishing process and enable Wiley to disseminate your work to the fullest extent, we need to have this Copyright Transfer Agreement signed and returned to us as soon as possible. If the Contribution is not accepted for publication this Agreement shall be null and void.

A. COPYRIGHT

1. The Contributor assigns to Wiley, during the full term of copyright and any extensions or renewals of that term, all copyright in and to the Contribution, including but not limited to the right to publish, republish, transmit, sell, distribute and otherwise use the Contribution and the material contained therein in electronic and print editions of the Journal and in derivative works throughout the world, in all languages and in all media of expression now known or later developed, and to license or permit others to do so.

2. Reproduction, posting, transmission or other distribution or use of the Contribution or any material contained therein, in any medium as permitted hereunder, requires a citation to the Journal and an appropriate credit to Wiley as Publisher, suitable in form and content as follows: (Title of Article, Author, Journal Title and Volume/Issue Copyright © [year] Wiley-Liss, Inc. or copyright owner as specified in the Journal.)

B. RETAINED RIGHTS

Notwithstanding the above, the Contributor or, if applicable, the Contributor's Employer, retains all proprietary rights other than copyright, such as patent rights, in any process, procedure or article of manufacture described in the Contribution, and the right to make oral presentations of material from the Contribution.

C. OTHER RIGHTS OF CONTRIBUTOR

Wiley grants back to the Contributor the following:

1. The right to share with colleagues print or electronic "preprints" of the unpublished Contribution, in form and content as accepted by Wiley for publication in the Journal. Such preprints may be posted as electronic files on the Contributor's own website for personal or professional use, or on the Contributor's internal university or corporate networks/intranet, or secure external website at the Contributor's institution, but not for commercial sale or for any systematic external distribution by a third party (e.g., a listserve or database connected to a public access server). Prior to publication, the Contributor must include the following notice on the preprint: "This is a preprint of an article accepted for publication in [Journal title] © copyright (year) (copyright owner as specified in the Journal)". After publication of the Contribution by Wiley, the preprint notice should be amended to read as follows: "This is a preprint of an article published in [include the complete citation information for the final version of the Contribution as published in the print edition of the Journal]", and should provide an electronic link to the Journal's WWW site, located at the following Wiley URL: http://www.interscience.Wiley.com/. The Contributor agrees not to update the preprint or replace it with the published version of the Contribution.

2. The right, without charge, to photocopy or to transmit online or to download, print out and distribute to a colleague a copy of the published Contribution in whole or in part, for the Contributor's personal or professional use, for the advancement of scholarly or scientific research or study, or for corporate informational purposes in accordance with Paragraph D.2 below.

3. The right to republish, without charge, in print format, all or part of the material from the published Contribution in a book written or edited by the Contributor.

4. The right to use selected figures and tables, and selected text (up to 250 words, exclusive of the abstract) from the Contribution, for the Contributor's own teaching purposes, or for incorporation within another work by the Contributor that is made part of an edited work published (in print or electronic format) by a third party, or for presentation in electronic format on an internal computer network or external website of the Contributor or the Contributor's employer.

5. The right to include the Contribution in a compilation for classroom use (course packs) to be distributed to students at the Contributor's institution free of charge or to be stored in electronic format in datarooms for access by students at the Contributor's institution as part of their course work (sometimes called "electronic reserve rooms") and for in-house training programs at the Contributor's employer.

D. CONTRIBUTIONS OWNED BY EMPLOYER

1. If the Contribution was written by the Contributor in the course of the Contributor's employment (as a "work-made-for-hire" in the course of employment), the Contribution is owned by the company/employer which must sign this Agreement (in addition to the Contributor's signature), in the space provided below. In such case, the company/employer hereby assigns to Wiley, during the full term of copyright, all copyright in and to the Contribution for the full term of copyright throughout the world as specified in paragraph A above.

2. In addition to the rights specified as retained in paragraph B above and the rights granted back to the Contributor pursuant to paragraph C above, Wiley hereby grants back, without charge, to such company/employer, its subsidiaries and divisions, the right to make copies of and distribute the published Contribution internally in print format or electronically on the Company's internal network. Upon payment of the Publisher's reprint fee, the institution may distribute (but not resell) print copies of the published Contribution externally. Although copies so made shall not be available for individual re-sale, they may be included by the company/employer as part of an information package included with software or other products offered for sale or license. Posting of the published Contribution by the institution on a public access website may only be done with Wiley's written permission, and payment of any applicable fee(s).

E. GOVERNMENT CONTRACTS

In the case of a Contribution prepared under U.S. Government contract or grant, the U.S. Government may reproduce, without charge, all or portions of the Contribution and may authorize others to do so, for official U.S. Government purposes only, if the U.S. Government contract or grant so requires. (U.S. Government Employees: see note at end).

F. COPYRIGHT NOTICE

The Contributor and the company/employer agree that any and all copies of the Contribution or any part thereof distributed or posted by them in print or electronic format as permitted herein will include the notice of copyright as stipulated in the Journal and a full citation to the Journal as published by Wiley.

G. CONTRIBUTOR'S REPRESENTATIONS

The Contributor represents that the Contribution is the Contributor's original work. If the Contribution was prepared jointly, the Contributor agrees to inform the co-Contributors of the terms of this Agreement and to obtain their signature to this Agreement or their written permission to sign on their behalf. The Contribution is submitted only to this Journal and has not been published before, except for "preprints" as permitted above. (If excerpts from copyrighted works owned by third parties are included, the Contributor will obtain written permission from the copyright owners for all uses as set forth in Wiley's permissions form or in the Journal's Instructions for Contributors, and show credit to the sources in the Contribution.) The Contributor also warrants that the Contribution contains no libelous or unlawful statements, does not infringe on the rights or privacy of others, or contain material or instructions that might cause harm or injury.

CHECK ONE:

[____]Contributor-owned work

_____ _____
Contributor's signature Date

_____
Type or print name and title

_____ _____
Co-contributor's signature Date

_____
Type or print name and title

ATTACH ADDITIONAL SIGNATURE PAGE AS NECESSARY

[____]Company/Institution-owned work (made-for-hire in the course of employment)

_____ _____
Company or Institution (Employer-for-Hire) Date

_____ _____
Authorized signature of Employer Date

[____]**U.S. Government work**

Note to U.S. Government Employees

A Contribution prepared by a U.S. federal government employee as part of the employee's official duties, or which is an official U.S. Government publication is called a "U.S. Government work," and is in the public domain in the United States. In such case, the employee may cross out Paragraph A.1 but must sign and return this Agreement. If the Contribution was not prepared as part of the employee's duties or is not an official U.S. Government publication, it is not a U.S. Government work.

[____]**U.K. Government work (Crown Copyright)**

Note to U.K. Government Employees

The rights in a Contribution prepared by an employee of a U.K. government department, agency or other Crown body as part of his/her official duties, or which is an official government publication, belong to the Crown. In such case, the Publisher will forward the relevant form to the Employee for signature.

3,3′-Diselenodipropionic Acid, an Efficient Peroxyl Radical Scavenger and a GPx Mimic, Protects Erythrocytes (RBCs) from AAPH-Induced Hemolysis

Amit Kunwar,[†] Beena Mishra,[†] Atanu Barik,[†] Liladhar B. Kumbhare,[‡] Ruchi Pandey,[§] Vimal K. Jain,[‡] and K. Indira Priyadarsini*,[†]

Radiation & Photochemistry Division, Chemistry Division, and Radiation Biology & Health Sciences Division, Bhabha Atomic Research Centre, Trombay, Mumbai-400085, India

Received April 27, 2007

3,3′-Diselenodipropionic acid (DSePA), a derivative of selenocystine, has been synthesized and examined for antioxidant activity, glutathione peroxidase (GPx) activity, and cytotoxicity. The effect of DSePA on membrane lipid peroxidation, release of hemoglobin, and intracellular K^+ ion as a consequence of erythrocyte (red blood cells or RBCs) oxidation by free radicals generated by 2,2′-azobis(2-amidinopropane) hydrochloride (AAPH) were used to evaluate the antioxidant ability. Lipid peroxidation, hemolysis, and K^+ ion loss in RBCs were assessed, respectively, by formation of thiobarbituric acid reactive substances (TBARS), absorbance of hemoglobin at 532 nm and flame photometry. The IC_{50} values for lipid peroxidation, hemolysis, and K^+ ion leakage were 45 ± 5, 20 ± 2, and 75 ± 8 μM, respectively. DSePA treatment prevented the depletion of glutathione (GSH) levels in RBCs from free-radical-induced stress. DSePA is a good peroxyl radical scavenger and the bimolecular rate constant for the reaction of DSePA with a model peroxyl radical, trichloromethyl peroxyl radical ($CCl_3O_2^{\bullet}$), was determined to be 2.7×10^8 M^{-1} s^{-1} using a pulse radiolysis technique. DSePA shows GPx activity with higher substrate specificity towards peroxides than thiols. The cytotoxicity of DSePA was studied in lymphocytes and EL4 tumor cells and the results showed that DSePA is nontoxic to these cells at the concentrations employed. These results when compared with two well-known selenium compounds, sodium selenite and ebselen, indicated that DSePA, although it shows lesser GPx activity, has higher free radical scavenging ability and lesser toxicity.

Introduction

Selenium is one of the essential micronutrients whose deficiency can lead to pathological states such as neurodegenerative diseases, cardiovascular diseases, etc. (*1–5*). Loss of selenium has also been observed in burn patients and some anti-inflammatory conditions (*6*). Selenium is a constituent of several redox active enzymes such as glutathione peroxidase (GPx), thioredoxin reductase (TRx), etc. So far, 34 selenium-containing proteins have been identified in eukaryotes (*5*). GPx is an antioxidant enzyme, playing a crucial role in combating oxidative stress (*2, 7*). Oxidative stress is a condition that is associated with excessive production of free radicals (*8*). In the last decade, several new selenium compounds have been developed that showed both GPx activity and free radical scavenging ability (*9–15*). However, most of the compounds showed only mixed success and one compound, ebselen, an aromatic selenide, showed promising GPx activity and was even tested in the clinic (*16*). However, it was later on found to show limited therapeutic utility. One of the constraints in the development of selenium compounds is their stability and poor water solubility. For a selenium compound to act as an antioxidant, it must show nucleophilicity necessary for GPx activity, free radical scavenging capability, water solubility and less toxicity. Recently Back et al. showed that certain aliphatic seleno-ethers and diselenides depending on the substitution on the aliphatic chain show higher GPx activity than ebselen (*17*).

Scheme 1

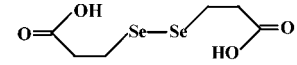

3,3'-Diselenodipropionic acid (DSePA)

With our recent interest in the design of water-soluble bioactive selenium compounds, we have examined a simple, stable, and water-soluble organoselenium compound, 3,3′-diselenodipropionic acid (DSePA), a diselenide, and an analogue of selenocystine for in vitro antioxidant activity, free radical reactions, GPx activity, and cytotoxicity. The compound, whose chemical structure is given in Scheme 1, was previously synthesized and tested as a GPx mimic using benzyl thiol and tert-butyl hydroperoxide as substrates by Back et al. (*17*). For antioxidant activity, DSePA has been tested for its ability to protect human red blood cells (RBCs) from free-radical-induced hemolysis. The oxidation of RBCs leading to hemolysis can serve as a model for the oxidative damage of biomembranes (*18–23*). Free radical reaction was initiated by the peroxyl radicals generated by thermal decomposition of an azo compound, 2,2′-azobis(2-amidinopropane) hydrochloride (AAPH), in the presence of oxygen (*20, 24*). Because both oxidative stress and GPx catalytic cycles can influence the GSH levels in cells, GSH levels were monitored. Also, the GPx activity and rate constant for the reaction of peroxyl radical with DSePA were estimated. The cytotoxicity of the compound at the concentra-

* Corresponding author. E-mail: kindira@barc.gov.in. Fax: 91-22-25505151.
[†] Radiation & Photochemistry Division, Bhabha Atomic Research Centre.
[‡] Chemistry Division, Bhabha Atomic Research Centre.
[§] Radiation Biology & Health Sciences Division, Bhabha Atomic Research Centre.

10.1021/tx700137a CCC: $37.00
Published on Web 09/28/2007

tions employed in these studies has been evaluated in lymphocytes and EL4 tumor cells. The results have been compared with sodium selenite, a well-known selenium compound used as selenium supplement, and ebselen, a potent GPx mimic.

Materials and Methods

Chemicals and Instruments. Thiobarbituric acid (TBA), butylated hydroxy toluene (BHT), (3-[4,5-dimethylthiazole-2-yl]-2,5-diphenyl tetrazolium bromide (MTT), cell culture medium RPMI 1640, HEPES buffer, 2,2′-azobis(2-amidinopropane) hydrochloride (AAPH), 5,5′-dithiobis-2-nitrobenzoic acid (DTNB), ebselen, and sodium selenite (Na_2SeO_3) were of the best purity available and obtained from commercial sources. GPx activity was determined using a standard kit (RS 504) obtained from Randox Laboratories, U.K. All the other chemicals were of analytical grade. Solutions were prepared in nanopure water. Absorption spectra were recorded on Hitachi spectrophotometer (model U 2001). The compound DSePA was synthesized (yield 63%; m.p. 135 °C) according to the literature reported method (*25*) and characterized by NMR, IR, and mass spectrometry. ^{1}H, ^{13}C{^{1}H}, and ^{77}Se{^{1}H} NMR spectra were recorded on a Bruker DPX-300 NMR spectrometer operating at 300, 75.47, and 57.24 MHz, respectively. Chemical shifts are relative to internal solvent peaks for ^{1}H and ^{13}C and external Me_2Se (secondary reference Ph_2Se_2 δ 463 ppm) for ^{77}Se NMR measurements. The IR spectrum was recorded as Nujol mull between CsI plates with Bomen MB-102 FT-IR spectrometer and the mass spectrum was recorded with Waters Q-TOF micro (Y-105) time of flight mass spectrometer. ^{1}H NMR (CD_3OD) δ: 2.81 (t, $SeCH_2$); 3.10 (t, CH_2CO) (COOH proton exchanged with CD_3OD). ^{13}C{^{1}H} NMR (CD_3OD) δ: 23.4 (s, $SeCH_2$); 35.4 (s, CH_2CO); 174.3 (s, CO). ^{77}Se{^{1}H} NMR (CD_3OD) δ: 322 (s). IR spectra: ν(C=O) 1694 cm^{-1}; Mass spectra: *m*/*z* 306 (molecular ion); 288 (M-H_2O). The *m*/*z* value given here is based on the ^{80}Se isotope with a natural abundance of 49.82%.

Preparation of RBCs. Blood samples were obtained by venipuncture from healthy volunteers with strict adherence to the ethical guidelines laid down by the institutional animal ethics committee of Bhabha Atomic Research Centre. Blood was collected in heparinized tubes and centrifuged for 10 min at 1000 g and 4° C using a cold centrifuge (Remi compufuge, CPR-24). Samples were washed three times with a phosphate-buffered saline (PBS: NaCl 150 mM, NaH_2PO_4 0.58 mM and Na_2HPO_4 3.4 mM, pH 7.4). Plasma and buffy coat were carefully removed by aspiration after each washing. RBCs were finally suspended in the buffer solution to obtain a hematocrit of approximately 50%, stored at 4° C, and used within 6 h. All the experiments were carried out in triplicate and the results are presented as means ± SEM, $n = 3$.

Measurement of Hemolysis. Hemolysis of RBCs was carried out by mixing a 5% suspension of RBCs in PBS under an air atmosphere with AAPH solution (final concentration 50 mM). This reaction mixture was incubated for 3 hours at 37°C with gentle shaking. The extent of hemolysis was determined spectrophotometrically by measuring the absorbance of haemolysate at 540 nm as described previously (*26*). For reference, RBCs were treated with distilled water and the absorbance of the haemolysate at 540 nm was used as 100% hemolysis. To test the effect of DSePA on hemolysis, RBCs were preincubated with varying concentration of DSePA at 37° C for 30 min, washed twice with cold PBS, and then subjected to hemolysis. This 30 min incubation time would ensure that DSePA is taken up by the RBCs.

Measurement of K^+ Ion Loss. Pecked RBCs were suspended in 3 mL of 10 mM PBS, containing varying amounts of DSePA to give 0.5% hematocrit. After 30 min of incubation at 37° C and two washes with cold PBS, AAPH (50 mM) was added and this system was incubated at room temperature for 3 h. After centrifugation at 1500 g for 10 min, the concentration of K^+ ion was measured in the supernatant using flame photometry (Chemito AA 203, atomic absorption spectrophotometer with programmable flame control unit). For reference of 100% intracellular K^+ ion, a sample of RBCs was haemolyzed in distilled water and the K^+ ion concentration was determined in the supernatant after centrifugation.

Membrane Lipid Peroxidation. Lipid peroxidation was assessed by measuring the thiobarbituric acid (TBA) reactive substances (TBARS). For this 5% suspension of RBCs in PBS (pH 7.4) was incubated under air atmosphere with varying concentration of DSePA at 37° C for 30 min, washed twice with cold PBS, and then incubated into a PBS solution of AAPH (50 mM) to initiate membrane damage. After incubation at room temperature for 3 h, the system was centrifuged at 1500 g for 10 min; the pellet was resuspended in to 300 μL of PBS (pH 7.4), to which 900 μL of TBA reagent (0.375% thiobarbituric acid, 0.25 M HCl, 15% trichloroacetic acid, and 6 mM EDTA) was added. After further treatment, TBARS were estimated by measuring the absorbance at 532 nm (*27*) and expressed per milligram of hemoglobin.

Glutathione Estimation. The concentration of glutathione in RBCs was determined using 5,5′-dithiobis-2-nitrobenzoic acid (DTNB) according to the reported method (*19*). In a typical experiment, a 5% suspension of RBCs in PBS (pH 7.4) was subjected to hemolysis by treatment with AAPH for 3 h in the presence of different concentrations of DSePA. The hemolysate was then used for estimation of GSH and expressed as nanomoles of DTNB per milligrams of hemoglobin.

Pulse Radiolysis Studies. Pulse radiolysis experiments were carried out with high-energy electron pulses (7 MeV, 500 ns) generated from a linear electron accelerator whose details are given elsewhere (*28*). Aerated aqueous solution of 0.01 M KSCN was used for determining the dose delivered per pulse (*29*). The dose per pulse was close to 10–12 Gy. Trichloromethyl peroxyl radicals ($CCl_3O_2^{\bullet}$) were generated by radiolysis of aerated aqueous solutions containing 48% 2-propanol and 4% CCl_4 (*30*).

GPx Activity. GPx activity was determined by following the decay of NADPH (0.34 mM) at 340 nm in the presence of glutathione reductase (0.5 mU/mL), GSH, cumene hydroperoxide (CuOOH), and DSePA. The initial rate (v) is calculated using the extinction coefficient as 6220 M^{-1} cm^{-1} and plotted against DSePA concentration to ensure linearity in the given range. In this linear range of concentration, Lineweaver−Burk (L−B) plots were made separately for GSH and CuOOH to find out the affinity of the enzyme DSePA to the two substrates individually. For these experiments, the concentration of DSePA is kept constant and v was determined at different concentrations of either GSH or CuOOH by fitting the data to the double reciprocal plot or L−B plot (eq 1).

$$\frac{1}{v} = \frac{K_m}{V_{max}}\frac{1}{[S]} + \frac{1}{V_{max}} \quad (1)$$

Here, V_{max} is the maximum rate of the enzymatic reaction, S is the concentration of either GSH or CuOOH, and K_m is the Michaelis−Menten constant. GPx units were estimated at different concentrations of DSePA (47–140 μM), Na_2SeO_3 (5–25 μM), and ebselen (100 μM dissolved in 1% acetonitrile) using the initial rates in terms of ΔA/min at 340 nm according to the procedure given in the literature (*31*). The molar concentration of DSePA required to oxidize 1 μmol of NADPH in 1 min is expressed as 1 unit of GPx.

Cytotoxicity Studies. Thymic lymphoma EL4 cells were obtained from National Centre for Cell Science (NCCS), Pune, India, and were maintained in RPMI-1640 medium; cells were routinely subcultured and maintained in a humidified atmosphere with 5% CO_2 at 37° C. Spleen cells were isolated from C57BL/6 mice as described earlier (*27*). Viability of EL4 cells (5×10^5 cells/mL) or splenic lymphocytes (5×10^6 cells/mL) in the presence of different concentration of DSePA at 24 and 48 h was estimated by the MTT (3-[4,5-dimethylthiazole-2-yl]-2,5-diphenyl tetrazolium bromide) dye conversion assay, (*32*) and the results were expressed as the mean absorbance ± SEM for four replicates.

Results

Inhibition of AAPH-Induced Lipid Peroxidation, Hemolysis, and K^+ Ion Leakage in Human RBCs by DSePA. RBC membranes are rich in polyunsaturated fatty acids, which are

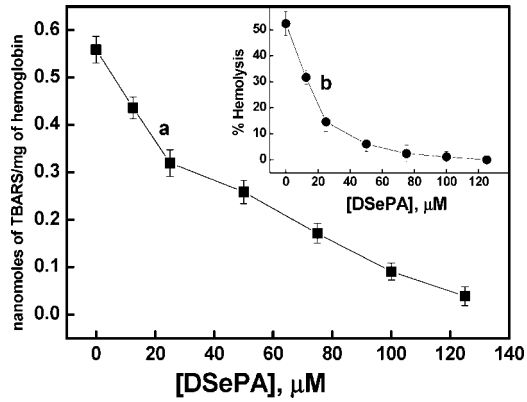

Figure 1. Variation of (a) lipid peroxidation and (b) percent hemolysis in human RBCs induced by 50 mM AAPH after incubation for 3 h at different concentrations of DSePA. Results are presented as mean ± SEM, $n = 3$.

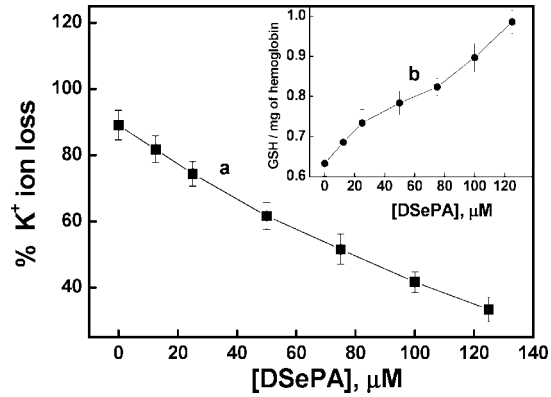

Figure 2. Variation (a) of K^+ ion loss and (b) glutathione levels in human RBCs incubated with 50 mM AAPH for 3 h in the presence of different concentrations of DSePA. Results are presented as mean ± SEM, $n = 3$.

susceptible to free-radical-mediated peroxidation, leading to damage of the membrane. When AAPH is added as initiator, it decomposes at physiological temperature (37° C) in aqueous solutions to generate alkyl radical (R″), which in the presence of oxygen is converted to the corresponding peroxyl radicals (R′OO•) (eqs 2 and 3). At 37° C in neutral water, the half life of AAPH is about 175 hours and generates radicals at a rate of 1.3×10^{-6} mol s^{-1} (*24*). These peroxyl radicals induce oxidation of polyunsaturated lipids (LH) in RBC membranes, (*23*) causing a chain reaction known as lipid peroxidation (eqs 4−6). As a result of this, the RBC membrane undergoes quick damage and losses its integrity, leading to the release of hemoglobin (hemolysis) and intracellular K^+ ions. When compounds like DSePA are present and if they can scavenge peroxyl radicals by converting them to nonreactive species (eq 7) the hemolysis may be inhibited.

$$\text{R'–N=N–R'} \rightarrow 2\text{R}^{\bullet} + \text{N}_2 \quad (2)$$

$$\text{R}^{\bullet} + \text{O}_2 \rightarrow \text{R'OO}^{\bullet} \quad (3)$$

$$\text{R'OO}^{\bullet} + \text{LH} \rightarrow \text{R'OOH} + \text{L}^{\bullet} \quad (4)$$

$$\text{L}^{\bullet} + \text{O}_2 \rightarrow \text{LOO}^{\bullet} \quad (5)$$

$$\text{LH} + \text{LOO}^{\bullet} \rightarrow \text{L}^{\bullet} + \text{LOOH} \quad (6)$$

$$\text{DSePA} + \text{LOO}^{\bullet} \xrightarrow{\text{H}^+} \text{DSePA}^{\bullet +} + \text{LOOH} \quad (7)$$

where, R′ is $-C(Me)_2-C(NH_2)=NH_2^+$

Figure 1a shows variation in TBARS in RBCs after being subjected to AAPH-induced damage in the presence and absence of different concentrations of DSePA. The level of TBARS was significantly increased after incubation of RBCs with AAPH as compared to the control sample. In the presence of DSePA, there was a significant decrease in TBARS formation and this inhibition increased with increasing DSePA concentration from 12.5 to 125 μM, from which the IC_{50} value, i.e., the concentration of DSePA required to inhibit TBARS formation by 50%, was found to be 45 ± 5 μM.

In the absence of AAPH, the RBCs were stable and the hemolysis was negligible. When aqueous suspension of RBCs was incubated with AAPH, about 52% hemolysis was observed. Hemolysis was monitored after DSePA addition to this reaction system in increasing concentrations (12.5–125 μM). It is evident from Figure 1b that the percent hemolysis progressively decreased with increasing concentration of DSePA, and at 125 μM DSePA, there was absolutely no hemolysis. The IC_{50} value, the concentration of DSePA required to inhibit hemolysis by 50%, was found to be 20 ± 2 μM.

The percent K^+ ion loss in RBCs after incubation with AAPH and its inhibition by increasing concentrations of DSePA are shown in Figure 2a. Incubation of RBCs with AAPH resulted in about 90% loss of intracellular potassium. This process was inhibited in a progressive manner when DSePA was added to the reaction system in increasing concentrations (12.5–125 μM). The IC_{50} value, i.e., the concentration of DSePA required to inhibit the loss of 50% K^+ ions, was 75 ± 8 μM.

Effect of DSePA on GSH Levels in RBCs after Hemolysis. Inset b of Figure 2 shows the change in GSH levels in RBCs after treatment with AAPH and also in presence of DSePA (*33*). The normal basal level of GSH in RBCs was found to be 1.07 ± 0.05 nmol/mg of hemoglobin, and after incubation with AAPH, the GSH level reduced to about 0.63 ± 0.03 nmol/mg of hemoglobin. Addition of DSePA in the concentration range of 12.5–125 μM to this reaction system prevented the reduction in GSH content in a concentration-dependent manner (Inset b of Figure 2).

GPx Activity. Selenium compounds are often very good mimics of intracellular GPx enzymes. The above studied antioxidant properties of DSePA may therefore be due to either its GPx activity, which causes enzymatic reduction of peroxide in presence of thiol, or direct free radical scavenging of the peroxyl radical (*16*). These two properties have been independently evaluated for DSePA. Initially, GPx enzyme activity was estimated at different concentrations of DSePA. Figure 3 shows the plot for the variation of the initial rate v, for the decay of NADPH, as a function of DSePA concentration. The plot is linear in the concentration range and did not reach saturation. From this linear plot, the average value of the GPx activity for DSePA was calculated to be 12.84 mM DSePA, equivalent to one unit of GPx. The GPx activity of DSePA may be due to its affinity for either GSH or CuOOH. To further understand this, we made separate L–B plots for GSH and CuOOH. An L–B plot for thiol was obtained (inset a of Figure 3) at different concentrations GSH (4–17 mM), keeping the concentration of DSePA (100 μM) and CuOOH (180 μM) fixed. From this, according to eq 1, we obtained K_m and V_{max} values for GSH of 10.2 mM and 4.8 μM/min, respectively. Similarly, the L–B plot for hydroperoxide was obtained (inset b of Figure 3) at different concentrations of CuOOH (0.9–1.44 mM), keeping the concentration of DSePA (100 μM) and GSH (4 mM) fixed; the K_m and V_{max} values for CuOOH were estimated to be 0.14 mM and 2.24 μM/min, respectively. The inverse of K_m is related to the binding affinity of the substrate to the enzyme. Thus, a lower

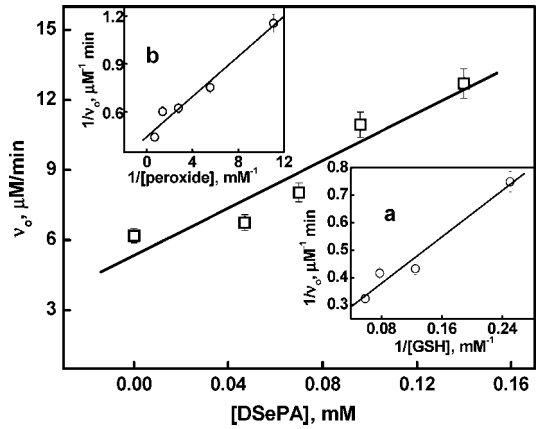

Figure 3. Variation in the initial rate of decay of NADPH at 340 nm as a function of the concentration of DSePA. Insets (a) and (b) show Lineweaver–Burk plots obtained on varying the concentration of GSH and cumene hydroperoxide (CuOOH), respectively.

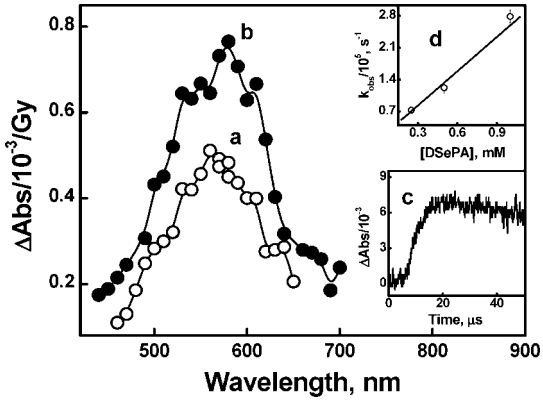

Figure 4. Difference absorption spectrum of the transient species produced on reaction of DSePA concentration (1 mM) with (a) $CCl_3O_2^{\bullet}$ and (b) $N_3^{\bullet}$ at pH 7. Inset (c) shows absorption–time plot for the formation of DSePA radical cation at 560 nm. Inset (d) shows variation in the observed pseudo-first order rate constant at 560 nm, as a function of DSePA.

value of K_m for CuOOH in comparison to GSH indicates that DSePA has a higher affinity or binding to the peroxide than GSH.

Pulse Radiolysis Study. The high affinity of DSePA for CuOOH and its antioxidant activity indicate that DSePA could be an effective scavenger of peroxyl radicals. To test this, we studied the direct reaction of peroxyl radical with DSePA using the pulse radiolysis technique. $CCl_3O_2^{\bullet}$ radicals are model peroxyl radicals, which can be conveniently produced by radiolysis of aqueous solutions of 2-propanol and CCl_4, and their reactions can be studied by pulse radiolysis (*30*). The reaction of DSePA with $CCl_3O_2^{\bullet}$ at pH 7 produced a transient radical species having an absorption spectrum in the wavelength range 300–600 nm, with a maximum at 560 nm (Figure 4a). $CCl_3O_2^{\bullet}$ radicals can react with DSePA by either electron transfer or H-atom abstraction (*30*). To understand this, we carried out independent experiments on the reaction of DSePA with a specific one-electron oxidant, $N_3^{\bullet}$, (*34*) and the results showed formation of a similar transient absorption spectrum (Figure 4 b). This confirms that DSePA reacts with $CCl_3O_2^{\bullet}$ preferentially by electron transfer, forming a selenium-centered radical cation ($DSePA^{\bullet+}$) as observed in several other organoselenium compounds (*35*). The bimolecular rate constant for the reaction of DSePA with $CCl_3O_2^{\bullet}$ was determined by following the build up kinetics of the transient at 560 nm (Figure 4, inset c) in the presence of different concentrations of DSePA

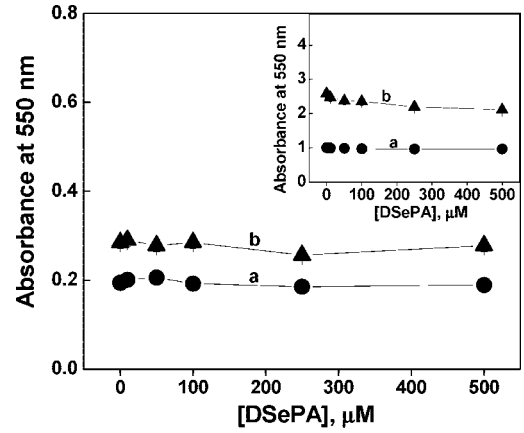

Figure 5. Effect of DSePA concentration on the viability of freshly isolated spleen lymphocytes (a) 24 and (b) 48 h assayed by MTT. Inset shows the effect of DSePA concentration on the viability of tumor cell line EL4 (a) 24 h and (b) 48 h assayed by MTT. Results are presented as mean ± SEM, $n = 4$.

and from the slope of the linear plot as given in the inset d of Figure 4; the rate constant was found to be 2.7×10^8 M^{-1} s^{-1}. Generally, rate constants for reactions of $CCl_3O_2^{\bullet}$ radicals with chain-breaking antioxidants, such as vitamin E, curcumin, etc., (*31*) are in the same range. Therefore, the antioxidant activity of DSePA may also arise by its peroxyl radical scavenging ability.

Cellular Cytotoxicity Studies. The effect of DSePA on cell viability was analyzed using normal quiescent splenic lymphocytes and their syngenic constitutively proliferating EL4 cells. Figure 5 and the inset show the viability of spleen cells and EL4 cell lines, cultured for 24 (curve a) and 48 h (curve b), respectively, in the presence of different concentrations of DSePA. It can been seen from Figure 5 that there was no effect of DSePA in the concentration range of 10–500 μM on the viability of either splenic lymphocytes or EL4 cell lines, confirming that DSePA is nontoxic to these cells under in vitro conditions.

Comparison between DSePA and Na_2SeO_3 and Ebselen. Because Na_2SeO_3 and ebselen are some of the most extensively studied selenium compounds for biological activities (*14, 36*), the present results on the antioxidant capacity and cellular cytotoxicity of DSePA were compared with those of Na_2SeO_3 and ebselen. Because of the limited solubility of ebselen, experiments could not be carried out over a wide range of concentrations; therefore, the results obtained at identical concentrations of Na_2SeO_3 and DSePA are discussed initially in detail. At a fixed concentration of 125 μM, the ability of DSePA and Na_2SeO_3 to protect human RBCs from hemoglobin loss, K^+ ion loss, lipid peroxidation, and glutathione depletion induced by AAPH was used to compare their antioxidant activity as shown in Figure 6. It is evident from the figure that DSePA is far superior to Na_2SeO_3 in protecting human RBCs from free-radical-induced damage. GPx activity for Na_2SeO_3, determined by a similar procedure in the concentration range from 5–25 μM, was found to be 1.3 mM of Na_2SeO_3, equivalent to one unit of GPx enzyme, indicating that Na_2SeO_3 exhibits much better GPx activity compared to DSePA. The comparative cellular cytotoxicity of the DSePA and Na_2SeO_3 suggests that although DSePA did not show toxicity to spleen lymphocytes and tumor cells up to a concentration of 500 μM, Na_2SeO_3 was toxic to both spleen lymphocytes and tumor cells, even at concentrations lower than 2.5 μM (*37*).

Similarly, at a 7.5 μM concentration of either ebselen or DSePA, similar percentage protection was observed toward

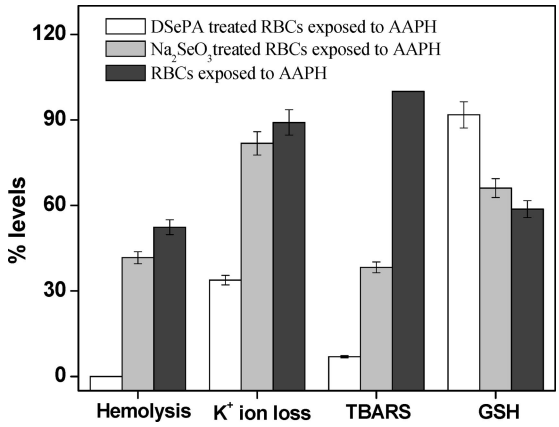

Figure 6. Bar graph showing the comparative effect of identical concentration (125 μM) of DSePA and Na_2SeO_3 on parameters of human RBCs oxidation such as hemolysis, K^+ ion loss, lipid peroxidation, and glutathione levels induced by 50 mM AAPH after 3 h of incubation. Results are presented as mean ± SEM, $n = 3$.

AAPH induced erythrocytes damage assessed by hemolysis, lipid peroxidation, and GSH levels. However, the GPx activity of ebselen was much higher, with one unit of GPx enzyme being equivalent to 2.35 mM of ebselen. The rate constant for the reaction $CCl_3O_2^{\bullet}$ peroxyl radical with ebselen has earlier been reported to be 2.8×10^8 M^{-1} s^{-1} (*38*).

Discussion

Hemolysis of human RBCs is a very good model for studying free-radical-induced oxidative damage to membranes for the development of antioxidants. Therefore, to evaluate the antioxidant activity of DSePA, we have evaluated lipid peroxidation of the membrane fatty acids, loss of hemoglobin, and release of intracellular K^+ ions in human RBCs treated with AAPH. The results obtained from these studies indicate that DSePA protects RBCs from AAPH-induced free radical damage. However, their IC_{50} values are not the same and follow the order of K^+ ion loss > lipid peroxidation > hemolysis. This is probably because a hemoglobin molecule with a large size is difficult to release from the damaged membranes, whereas K^+ ions, being smaller in size, can be leaked even with a slight disturbance in the membrane structure. Thus, a concentration of DSePA showing little protection to membrane damage (assessed in terms of TBARS) can have a significant impact on the prevention of hemoglobin loss from RBCs, while to prevent the loss of intracellular K^+ ions, a much higher concentration of DSePA is required. Such requirements of high concentrations to prevent K^+ ion loss leaves a doubt on its therapeutic utility, but because of low cytotoxicity of DSePA, this may not be a serious limitation.

GSH, a tripeptide containing cysteine, is the most abundant thiol present in mammalian cells (*13, 39*). GSH, along with other reduced thiols, performs a number of vital cell functions, including maintaining the essential thiol status of proteins by preventing oxidation of sulfahydryl groups or by reducing disulphide bonds induced by oxidative stress, or by scavenging free radicals. Thiols are also involved in the GPx cycle. Because of all these processes, during oxidative stress, the cellular pool of GSH is depleted. Exogenously applied antioxidants protect GSH levels in cells by preventing them from being consumed in reaction with free radicals (*39*). Our results indicate that the GSH levels come down significantly in RBCs after AAPH incubation, but pretreatment with DSePA in the concentration range prevents the decrease in GSH level. This effect could be due to its ability to either scavenge peroxyl radicals or act as a GPx mimic. For this, we evaluated the GPx activity of the compound by estimating K_m values for peroxide and thiol separately. The results indicated that DSePA has more affinity toward the peroxide than the thiol. The GPx activity of DSePA in terms of GPx units indicates that it has lower activity than well-known standards such as sodium selenite or ebselen. Although their mechanism of GPx action may be very much different, such comparisons are necessary for evaluating this compound as a GPx mimic.

Scheme 2

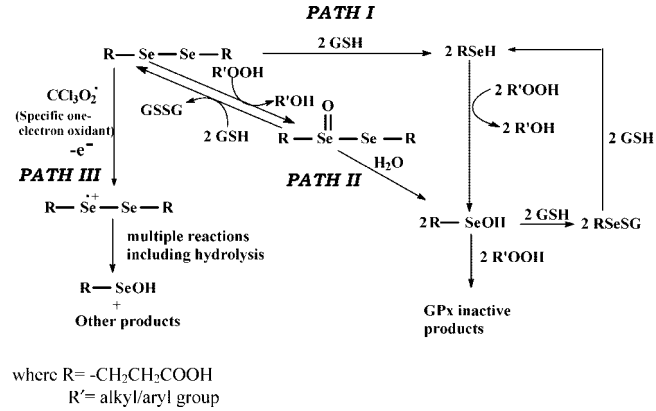

where R= $-CH_2CH_2COOH$
R′= alkyl/aryl group

To understand this behavior, we tried to relate different steps involved in the GPx cycle of DSePA. A diselenide can show its GPx activity through two mechanisms (Scheme 2). Path I: Conversion to a selenol (RSeH) in the presence of GSH, which on reaction with hydroperoxides gets oxidized to selenenic acid (RSeOH). This selenenic acid is converted back to the selenol on two-step reaction with 2 mol of GSH. (*15*) Path II: A diselenide can directly react with a hydroperoixde to form the diselenide monoxide (RSeSeOR), which may react either with thiol to be converted back to the diselenide or with water to form RSeOH, which can again be regenerated back to selenol by the thiols, as observed in most selenium GPx mimics (*17*). However, some recent reports by Back et al. indicate that aliphatic selenenic acids (like DSePA) in the presence of excess hydroperoxide may undergo further oxidation to form seleninic acid (RSeOOH), which may finally be converted into smaller products, such as acrylic acid, that do not cause recycling of the enzyme (*17*). Therefore, from the above results, it can be inferred that the GPx activity of DSePA may arise through the oxidation mechanism.

In addition to the GPx activity, DSePA is a good scavenger of peroxyl radicals and the rate constant is comparable to well-known GPx mimic ebselen and chain-breaking antioxidants like vitamin E. The reaction causes one-electron oxidation, forming $DSePA^{\bullet+}$ as seen by the transient spectrum. This indicates that DSePA is easy to undergo one-electron oxidation, mainly because of the increase in electron density on the selenium atom by the electron-donating carboxylate groups present in the γ-position and subsequent stability of the radical cation by the two selenium atoms (*35*). Such easy oxidation makes DSePA a very efficient scavenger of oxidizing free radicals. However, the fate of such a radical cation is not clear. One possible reaction is its hydrolysis, as observed in the case of disulfide radical cations (*40*), to form RSeOH as one of the products, which may participate in GPx activity by Path II. All these reactions are depicted in Path III of Scheme 2.

At this stage, we felt it was necessary to evaluate toxicity to normal and tumor cells. Thus, cytotoxicity studies of DSePA in

splenic lymphocytes and EL4 cell lines indicated that at the concentrations employed in the present study, DSePA is nontoxic to both normal and tumor cells. Also, our preliminary in vivo studies showed an increase in the GPx activity in mouse fed with DSePA at a dose of 1 mg/kg of body weight (results not included).

Finally, all these results on DSePA when compared with pharmacologically active selenium compounds like sodium selenite and ebselen indicated that DSePA is far superior to sodium selenite and comparable to ebselen in protecting RBCs from hemolysis. Both ebselen and DSePA are excellent scavengers of peroxyl radicals. However, the GPx activity of either sodium selenite or ebselen is much higher than that of DSePA. Even then both sodium selenite and ebselen suffer from the drawbacks of either high toxicity or poor water solubility. Considering all these factors, it appears that DSePA may be considered as a simple, stable, and water-soluble compound, which can be used as a model in the design and synthesis of more active and potent selenium antioxidants having high free radical scavenging ability, good GPx activity, low cytotoxicity, and water solubility.

Acknowledgment. The authors are thankful to Dr B. Venkatramani for help in the flame photometry experiment and Dr. T. Mukherjee and Dr. S. K. Sarkar for their constant encouragement and support.

References

(1) Brenneisen, P., Steinbrenner, H., and Sies, H. (2005) Selenium, oxidative stress, and health aspects. *Mol. Aspects Med. 26*, 256–267.
(2) Arteel, G. E., and Sies, H. (2001) The biochemistry of selenium and the glutathione system. *Environ. Toxicol. Pharmacol. 10*, 153–158.
(3) Tapiero, H., Townsend, D. M., and Tew, K. D. (2003) The antioxidant role of selenium and selenol-compounds. *Biomed. Pharmacother. 57*, 134–144.
(4) Madea, H., Katayama, K., Matsuno, H., and Uno, T. (2006) 3′-(2,4-Dinitrobenzenesulfonyl)-2′,7′-dimethylfluorescein as a fluorescent probe for selenols. *Angew. Chem., Int. Ed. 45*, 1810–1813.
(5) Rayman, M. P. (2000) The importance of selenium to human health. *Lancet 356*, 233–241.
(6) Agay, D., Sandre, C., Ducros, V., Faure, H., Cruz, C., Alonso, A., Roussel, A-M., and Chancerelle, Y. (2005) Optimization of selenium status by a single intraperitoneal injection of selenium in Se- deficient rat: Possible application to burned patient treatment. *Free Radical Biol. Med. 39*, 762–768.
(7) Mugesh, G., and du Mont, W.-W. (2001) Structure–activity correlation between natural glutathione peroxidase (GPx) and mimics: A biomimetic concept for the design and synthesis of more efficient GPx mimics. *Chem.—Eur. J. 7*, 1365–1370.
(8) Halliwell, B., and Gutteridge, J. M. C. (1989) *Free Radicals in Biology and Medicine*. Clarendon, Oxford, U.K.
(9) Klayman, D. L., and Gunther, W. H. H. (1973) *Organic Selenium Compounds: Their Chemistry and Biology*. Wiley, New York.
(10) Bock, A. (1994) Selenium Proteins Containing Selenocysteine. In *Encyclopedia of Inorganic Chemistry* (King, R. B., Ed.), *Vol. 7*, pp 3700–3709, Wiley, New York.
(11) Metanis, N., Keinan, E., and Dawson, P. E. (2006) Synthetic seleno-glutaredoxin 3 analogues are highly reducing oxidoreductases with enhanced catalytic efficiency. *J. Am. Chem. Soc. 128*, 16684–16691.
(12) Sagher, D., Brunell, D., Brot, N., Vallee, B. L., and Weissbach, H. (2006) Selenocompounds can serve as oxido-reductants with the methionine sulfoxide reductase enzymes. *J. Biol. Chem. 281*, 31184–31187.
(13) Nogueira, C. W., Zeni, G., and Rocha, J. B. T. (2004) Organoselenium and Organotellurium compounds: Toxicology and Pharmacology. *Chem. Rev. 104*, 6255–6285.
(14) Mugesh, G., du Mont, W.-W., and Sies, H. (2001) Chemistry of biologically important synthetic organoselenium compounds. *Chem. Rev. 101*, 2125–2179.
(15) Mishra, B., Priyadarsini, K. I., Mohan, H., and Mugesh, G. (2006) Horseradish peroxidase inhibition and antioxidant activity of ebselen and related organoselenium compounds. *Bioorg. Med. Chem. Lett. 16*, 5335–5338.
(16) Parnham, M. J., and Sies, H. (2000) Ebselen: Prospective therapy for cerebral ischemia. *Exp. Opin. Invest. Drugs 9*, 607–619.
(17) Back, T. G., and Moussa, Z. (2003) Diselenides and allyl selenides as glutathione peroxidase mimetics. Remarkable activity of cyclic seleninates produced in situ by the oxidation of allyl ω-hydroxyalkyl selenides. *J. Am. Chem. Soc. 125*, 13455–13460.
(18) Chwalek, M., Lalun, N., Bobichon, H., Plé, K., and Voutquenne-Nazabadioko, L. (2006) Structure-activity relationships of some hederagenin diglycosides: Haemolysis, cytotoxicity and apoptosis induction. *Biochim. Biophys. Acta 1760*, 1418–1427.
(19) El-Missiry, M. A., and Abou-Seif, M. (2000) Photosensitization induced reactive oxygen species and oxidative damage in human erythrocytes. *Cancer Lett. 158*, 155–163.
(20) Niki, E., Komuro, E., Takahashi, M., Urano, S., Ito, E., and Terao, K. (1988) Oxidative hemolysis of erythrocytes and its inhibition by free radical scavengers. *J. Biol. Chem. 263*, 19809–19814.
(21) Ali, I., Gatasheh, M. K. M., and Naseem, I. (2000) Hemolysis of human red blood cells by riboflavin-Cu(II) system. *Biochim. Biophys. Acta 1523*, 225–229.
(22) Vosters, O., and Nève, J. (2002) Inhibitory effects of thiol-containing drugs on erythrocyte oxidative damages investigated with an improved assay system. *Talanta 57*, 595–600.
(23) Deng, S.-L., Cheng, W.-F., Zhou, B., Yang, L., and Liu, Z.-L. (2006) Protective effect of curcumin and its analogues against free radical-induced oxidative haemolysis of human red blood cells. *Food Chem. 98*, 112–119.
(24) Niki, E. (1990) Free radical initiators as source of water or lipid soluble peroxyl radicals. *Methods Enzymol. 186*, 100–108.
(25) Arnold, A. P., Tan, K. S., and Rabenstein, D. L. (1986) Nuclear magnetic resonance studies of the solution chemistry of metal complexes. 23. Complexation of methylmercury by selenohydryl-containing amino acids and related molecules. *Inorg. Chem. 25*, 2433–2437.
(26) Kwak, C. S., Mun, K. C., and Suh, S. I. (2002) Production of oxygen free radicals and of hemolysis by cyclosporine. *Transplant. Proc. 34*, 2654–2655.
(27) Santosh Kumar, S., Shankar, B., and Sainis, K. B. (2004) Effect of chlorophyllin against oxidative stree in splenic lymphocytes in vitro and in vivo. *Biochim. Biophys. Acta 1672*, 100–111.
(28) Guha, S. N., Moorthy, P. N., Kishore, K., Naik, D. B., and Rao, K. N. (1987) One electron reduction of thionine studied by pulse radiolysis. *Proc. Indian Acad. Sci. (Chem. Sci.) 99*, 261–271.
(29) Fielden, E. M. (1984) Chemical dosimetry of pulsed electron and X-ray sources in the 1–20 MeV range. In *The Study of Fast Processes and Transient Species by Electron Pulse Radiolysis* (Baxendale, J. H., and Busi, F., Eds.), pp 49–62, D. Reidel, Dordrecht, The Netherlands,
(30) Alfassi, Z. B., Mosseri, S., and Neta, P. (1987) Halogenated alkyl peroxyl radicals as oxidants: Effects of solvent and of substituents on rates of electron transfer. *J. Phys. Chem. 91*, 3383–3385.
(31) Boyer, R. (2001) *Modern Experimental Biochemistry*. Pearson Education, Singapore.
(32) Mosmann, T. (1983) Rapid colorimetric assay for cellular growth and survival: application to proliferation and cytotoxicity assays. *J. Immunol. Methods 65*, 55–63.
(33) Here, although we consider this as measurement of GSH, it may correspond to total reduced thiols present in the RBCs; however, no attempt has been made to separately estimate GSH from other thiols.
(34) Alfassi, Z. B., and Schuler, R. H. (1985) Reaction of azide radicals with aromatic compounds. Azide as a selective oxidant. *J. Phys. Chem. 89*, 3359–3363.
(35) Mishra, B., Priyadarsini, K. I., and Mohan, H. (2006) Effect of pH on one electron oxidation of organoselenium compounds in aqueous solutions. *J. Phys. Chem. A 110*, 1894–1900.
(36) Müller, A. S., and Pallauf, J. (2003) Effect of increasing selenite concentrations, vitamin E supplementation and different fetal calf serum content on GPx1 activity in primary cultured rabbit hepatocytes. *J. Trace Elem. Med. Biol. 17*, 183–192.
(37) Zhong, W., and Oberley, T. D. (2001) Redox-mediated effects of selenium on apoptosis and cell cycle in the LNCaP human prostate cancer cell line. *Cancer Res. 61*, 7071–7078.
(38) Schöneich, C., Narayanaswami, V., Asmus, K. D., and Sies, H. (1990) Reactivity of ebselen and related selenoorganic compounds with 1,2-dichloroethane radical cations and halogenated peroxyl radicals. *Arch. Biochem. Biophys. 282*, 18–25.
(39) Vivancos, M., and Moreno, J. J. (2005) β-Sitosterol modulates antioxidant enzyme response in RAW 264.7 macrophages. *Free Radic. Biol. Med. 39*, 91–97.
(40) Asmus, K.-D., and Bonifačič, M. (1999) Sulfur Centered Reactive Intermediates as Studied by Radiation Chemical and Complementary Techniques. In *S-centered Radicals* (Alfassi, Z. B., Eds.), pp 142–145, John Wiley & Sons, New York.

TX700137A

Chemico-Biological Interactions 174 (2008) 134–139

Contents lists available at ScienceDirect

Chemico-Biological Interactions

journal homepage: www.elsevier.com/locate/chembioint

Concentration dependent antioxidant/pro-oxidant activity of curcumin Studies from AAPH induced hemolysis of RBCs

Arnab Banerjee[a], A. Kunwar[b], B. Mishra[b], K.I. Priyadarsini[b,*]

[a] Department of Biotechnology, Kumararani Meena Muthiah College of Arts and Science, Chennai 600020, India
[b] Radiation & Photochemistry Division, Bhabha Atomic Research Center, Trombay, Mumbai 400085, India

ARTICLE INFO

Article history:
Received 12 February 2008
Received in revised form 5 May 2008
Accepted 6 May 2008
Available online 15 May 2008

Keywords:
RBCs
Curcumin
Antioxidant
Pro-oxidant
Hemolysis
AAPH

ABSTRACT

The antioxidant properties of curcumin have been studied by evaluating its ability to protect RBCs from AAPH (2,2′-azobis (2-amidinopropane) hydrochloride) induced oxidative damage. RBCs are susceptible to oxidative damage, resulting in peroxidation of the membrane lipids, release of hemoglobin (hemolysis), release of intracellular K^+ ions and depletion of glutathione (GSH). In this paper, lipid peroxidation, hemolysis and K^+ ion loss in RBCs were assessed respectively by formation of thiobarbituric acid reactive substances (TBARS), absorbance of hemoglobin at 532 nm and flame photometry. The treatment of RBCs with curcumin showed concentration dependant decrease in level of TBARS and hemolysis. The IC_{50} values for inhibition of lipid peroxidation and hemolysis were estimated to be 23.2 ± 2.5 and 43 ± 5 μM respectively. However in contrast to the above mentioned effects, curcumin in similar concentration range, did not prevent release of intracellular K^+ ions during the process of hemolysis, rather curcumin induced its release even in the absence of hemolysis. The ability of curcumin to prevent oxidation of intracellular GSH due to hemolysis showed mixed results. At low concentrations of curcumin (<10 μM) it prevented GSH depletion and at higher concentrations, the GSH levels decreased gradually. Curcumin scavenges the peroxyl radical generated from AAPH. Based on these results, it is concluded that curcumin exhibits both antioxidant/pro-oxidant activity, in a concentration dependent manner.

1. Introduction

Aerobic organisms generate reactive oxygen species (ROS) such as hydroxyl radicals, superoxide, peroxyl radicals etc. during normal metabolism [1,2]. These ROS when produced in excess can cause harmful effects on living cells, resulting into irreparable damage to cellular macromolecules such as lipids, proteins, nucleic acids etc. [1,2]. Curcumin (diferuloylmethane), a dietary pigment responsible for the yellow color of turmeric, has been used in traditional medicine [3–5]. Extensive research within the past one decade has confirmed that curcumin possesses antioxidant activity and mediates anti-inflammatory effects [6–10]. Curcumin has been shown to inhibit lipid peroxidation, and effectively scavenge superoxide and peroxyl radicals [7]. It also shows anti-tumor activity, by suppressing the proliferation of a wide variety of tumor cells [3–5,11,12]. It has been known to upregulate several important antioxidant genes such as *HO*-1, *γ-GCS* within cells during oxidative stress [6,9,13,14]. In contrast to these studies some reports suggest that curcumin shows DNA damaging property and leads to induction of apoptosis in cells [15,16]. Curcumin-mediated apoptosis was closely related to the increase in intracellular ROS [8,17–19]. All these reports suggest that curcumin exhibits both antioxidant and pro-oxidant activities in different cells. Therefore in this present work, we have investigated the differential antioxidant/pro-oxidant behavior of curcumin by following

* Corresponding author. Fax: +91 22 25505151.
E-mail address: kindira@barc.gov.in (K.I. Priyadarsini).

0009-2797/$ – see front matter © 2008 Elsevier Ireland Ltd. All rights reserved.
doi:10.1016/j.cbi.2008.05.009

its ability to protect human RBCs from free radical induced damages. RBCs are enucleated cells, containing polyunsaturated fatty acids in their cell membrane [20]. The major protein component found within these RBCs is the red pigment hemoglobin (Hb) [20]. RBCs are fragile cells, and are highly susceptible to free radical induced damage of cell membrane (lipid peroxidation) leading to leakage of Hb (hemolysis) from within [20–23]. K^+ ions present within the cell, which maintains the osmotic balance, is prone to leakage following hemolysis [23,24]. Therefore, oxidative hemolysis of RBCs and its protection by compounds act as a good model system to screen the test compounds for their antioxidant/pro-oxidant behavior [20,23,25–27]. This model is simple to study and obtain easily accessible results [20]. Hemolysis, was initiated by the peroxyl radicals generated by thermal decomposition of an azo compound 2,2′-azobis(2-amidinopropane) hydrochloride (AAPH) in the presence of oxygen [20,28]. Since ROS can influence the reduced glutathione (GSH) concentration in cells, GSH levels were also monitored following hemolysis [22,23]. There are a few reports in literature on effect of curcumin on AAPH induced hemolysis of erythrocytes and LDL oxidation [29,30]. However in the present study, hemolysis is monitored by different markers like release of hemoglobin, lipid peroxidation, K^+ ion loss, change in GSH levels and finally the results correlated with the scavenging kinetics of AAPH peroxyl radicals by curcumin.

2. Materials and methods

Curcumin, dimethyl sulphoxide (DMSO), thiobarbituric acid (TBA), butylated hydroxy toluene (BHT), Tris base, 2,2′-azobis(2-amidinopropane) hydrochloride, 5,5′-dithiobis-2-nitrobenzoic acid (DTNB), ethylene diamine tetra acetic acid (EDTA) were of the best purity available and obtained from commercial sources. All the other chemicals were of analytical grade. Wherever required solutions were prepared in nano-pure water and autoclaved. Absorption spectra were recorded on Hitachi spectrophotometer (model U 2001).

2.1. Preparation of RBCs

Blood samples were obtained by venipuncture from healthy volunteers with strict adherence to the ethical guidelines laid down by the institutional animal ethics committee of Bhabha Atomic Research Centre. Blood was collected in heparinised tubes and centrifuged for 10 min at $1000 \times g$ and 4 °C using a cold centrifuge (Remi compufuge, CPR-24). Samples were washed three times with a phosphate buffered saline (PBS: NaCl 150 mM, KH_2PO_4 0.58 mM and Na_2HPO_4 3.4 mM, pH 7.4). Plasma and buffy coat were carefully removed by aspiration after each washing. RBCs were finally suspended in the buffer solution to obtain a hematocrit of approximately 50%, stored at 4 °C and were used within 6 h. All the experiments were carried out in triplicate and the results are presented as means ± S.E.M., $n = 3$.

2.2. Measurement of hemolysis

Hemolysis of RBCs was carried out by mixing 5% suspension of RBCs in PBS with AAPH solution (final concentration 50 mM). This reaction mixture was incubated for 3 h at 37 °C with gentle shaking. The extent of hemolysis was determined spectrophotometrically by measuring the absorbance of hemolysate at 540 nm as described previously [21]. For reference, RBCs were treated with distilled water and the absorbance of the hemolysate at 540 nm was used as 100% hemolysis. To test the effect of curcumin on hemolysis, RBCs were pre-incubated with varying concentration of curcumin at 37 °C for 30 min, washed twice with cold PBS and then subjected to hemolysis. This 30 min incubation time would ensure that curcumin is taken up by the RBCs.

2.3. Membrane lipid peroxidation

Lipid peroxidation was assessed by measuring the thiobarbituric acid (TBA) reactive substances (TBARS). For this 5% suspension of RBCs in PBS (pH 7.4) was incubated under air atmosphere with varying concentration of curcumin at 37 °C for 30 min, washed twice with cold PBS and then incubated into a PBS solution of AAPH (50 mM) to initiate membrane damage. After incubation at room temperature for 3 h, the system was centrifuged at $1500 \times g$ for 10 min and the pellet was resuspended in to 300 μl PBS (pH 7.4) to which 900 μl of TBA reagent (0.375% thiobarbituric acid, 0.25 M HCl, 15% trichloroacetic acid and 6 mM EDTA) was added and after further treatment, TBARS were estimated by measuring the absorbance at 535 nm [23] and expressed as per mg of hemoglobin.

The IC_{50} value i.e. the concentration of curcumin required to inhibit, hemolysis or lipid peroxidation by 50%, was determined by plotting the percent hemolysis, or TBARS levels respectively as a function of curcumin concentration, and from the plot, the concentration of curcumin required to reduce the activity by 50% was identified.

2.4. Measurement of K^+ ion loss

Pecked RBCs were suspended in 3 ml of 10 mM PBS, containing varying amount of curcumin to give 0.5% hematocrit. After 30 min of incubation at 37 °C and two washes with cold PBS, AAPH (50 mM) was added and this system was incubated at room temperature for 3 h. After centrifugation at $1500 \times g$ for 10 min, the concentration of K^+ ion was measured in the supernatant using flame photometry (Chemito AA 203, atomic absorption spectrophotometer with programmable flame control unit) [23]. For reference of 100% intracellular K^+ ion, a sample of RBCs was hemolysed in distilled water and the K^+ ion concentration was determined in the supernatant after centrifugation.

2.5. Glutathione estimation

The concentration of reduced glutathione in RBCs was determined using 5,5′-dithiobis-2-nitrobenzoic acid according to the reported method [22,23,31]. In a typical experiment, 5% suspension of RBCs in PBS (pH 7.4) was

subjected to hemolysis by treatment with AAPH for 3 h, in presence of different concentrations of curcumin. The hemolysate was precipitated using 10% TCA, centrifuged and the supernatant used for the estimation of free non protein bound reduced GSH and expressed as nmol DTNB per mg of hemoglobin.

2.6. Study of the reaction of curcumin with AAPH

The rate constant for the reaction of curcumin with AAPH was estimated by following the time dependent changes in the absorbance of curcumin at 435 nm in presence of AAPH and fitting the absorption–time plot to first order exponential function as given below:

$$A_t = A_o\, e^{-(k_{obs}t)} \quad (1)$$

here A_o and A_t represent the respective initial absorbance and absorbance at given time "t" at 435 nm. k_{obs} is the observed first order decay rate constant. This k_{obs} was estimated at four different curcumin concentrations (10–50 μM) and the average value of k_{obs} divided by curcumin concentration is considered as the bimolecular rate constant for the reaction of AAPH with curcumin.

3. Results

When AAPH is added as initiator, it decomposes at physiological temperature (37 °C) in aqueous solutions to generate alkyl radical (R′•), which in presence of oxygen is converted to the corresponding peroxyl radicals (R′OO•) Eqs. (2) and (3). At 37 °C in neutral water, the half-life of AAPH is about 175 h and generates radicals at a rate of 1.3×10^{-6} [AAPH]/s [28]. These peroxyl radicals induce oxidation of polyunsaturated lipids (LH) in RBC membranes causing a chain reaction known as lipid peroxidation Eqs. (4–6). As a result of this lipid peroxidation, the RBC membrane undergoes quick damage and losses its integrity, leading to the release of hemoglobin (hemolysis) and intracellular K^+ ions. When compounds like curcumin are present and if they can scavenge peroxyl radicals, and convert them to non-reactive species Eq. (7), the hemolysis can be inhibited.

$$R'\text{–}N{=}N\text{–}R' \rightarrow 2R'^{\bullet} + N_2 \quad (2)$$

$$R'^{\bullet} + O_2 \rightarrow R'OO^{\bullet} \quad (3)$$

$$R'OO^{\bullet} + LH \rightarrow R'OOH + L^{\bullet} \quad (4)$$

$$L^{\bullet} + O_2 \rightarrow LOO^{\bullet} \quad (5)$$

$$LH + LOO^{\bullet} \rightarrow L^{\bullet} + LOOH \quad (6)$$

$$\text{Curcumin} + LOO^{\bullet} \xrightarrow{H^+} \text{Curcumin radical} + LOOH \quad (7)$$

where R′ is $-C(Me)_2-C(NH_2){=}NH_2^+$

3.1. Inhibition of AAPH induced hemolysis in human RBCs by curcumin

In the absence of AAPH, RBCs were stable and the hemolysis was negligible. When aqueous suspension of RBCs was incubated with AAPH, about 53% of hemolysis was observed. Fig. 1(a) shows variation in percent hemolysis in RBCs pre-incubated with increasing concentrations of curcumin (5–50 μM) for 30 min and subjected to hemolysis. It is evident from Fig. 1(a) that the percent hemolysis gradually decreased with increasing concentration of curcumin, from which the IC_{50} value, was found to be 43 ± 5 μM. Fig. 1(b) shows variation in percent hemolysis in RBCs incubated simultaneously with increasing concentrations of curcumin (5–50 μM) and AAPH. It is evident from Fig. 1(b) that the percent hemolysis progressively decreased with increasing concentration of curcumin, from which the IC_{50} value was found to be 8 ± 0.6 μM. The percent hemolysis in RBCs incubated with curcumin (5–50 μM) in the absence of AAPH was almost identical to that of control sample indicating curcumin itself could not induce hemolysis.

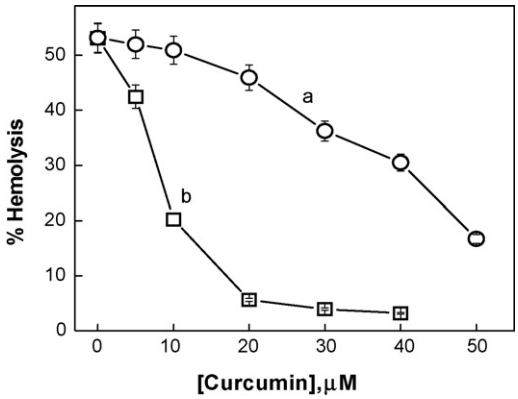

Fig. 1. (a) Variation in percent hemolysis in human RBCs pre-incubated with different concentrations of curcumin and then subjected to hemolysis by 50 mM AAPH for 3 h. (b) Variation in percent hemolysis in human RBCs incubated simultaneously with 50 mM AAPH and different concentrations of curcumin for 3 h. Results are presented as means ± S.E.M., $n = 3$.

3.2. Inhibition of AAPH induced lipid peroxidation in human RBCs by curcumin

Fig. 2 shows variation in TBARS in RBCs after subjecting to AAPH induced damage in the presence and absence of different concentrations of curcumin. The level of TBARS

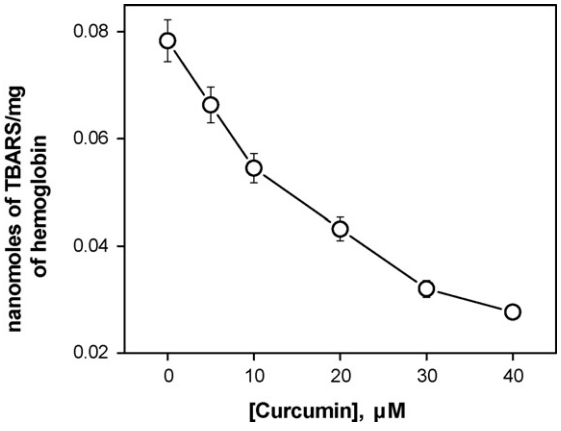

Fig. 2. Variation in TBARS estimated for lipid peroxidation in human RBCs induced by 50 mM AAPH after incubation for 3 h at different concentrations of curcumin. Results are presented as means ± S.E.M., $n = 3$.

was significantly increased after incubation of RBCs with AAPH as compared to the control sample. In the presence of curcumin, there was gradual decrease in TBARS formation and this inhibition increased with increasing curcumin concentration from 5 to 40 μM, from which the IC_{50} value was found to be 23.2 ± 2.5 μM. The incubation of RBCs with curcumin in the absence of AAPH did not show any significant change in the level of TBARS as compared to control sample.

3.3. Inhibition of AAPH induced K^+ ion leakage in human RBCs by curcumin

In the absence of AAPH, the RBCs were stable and the K^+ ion leakage was negligible. When aqueous suspension of RBCs was incubated with AAPH, about 79% of K^+ ion leakage was observed. Fig. 3 shows the variation in percent K^+ ion leakage from RBCs pre-incubated with increasing concentrations of curcumin (5–40 μM) for 30 min and subjected to hemolysis. It is evident from Fig. 3 that the percent K^+ ion leakage is lower in curcumin pretreated samples compared to the control sample. However in each case, the K^+ ion leakage increased with increasing concentration of curcumin. Inset of Fig. 3 shows variation in percent K^+ ion loss in RBCs after incubation with different concentrations of curcumin (5–100 μM) for 3 h in the absence of AAPH. From the figure it is clear that the percent K^+ ion loss is significantly higher in curcumin treated samples as compared to control sample. The percent K^+ ion loss was almost identical (nearly 47%) at all the concentrations of curcumin (5–100 μM) tested in present study.

3.4. Effect of curcumin on GSH levels in RBCs after hemolysis

Fig. 4 shows change in GSH level in RBCs after treatment with AAPH and also in presence of increasing concentration of curcumin (5–40 μM). The normal basal level of GSH in RBCs was found to be 2.74 ± 0.05 nmol/mg of hemoglobin

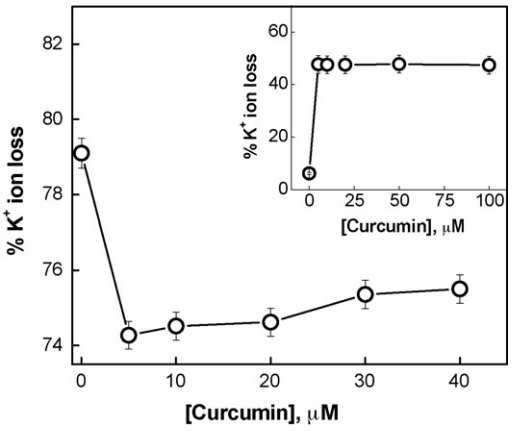

Fig. 3. Variation in K^+ ion loss estimated by flame photometry in human RBCs incubated with 50 mM AAPH for 3 h in presence of different concentrations of curcumin. Inset shows variation in K^+ ion loss in human RBCs incubated with different concentrations of curcumin without any added AAPH. Results are presented as means ± S.E.M., $n = 3$.

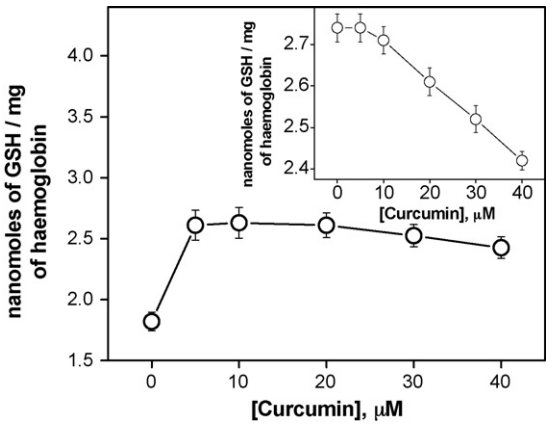

Fig. 4. Variation in glutathione (GSH) levels in human RBCs incubated with 50 mM AAPH for 3 h in presence of different concentrations of curcumin. Inset shows variation in glutathione levels in human RBCs incubated with different concentrations of curcumin without any added AAPH. Results are presented as means ± S.E.M., $n = 3$.

and after incubation with AAPH, the GSH level reduced to about 1.82 ± 0.03 nmol/mg of hemoglobin. Addition of curcumin to this reaction system prevented the reduction in GSH content in a concentration dependant manner up to 10 μM. However at higher concentrations of curcumin treatment, GSH content reduced in a concentration dependant manner. Inset of Fig. 3 shows variation in GSH level in RBCs after incubation with different concentrations of curcumin (5–40 μM) for 3 h in the absence of AAPH. From the figure it is clear that the level of GSH in curcumin treated RBCs was almost constant up to treatment concentration of 10 μM, however beyond that a concentration dependant decrease in level of GSH was observed.

3.5. Reaction of curcumin with AAPH peroxyl radicals

Curcumin exhibits a broad absorption spectrum in PBS solution containing 1% DMSO with maximum absorption at ~435 nm, while that of 50 mM AAPH at pH 7 showed absorption maximum at 350 nm, with no absorption at wavelength >400 nm (Fig. 5a and b). On incubating with AAPH, for 30 min the absorption spectrum of curcumin changed significantly and the absorbance due to curcumin decreased completely. Fig. 5c and d, show spectra recorded at two different times 5 and 30 min after incubation with AAPH. Curcumin itself undergoes degradation in aqueous medium and the absorbance decays with the half-life of 96.7 min (Fig. 5e). The decay of curcumin becomes faster in the presence of AAPH with the half-life of 4.5 min. The absorption–time plot (Fig. 5f) shows the decay of the parent curcumin (30 μM) absorption at 435 nm after mixing with AAPH. As seen in the Fig. 5 this is much faster than the self decay of curcumin, therefore the self decay of curcumin can be ignored under these conditions. The rate constant for the reaction between curcumin and AAPH was calculated by following the decay of curcumin at different concentration (10–50 μM) in presence of AAPH. The k_{obs} was obtained by fitting the decay trace to a first order exponential function (Eq. (1)), at a given concentration of curcumin and from which the bimolecular rate constant for the reaction (8) was

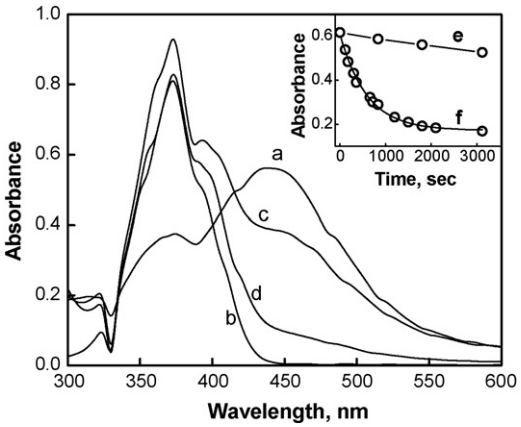

Fig. 5. Absorption spectra of (a) 25 μM curcumin, (b) 50 mM AAPH in PBS buffer containing 1% DMSO. (c) and (d) correspond to the spectra obtained on mixing 25 μM curcumin with 50 mM AAPH after 5 and 30 min respectively. Inset shows the change in absorbance of 30 μM curcumin at 435 nm as a function of time in (e) the absence and (f) in presence of 50 mM AAPH at pH 7.

estimated to be $63.4 \pm 12.7\ M^{-1}\ s^{-1}$. Due to slow rate limiting decomposition of AAPH this value may not be a true representation of the rate constant for the overall reaction (8) but it certainly confirms direct reaction of AAPH radicals with curcumin.

$$\text{AAPH} \rightarrow [\text{Peroxylradical}] + \text{Curcumin} \rightarrow \text{Product} \qquad (8)$$

Earlier using pulse radiolysis technique, it has been reported that curcumin reacts with trichloromethyl peroxyl radical and lineolic peroxyl radical with rate constant of 5×10^8 and $5.3 \times 10^5\ M^{-1}\ s^{-1}$ respectively [7]. The low apparent rate constant with AAPH is mainly due to slow rate limiting release ($1.3 \times 10^{-6}\ s^{-1}$) of peroxyl radicals from AAPH decomposition [28].

4. Discussion

Hemolysis of human RBCs is a very good model for studying free radical induced oxidative damage to membranes and to evaluate the antioxidant activity of new compounds [20,23,25–27]. Therefore to evaluate the antioxidant activity of curcumin, lipid peroxidation of the membrane fatty acids, loss of hemoglobin and release of intracellular K^+ ions have been estimated in human RBCs treated with AAPH [20,28]. The results obtained from these studies indicate that curcumin by itself did not cause either lipid peroxidation or hemolysis to RBCs, and showed significant protection from AAPH induced lipid peroxidation and hemolysis. Curcumin has also been shown to react with the peroxyl radicals generated from AAPH. Thus the overall effect of curcumin on AAPH induced protection of RBCs may be either due to direct chemical neutralization of peroxyl radicals generated from AAPH or its cellular uptake. To find out more about these possibilities hemolysis experiments were carried out in two different conditions. In the first condition, the RBCs were incubated with curcumin for 30 min prior to AAPH addition and in the second condition the RBCs were treated with curcumin and AAPH simultaneously. The IC_{50} values estimated for these two systems indicated higher value for the former compared to the latter. The results suggest that when RBCs are preincubated with curcumin for 30 min, majority of curcumin may have been taken up by the RBCs, leaving very minute amounts of curcumin in the extra-cellular aqueous medium to be scavenged by the peroxyl radicals and therefore elevating the IC_{50} value. However when RBCs were treated with curcumin and AAPH simultaneously more curcumin is available to be scavenged by the peroxyl radicals, resulting in low IC_{50} value. Therefore in all the further experiments we followed the incubation of RBCs with curcumin prior to AAPH treatment in order to avoid direct chemical neutralization of peroxyl radicals by curcumin generated from AAPH.

Like in lipid peroxidation and hemolysis assays, curcumin did not show progressive inhibition of K^+ ion loss and reduced GSH depletion under AAPH treated condition thus making us unable to estimate their IC_{50} values. Curcumin treated samples showed lower percent of K^+ ion loss as compared to AAPH treated samples. However in each case, the percent K^+ ion loss increased with increasing concentrations of curcumin. Therefore to know whether curcumin itself has any effect on K^+ ion loss, we looked at the loss of K^+ ion in only curcumin treated samples. The results clearly suggest that curcumin at concentration as low as 5 μM drastically increased the loss of K^+ ions (47%) from RBCs. With the increasing curcumin concentration, the percent of K^+ ion loss remained almost the same suggesting the saturation effect of curcumin on K^+ ion loss. The ability of curcumin to induce K^+ ion loss may be because of its effect on Na^+/K^+ ion channels present on RBC membranes. This indicates that curcumin may not be acting as a simple antioxidant but probably has a pro-oxidant effect.

GSH is the most abundant thiols present in mammalian cells [22,23,32]. It performs a number of vital cell functions including maintaining the essential thiol status of proteins by preventing oxidation of sulfahydryl groups or by reducing disulphide bonds induced by oxidative stress, or by scavenging free radicals. During oxidative stress, the cellular pool of GSH is depleted. Exogenously applied antioxidants protect GSH levels in cells by preventing them from being consumed in reaction with free radicals [33]. Our results indicate that the GSH levels come down significantly in RBCs after AAPH incubation, but treatment with curcumin in the concentration range from 5 to 10 μM significantly prevents the decrease in GSH level. However further increase in concentration of curcumin showed decrease in GSH level in a concentration dependant manner. Curcumin treatment alone without AAPH did not show much effect on GSH level in the concentration range up to 10 μM, and further increase up to 40 μM resulted in significant decrease of GSH level, probably due to the direct reaction of curcumin with GSH [34]. Some reports suggest that curcumin reacts with ROS and generates less reactive phenoxyl radical Eq. (7) [7,33]. Therefore the observed decrease in GSH level in curcumin (>10 μM) pretreated samples after exposure to AAPH could also be due to the excess accumulation of phenoxyl radicals and thereby oxidation of cellular GSH to GSSG [33]. Hence this observation indicates that curcumin at higher concentrations (>10 μM) shows pro-oxidant behavior.

Earlier Deng et al. have also shown the protection of RBCs from oxidative hemolysis by curcumin [26]. In this study the authors looked at the inhibition of hemoglobin leakage by curcumin and thus explained the antioxidant activity of curcumin, which is in agreement with our results. In present study, apart from hemoglobin leakage several other sensitive parameters associated with oxidative hemolysis such as K^+ ion leakage and glutathione depletion have been taken in to care therefore making us enable to identify the dual activity of antioxidant and pro-oxidant associated with curcumin. In this respect, it is worth mentioning that most of the in vivo studies dealing with curcumin as an anti-tumor agent discuss about its poor bioavailability as low blood levels are achieved after excessive oral administration (8 g/day) [5]. Our results compliment these studies and suggest that at low blood levels, curcumin shows antioxidant activity on RBCs, which is desired along with its anti-tumor activity. In conclusion curcumin shows both antioxidant and pro-oxidant activity in RBCs hemolysis model and at high curcumin concentration, it is the later one, which predominates over the former.

References

[1] B. Halliwell, J.M.C. Gutteridge, Free Radicals in Biology and Medicine, Oxford University Press, New York, 1999.
[2] R. Stocker, B. Frei, Endogenous Antioxidant Defenses in Human Blood Plasma. Oxidative Stress: Oxidants and Antioxidants, Academic Press, London, 1991.
[3] S. Shishodia, G. Sethi, B.B. Aggarwal, Curcumin: getting back to the roots, Ann. N.Y. Acad. Sci. 1056 (2005) 206–217.
[4] B.B. Aggarwal, C. Sundaram, N. Malani, H. Ichikawa, Curcumin: The Indian Solid Gold. The Molecular Targets and Therapeutic Uses of Curcumin in Health and Disease, Springer, NY, USA, 2007.
[5] R.A. Sharma, A.J. Gescher, W.P. Steward, Curcumin: the story so far, Eur. J. Cancer 41 (2005) 1955–1968.
[6] I. Rahman, S.K. Biswas, P.A. Kirkham, Regulation of inflation and redox signaling by dietary polyphenol, Biochem. Pharmacol. 72 (2006) 1439–1452.
[7] K.I. Priyadarsini, Free radical reactions of curcumin in model membranes, Free Radical Biol. Med. 23 (1997) 838–844.
[8] E.M. Strasser, B. Wessner, N. Manhart, E. Roth, The relationship between the anti-inflammatory effects of curcumin and cellular glutathione content in myelomonocytic cells, Biochem. Pharmacol. 70 (2005) 552–559.
[9] R. Motterlini, R. Foresti, R. Bassi, C.J. Green, Curcumin, an antioxidant and anti-inflammatory agent, induces heme oxygenase-1 and protects endothelial cells against oxidative stress, Free Radical Biol. Med. 28 (2000) 1303–1312.
[10] S.K. Sandur, H. Ichikawa, M.K. Pandey, A.B. Kunnumakkara, B. Sung, G. Sethi, B.B. Aggrawal, Role of pro-oxidants and antioxidants in the anti-inflammatory and apoptotic effects of curcumin (diferuloylmethane), Free Radical Biol. Med. 43 (2007) 568–580.
[11] B.B. Agarwal, A. Kumar, A.C. Bharti, Anticancer potential of curcumin: preclinical and clinical studies, Anticancer Res. 23 (2003) 363–398.
[12] M.L. Kuo, T.S. Huang, J.K. Lin, Curcumin an antioxidant and anti-tumor promoter, induces apoptosis in human leukemia cells, Biochim. Biophys. Acta 1317 (1996) 95–100.
[13] E. Balogun, M. Hoque, P. Gong, E. Killeen, C.J. Green, R. Foresti, J. Alam, R. Motterlini, Curcumin activates the haem oxygenase-1 gene via regulation of Nrf2 and the antioxidant-responsive element, Biochem. J. 371 (2003) 887–895.
[14] S.W. Rushworth, R.M. Ogborne, C.A. Charalambos, M.A. O'Connell, Role of PKC δ in curcumin-induced antioxidant response element-mediated gene expression in human monocytes, Biochem. Biophys. Res. Commun. 341 (2006) 1007–1016.
[15] M. Yoshino, M. Haneda, M. Naruse, H.H. Htay, R. Tsubouchi, Q. Shanlou, L. WeiHua, K. Murakami, T. Yokochi, Prooxidant activity of curcumin: copper-dependent formation of 8-hydroxy-2′-deoxyguanosine in DNA and induction of apoptotic cell death, Toxicol. in Vitro 18 (2004) 783–789.
[16] H. Ahsan, N. Parveen, N.U. Khan, S.M. Hadi, Pro-oxidant, antioxidant and cleavage activities on DNA of curcumin and its derivatives demethoxycurcumin and bisdemethoxycurcumin, Chem. Biol. Interact. 121 (1999) 161–175.
[17] S. Bhaumik, R. Anjum, N. Rangaraj, B.V. Pardhasaradhi, A. Khar, Curcumin mediated apoptosis in AK-5 tumor cells involves the production of reactive oxygen intermediates, FEBS Lett. 456 (1999) 311–314.
[18] J. Chen, D. Wanming, D. Zhang, Q. Liu, J. Kang, Water soluble antioxidants improve the antioxidant and anticancer activity of low concentrations of curcumin in human leukaemia cells, Pharmazie 60 (2005) 57–61.
[19] J. Fang, J. Lu, A. Holmgren, Thioredoxin reductase is irreversibly modified by curcumin: a novel molecular mechanism for its anticancer activity, J. Biol. Chem. 280 (2005) 25284–25290.
[20] E. Niki, E. Komuro, M. Takahashi, S. Urano, E. Ito, K. Terao, Oxidative hemolysis of erythrocytes and its inhibition by free radical scavengers, J. Biol. Chem. 263 (1988) 19809–19814.
[21] C.S. Kwak, K.C. Mun, S.I. Suh, Production of oxygen free radicals and of hemolysis by cyclosporine, Transplant. Proc. 34 (2002) 2654–2655.
[22] M.A. El-Missiry, M. Abou-Seif, Photosensitization induced reactive oxygen species and oxidative damage in human erythrocytes, Cancer Lett. 158 (2000) 155–163.
[23] A. Kunwar, B. Mishra, A. Barik, L.B. Kumbhare, R. Pandey, V.K. Jain, K.I. Priyadarsini, 3,3′-Diselenodipropionic acid, an efficient peroxyl radical scavenger and a GPx mimic, protects erythrocytes (RBCs) from AAPH-induced hemolysis, Chem. Res. Toxicol. 20 (2007) 1482–1487.
[24] I. Ali, M.K.M. Gatasheh, I. Naseem, Hemolysis of human red blood cells by riboflavin-Cu(II) system, Biochim. Biophys. Acta 1523 (2000) 225–229.
[25] O. Vosters, J. Nève, Inhibitory effects of thiol-containing drugs on erythrocyte oxidative damages investigated with an improved assay system, Talanta 57 (2002) 595–600.
[26] S.-L. Deng, W.-F. Cheng, B. Zhou, L. Yang, Z.-L. Liu, Protective effect of curcumin and its analogues against free radical –induced oxidative haemolysis of human red blood cells, Food Chem. 98 (2006) 112–119.
[27] M. Chwalek, N. Lalun, H. Bobichon, K. Plé, L. Voutquenne-Nazabadioko, Structure–activity relationships of some hederagenin diglycosides: haemolysis, cytotoxicity and apoptosis induction, Biochim. Biophys. Acta 1760 (2006) 1418–1427.
[28] E. Niki, Free radical initiators as source of water or lipid soluble peroxyl radicals, Methods Enzymol. 186 (1990) 100–108.
[29] P. Somparn, C. Phisalaphong, S. Nakornchai, S. Unchern, N.P. Morales, Comparative antioxidant activities of curcumin and its demethoxy and hydrogenated derivatives, Biol. Pharm. Bull. 30 (2007) 74–78.
[30] W.-C Chen, S.-L. Deng, B. Zhou, L. Yang, Z.-L. Liu, Curcumin and its analogues as potent inhibitors of low density lipoproteins oxidation: H-atom abstraction from the phenolic groups and possible involvement of the 4-hydroxy-3-methoxyl phenyl groups, Free Radical Biol. Med. 40 (2006) 526–535.
[31] E. Beutler (Ed.), Red Cell Metabolism. A Manual of Biochemical Methods, vol. 89, Grune & Stratton, New York, 1982, pp. 137–140.
[32] M. Vivancos, J.J. Moreno, β–Sitosterol modulates antioxidant enzyme response in RAW 264.7 macrophages, Free Radical Biol. Med. 39 (2005) 91–97.
[33] G. Galati, O. Sabzevari, J.X. Wilson, P.J. O'Brien, Prooxidant activity and cellular effects of the phenoxyl radicals of dietary flavonoids and other polyphenolics, Toxicology 177 (2002) 91–104.
[34] S. Awasthi, U. Pandya, S.S. Singhal, J.T. Lin, V. Thiviyanathan, W.E. Seifert Jr., Y.C. Awasthi, G.A. Ansari, Curcumin-glutathione interactions and the role of human glutathione S-transferase P1-1, Chem. Biol. Interact. 128 (2000) 19–38.

Available online at www.sciencedirect.com
ScienceDirect
Biochimica et Biophysica Acta 1780 (2008) 673–679
Biochimica et Biophysica Acta
BBA
www.elsevier.com/locate/bbagen

Quantitative cellular uptake, localization and cytotoxicity of curcumin in normal and tumor cells

A. Kunwar [a], A. Barik [a], B. Mishra [a], K. Rathinasamy [b], R. Pandey [c], K.I. Priyadarsini [a,*]

[a] *Radiation and Photochemistry Division, Bhabha Atomic Research Centre, Trombay, Mumbai, 400 085, India*
[b] *School of Biosciences and Bioengineering, IIT-Bombay, Mumbai, 400 076, India*
[c] *Radiation Biology and Health Sciences Division, Bhabha Atomic Research Centre, Trombay, Mumbai, 400 085, India*

Received 27 June 2007; received in revised form 16 November 2007; accepted 29 November 2007
Available online 15 December 2007

Abstract

Using absorption and fluorescence spectroscopic methods, quantitative cellular uptake of curcumin, an antioxidant and anti-tumor agent from *Curcuma longa*, was calculated in two types of normal cells: spleen lymphocytes, and NIH3T3 and two tumor cell lines: EL4 and MCF7. Both the uptake and fluorescence intensity of curcumin were significantly higher in tumor cells compared to the normal cells. A linear dependency on the uptake was observed with treatment concentration of curcumin. Using laser confocal microscopy, intracellular localization of curcumin was monitored and the results indicated that curcumin is located both in the cell membrane and the nucleus. Sub-cellular fractionation of curcumin-loaded MCF7 cells supported the differential distribution of curcumin in membrane, cytoplasm and nuclear compartments of cell with maximum localization in the membrane. Cytotoxicity studies in different cell lines indicated that the toxicity of curcumin increased with increasing uptake.

Keywords: Curcumin; Cellular uptake; Tumor cell; Nuclear localization; Fluorescence; Cytotoxicity

1. Introduction

Curcumin (1,7-bis(4-hydroxy 3-methoxy phenyl)-1,6-heptadiene-3, 5-dione) is a polyphenolic pigment isolated from the rhizomes of *Curcuma longa* (turmeric), a medicinal plant widely used in the ancient Indian and Chinese medicine [1,2]. Traditionally it has been in the practice for the treatment of common cold, skin diseases, wound healing, inflammation etc. [1,2]. Recent scientific research has confirmed that curcumin possesses antioxidant, anti-inflammatory, antibacterial, anti-amyloid properties and suppresses proliferation of a wide variety of tumor cells [3–6]. At present, there are several ongoing clinical trials for the treatment of different types of cancers like pancreatic cancer, multiple myeloma and colorectal cancer. The remarkable pharmacological activity of curcumin is attributed to its ability to act on multiple intracellular targets and effectively scavenge reactive oxygen species [7,8]. Pharmacologically curcumin has been found to be safe even at doses of 8g/day [4].

In spite of great advancement on the therapeutic research of curcumin, there are still very few studies reporting the methodologies to quantitatively estimate intracellular curcumin uptake and localization. Recently we developed a method to estimate curcumin in cells by following absorption and fluorescence spectroscopy under different treatment concentrations of curcumin, delivery vehicles like liposomes, albumins etc. [9]. In the present study, we extended cellular uptake measurements in four different cell types, such as two normal cells, *viz.*, mouse spleen lymphocytes, NIH3T3 (mouse fibroblast cells), and two tumor cell lines, *viz.*, EL4 (T cell lymphoma of murine origin) and MCF7 (breast cancer cells of human origin). Mouse spleen lymphocytes and EL4 cells grow in suspension and are of lymphoid origin, while NIH3T3 and MCF7 are adherent cell lines [10]. Following absorption spectrum of curcumin in the cell lysate and the fluorescence spectra of cellular curcumin, quantitative uptake was calculated and from fluorescence spectral maxima, attempts have been made to understand the interaction of curcumin with different types of cells. Further,

* Corresponding author. Fax: +91 22 25505151.
E-mail address: kindira@barc.gov.in (K.I. Priyadarsini).

0304-4165/$ - see front matter © 2007 Elsevier B.V. All rights reserved.
doi:10.1016/j.bbagen.2007.11.016

monitoring curcumin fluorescence by confocal microscopy and by sub-cellular fractionation, an attempt has been made to understand its intracellular localization. Finally the cytotoxicity of curcumin in the cell lines was determined and compared with the uptake.

2. Materials and methods

2.1. Chemicals and equipments

Curcumin (CI 7500), 4′6-diamidino-2-phenylindol (DAPI), cell culture medium (RPMI 1640 and DMEM) from Sigma/Aldrich, USA, cell proliferation kit from Roche Biochem, Germany, and HPLC grade DMSO from Spectro Chem. India were procured from the local agents. The purity of curcumin was confirmed by TLC and HPLC. Mouse spleen lymphocytes were freshly isolated as given in Ref. [9], and EL4, MCF7, and NIH3T3 cell lines were obtained from National Centre for Cell Science (NCCS), India. Absorption spectra were recorded on a JASCO V-530 spectrophotometer and fluorescence spectra were recorded on a Hitachi F-4010 fluorimeter. Solutions were prepared in nanopure water from a Millipore Milli-Q system.

2.2. Cell culture and uptake studies

EL4 cell line in suspension with RPMI medium, MCF7 cell line as adherent in DMEM medium, NIH3T3 cell line as adherent in RPMI medium and freshly isolated spleen lymphocytes as suspension in RPMI medium were cultured and supplemented with 10% fetal bovine serum. 10 mM stock solutions of curcumin were prepared in DMSO and diluted with the culture medium to get the desired concentration. The concentration of DMSO varied from 0.1 to 0.8%, to achieve different curcumin concentrations ranging from 10 to 80 nmol/ml, and was within the permissible limits of toxicity (<1%) [11]. For loading of curcumin, the cells ($\sim 1\times10^6$ cells/ml) were incubated with curcumin (at a concentration of 10 or 20 nmol/ml) for 4 h, spinned down at 1000 rpm in Beckman centrifuge for 5 min and washed thrice with cold phosphate buffered saline (PBS). The cells were re-suspended in to 1 ml of PBS and subjected to fluorescence spectral studies [9]. For the estimation of cellular uptake, after spinning down the curcumin-loaded cells, the pellet was dried and suspended in to 1 ml of methanol and sonicated till curcumin is completely extracted into the methanol fraction. The lysate was centrifuged at 10,000 rpm for 5 min, absorption spectra of supernatant containing methanolic curcumin were recorded and from the absorbance at 428 nm and extinction coefficient of 48,000 M^{-1} cm^{-1}, the total cellular uptake was estimated [9]. Treatment at each concentration was done in triplicate and the estimated uptake at each concentration was normalised to 1 nmol/ml of curcumin treatment. The uptake values represented in Table 1, as pmol/million cells, are the average of six different normalised estimations at two different treatment concentration of curcumin (10 and 20 nmol/ml). Vehicle control was kept for each cell line.

2.3. Confocal microscopy and image analysis

Slides for confocal microscopy of lymphocytes and EL4 cells were prepared by fixing curcumin-loaded cells in 1% paraformaldehyde (PFA) in PBS for 15 min at 4 °C. 50 μl of cell suspension in PBS was spread on to confocal slide using cytocentrifuge, air dried and sealed with cover slip using mounting medium. For MCF7 and NIH3T3 cells, similar procedure was adopted except that these cells were first adhered to sterile coverslip and then processed for fixation. Fluorescence imaging of cells was performed with an Olympus Fluoview 500 confocal laser-scanning microscope (Olympus, Tokyo, Japan) equipped with a multi-Argon laser for excitation at 458, 488 and 515 nm [12]. The images of cells were acquired in the emission mode either with a 20× or a 60× water immersion objective after exciting the sample at 458 nm using barrier filter. Although, the absorption maximum of curcumin is at ~ 420 nm, at 458 nm, it has considerable absorption (45 to 70% of the maximum absorption in different cells). DAPI stained cells were excited using Coherent Mira 900F Titanium: Saphire infrared laser (Coherent Verdi-V5, Santa Clara, CA, USA) tuned to 720 nm and the fluorescence in the wavelength range of 400–470 nm was collected. This two-photon imaging avoids the photobleaching that could happen due to UV laser. At least five monochrome images were accumulated from five different microscopic fields of the same slide. The desired region on each fluorescent cell was selected and the mean fluorescence intensity/area for the region was determined using the Fluoview software and the average values of 15 different regions are presented in Table 1. To quantify the co-localization of fluorescent probes (curcumin and DAPI), images acquired separately for each of the probe were merged using the software.

2.4. Sub-cellular fractionation

MCF7 cells ($\sim 2\times10^6$ cells) were incubated with curcumin (at a concentration of 20 nmol/ml) for 4 h. Following treatment, the sub-cellular fractionation was performed using differential centrifugation protocol described earlier [13] with certain modifications. In brief the treated cells were suspended in to 0.5 ml of hypotonic lysis buffer, allowed to swell on ice for 15 min, and then Nonidet P-40 (0.6%) was added. The sample was homogenised and subjected to varying centrifugal speed of 2000×g for 10 min, 10,000×g for 15 min and 100,000×g for 45 min respectively to collect the nuclear, mitochondrial and membrane fractions in the form of pellets and the cytosolic fraction as supernatant. All the pellet fractions were washed thrice with cold PBS, air dried, suspended in to 0.5 ml of methanol and sonicated to extract the curcumin completely in methanol. The cytosolic fraction was vacuum dried and suspended in to 0.5 ml of methanol. Absorption spectra of methanolic curcumin from all the fractions were recorded as described above.

2.5. Cytotoxicity studies

The cytotoxic activity of curcumin in different cell lines and spleen cells was assessed by the MTT (3-[4,5-dimethylthiazole-2-yl]-2,5-diphenyl tetrazolium bromide) dye conversion assay [14]. Briefly, 5×10^4 cells were cultured in 100 μl volume of tissue culture medium in a 96 well plate in the absence and presence of different concentrations of curcumin and after 24 h, the cells were washed once and further incubated for 4 h with MTT dye. The blue formazan precipitate obtained was dissolved using solubilization buffer, kept overnight at 37 °C and the absorbance at 550 nm was measured using a scanning plate reader (Bio-Tek Instruments, USA). The results were expressed as the mean absorbance±SEM for four replicates.

Table 1
Cellular uptake, fluorescence spectral properties, and intensity variations of curcumin in different cells

Cell lines	λ_{fl}, nm (λ_{ex}=420 nm)	Average normalised cellular uptake (pmol/10^6 cells)	Fl. intensity/pmol of curcumin uptake (λ_{ex}=420 nm)	Confocal imaging data Fl. intensity/area of cell (λ_{ex}=458 nm)		
				Control	Treated	Difference
Spleen lymphocytes	504	23.2±4.3	0.023±0.004	69±12	125±35	56±35
EL4	500	34.5±6.4[a, b]	0.064±0.01[a, b]	106±8	212±23	106±23[a, b]
NIH3T3	535	22.6±6.8	0.007±0.002	220±27	259±60	39±5
MCF7	520	44.2±7.2[a, b]	0.067±0.01[a, b]	208±66	382±91	174±91[a, b]

[a] Significant against spleen lymphocytes at $P<0.05$.
[b] Significant against NIH3T3 cell line at $P<0.05$.

2.6. Statistical analysis

The statistical analysis between different groups for significance was done using Student's t test. A value of $P<0.05$ was considered as statistically significant.

3. Results

3.1. Uptake measurements

Fig. 1 shows representative absorption spectra (a–e) of methanolic curcumin extracted from MCF7 cells, after treatment with different concentrations (5 to 80 nmol/ml) of curcumin and the inset shows linear plot for the variation of cellular uptake as a function of curcumin treatment concentration. Similarly cellular uptake of curcumin by the two other cell lines (EL4, and NIH3T3) and spleen lymphocytes were calculated at different curcumin treatment concentrations of 10 and 20 nmol/ml (figure not shown). The results indicated that the uptake increased with increasing concentration of curcumin treatment in all the different cells and nearly doubled when treatment concentration was doubled. After normalization, cellular uptake was calculated and the average values are listed in Table 1. It can be seen that the tumor cells (EL4 and MCF7) showed significantly higher uptake as compared to normal cells (NIH3T3 and lymphocytes).

3.2. Fluorescence spectroscopic studies of intracellular curcumin

In the earlier studies it has been shown that curcumin exhibits weak fluorescence with featureless and broad maximum ~550 nm in aqueous methanol solution, however in presence of phosphatidylcholine (PC) liposome or human serum albumin (HSA) protein its fluorescence intensity is significantly enhanced along with large blue shift in the fluorescence maximum with their respective values at 498 nm and 515 nm for liposomes and HSA protein [9]. Representative fluorescence spectra of curcumin in PC liposomes and HSA protein are given in the inset (a and b) of Fig. 2. The fluorescence maxima and intensity changes suggest that the fluorescence of curcumin is sensitive to the specific hydrophobic environments in the lipids and proteins. Since living cells are rich, and also differ in lipid and protein content, change in fluorescence spectral behaviour of curcumin is expected upon interaction with living cells. In order to explore these possibilities, the four different kinds of cells; spleen lymphocytes, EL4, NIH3T3 and MCF7 were loaded with curcumin and subjected to steady state fluorescence measurement.

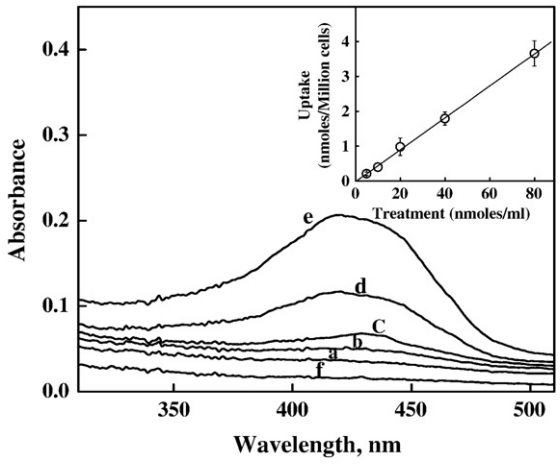

Fig. 1. Absorption spectra (a–e) of curcumin extracted in to 1 ml of methanol from MCF7 cells (2×10^6) after treatment with curcumin (at a concentration of 5 to 80 nmol/ml in aqueous-DMSO) for 4 h. Spectrum (f) represents the control MCF7 cells (2×10^6) treated with aqueous-DMSO without any curcumin. Inset shows variation in the total cellular uptake (without normalization with curcumin treatment) as a function of curcumin treatment. Results are presented as means±SEM, $n=3$.

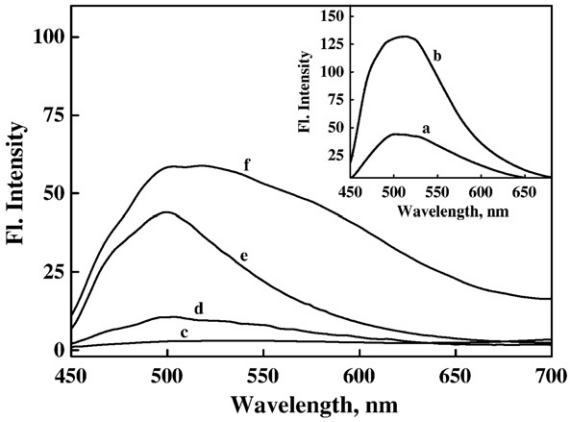

Fig. 2. Fluorescence spectra of curcumin in different systems, after excitation at 420 nm. Inset: (a) PC liposomes (b) HSA protein; main figure: (c) NIH3T3, (d) spleen lymphocytes, (e) EL4 and (f) MCF7 cells. The cells for recording fluorescence spectra were treated with 20 nmol/ml aqueous-DMSO solution of curcumin.

Fig. 2 gives the fluorescence spectra of curcumin-loaded cells (spectra c–f), after excitation at 420 nm. The fluorescence spectrum of curcumin in lymphocytes and EL4 cells is sharp and the maximum is at 500 to 505 nm, while those in MCF7 and NIH3T3 cells are broad with maximum at 520 to 535 nm. The fluorescence intensity, when compared in these four sets of cells, showed higher intensity in the two tumor cell lines. One of the reasons for such increase in fluorescence could be due to its increased uptake. To verify this, we calculated the fluorescence intensity to the same level of uptake and compared the fluorescence per unit uptake and the results are listed in Table 1. It is clear that the fluorescence is at least 3–8 times more intense in the tumor cells than that in normal cells. The shift in fluorescence spectra and intensity variations clearly indicate that curcumin experiences different hydrophobic environments inside the tumor cells and interacts with them differently.

3.3. Fluorescence microscopy studies

The above observed fluorescence changes, prompted us to understand its intracellular localization. Figs. 3A, B and 4A, B give the confocal images of curcumin treated lymphocytes, EL4, NIH3T3 and MCF7 cells respectively along with their corresponding phase contrast images and a few magnified

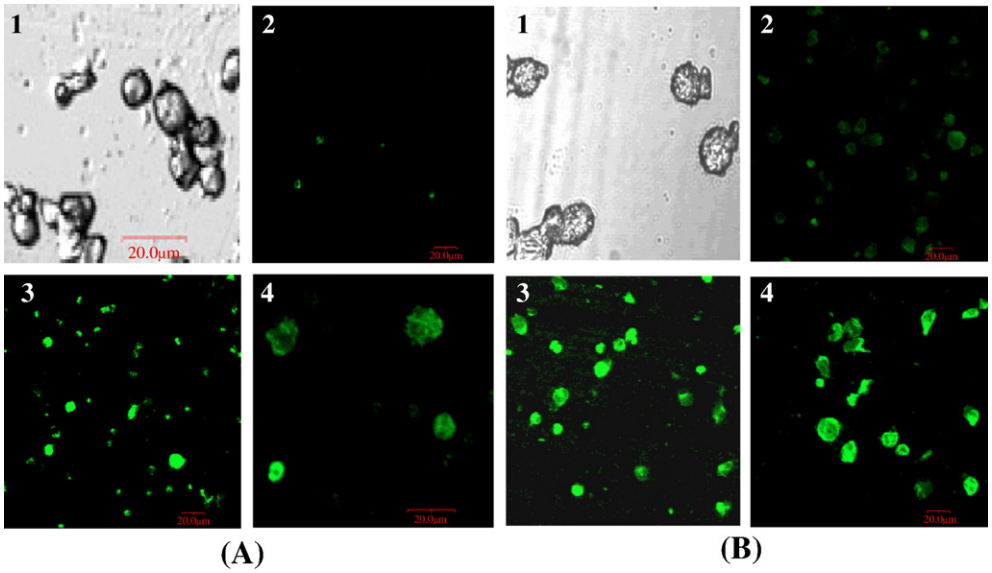

Fig. 3. Confocal micrographs of cells after treating with curcumin at concentration of 10 nmol/ml. (A) Spleen lymphocytes (20× objective); 1 — Phase contrast image, 2 — Cells without curcumin treatment, 3 — Cells treated with curcumin (2× zoom), 4 — Cells treated with curcumin (6× zoom). (B) EL4 cells (20× objective); 1 — Phase contrast image, 2 — Cells without curcumin treatment, 3 — Cells treated with curcumin (2× zoom), 4 — Cells treated with curcumin (3× zoom). Excitation wavelength 458 nm.

images. From these images, the average fluorescence intensity per unit area was calculated and listed in Table 1. The results supported our earlier observation that curcumin exhibits more fluorescence in tumor cell lines. Curcumin, being a lipophilic molecule, is expected to be localised in the membrane. However, the images of EL4 and lymphocytes show emission from the entire cells. Since in these cells, majority of the cell volume is occupied by the nucleus with very little cytoplasm, the emission could be from both the membrane and the nucleus.

In case of MCF7 and NIH3T3 cells, due to their distinct morphology, fluorescence images indicate selective localization of curcumin in the cell membrane and the nucleus. To confirm its nuclear localization, these cells were subjected to dual staining for which the cells treated with curcumin were thoroughly

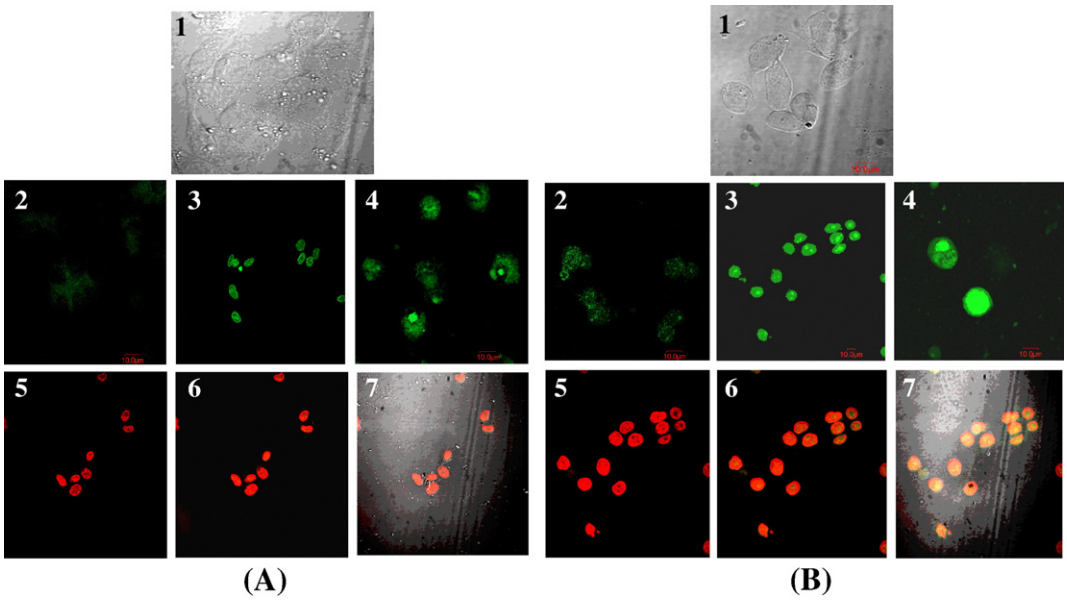

Fig. 4. Confocal micrographs of cells after treating with curcumin at concentration of 10 nmol/ml. (A) NIH3T3 cells (60× objective); 1 — Phase contrast image, 2 — Cells without curcumin treatment, 3 — Cells treated with curcumin (1× zoom), 4 — Cells treated with curcumin (2× zoom), 5 — Cells stained with DAPI (1× zoom), 6 — Images 4 and 5 merged together (1× zoom), 7 — Images 4 and 5 merged with image 1 (1× zoom). (B) MCF7 cells (60× objective); 1 — Phase contrast image, 2 — Cells without curcumin treatment, 3 — Cells treated with curcumin (1× zoom), 4 — Cells treated with curcumin (2× zoom), 5 — Cells stained with DAPI (1× zoom), 6 — Images 4 and 5 merged together (1× zoom), 7 — Images 4 and 5 merged with image 1 (1× zoom). For curcumin, λ_{ex} — 458 nm and DAPI, λ_{ex} — 720 nm, two photon.

washed, stained with DAPI, a DNA selective fluorescent probe [15] and after fixation, the images were recorded. The fluorescence from curcumin was pseudocolored as green and that from DAPI as red (Images 3, and 5 of Fig. 4A and B respectively). The superimposed images as shown in images 6 and 7 of Fig. 4A and B respectively for NIH3T3 and MCF7 cells, clearly indicate green and red areas overlapping, confirming the co-localization of curcumin and DAPI in the nucleus.

An attempt has also been made to follow the cellular localization of curcumin as a function of time in MCF7 cells. In the absence of live cell imaging technique this could be done only by treating the cells with curcumin for different time periods (0.5 to 8 h), and after treatment, the confocal fluorescence images were captured. Fig. 5A and B respectively show the confocal micrographs and the plot of mean fluorescence intensity/area of MCF7 cells at different treatment times. From the figure it is clear that the fluorescence of curcumin could be observed as early as 0.5 h within the cell and at this time point the intensity was observed uniformly from the entire cell. With progress of time (2 to 8 h), the fluorescence intensity appears to be localised into various compartments. This makes us speculate that incubation time of 0.5 to 2 h may be enough for maximum cellular uptake of curcumin.

3.4. Sub-cellular distribution of curcumin

Since MCF7 cell lines showed maximum uptake of curcumin and exhibit clear differential distribution, further studies were carried out to estimate the different sub-cellular distribution of curcumin. The absorption spectra of methanolic curcumin from different sub-cellular fractions of MCF7 have been shown in Fig. 6 and by comparing the absorbance at 428 nm, the percentage distribution of curcumin in different cellular compartments was calculated and shown as inset of Fig. 6. The figure confirms that the membrane fraction showed significantly highest percentage of curcumin and the differential uptake in sub-cellular components is in the order membrane > cytoplasm > nucleus > mitochondria. Although these studies are too preliminary and need more confirmative studies, they support the previous re-

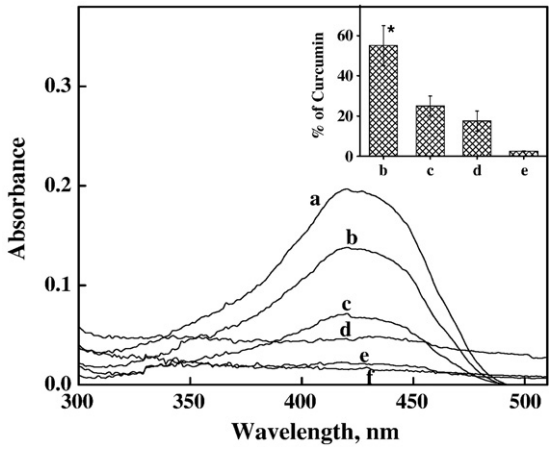

Fig. 6. Absorption spectra of curcumin extracted in to 0.5 ml of methanol from different sub-cellular fractions of MCF7 cells (2×10^6) after treatment with 20 nmol/ml of curcumin in aqueous-DMSO for 4 h: a — Total cellular fraction, b — Membrane fraction, c — Cytoplasmic fraction, d — Nuclear fraction, e — Mitochondrial fraction, f — Control. Inset shows variation in percent curcumin in different sub-cellular fractions. Control represents cells (2×10^6) treated with aqueous-DMSO. Results presented as means ± SEM, $n=3$. *Significant against cytoplasmic, nuclear and mitochondrial fractions at $P<0.05$.

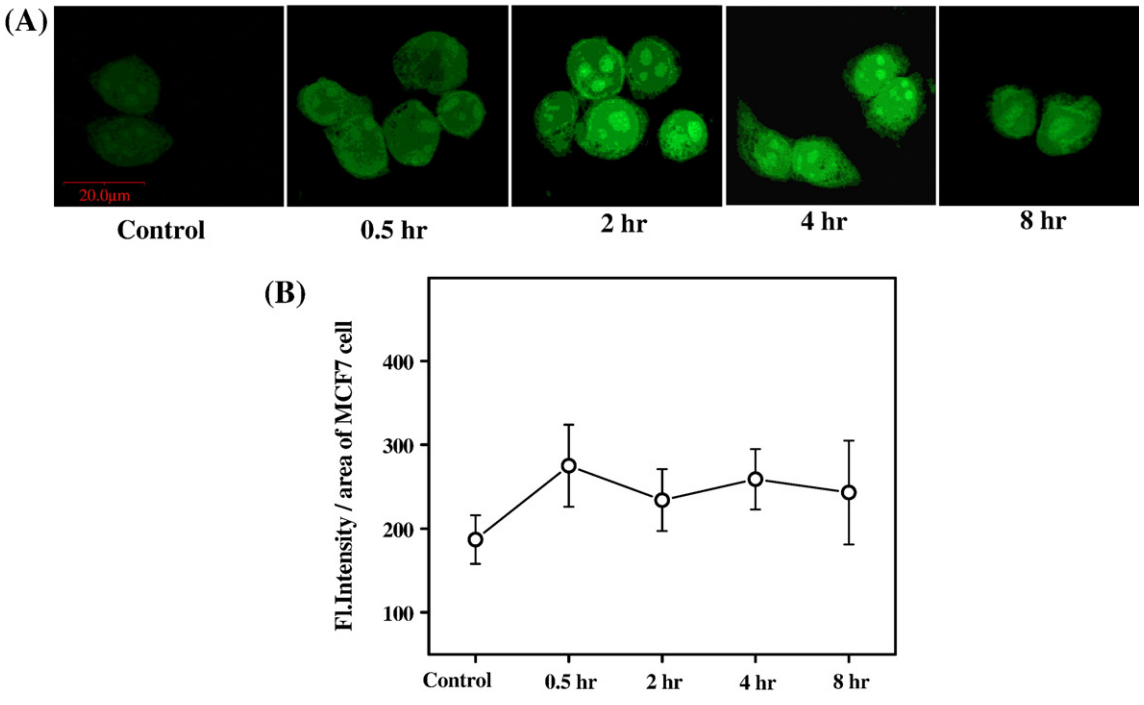

Fig. 5. (A) Confocal micrographs of MCF7 cells (60× objective, 2× zoom) at different time points (0.5 h to 8 h) after treatment with curcumin at concentration of 10 nmol/ml. (B) Line graph showing variation in fluorescence intensity/area at different time points. Excitation wavelength 458 nm.

Table 2
Effect of curcumin on the viability of different cell lines assayed by MTT

Treatment (curcumin)	MCF-7 λ_{abs} 550 nm	EL4 λ_{abs} 550 nm	NIH3T3 λ_{abs} 550 nm
Control	0.83±0.01	0.79±0.02	0.44±0.01
20 nmol/ml	0.65±0.02[a]	0.56±0.01[a, b]	0.37±0.01
Cytotoxicity (%)	22%	30%	16%
40 nmol/ml	0.50±0.01[a]	0.30±0.01[a, b]	0.29±0.01
Cytotoxicity (%)	41%	63%	35%

[a] Significant against NIH3T3 cell line at $P<0.05$.
[b] Significant against MCF7 cell line at $P<0.05$.

ports that the cell membrane is the preferred site of localization for curcumin and curcumin is localised in the nucleus too.

3.5. Cytotoxicity measurements

Table 2 shows the cytotoxic effect of curcumin at concentrations of 20 to 40 nmol/ml in different cell lines. The results indicate that there is an increase in the cytotoxicity in individual cell line with increasing concentration of curcumin treatment. Tumor cells EL4 and MCF7 showed significantly higher sensitivity towards the cytotoxic activity of curcumin compared to normal fibroblast cells NIH3T3. Between the tumor cells, EL4 showed significantly higher toxicity compared to MCF7 even at lesser uptake, indicating that the cells of lymphoid origin experience more toxicity of curcumin. The above observations have been represented in Fig. 7, as change in cytotoxicity against total cellular uptake at different treatment conditions. The treatment of the cell lines with curcumin at a concentration of 10 nmol/ml showed only little toxicity. This experiment with normal spleen lymphocytes was not reported as large fluctuations were observed in their viability in 24 h time period.

4. Discussion

In spite of all the advancement on curcumin research, there are a very few papers addressing its cellular uptake, and localization. In this paper, applying absorption and unique fluorescence spectral properties of curcumin, we made an attempt to measure quantitative uptake and intracellular localization of curcumin in four different cell types and tried to correlate these results with its cytotoxicity.

Our results clearly support the earlier reported observation, that tumor cells show preferential uptake of curcumin compared to normal cells. Curcumin being a lipophilic molecule interacts with cellular membrane and is subsequently transported inside the cell. Among various factors that are responsible for higher curcumin uptake in tumor cells against normal cells could be their differences in membrane structure, protein composition and bigger size [16,17].

The fluorescence spectra of cellular curcumin showed two interesting factors. The fluorescence intensity is always higher in tumor cells compared to normal cells and the fluorescence maximum of curcumin in suspension cells is more blue shifted as compared to that in adherent cells. Several recent reports indicate that the fluorescence maximum and fluorescence quantum yield of curcumin are highly sensitive to the medium polarity and availability of the hydrophobic pockets such as protein and lipid [9,18–25]. The present observations clearly indicate that curcumin interacts differently with different cells. Although there are no reports available in literature on differential polarity of these different cells, the observed fluorescence spectral changes however suggest differences in the protein and lipid composition of these cells. The more polar environment in the adherent cells could be due to adhering proteins (cadherins) and several cell–cell junction (gap junction, tight junction and adherent junction) proteins [26–29]. However in tumor cells of adherent type such as MCF7 other factors like differential pool of cytoplasmic proteins (resulting from altered gene expression) and the difference in the composition of membrane lipids can also contribute towards the intracellular microenvironment or hydrophobicity [30–32]. These significantly prominent fluorescence changes of curcumin also indicate that curcumin can be used as a new probe to understand the behaviour of different cell types.

Our preliminary fluorescence imaging studies are very encouraging and clearly show localization of curcumin inside the cells. In all the cells, curcumin fluorescence could be seen in the membrane but in MCF7 and NIH3T3 cells, due to their distinct morphology, localization inside the nucleus is also observed. Studies on isolation of curcumin from sub-cellular fractions also confirmed the differential localization of curcumin in the membrane, cytoplasm and nuclear compartments of the cell with preferred localization in the membrane. The localization of curcumin in the nucleus is a new and unexpected observation, which needs to be addressed in the future. To understand this, more detailed experiments are needed with special emphasis on identification of the cellular proteins that specifically interact with curcumin and helping its transport to nucleus. The cytotoxicity studies support the previously reported observation that

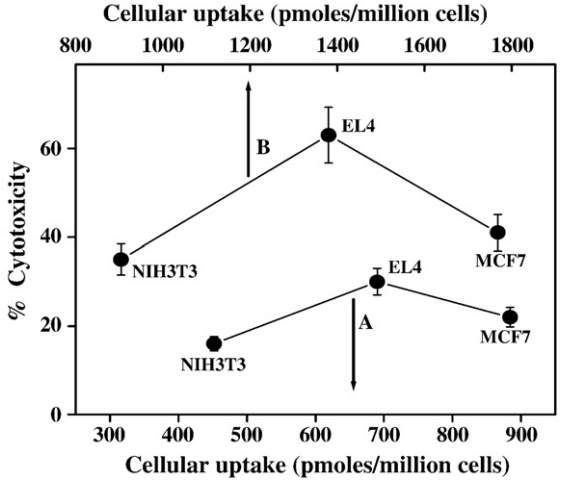

Fig. 7. Change in cytotoxicity of curcumin, assayed by MTT, against cellular uptake for different cells at two different treatment conditions. (A) 20 nmol curcumin/ml and (B) 40 nmol curcumin/ml. Results are presented as means±SEM, $n=3$.

curcumin shows toxicity to tumor cells. In addition to this, our limited studies indicate that there is no general correlation between uptake and toxicity. It appears that the cells of lymphoid origin are more sensitive to curcumin than the non-lymphoid cells even when these cells showed lesser uptake. However in all the individual cell lines, the toxicity clearly increased with increased curcumin uptake.

In conclusion, our present studies give a method to estimate quantitative uptake of curcumin and the results provide confirmation that tumor cells preferentially take up more curcumin. The fluorescence spectrum of curcumin in tumor cells is easy to detect and can be used as a marker to understand its interaction with different cellular proteins. The fluorescence imaging studies show localization in the cells and a surprising observation of its nuclear localization, this provides a chance to explore new avenues of research to understand its interactions with different nuclear factors and target proteins.

Acknowledgements

The authors are thankful to Drs. T. Mukherjee, K. B. Sainis, and S. K. Sarkar, of Bhabha Atomic Research Centre for the encouragement and support and Prof. Dulal Panda, IIT-Bombay, for helping in confocal imaging studies. The authors are grateful to Prof. Bharat B. Aggarwal, MD Anderson, Texas, USA for several useful suggestions and encouragement on curcumin research.

References

[1] B.B. Aggarwal, C. Sundaram, N. Malani, H. Ichikawa, Curcumin: the Indian solid gold, in: B.B. Aggarwal, S. Young-Joon, S. Shishodia (Eds.), The Molecular Targets and Therapeutic Uses of Curcumin in Health and Disease, Springer, NY USA, 2007, pp. 1–76.
[2] I. Chattopadhyay, K. Biswas, U. Bandyopadhyay, R.K. Banerjee, Turmeric and curcumin: biological actions and medicinal applications, Curr. Sci. 87 (2004) 44–53.
[3] B.B. Aggarwal, A. Kumar, A.C. Bharti, Anticancer potential of curcumin: preclinical and clinical studies, Anticancer Res. 23 (2003) 363–398.
[4] R.A. Sharma, A.J. Gescher, W.P. Steward, Curcumin: the story so far, Eur. J. Cancer 41 (2005) 1955–1968.
[5] S. Singh, A. Khar, Biological effects of curcumin and its role in cancer chemoprevention and therapy, Anticancer Agents Med. Chem. 6 (2006) 933–946.
[6] S. Shishodia, G. Sethi, B.B. Aggarwal, Curcumin: getting back to the roots, Ann. N.Y. Acad. Sci. 1056 (2005) 206–217.
[7] S. Singh, From exotic spice to modern drug, Cell 130 (2007) 765–768.
[8] K.I. Priyadarsini, Free radical reactions of curcumin in membrane model, Free Radic. Biol. Med. 23 (1997) 838–846.
[9] A. Kunwar, A. Barik, R. Pandey, K.I. Priyadarsini, Transport of liposomal and albumin loaded curcumin to living cells: an absorption and fluorescence study, Biochim. Biophys. Acta 1760 (2006) 1513–1520.
[10] http://www.atcc.org/common/catalog/cellBiology/cellBiologyIndex.cfm
[11] A.B. Trivedi, N. Kitabatake, E. Doi, Toxicity of dimethyl sulphoxide as a solvent in bioassay system with HeLa cells evaluated colorimetrically with 3-(4,5-dimethyl thiazol-2-yl)-2,5-diphenyl-tetrazolium bromide, Agric. Biol. Chem. 54 (1990) 2961–2966.
[12] Z. Földes-Papp, U. Demel, G.P. Tilz, Laser scanning confocal fluorescence microscopy: an overview, Int. Immunopharmacology 3 (2003) 1715–1729.
[13] L. Coda, A.E. Salcini, S. Confalonieri, G. Pelicci, T. Sorkina, A. Sorkin, P.G. Pelicci, P.P. Di Fiore, Eps15R is a tyrosine kinase substrate with characteristics of a docking protein possibly involved in coated pits-mediated internalization, J. Biol. Chem. 273 (1998) 3003–3012.
[14] T. Mosmann, Rapid colorimetric assay for cellular growth and survival: application to proliferation and cytotoxicity assays, J. Immunol. Methods 65 (1983) 55–63.
[15] T. Suzui, K. Fujikura, T. Higashiyama, K. Takata, DNA staining for fluorescence and laser confocal microscopy, J. Histochem. Cytochem. 45 (1997) 49–53.
[16] S.J. Singer, The molecular organization of membranes, Ann. Rev. Biochem. 43 (1974) 805–833.
[17] S.J. Singer, Some early history of membrane molecular biology, Ann. Rev. Physiology 66 (2004) 1–27.
[18] C.F. Chignell, P. Bilski, K.J. Reszka, A.N. Motten, R.H. Sik, T.A. Dhal, Spectral and photochemical properties of curcumin, Photochem. Photobiol. 59 (1994) 295–302.
[19] P.H. Bong, Spectral and photophysical behaviours of curcumin and curcuminoids, Bull. Korean Chem. Soc. 21 (2000) 81–86.
[20] S.M. Khopde, K.I. Priyadarsini, D.K. Palit, T. Mukherjee, Effect of solvent on the excited state photophysical properties of curcumin, Photochem. Photobiol. 72 (2000) 625–631.
[21] G. Began, E. Sudharshan, K.U. Sankar, A.G. Appu Rao, Interaction of curcumin with phosphatidylcholine: a spectrofluorometric study, J. Agric. Food Chem. 47 (1999) 4992–4997.
[22] M.O. Iwunze, Binding and distribution characteristics of curcumin solubilised in CTAB micelle, J. Mol. Liquids 111 (2004) 161–165.
[23] A. Barik, K.I. Priyadarsini, H. Mohan, Photophysical studies on binding of curcumin to bovine serum albumin, Photochem. Photobiol. 77 (2003) 597–603.
[24] F. Wang, J. Yang, X. Wu, S. Liu, Study of the interaction of proteins with curcumin and SDS and its analytical application, Spectrochim. Acta A Mol. Biomol. Spectros. 61 (2005) 2650–2656.
[25] A. Barik, B. Mishra, A. Kunwar, K.I. Priyadarsini, Interaction of curcumin with human serum albumin: thermodynamic properties, fluorescence energy transfer and denaturation effects, Chem. Phys. Lett. 436 (2007) 239–243.
[26] S.M. Troyanovsky, Mechanism of cell–cell adhesion complex assembly, Curr. Opin. Cell Biol. 11 (1999) 561–566.
[27] D.A. Leckband Prakasam, Mechanism and dynamics of cadherin adhesion, Ann. Rev. Biomed. Eng. 8 (2006) 259–287.
[28] S.T. Suzuki, Structure and function of cadherins, Tanpakushitsu Kakusan Koso 51 (2006) 629–635.
[29] P. Savagner, Leaving the neighborhood: molecular mechanisms involved during epithelial–mesenchymal transition, BioEssays 23 (2001) 912–923.
[30] T.A. Sellers, J.R. Yates, Review of proteomics with applications to genetic epidemiology, Genetic Epidemiology 24 (2003) 83–98.
[31] C.P. Paweletz, J.W. Gillespie, D.K. Ornstein, N.L. Simone, M.R. Brown, K.A. Cole, O. Wang, J. Huang, Hu Nan, T. Yip, W.E. Rich, E.C. Kohn, M.W. Linehan, T. Weber, P. Taylor, M.R. Emmert-Buck, L.A. Liotta, E.F. Petricoin, Rapid protein display profiling of cancer progression directly from human tissue using a protein biochip, Drug Development Research 49 (2000) 34–42.
[32] K. Glunde, J. Chunfa, Z.M. Bhujwalla, Molecular causes of the aberrant choline phospholipid metabolism in breast cancer, Cancer Research 64 (2004) 4270–4276.

European Journal of Pharmacology 611 (2009) 8–16

Contents lists available at ScienceDirect

European Journal of Pharmacology

journal homepage: www.elsevier.com/locate/ejphar

Molecular and Cellular Pharmacology

Curcumin mediates time and concentration dependent regulation of redox homeostasis leading to cytotoxicity in macrophage cells

Amit Kunwar [a,*], Santosh K. Sandur [b], Malini Krishna [b], Kavirayani I. Priyadarsini [a]

[a] Radiation & Photochemistry Division, Bhabha Atomic Research Centre, Trombay, Mumbai-400085, India
[b] Radiation Biology & Health Sciences Division, Bhabha Atomic Research Centre, Trombay, Mumbai-400085, India

ARTICLE INFO

Article history:
Received 14 November 2008
Received in revised form 12 March 2009
Accepted 23 March 2009
Available online 1 April 2009

Keywords:
Curcumin
Reactive oxygen species
Thiols
Antioxidant genes
γ-radiation

ABSTRACT

The present study was designed to test a hypothesis that curcumin may be modulating oxidative stress parameters including reactive oxygen species, non-protein thiols and expression of antioxidant genes in a concentration and time dependent manner in exhibiting cytotoxic effects in macrophage cell line RAW 264.7. The results have shown that curcumin elevated the reactive oxygen species levels accompanied by a decrease in levels of intracellular non-protein thiols at 2 h after its addition to cells. However, the levels of reactive oxygen species decreased and non-protein thiols content increased at 18 h after its addition. Whereas the expression of *glutathione peroxidase* (*GPx*), *catalase*, *Cu,Zn-superoxide dismutase* (*Cu,Zn-SOD*) and *heme oxygenase-1* (*HO-1*) increased with curcumin concentration and also with increase in time of incubation, the expression of *Mn- superoxide dismutase* (*Mn-SOD*) showed concentration dependant repression upon treatment with curcumin. The cell viability was significantly reduced at high concentration (25 μM) of curcumin treatment but not at low concentration (5 μM). Curcumin at 5 μM scavenged γ-radiation induced reactive oxygen species and inhibited cell death. On the contrary, at 25 μM, curcumin increased radiation induced reactive oxygen species production and augmented cell death. Interestingly pretreatment with reducing agents glutathione (GSH) or N-acetyl-cysteine (NAC), modified the curcumin mediated redox changes and cell death differentially, due to the inhibition of cellular uptake of curcumin by GSH but not by NAC. The important finding of the study is that the concentration and time dependent dual effect of curcumin may be attributed to changes in oxidative stress and antioxidant gene expression levels leading to inhibition or promotion of cell death.

1. Introduction

Curcumin (Diferuloylmethane), a principal phenolic pigment present in turmeric, is used commercially as a spice/food colouring agent and has been widely employed in ancient Indian and Chinese medicine (Chattopadhyay et al., 2004; Aggarwal et al., 2007). Recent scientific research has confirmed that curcumin possesses anti-inflammatory, antibacterial, anti-amyloid properties, suppresses proliferation of a wide variety of tumor cells and also acts as an antioxidant in normal tissues and cells (Sharma, 1976; Aggarwal et al., 2003; Sharma et al., 2005; Shishodia et al., 2005; Singh and Khar, 2006; Rahman et al., 2006; Singh, 2007; Fiala et al., 2007). The extensive research on curcumin's chemical biology in the past one decade suggested that it effectively scavenged reactive oxygen species like peroxyl and hydroxyl radicals. It inhibited reactive oxygen species induced lipid peroxidation and up regulated expression of several phase II detoxifying enzymes via the activation of the antioxidant response element (Priyadarsini, 1997; Motterlini et al., 2000; Balogun et al., 2003; Iqbal et al., 2003; Rahman et al., 2006; Rushworth et al., 2006; Wei et al., 2006; Surh et al., 2008).

In contrast to these reports, curcumin has also been shown to promote oxidative stress in transformed cells in culture. These effects are associated with loss of mitochondrial functions and oxidative DNA damage resulting in apoptosis, which has been attributed as one of the mechanisms associated with the antitumor activity of curcumin (Bhaumik et al., 1999; Morin et al., 2001; Syng-Ai et al., 2004; Jung et al., 2005; Fang et al., 2005; Sandur et al., 2007a; Li et al., 2008). Recently it has been reported that curcumin scavenged reactive oxygen species at low concentrations and induced their production at high concentrations in HL-60 cells (Chen et al., 2005). These observations indicated that curcumin may exhibit both antioxidant and prooxidant effects depending on the cell type. However, the mechanism responsible for such differential effects of curcumin is not clearly understood. It is suggested that curcumin may exert beneficial or cytotoxic actions through modulation of cellular reactive oxygen species levels, non-protein thiols content and the antioxidants enzymes including superoxide dismutase (SOD) family, catalase, glutathione peroxidase (GPx) and heme oxygenase (HO-1) (Balogun et al., 2003; Matés, 2000; Han et al., 2005; Maclachlan et al., 2005; Surh et al., 2008). The present study, therefore, was designed to test a hypothesis that curcumin may be

* Corresponding author. Fax: +91 22 25505151.
E-mail address: kamit@barc.gov.in (A. Kunwar).

0014-2999/$ – see front matter © 2009 Elsevier B.V. All rights reserved.
doi:10.1016/j.ejphar.2009.03.060

modulating oxidative stress parameters including reactive oxygen species, non-protein thiols and expression of antioxidant genes in a concentration and time dependent manner and subsequently influencing cell viability in murine macrophage cell line RAW 264.7. Since glutathione (GSH) has been shown to chemically interact with curcumin through Michael addition reaction (Awasthi et al., 2000), the curcumin induced cellular modifications in presence of GSH or N-acetyl cysteine (NAC) was also studied. Further, the ability of curcumin to modulate γ-radiation-induced oxidative stress and cell death was investigated in these cells. The information gained from these studies would provide a line of evidence to support the existence of a concentration and time dependent differential changes in oxidative stress and antioxidant gene expression levels as part of the molecular mechanism leading to either beneficial or cytotoxic actions as caused by curcumin.

2. Materials and methods

2.1. Chemicals

Curcumin (CI 7500), GSH, NAC, 5,5′-dithiobis-2-nitrobenzoic acid (DTNB), diethyl pyrocarbonate (DEPC), tris base and Dulbecco's modified essential medium (DMEM) were purchased from Sigma Chemical Company, USA. Penicillin, streptomycin, fetal calf serum and reverse transcription–polymerase chain reaction (RT-PCR) kit were procured from Invitrogen, USA. Total RNA isolation kit was obtained from Roche Biochem, Germany. Dichlorofluorescein diacetate (DCF-DA) was obtained from Molecular probes, USA. High performance liquid chromatography (HPLC) grade dimethyl sulphoxide (DMSO) was procured from Spectro Chem (India). All the other chemicals with maximum available purity were purchased from reputed local manufacturers/suppliers. The purity of curcumin was confirmed by thin layer chromatography and HPLC**.** The gene specific primers for RT-PCR were custom synthesized from the local agents. The reagent solutions were prepared in nanopure water from a Millipore Milli-Q system just before the use. Absorption spectra were recorded on a JASCO V-530 spectrophotometer and fluorescence intensity was recorded on a Hitachi F-4010 fluorimeter. PCR was performed on Techne thermocycler (Model no. — TC512, UK).

2.2. Cell culture and treatment

The murine macrophage cell line RAW 264.7 was obtained from National Centre for Cell Science, India. The cells were cultured in DMEM supplemented with 10% fetal calf serum, 100 μg/ml streptomycin and 100 U/ml penicillin and maintained at 37 °C under 5% CO_2 and humidified air. The cells in DMEM medium were seeded (1×10^6 cells/ml) in six-well culture plates and kept overnight for attachment. The medium was changed before treating the cells with different reagents for desired time points. 20 mM stock solution of curcumin was prepared in DMSO and diluted with the culture medium to get the desired concentration. The maximum concentration of DMSO was within permissible limits of toxicity ($\leq$0.1%). Appropriate DMSO controls were taken in all the experiments.

2.3. Measurement of reactive oxygen species

Intracellular levels of reactive oxygen species were estimated using a cell permeable oxidation sensitive probe DCF-DA whose fluorescence intensity increases after oxidation to dichlorofluorescein (DCF) by reactive oxygen species. The cells treated with different agents were harvested at different time points by centrifugation at 900 ×*g* and were washed three times with cold phosphate buffer saline (PBS). The cells were incubated with oxidation sensitive DCF-DA (a final concentration of 10 μM) in PBS for 30 min at 37 °C (Sandur et al., 2007a; Hail, 2008). The cells were again washed three times with cold PBS to remove the extracellular probe and were lysed in PBS containing 1% Tween 20. The supernatant was assayed for DCF fluorescence (excitation at 480 nm and emission at 530 nm). Curcumin has absorption maximum at 420 nm; therefore it does not show considerable absorption at 480 nm. However, to avoid any interference due to emission from curcumin excitation to the fluorescence emission, all the reactive oxygen species measurements in presence of curcumin using DCF-DA probe were subtracted with appropriate control samples treated with curcumin without adding the probe. The representative values are expressed as mean fluorescence intensity at 530 nm.

2.4. Measurement of intracellular non-protein thiols content

The concentration of non-protein thiols content in cells was determined using DTNB according to the reported method (Sedlak and Lindsay, 1968; Kunwar et al., 2007). This assay is based on the principle of formation of yellow color by sulfhydryl groups (-SH) with DTNB. The cells were suspended in to 0.2 ml of 10 mM Tris/HCl, pH 7.4, and disrupted two times using a bioruptor (Cosmos Bio, Tokyo, Japan) at 200 W for 30 s each. Protein estimation in the cell lysate was carried out by DC protein assay kit (Bio-Rad, U.S.A). Further the cell lysate was precipitated using 10% trichloro acid, and the supernatant was mixed with 6 μM DTNB and incubated for 10 min and absorbance measured at 412 nm against appropriate control samples that were processed in parallel without adding the DTNB. The non-protein thiols content was expressed as nmol of reduced thiol per μg of protein. Although GSH forms the majority of DTNB reactive thiols, the small-molecular-weight thiols other than GSH too react with DTNB. Therefore, the total DTNB reactive thiols have been addressed as non-protein thiols throughout the text.

2.5. RNA isolation and RT-PCR

All pipette tips, Eppendorf tubes and glassware were treated with DEPC to destroy ribonucleases. Cells were harvested at different time points and washed three times with cold PBS. Total RNA was isolated using RNA isolation kit (Roche Biochem, Germany) and was eluted in 50 μl deionised DEPC-treated water (Kurrey et al., 2005). 2 μg of total RNA was used for the synthesis of cDNA by reverse transcription (cDNA synthesis kit, Invitrogen, USA). cDNA was amplified using 1 μl of the reaction products in 25 μl with 10 pmole of the primers for 35 cycles. Each cycle consisted of 30 s of denaturation at 94 °C, 30 s of annealing and 60 s of extension at 72°C. The primers used for cDNA amplification (forward and reverse respectively) were as follows:

Mn-SOD	5′-GCACATTAACGCGCAGATCA-3′
	5′-AGCCTCCAGCAACTCTCCTT-3′
Cu,Zn-SOD	5′-AAGGCCGTGTGCGTGCTGAA-3′
	5′-CAGGTCTCCAACATGCCTCT-3′
Catalase	5′-GCAG ATACCTGTGAACTGTC-3′
	5′-GTAGAATGTCCGCACCTGAG-3′
GPx	5′-CCTCAAGTACGTCCGACCTG-3′
	5′-GTAGAATGTCCGCACCTGAG-3′
HO-1	5′-AACAAGCAGAACCCAGTC-3′
	5′-TGTCATCTCCAGAGTGTTC-3′
β-actin	5′-TGGAATCCTGTGGCATCCATGAAAC-3′
	5′-TAAAACGCAGCTCAGTAACAGTCCG-3′
Bcl-2	5′-TGCACCTGACGCCCTTCAC-3′
	5′-TAGCTGATTCGACCATTTGCCTGA-3′
Bcl-XL	5′-TGGTCGACTTTCTCTCCTAC-3′
	5′-GAGATCCACAAAAGTGTCCC-3′

β-actin was used as internal control in all the reactions. The band intensity was quantified by gelquant software (version 2.7 DNR imaging systems Ltd. Israel). Fold changes were calculated after normalization to β-actin.

2.6. Irradiation protocol

The curcumin treated and untreated cells were exposed to γ-radiation to an absorbed dose of 2 Gy using a ^{60}Co γ-source at a dose rate of 4 Gy min^{-1} as measured by standard Fricke dosimeter (Spinks and Woods, 1990). After irradiation, fetal calf serum was added at a concentration of 5% v/v and cells were incubated at 37 °C in humidified incubator with 5% CO_2 in air for different time intervals.

2.7. Measurement of cell viability

The viability of cells was determined by trypan blue dye exclusion test using a hemocytometer (Tolnai, 1975). For this experiment 2×10^4 untreated (control) or curcumin treated cells were added to each well of 24-well plates in one ml of tissue culture medium in triplicate. After 24 h of addition floating cells in the medium of each well were transferred to centrifuge tubes. Adherent cells were detached and were added to the corresponding floating cells before centrifugation. The pellet was suspended and 0.14% trypan blue was mixed with the same volume of cell suspension and 5 min later the stained (dead) and unstained (viable) cells were counted in hemocytometer. The cell viability for each group was calculated as percentage (%). % viability = (the number of living cells ÷ total number of cells including living and dead) × 100.

2.8. Cell uptake studies

The cellular uptake of curcumin was calculated using the method reported earlier from our lab (Kunwar et al., 2006, 2008). In brief cells were plated at ~1×10^6 cells/ml in 24 well plate and incubated with 20 μM of curcumin for 4 h. The cell pellet after washing with ice cold PBS, was suspended in to 500 μl of methanol and sonicated for 5 min. The absorbance of the supernatant at 428 nm, after centrifugation was recorded and using the molar absorption coefficient, the amount of curcumin taken up by cells was estimated. The results were normalized to 1 nmol of curcumin added/million cells/ml and cell uptake was expressed as pmol/million cells.

2.9. Statistical analysis

The results have been presented as mean ± S.E.M. for two independent experiments run in triplicates. Data were analyzed by one-way and two-way ANOVA of SPSS software (version 8.0.0) to confirm the variability of data and for multiple comparisons of means. P values ≤ 0.05 were considered as statistically significant.

3. Results

3.1. Biphasic effects of curcumin on reactive oxygen species levels and non-protein thiols content

Fig. 1A and B show the representative fluorescent intensities of DCF indicating levels of reactive oxygen species at 2 and 18 h after curcumin (1–25 μM) addition to cells. Curcumin increased reactive oxygen species levels steadily up to 25 μM concentration at 2 h after addition to cells. However the reactive oxygen species levels dropped below the control levels at 18 h after addition. The levels of non-protein thiols content were measured at the same time points after curcumin addition and it indicated that the basal levels of non-protein thiols content (0.251 ± 0.015 nmol/μg of protein) decreased at 2 h (Fig. 1C). Interestingly, at later time point (18 h) the levels of non-protein thiols increased significantly with increasing concentration (1–25 μM) of curcumin (Fig. 1D).

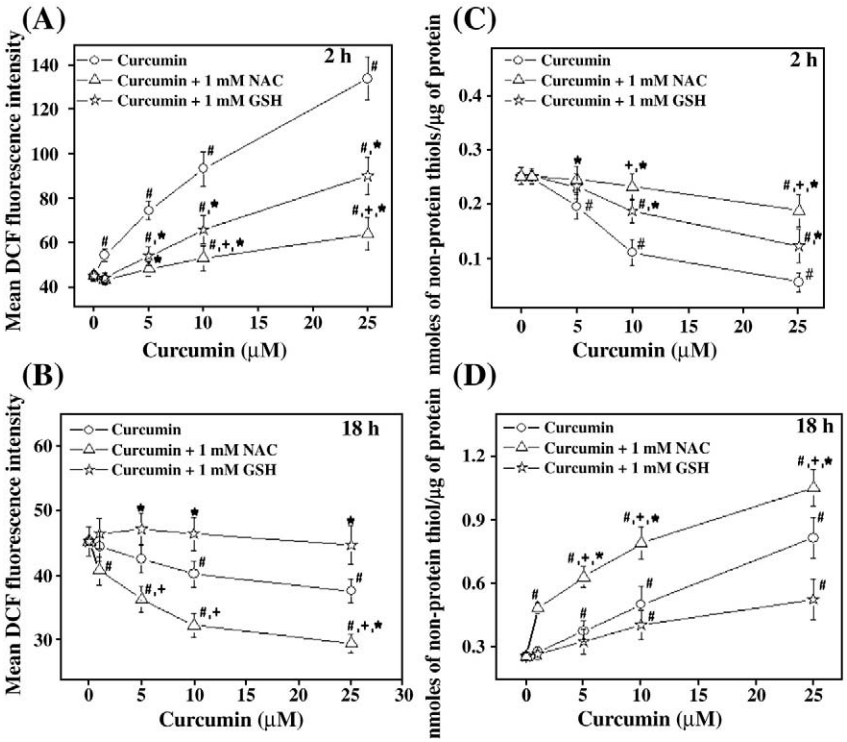

Fig. 1. Effect of curcumin (1–25 μM) on reactive oxygen species levels and non-protein thiols content at two different timepoints 2 h (A & C) and 18 h (B & D) after its addition and modulation by NAC (1 mM) or GSH (1 mM). The GSH or NAC was added to cell culture 2 h prior to addition of curcumin. Results presented as mean ± S.E.M. for $n=3$. $^{\#}P<0.05$ as compared to reactive oxygen species or non-protein thiols levels of control cells.$^{*}P<0.05$ as compared to reactive oxygen species or non-protein thiols levels of cells treated with curcumin at a particular concentration. $^{+}P<0.05$ as compared to reactive oxygen species or non-protein thiols levels of cells treated with curcumin at a particular concentration in presence of GSH.

Taken together these results suggest that curcumin modified the redox environment within cells in a concentration and time dependent manner. Further to know whether curcumin mediated changes in redox environment in cells could be restored by the addition of water soluble antioxidants like GSH or NAC, the cells were treated with 1 mM concentration of NAC or GSH for 2 h prior to addition of curcumin (1–25 μM). The reactive oxygen species levels and non-protein thiols content were measured at 2 and 18 h respectively. Exogenous addition of GSH or NAC prior to curcumin addition significantly decreased the reactive oxygen species generation at 2 h (Fig. 1A). The NAC was more effective than GSH in this respect. At later time point (18 h) the NAC and curcumin treated cells showed lower reactive oxygen species levels than the cells treated with curcumin alone (Fig. 1B). Similarly, pretreatment with NAC or GSH abrogated curcumin mediated decrease in the levels of non-protein thiols at early time point (2 h) (Fig. 1C). However, at a later time point (18 h), NAC potentiated the curcumin mediated increase in non-protein thiols levels while GSH decreased it (Fig. 1D). Thus NAC and GSH had an opposing effect on curcumin-mediated changes in levels of non-protein thiols at 18 h. The group treated with GSH alone did not bring down basal levels of reactive oxygen species. However, non-protein thiols content increased marginally from basal levels of 0.251 ± 0.015 nmol/μg of protein to 0.264 ± 0.018 nmol/μg of protein at 18 h. Interestingly, addition of NAC alone reduced basal levels of reactive oxygen species by 11% at 2 h and by 25% at 18 h, while non-protein thiols content increased to 0.371 ± 0.049 nmol/μg of protein at 2 h and 0.568 ± 0.085 nmol/μg of protein at 18 h compared to basal levels.

3.2. Effects of curcumin on the expression of antioxidant genes

Experiments were carried out to monitor the effects of low (5 μM) and high (25 μM) concentrations of curcumin on cellular antioxidant mechanisms. Antioxidant enzymes such as Mn-SOD, Cu,Zn-SOD, catalase, GPx and HO-1 play an important role in maintaining the redox homeostasis within the cells. Therefore expression of these enzymes at mRNA level was monitored in the cells at 6 and 18 h after curcumin addition. Curcumin upregulated the mRNA levels of *GPx*, *catalase* and *Cu,Zn-SOD* genes over the control in a concentration and time dependent manner with peak levels observed at 18 h after addition (Fig. 2A–D). The relative increase in the expression of *GPx* gene upon treatment with 5 and 25 μM curcumin was significantly higher as compared to increase in the expression of *catalase* and *Cu, Zn-SOD* genes. Although *HO-1* gene also showed an increase in the levels of mRNA with increase in concentration of curcumin from 5 to 25 μM, the peak level was observed at 6 h instead of 18 h (Fig. 2A–D). In contrast, the *Mn-SOD* gene showed time dependent decrease upon treatment with 5 and 25 μM curcumin (Fig. 2A–D).

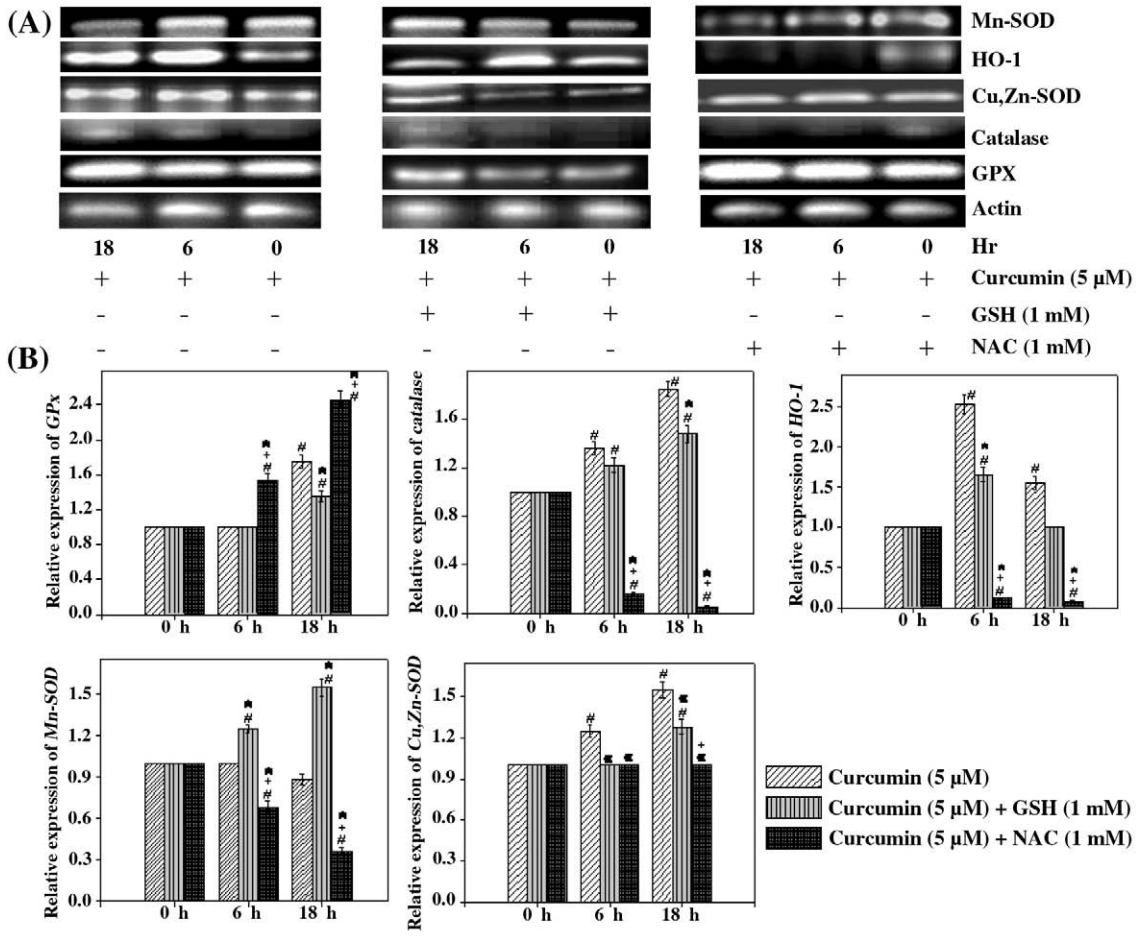

Fig. 2. Effect of curcumin concentration on the mRNA expression of antioxidant genes (*GPx*, *catalase*, *HO-1*, *Cu,Zn-SOD* and *Mn-SOD)* at 6 and 18 h after its addition and modulation by NAC (1 mM) or GSH (1 mM). (A) RT-PCR analysis at 5 μM curcumin in absence and presence of NAC or GSH. (B) Bar graph showing time dependant variation in the relative expression of the genes at 5 μM curcumin and in combination with NAC or GSH. (C) RT-PCR analysis of the genes at 25 μM curcumin both in absence and presence of NAC or GSH. (D) Bar graph showing time dependant variation in the relative expression of the genes at 25 μM curcumin and in combination with NAC or GSH. The GSH or NAC was added to cell culture 2 h prior to addition of curcumin. β-actin mRNA expression was used as an internal control. Results presented as mean ± S.E.M. for $n = 3$. $^{\#}P<0.05$ as compared to mRNA expression levels of control cells. $^{*}P<0.05$ as compared to mRNA expression levels of cells treated with curcumin at a particular timepoint. $^{+}P<0.05$ as compared to mRNA expression levels of cells treated with curcumin at any time point in presence of GSH.

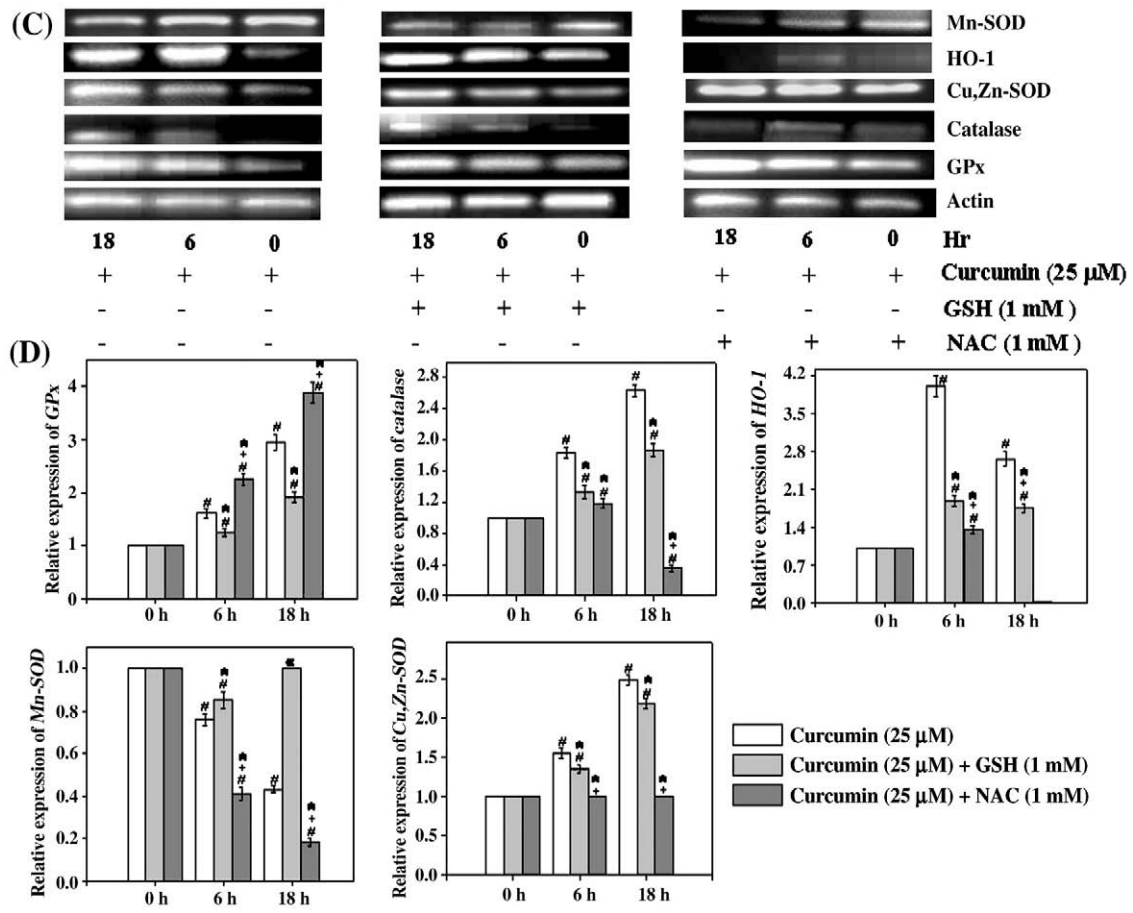

Fig. 2 (*continued*).

Pretreatment of cells with 1 mM GSH or NAC for 2 h modulated the curcumin's effect on gene expression. Pretreatment with GSH reduced the magnitude of induction in the expression of *GPx*, *catalase*, *Cu,Zn-SOD* and *HO-1* genes at both the time points (Fig. 2A–D). Interestingly, GSH also restored the suppression of *Mn-SOD* gene expression after treatment with curcumin (5 and 25 μM) (Fig. 2A–D). On the other hand cells pretreated with NAC showed an increase in the expression of *GPx* gene and decrease in the expression of *catalase, Cu,Zn-SOD, HO-1* and *Mn-SOD* genes at 6 and 18 h as compared to curcumin treatment alone (Fig. 2A–D). These results indicated a differential effect of GSH and NAC on curcumin induced gene expression in RAW cells. The group treated with GSH alone did not show changes in the expression of all the five antioxidant genes at 6 and 18 h compared to control levels (supplementary data). However, the group treated with NAC showed significant upregulation of *GPx* at 18 h, repression of *Mn-SOD* and *HO-1* at both timepoints. However, the expression of *catalase* and *Cu,Zn-SOD* was comparable to control levels (Supplementary data).

3.3. Effect of curcumin on cell viability

To investigate, how changes in the redox environment induced by curcumin affect cell viability, cells were incubated with curcumin (5 and 25 μM) for 24 h. The % cell viability under different treatment conditions has been shown in Fig. 3A. The figure clearly reveals that treatment at 5 μM curcumin resulted marginal decrease in cell viability while that at 25 μM showed significant reduction. Addition of GSH or NAC resulted in the complete recovery of viability in cells treated with 5 μM of curcumin. However, at 25 μM of curcumin, NAC offered better protection than GSH. Treatment with NAC or GSH alone did not induce loss of cell viability. Further mRNA expression levels of antiapoptotic genes such as *Bcl-2* and *Bcl-XL* were measured at 18 h after curcumin addition. The results showed that significant decrease in the mRNA expression levels of *Bcl-2* and *Bcl-XL* genes was seen only at 25 μM curcumin (Fig. 3B and C). However, treatment with 1 mM NAC or GSH prior to curcumin (5 and 25 μM) addition abrogated curcumin mediated decrease in expression of antiapoptotic genes and NAC was better than GSH in its action (Fig. 3B and C). The group treated with GSH alone did not change the mRNA expression levels of *Bcl-2* and *Bcl-XL*, while NAC showed significant upregulation of these genes (Fig. 3B and C).

3.4. Effect of GSH or NAC on cellular uptake of curcumin

In order to understand the mechanism responsible for differential effects of NAC or GSH on curcumin induced redox changes, uptake of curcumin in cells in presence of GSH or NAC was estimated. The cells were incubated with 20 μM of curcumin in presence or absence of 1 mM GSH or NAC for 4 h. Fig. 4A shows the absorption spectrum of intracellular curcumin and Fig. 4B shows relative uptakes in pmol/million cells under different treatment conditions. The basal level of cellular uptake of curcumin was about 17.5 ± 3.1 pmol/million cells. In the presence of NAC, the cellular uptake was marginally decreased to 14.7 ± 2.8 pmol/million cells. However, in the presence of GSH, it was significantly reduced to 8.75 ± 2.3 pmol/million cells. These results suggest that pretreatment with GSH inhibited the cellular uptake of curcumin, while NAC was less effective.

3.5. Concentration dependent response of curcumin to γ-irradiation

To investigate the concentration dependant differential antioxidant and pro-oxidant activity, the curcumin (5 and 25 μM) treated

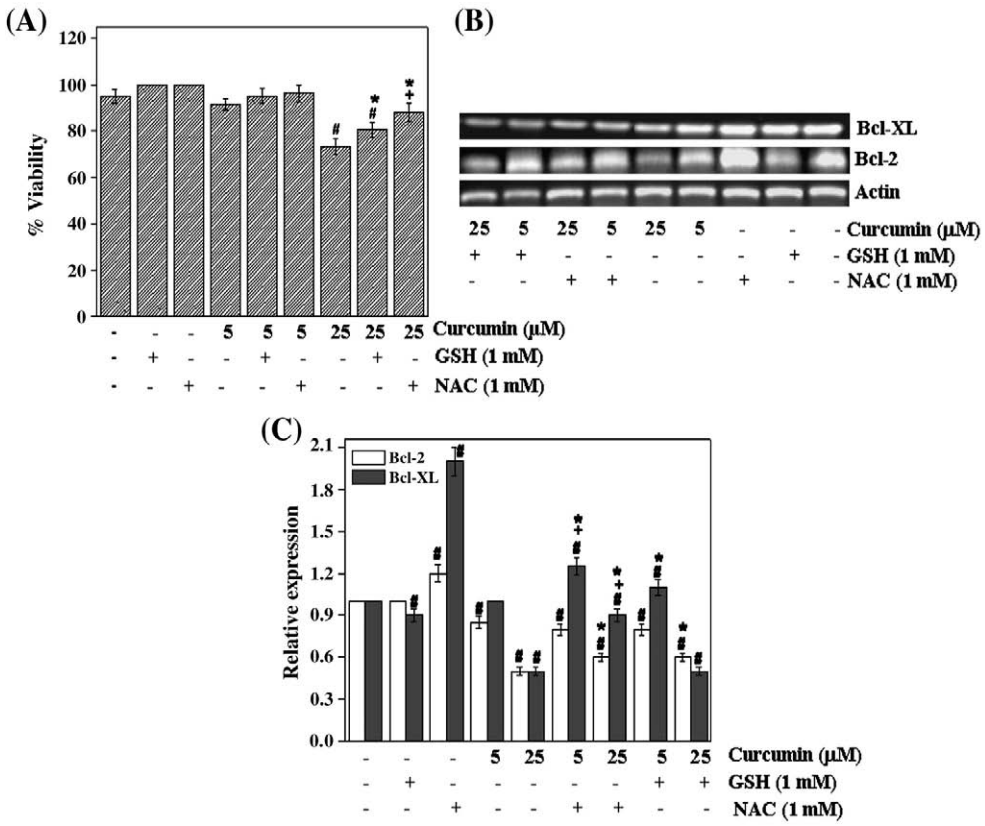

Fig. 3. Effect of curcumin (5 or 25 μM) in combination with NAC (1 mM) or GSH (1 mM) on cell viability. (A) Bar graph showing variation in the cell viability. (B) RT-PCR analysis showing comparative expression of antiapoptotic genes *Bcl-2* and *Bcl-XL* in cells. (C) Analysis of the relative expression of above genes under different treatment conditions. The GSH or NAC was added to cell culture 2 h prior to addition of curcumin. β-actin mRNA expression was used as an internal control. Results presented as mean ± S.E.M. for $n = 3$. $^{\#}P<0.05$ as compared to control cells. $^{*}P<0.05$ as compared to cells treated with curcumin. $^{+}P<0.05$ as compared to cells treated with curcumin in presence of GSH.

cells were exposed to γ-radiation (absorbed dose, 2 Gy) and examined for the reactive oxygen species levels at 2 h, expression of anti-apoptotic markers such as *Bcl-2* and *Bcl-XL* at 18 h and cell viability at 24 h. Fig. 5A shows the intracellular reactive oxygen species levels under different treatment conditions. Exposure of cells to γ-radiation elevated reactive oxygen species levels, which was marginally lowered in presence of 5 μM curcumin, while at 25 μM curcumin, the reactive oxygen species levels significantly increased. However, when cells were treated with curcumin (5 and 25 μM) in combination with 1 mM GSH or NAC, the radiation induced reactive oxygen species levels decreased significantly. NAC was again more effective than GSH. Further, the mRNA levels of *Bcl-2* and *Bcl-XL* and cell viability, assessed under the same conditions showed that γ-radiation suppressed the expression of anti-apoptotic genes and reduced the cell viability (Fig. 5B, C and D). Curcumin at 5 μM partially inhibited the radiation-mediated repression of *Bcl-2* and *Bcl-XL* genes while 25 μM of curcumin further suppressed radiation induced abrogation of these genes (Fig. 5B and C). Similar changes in cell viability were observed when cells treated with curcumin (5 and 25 μM) were exposed to radiation (Fig. 5D). The treatment with NAC or GSH prior to

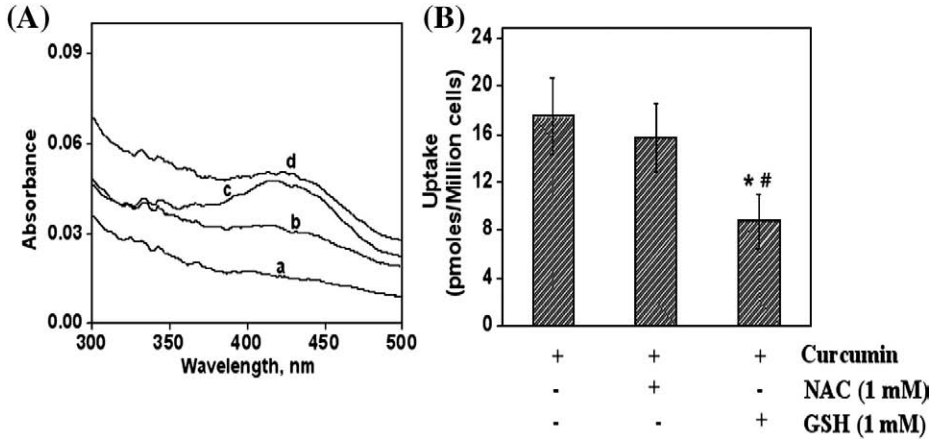

Fig. 4. Effect of NAC (1 mM) or GSH (1 mM) on cellular uptake of curcumin: (A) Absorption spectra of methanolic curcumin from cells (a) control cells (b) cells treated with 20 μM curcumin and GSH (c) cells treated with 20 μM curcumin and NAC (d) cells treated with 20 μM curcumin only. (B) Bar graph showing relative cellular uptake under various treatment conditions as mentioned above in pmol/million cells after normalization to 1 nmol of curcumin added/million cells/ml. Results presented as mean ± S.E.M. for $n = 3$. $^{*}P<0.05$ as compared to curcumin treated group. $^{\#}P<0.05$ as compared to curcumin and NAC treated group.

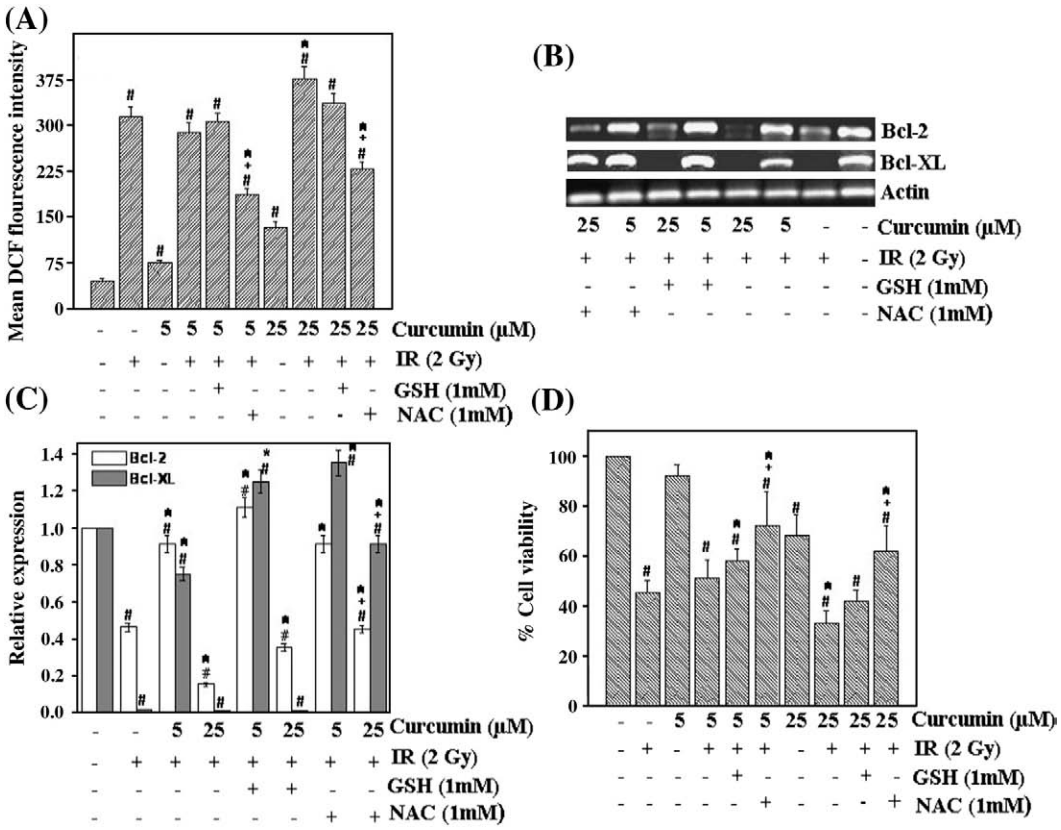

Fig. 5. Effect of curcumin pretreatment at 5 or 25 μM concentration in combination with NAC (1 mM) or GSH (1 mM) on γ-radiation (absorbed dose, 2 Gy) induced oxidative stress in cells. (A) reactive oxygen species levels. (B) RT-PCR analysis showing comparative expression of antiapoptotic genes *Bcl-2* and *Bcl-XL*. (C) Analysis of the relative expression of the above genes under different treatment conditions. (D) Bar graph showing variation in the cell viability. β-actin mRNA expression was used as an internal control. Results presented as mean ± S.E.M. for $n = 3$. $^{\#}P<0.05$ as compared to control cells. $^{*}P<0.05$ as compared cells treated with curcumin. $^{+}P<0.05$ as compared to cells treated with curcumin in presence of GSH.

curcumin addition and exposure to γ-radiation partially inhibited the radiation-mediated decrease in expression of antiapoptotic genes and loss of viability in cells and between the two NAC was better than GSH.

4. Discussion

The circulating monocytes are continuously exposed to oxidative stress and play a key role in inflammation (Rushworth et al., 2006). Curcumin, a well-known antioxidant molecule from the rhizomes of *Curcuma longa* exerts antioxidative and anti-inflammatory effects in monocytes and other cell types and presently in different stages of clinical trials as antitumor agent (Aggarwal et al., 2003; Rushworth et al., 2006; Aggarwal et al., 2007). Besides its antioxidative effects, there is also an increasing evidence that curcumin exhibits pro-oxidative toxicity in proliferating or tumor cells (Bhaumik et al., 1999; Morin et al., 2001; Syng-Ai et al., 2004; Jung et al., 2005; Fang et al., 2005; Sandur et al., 2007a; Li et al., 2008). Therefore it is essential to understand the conditions under which curcumin acts as an antioxidant or pro-oxidant in macrophage cells. In order to address this problem, the present studies were performed by monitoring the changes in cellular redox environment in a concentration and time dependent manner in RAW 264.7 cells. GSH is the major intracellular reducing agent present in millimolar concentrations that protects cells from the oxidants. Exogenously added GSH is cell impermeable (Schafer and Buettner, 2001). Therefore to mimic intracellular concentrations of GSH and to investigate the influence of exogenous GSH on curcumin uptake by cells and its redox modulating ability, the cells were treated with 1 mM concentration of GSH prior to curcumin addition. Since NAC is another thiol containing reducing agent which is permeable to cell and exerts antioxidant effects by increasing intracellular GSH contents, the effect of NAC on curcumin induced modifications was also investigated at equimolar concentration (Hoffer et al., 1997).

Treatment of cells with curcumin (1–25 μM) elevated the DCF fluorescence (reactive oxygen species levels) at 2 h in a concentration dependent manner, similar to the earlier observations (Sandur et al., 2007b). This increase in reactive oxygen species levels at 2 h was also accompanied by decrease in the levels of intracellular non-protein thiols indicating that curcumin provoked oxidative stress early after its addition. Interestingly, we observed that reactive oxygen species levels decreased below basal levels at 18 h after curcumin addition suggesting that the pro-oxidant activity of curcumin was only transient. The mechanism by which curcumin induces reactive oxygen species is not clear. However, it has been proposed that curcumin binds to thioredoxin reductase, thus converting its activity to NADPH oxidase (Fang et al., 2005), which leads to the production of reactive oxygen species. The most important intracellular antioxidant GSH constitutes major non-protein thiols in cells (Sedlack and L'Hanus, 1982; Dickinson and Forman, 2002). The decreased levels of non-protein thiols at early time point (2 h) after curcumin addition may be due to oxidation of GSH to GSSG by reactive oxygen species or due to formation of Michael adduct between GSH and curcumin. However when low concentration of curcumin is available within cells due to poor cellular uptake, reactions of curcumin with GSH are not likely to play a prominent role in lowering non-protein thiols content. The incubation of cells with curcumin for 18 h led to significant increase in levels of non-protein thiols in a concentration dependent manner. The observed increase in non-protein thiols content also ruled out the possibility of formation of Michael adduct of curcumin with GSH in cells, since this reaction would also tend to decrease the non-protein

thiols content. One of the reasons responsible for these observations appear to be the oxidative stress mediated depletion of GSH leading to induction of its intracellular synthesis (Sedlack and L'Hanus, 1982). Additionally curcumin is also reported to increase the biosynthesis of GSH by stimulating the γ-glutamate–cysteine ligase activity (Biswas et al., 2005; Rushworth et al., 2006; Strasser et al., 2005).

Our investigations on the expression of antioxidant enzymes at 6 and 18 h after treatment with 5 or 25 μM curcumin, showed induction of *GPx*, *catalase*, *HO-1* and *Cu,Zn-SOD* genes with increasing time and concentration. Although the exact mechanism(s) by which curcumin activates the expression of these genes is not clearly understood, the observed increase in expression of some of the antioxidant genes like *GPx* and *HO-1* after curcumin addition to cells may be attributed to activation of transcription factor Nrf-2 as reported by Surh et al. (2008). These time course studies reveal that antioxidant effects precede pro-oxidant effects of curcumin. These studies also indicate that the reduced reactive oxygen species levels at 18 h after curcumin addition to cells may be due to elevated *GPx*, *Cu,Zn -SOD* expressions and non-protein thiols levels in the present study.

A striking observation of the present study is that curcumin reduced the *Mn-SOD* gene expression. The transcription factor NF-κB regulates the expression of *Mn-SOD* gene (Murley et al., 2006) and curcumin is a known suppressor of basal and induced NF-κB levels (Shishodia et al., 2005; Duvoix et al., 2005; Sandur et al., 2007a; Everett et al., 2007). Therefore the observed decrease in the *Mn-SOD* expression levels upon curcumin treatment can directly be attributed to inhibition of NF-κB.

The assessment of cell viability at 24 h revealed that curcumin did not induce loss of viability at 5 μM, however lower but significant loss of viability was observed at 25 μM. These results suggest that despite increased expression of antioxidant genes at 25 μM of curcumin, the cells did not survive. The loss of cell viability after treatment at 25 μM curcumin was also evident in terms of the decrease in the expression of antiapototic genes such as *Bcl-2* and *Bcl-XL*, which are required for cell survival. This observed loss of viability may be due to irreversible damage caused by increased production of reactive oxygen species at early time point (2 h), decreased *Mn-SOD* expression and induction of apoptosis. Earlier reports support this argument that increased reactive oxygen species levels leads to cell death and Mn-SOD is essential to protect the cells from mitochondrial oxidative stress (Lebovitz et al., 1996; Liu et al., 2005).

Further the effects of exogenously added reducing agents on curcumin-mediated cellular modifications were studied by pre-treating the cells with GSH or NAC. GSH inhibited curcumin induced oxidative stress and antioxidant effects at 2 and 18 h respectively. However, NAC inhibited the pro-oxidant effects of curcumin at early time point (2 h) and augmented the non-protein thiols levels at 18 h. NAC is a cell permeable reducing agent and acts as a precursor for the synthesis of intracellular GSH (Hoffer et al., 1997). This may be the reason for the additive effect of NAC on curcumin-mediated increase in non-protein thiols levels at 18 h. GSH also lowered the curcumin induced expressions of *GPx*, *Cu,Zn-SOD* and *HO-1* genes and increased the expression of *Mn-SOD* gene. While, NAC increased the curcumin induced expression of *GPx* and reduced the expression of all the other genes examined. The enhanced expression of *GPx* in the presence of NAC may be due to increased intracellular synthesis of GSH (Vivancos and Moreno, 2005). Pretreatment with equimolar (1 mM) concentration of GSH or NAC inhibited curcumin induced cell death however; NAC was more effective than GSH. This differential action could be due to their ability to inhibit cellular uptake of curcumin as GSH is impermeable to cells (Schafer and Buettner, 2001). Our experiments indeed showed that GSH significantly inhibited the cellular uptake of curcumin; however, pretreatment with NAC did not affect curcumin uptake by the cells. The mechanism(s) by which exogenously added GSH prevents the cellular uptake of curcumin is not known. Probably Michael addition reaction of curcumin with GSH in the cell culture medium may be responsible for this observation (Awasthi et al., 2000; Usta et al., 2007).

Studies on the effects of curcumin in combinations with GSH or NAC against γ-radiation induced oxidative stress in RAW cells showed interesting results. At 5 μM, curcumin decreased radiation induced reactive oxygen species production at 2 h and inhibited the loss of cell viability at 24 h only marginally. However, at 25 μM, curcumin significantly enhanced both radiation induced reactive oxygen species production and loss of cell viability. The protective effects at 5 μM were in correlation with the restoration of γ-irradiation induced decrease in *Bcl-2* and *Bcl-XL* expressions, while at 25 μM it completely abolished their expression. As expected, both GSH and NAC enhanced the radioprotective action of curcumin at 5 μM and inhibited the sensitizing activity at 25 μM.

In conclusion, the present studies confirm that both concentration and time of incubation with curcumin differentially modulate levels of reactive oxygen species, non-protein thiols and mRNA expression levels of antioxidant genes in RAW 264.7 cell. Curcumin mediated pro-oxidant action and decrease in *Mn-SOD* expression levels soon after its addition may be responsible for the loss of cell viability at higher concentrations. Reducing agents, GSH or NAC differentially modulated the activity of curcumin and its uptake. Thus, combination of low concentrations of curcumin with reducing agents is a better strategy to improve the antioxidant levels in cells. These studies would also help in the development of new curcumin treatment regimes for its therapeutic applications.

Acknowledgements

The authors are thankful to Drs. K. B. Sainis, T. Mukherjee, and S.K. Sarkar, for their encouragement and support to this work.

Appendix A. Supplementary data

Supplementary data associated with this article can be found, in the online version, at doi:10.1016/j.ejphar.2009.03.060.

References

Aggarwal, B.B., Kumar, A., Bharti, A.C., 2003. Anticancer potential of curcumin: preclinical and clinical studies. Anticancer Res. 23, 363–398.
Aggarwal, B.B., Sundaram, C., Malani, N., Ichikawa, H., 2007. Curcumin: the Indian solid gold. The Molecular Targets and Therapeutic Uses of Curcumin in Health and Disease. Springer, NY USA.
Awasthi, S., Pandya, U., Singhal, S.S., Lin, J.T., Thiviyanathan, V., Seifert Jr., W.E., Awasthi, Y.C., Ansari, G.A., 2000. Curcumin-glutathione interactions and the role of human glutathione *S*-transferase P1-1. Chem. Biol. Interact 128, 19–38.
Balogun, E., Hoque, M., Gong, P., Killeen, E., Green, C.J., Foresti, R., Alam, J., Motterlini, R., 2003. Curcumin activates the haem oxygenase-1 gene via regulation of Nrf2 and the antioxidant-responsive element. Biochem. J. 371, 887–895.
Bhaumik, S., Anjum, R., Rangaraj, N., Pardhasaradhi, B.V., Khar, A., 1999. Curcumin mediated apoptosis in AK-5 tumor cells involves the production of reactive oxygen intermediates. FEBS Lett. 456, 311–314.
Biswas, S.K., McClure, D., Jimenez, L.A., Megson, I.L., Rahman, I., 2005. Curcumin induces glutathione biosynthesis and inhibits NF-kappaB activation and interleukin-8 release in alveolar epithelial cells: mechanism of free radical scavenging activity. Antioxid. Redox Signal. 7, 32–41.
Chattopadhyay, I., Biswas, K., Bandyopadhyay, U., Banerjee, R.K., 2004. Turmeric and curcumin: biological actions and medicinal applications. Curr. Sci. 87, 44–53.
Chen, J., Wanming, D., Zhang, D., Liu, Q., Kang, J., 2005. Water-soluble antioxidants improve the antioxidant and anticancer activity of low concentrations of curcumin in human leukemia cells. Pharmazie 60, 57–61.
Dickinson, D.A., Forman, H.J., 2002. Cellular glutathione and thiols metabolism. Biochem. Pharmacol. 64, 1019–1026.
Duvoix, A., Blasius, R., Delhalle, S., Schnekenburger, M., Morceau, F., Henry, E., Dicato, M., Diederich, M., 2005. Chemopreventive and therapeutic effects of curcumin. Cancer Lett. 223, 181–190.
Everett, P.C., Meyers, J.A., Makkinje, A., Rabbi, M., Lerner, A., 2007. Preclinical assessment of curcumin as a potential therapy for B-CLL. Am. J. Hematol. 82, 22–30.
Fang, J., Lu, J., Holmgren, A., 2005. Thioredoxin reductase is irreversibly modified by curcumin: a novel molecular mechanism for its anticancer activity. J. Biol. Chem. 280, 25284–25290.
Fiala, M., Liu, P.T., Espinosa-Jeffrey, A., Rosenthal, M.J., Bernard, G., Ringman, J.M., Sayre, J., Zhang, L., Zaghi, J., Dejbakhsh, S., Chiang, B., Hui, J., Mahanian, M., Baghaee, A.,

Hong, P., Cashman, J., 2007. Innate immunity and transcription of MGAT-III and Toll-like receptors in Alzheimer's disease patients are improved by bisdemethoxycurcumin. Proc. Natl. Acad. Sci. 104, 12849–12854.
Hail Jr., N., 2008. Mitochondrial reactive oxygen species affect sensitivity to curcumin-induced apoptosis. Free Radic. Biol. Med. 44, 1382–1393.
Han, Y., Son, S.-J., Akhalaia, M., Platonov, A., Son, H.-J., Lee, K.-H., Yun, Y.-S., Song, J.-Y., 2005. Modulation of radiation induced disturbances of antioxidant defense systems by ginsan, vol. 2. eCAM, pp. 529–536.
Hoffer, E.L., Shenker, Y., Baum, Y., Tabak, A., 1997. Paraquat-induced formation of leukotriene B4 in rat lungs: modulation by N-acetylcysteine. Free Radic. Biol. Med. 22, 567–572.
Iqbal, M., Sharma, S.D., Okazaki, Y., Fujisawa, M., Okada, S., 2003. Dietary supplementation of curcumin enhances antioxidant and phase II metabolising enzymes in ddY male mice: possible role in protection against chemical carcinogenesis and toxicity. Pharmacol. Toxicol. 92, 33–38.
Jung, E.M., Lim, J.H., Lee, T.J., Park, J.W., Choi, K.S., Kwon, T.K., 2005. Curcumin sensitises tumor necrosis factor-related apoptosis-inducing ligand (TRAIL)-induced apoptosis through reactive oxygen species-mediated upregulation of death receptor 5 (DR5). Carcinogenesis 26, 1905–1913.
Kunwar, A., Barik, A., Pandey, R., Priyadarsini, K.I., 2006. Transport of liposomal and albumin loaded curcumin to living cells: an absorption and fluorescence spectroscopic study. Biochim. Biophys. Acta 1760, 1513–1520.
Kunwar, A., Mishra, B., Barik, A., Kumbhare, L.B., Pandey, R., Jain, V.K., Priyadarsini, K.I., 2007. 3,3'-Diselenodipropionic acid, an efficient peroxyl radical scavenger and a GPx mimic, protects erythrocytes (RBCs) from AAPH-induced hemolysis. Chem. Res. Toxicol. 20, 1482–1487.
Kunwar, A., Barik, A., Mishra, B., Rathinasamy, K., Pandey, R., Priyadarsini, K.I., 2008. Quantitative cellular uptake, localization and cytotoxicity of curcumin in normal and tumor cells. Biochim. Biophys. Acta 1780, 673–679.
Kurrey, N.K., Amit, K., Bapat, S.A., 2005. Snail and slug are major determinants of ovarian cancer invasiveness at the transcription level. Gynecol. Oncol. 97, 155–165.
Lebovitz, R.M., Zhang, H., Vogel, H., Cartwright, J., Dionne, L., Lu, N., Huang, S., Matzuk, M.M., 1996. Neurodegeneration, myocardial injury, and perinatal death in mitochondrial superoxide dismutase-deficient mice. Proc. Natl. Acad. Sci. U.S.A. 93, 9782–9787.
Li, H., Berlo, D., Shi, T., Speit, G., Knaapen, Ad.M., Borm, P.J.A., Albrecht, C., Schins, R.P.F., 2008. Curcumin protects against cytotoxic and inflammatory effects of quartz particles but causes oxidative DNA damage in a rat lung epithelial cell line. Toxicol. Appl. Pharmacol. 227, 115–124.
Liu, Y., Borchert, G.L., Donald, S.P., Surazynski, A., Hu, C., Weydert, C.J., Oberley, L.W., Phang, J.M., 2005. MnSOD inhibits proline oxidase-induced apoptosis in colorectal cancer cells. Carcinogenesis 26, 1335–1342.
Maclachlan, T., Narayanan, B., Gerlach, V.L., Smithson, G., Gerwien, R.W., Folkerts, O., Fey, E.G., Watkins, B., Seed, T., Alvarez, E., 2005. Human fibroblast growth factor 20 (FGF-20; CG53135-05): a novel cytoprotectant with radioprotective potential. Int. J. Radiat. Biol. 81, 567–579.
Matés, J.M., 2000. Effects of antioxidant enzymes in the molecular control of reactive oxygen species toxicology. Toxicology 153, 83–104.
Morin, D., Barthelemy, S., Zini, R., Labidalle, S., Tillement, J.P., 2001. Curcumin induces the mitochondrial permeability transition pore mediated by membrane protein thiol oxidation. FEBS lett. 495, 131–136.
Motterlini, R., Foresti, R., Bassi, R., Green, C.J., 2000. Curcumin, an antioxidant and anti-inflammatory agent, induces heme oxygenase-1 and protects endothelial cells against oxidative stress. Free Radic. Biol. Med. 28, 1303–1312.
Murley, J.S., Kataoka, Y., Weydert, C.Y., Oberley, L.W., Grdina, D.J., 2006. Delayed radioprotection by nuclear transcription factor κB-mediated induction of manganese superoxide dismutase in human microvascular endothelial cells after exposure to the free radical scavenger WR1065. Free Radic. Biol. Med. 40, 1004–1016.
Priyadarsini, K.I., 1997. Free radical reactions of curcumin in membrane model. Free Radic. Biol. Med. 23, 838–846.
Rahman, I., Biswas, S.K., Kirkham, P.A., 2006. Regulation of inflammation and redox signaling by dietary polyphenol. Biochem. Pharmacol. 72, 1439–1452.
Rushworth, S.W., Ogborne, R.M., Charalambos, C.A., O'Connell, M.A., 2006. Role of PKC δ in curcumin-induced antioxidant response element-mediated gene expression in human monocytes. Biochem. Biophys. Res. Commun. 341, 1007–1016.
Sandur, S.K., Ichikawa, H., Pandey, M.K., Kunnumakkara, A.B., Sung, B., Sethi, G., Aggarwal, B.B., 2007a. Role of pro-oxidants and antioxidants in the anti-inflammatory and apoptotic effects of curcumin (diferuloylmethane). Free Radic. Biol. Med. 43, 568–580.
Sandur, S.K., Pandey, M.K., Sung, B., Ahn, K.S., Murakami, A., Sethi, G., Limtrakul, P., Badmaev, V., Aggarwal, B.B., 2007b. Curcumin, demethoxycurcumin, bisdemethoxycurcumin, tetrahydrocurcumin and turmerones differentially regulate anti-inflammatory and anti-proliferative responses through a ROS-independent mechanism. Carcinogenesis 28, 1765–1773.
Schafer, F.Q., Buettner, G.R., 2001. Redox environment of the cell as viewed through the redox state of the glutathione disulfide/glutathione couple. Free Radic. Biol. Med. 30, 1191–1212.
Sedlack, J., L'Hanus, 1982. Changes in glutathione, protein bound SH-groups concentrations in rat adrenals under acute and repeated stress. Endocrinol. Exp. 16, 103–109.
Sedlak, J., Lindsay, R., 1968. Estimation of total, protein-bound, and nonprotein sulfhydryl groups in tissue with Ellman's reagent. Anal. Biochem. 25, 192–205.
Sharma, O.P., 1976. Antioxidant activity of curcumin and related compounds. Biochem. Pharmacol. 25, 1811–1812.
Sharma, R.A., Gescher, A.J., Steward, W.P., 2005. Curcumin: the story so far. Eur. J. Cancer 41, 1955–1968.
Shishodia, S., Sethi, G., Aggarwal, B.B., 2005. Curcumin: getting back to the roots. Ann. N.Y. Acad. Sci. 1056, 206–217.
Singh, S., 2007. From exotic spice to modern drug. Cell 130, 765–768.
Singh, S., Khar, A., 2006. Biological effects of curcumin and its role in cancer chemoprevention and therapy. Anticancer Agents Med. Chem. 6, 933–946.
Spinks, J.W.T., Woods, R.J., 1990. An introduction to radiation chemistry. Weily Interscience Publication, pp. 95–101.
Strasser, E.M., Wessner, B., Manhart, N., Roth, E., 2005. The relationship between the anti-inflammatory effects of curcumin and cellular glutathione content in myelomonocytic cells. Biochem. Pharmacol. 70, 552–559.
Surh, Y.J., Kundu, J.K., Na, H.K., 2008. Nrf2 as a master redox switch in turning on the cellular signaling involved in the induction of cytoprotective genes by some chemopreventive phytochemicals. Planta Med. 74, 1526–1539.
Syng-Ai, C., Kumari, A.L., Khar, A., 2004. Effect of curcumin on normal and tumor cells: role of glutathione and bcl-2. Mol. Cancer Ther. 3, 1101–1108.
Tolnai, S., 1975. A method for viable cell count. Methods Cell Sci. 1, 37–38.
Usta, M., Wortelboer, H.M., Vervoort, J., Boersma, M.G., Rietjens, I.M., Van Bladeren, P.J., Cnubben, N.H., 2007. Human glutathione S-transferase-mediated glutathione conjugation of curcumin and efflux of these conjugates in Caco-2 cells. Chem. Res. Toxicol. 20, 1895–1902.
Vivancos, M., Moreno, J.J., 2005. β-Sitosterol modulates antioxidant enzyme response in RAW 264.7 macrophages. Free Radic. Biol. Med. 39, 91–97.
Wei, Q.Y., Chen, W.F., Zhou, B., Yang, L., Liu, Z.L., 2006. Inhibition of lipid peroxidation and protein oxidation in rat liver mitochondria by curcumin and its analogues. Biochim. Biophys. Acta 1760, 70–77.

Free Radical Biology & Medicine 48 (2010) 399–410

Contents lists available at ScienceDirect

Free Radical Biology & Medicine

journal homepage: www.elsevier.com/locate/freeradbiomed

Original Contribution

In vivo radioprotection studies of 3,3′-diselenodipropionic acid, a selenocystine derivative

Amit Kunwar [a], P. Bansal [b], S. Jaya Kumar [c], P.P. Bag [a], P. Paul [b], N.D. Reddy [b], L.B. Kumbhare [d], V.K. Jain [d], R.C. Chaubey [c], M.K. Unnikrishnan [b,*], K.I. Priyadarsini [a,*]

[a] Radiation & Photochemistry Division, Bhabha Atomic Research Centre, Trombay, Mumbai 400085, India
[b] Department of Pharmacology, Manipal College of Pharmaceutical Sciences, Manipal 576104, India
[c] Radiation Biology & Health Sciences Division, Bhabha Atomic Research Centre, Trombay, Mumbai 400085, India
[d] Chemistry Division, Bhabha Atomic Research Centre, Trombay, Mumbai 400085, India

ARTICLE INFO

Article history:
Received 20 June 2009
Revised 5 November 2009
Accepted 12 November 2009
Available online 18 November 2009

Keywords:
3,3′-Diselenodipropionic acid
Radioprotection
Antioxidant enzymes
DNA damage
Apoptosis
Survival
Free radicals

ABSTRACT

3,3′-Diselenodipropionic acid (DSePA), a diselenide and a derivative of selenocystine, was evaluated for in vivo radioprotective effects in Swiss albino mice, at an intraperitoneal dose of 2 mg/kg body wt, for 5 days before whole-body exposure to γ-radiation. The radioprotective efficacy was evaluated by assessing protection of the hepatic tissue, the spleen, and the gastrointestinal (GI) tract and survival against sub- and supralethal doses of γ-radiation. DSePA inhibited radiation-induced hepatic lipid peroxidation, protein carbonylation, loss of hepatic function, and damage to the hepatic architecture. DSePA also attenuated the depletion of endogenous antioxidants such as glutathione, glutathione peroxidase, superoxide dismutase, and catalase in the livers of irradiated mice. DSePA also restored the radiation-induced reduction in villus height, crypt cell numbers, and spleen cellularity, indicating protective effects on the GI tract and the hematopoietic system. The results from single-cell gel electrophoresis of the peripheral blood leukocytes showed that DSePA can attenuate radiation-induced DNA damage. The mRNA expression analysis of genes revealed that DSePA augmented *GADD45α* and inhibited *p21* in both spleen and liver tissues. DSePA also inhibited radiation-induced apoptosis in the spleen and reversed radiation-induced alterations in the expression of the proapoptotic *BAX* and the antiapoptotic *Bcl-2* genes. In line with these observations, DSePA improved the 30-day survival of irradiated mice by 35.3%. In conclusion, these findings clearly confirm that DSePA exhibits protective effects against whole-body γ-radiation and the probable mechanisms of action involve the maintenance of antioxidant enzymes, prophylactic action through the attenuation of the DNA damage, and inhibition of apoptosis.

Radiotherapy, a major treatment option for cancers, suffers from an important drawback because normal cells in the vicinity of the tumor could also get exposed to the radiation [1]. Ionizing radiation causes radiolysis of cellular water, generating reactive oxygen species (ROS), which damage organelles. Radioprotectors protect the normal cells from the unwanted radiation damage [2,3]. Since the beginning of the nuclear era, despite extensive research on the development of radioprotectors from natural and synthetic compounds, success has been limited [1–5]. The only clinically acceptable radioprotector, amifostine (an aminothiol), has inherent dose-limiting toxicities and has therefore stimulated extensive search for nontoxic, effective, and alternative radioprotectors [1].

Selenium is a micronutrient, whose deficiency leads to several disorders including neurodegenerative diseases, cardiovascular diseases, arthritis, cancer, cataracts, etc., in humans [6–9]. Its role in chemoprevention, immunomodulation, and anti-inflammatory effects has also been established by several studies involving dietary supplementation with low, nontoxic doses of selenium [8,10–13]. In biological systems, selenium exists in the form of selenoproteins. So far, 25 selenium-containing proteins have been identified in humans, the most important among these being glutathione peroxidase (GPx) [6–8,14,15]. GPx, an antioxidant enzyme, is an important mediator for most of the physiological functions shown by selenium [16]. In the search for effective antioxidants, several research groups are involved in the synthesis of water-soluble, nontoxic selenium compounds with GPx-mimicking activity [17]. In this context, we have recently reported the ROS-scavenging ability and GPx-mimicking activity of a simple, stable, and water-soluble organoselenium compound, 3,3′-diselenodipropionic acid (DSePA) [18,19]. Its antioxidant activity has been confirmed by its ability to protect human erythrocytes from free radical-induced oxidative hemolysis [18]. Preliminary cytotoxicity studies on spleen lymphocytes revealed that DSePA is nontoxic up to 500 μM concentration [18]. These promising results prompted us to

* Corresponding authors. Fax: +91 22 25505151.
E-mail addresses: mkunnikrishnan@gmail.com (M.K. Unnikrishnan), kindira@barc.gov.in (K.I. Priyadarsini).

0891-5849/$ – see front matter © 2009 Elsevier Inc. All rights reserved.
doi:10.1016/j.freeradbiomed.2009.11.009

hypothesize that DSePA might have the potential to protect tissues and organ systems against radiation damage. A recent report by Tak and Park showed that ebselen, an aromatic selenide and potent GPx mimic, exhibits excellent radioprotective activity in both cultured cells and mice, supporting the current hypothesis on application of organoselenium compounds for radioprotection [20]. Therefore, this study investigated the radioprotective effects of DSePA in irradiated Swiss albino mice. The effects of DSePA on the regulation of cellular antioxidant levels, oxidative stress, and apoptosis induced by ionizing radiation have been included. The chemical structure of DSePA is given in Scheme 1.

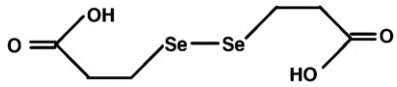

Scheme 1. 3,3′-Diselenodipropionic acid (DSePA).

Materials and methods

Chemicals and animals

Thiobarbituric acid, trichloroacetic acid, butylated hydroxy toluene, 5,5′-dithiobis-2-nitrobenzoic acid, dinitrophenylhydrazine (DNPH), diethyl pyrocarbonate, SYBR Green-II dye, sodium dodecyl sulfate, aspartate, alanine, α-ketoglutarate, sodium sarcosinate, tris base, high- and low-melting-point agarose, ethidium bromide, hydrogen peroxide, xanthine, NADPH, EDTA, Triton X-100, proteinase K, cytochrome *c*, and RNase were purchased from Sigma Chemicals (St. Louis, MO, USA). RT-PCR kit was procured from Invitrogen (Carlsbad, CA, USA). Total RNA isolation kit was obtained from Roche Biochem (Germany). Xanthine oxidase, caspase-3 activity assay kit (QIA 70), and fluorescein frag EL DNA fragmentation detection kit (QIA 39) were obtained from Calbiochem (San Diego, CA, USA). GPx activity was determined using a standard kit (RS 504) obtained from Randox Laboratories (UK). Protein content was determined using bovine serum albumin as a standard protein using a standard kit from M/s Bangalore (Genei, India). All other chemicals with maximum available purity were purchased from reputable local manufacturers/suppliers. The gene-specific primers for reverse transcriptase–polymerase chain reaction (RT-PCR) were custom synthesized from local agents. DSePA was synthesized in our laboratory and characterized as described in our earlier reports [18,19]. The reagent solutions were prepared in Nanopure water from a Millipore Milli-Q system just before use. Absorption spectra were recorded on a JASCO V-530 spectrophotometer and PCR was performed on an Eppendorf gradient cycler. All the in vivo studies were carried out in 7- to 8-week-old male Swiss albino mice weighing around 20–25 g, housed under standard conditions by the Animal House Facility of the Bhabha Atomic Research Centre, Mumbai, and Kasturba Medical College, Manipal, and the experiments were conducted with strict adherence to the ethical guidelines laid down by the Institutional Animal Ethics Committee.

Acute toxicity studies

The acute toxicity of DSePA was determined in fasting mice according to the previously published procedure [21]. Animals were divided into groups of 10 and were injected with DSePA intraperitoneally (ip) in the dose range of 0.25 to 120 mg/kg body wt, observed continuously for 2 h, then frequently up to 6 h, and daily thereafter for 30 days, and mortality, if any, was recorded. The control group was injected ip with saline.

Experimental design for radioprotection studies

Very low nontoxic doses of DSePA were used for investigating its radioprotective potential. DSePA at 2 mg/kg body wt was administered ip for 5 consecutive days before the irradiation. The mice were grouped as follows: Group I, sham control, normal saline; Group II, radiation control; Group III, DSePA control, received DSePA at 2 mg/kg ip for 5 consecutive days; and Group IV, DSePA pretreatment at 2 mg/kg ip daily for 5 consecutive days, followed by irradiation.

Mice were then randomized, placed in ventilated Perspex containers, and subjected to whole body γ-irradiation from a ^{60}Co Theratron–780 (Atomic Energy of Canada Ltd, Canada) at a dose rate of 0.52 Gy/min and an SSD of 100 cm at the Bhabha Atomic Research Centre and from a ^{60}Co Theratron teletherapy unit (Siemens, Germany) at a dose rate of 1.66 Gy/min and an SSD of 55.1 cm at Shirdi Sai Baba Caner Hospital, Manipal. Radiation dose was fixed according to the previous standardizations, in such a way that the irradiated groups suffered significantly greater radiation damage than control groups [21]. After irradiation, the animals were housed under normal laboratory conditions before being sacrificed to study the effects on their hepatic, hematopoietic, and gastrointestinal (GI) systems.

Biochemical assays

The hepatic tissues were homogenized using a Branson sonifier (250; VWR Scientific, Danbury, CT, USA) and centrifuged at 800 *g* for 5 min and the supernatant was used for the estimation of superoxide dismutase (SOD), catalase, thiobarbituric acid-reactive substances (TBARS), glutathione (GSH), and total thiol content using standard spectrophotometric assays as described in previous publications [18,22–25]. The GPx activity and protein content in the tissue fraction were estimated using a standard kit as per the manufacturer's instructions. Protein carbonylation in the liver homogenate was assayed spectrophotometrically using the DNPH labeling procedure as described earlier [26].

Evaluation of hepatic function

Blood samples were collected, serum was separated, and serum alanine aminotransferase (ALT) and aspartate aminotransferase (AST) levels were estimated by the reported method [27]. Activities are expressed as international units/liter.

DNA fragmentation assay in hepatic tissue

The DNA fragmentation assay in hepatic tissue was performed according to a previously described method [28]. Genomic DNA was quantified by measuring the absorbance at 260 nm. DNA fragmentation was studied by electrophoresis on a 1.5% agarose gel and the pattern of fragmentation was visualized by a gel documentation unit (U-Genius, Syngene, Germany).

Gene expression analysis at mRNA level by RT-PCR

Total RNA was isolated from the spleen and the hepatic tissue and 2 μg of total RNA was used for the synthesis of cDNA by reverse transcription. The cDNA was amplified using 1 μl of the reaction products in 25 μl with 10 pmol of the primers for 35 cycles. Each cycle consisted of 30 s of denaturation at 94°C, 30 s of annealing at 57°C, and 60 s of extension at 72°C. The primers used for cDNA amplification (forward and reverse) included GAPDH, 5′-AATGTGTCCGTCGTGGATCTGA-3′, 5′-GATGCCTGCTTCACCACCTTCT-3′; p21, 5′-ATGTCCAATCCTGGTGATGT-3′, 5′-TGCAGCAGGGCAGAGGAAGT-3′; GADD45α, 5′-TGGTGACGAACCCACATTCAT-3′, 5′-ACCCACTGATCCATGTAGCGAC-3′; Bcl-2, 5′-TTCGCAGCGATGTCCAGTCAGCT-3′, 5′-

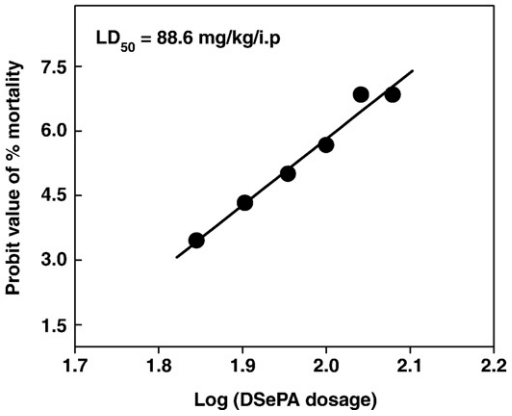

Fig. 1. Determination of LD_{50} dosage of DSePA in Swiss albino mice ($n=10$).

TGAAGAGTTCTTCCAACCACCGT-3′; and BAX, 5′-ATGCGTCCACCAAA-GAAGCTGA-3′, 5′-AGCAATCATCCTCTGCAGCTCC-3′.

Glyceraldehyde-3-phosphate dehydrogenase (*GAPDH*) was used as internal control in all reactions. The band intensity was quantified by GelQuant software (version 2.7; DNR Imaging Systems Ltd., Israel). Relative changes were calculated after normalization to *GAPDH*.

Alkaline single-cell gel electrophoresis (comet assay)

Blood from the tail of each animal was collected in heparinized vials and two microscopy slides from the blood samples of each animal were prepared and processed for comet assay as described previously [29]. The slides were immersed in lysis buffer for 1 h at 4°C and equilibrated in alkaline solution for 20 min, followed by electrophoresis for 30 min at 22 V, 299 mA. After electrophoresis, the slides were neutralized and stained by 5× SYBR Green-II dye. The images were captured using a Carl Zeiss Axioplan fluorescence microscope (Germany). Fifty images per slide were analyzed for percentage DNA content in the tail, tail length (TL), tail moment (TM), and olive tail moment (OTM) using CASP software.

Endogenous spleen colony assay

Animals were sacrificed and the spleens were removed immediately, blotted free of blood, and weighed and the spleen index was calculated (spleen index = (spleen wt/body wt) × 100). Subsequently, the spleens were fixed in Bouin's fixative and the spleen colony-forming units (CFUs) were counted manually as described previously [21].

Apoptosis assay in splenocytes and tissue sections

Animals from the various groups were sacrificed immediately after irradiation, spleens were removed, and splenocytes were isolated as described previously [22]. After the splenocyte viability was checked by trypan blue dye exclusion test, 1×10^6 cells/ml per well were seeded in six-well plates and incubated for 18 h at 37°C. The cells were collected by centrifugation, washed three times with cold PBS, and processed for caspase-3 activity and TUNEL staining, using standard kits, and the TUNEL-positive cells were quantified using fluorescence confocal microscopy and a Partec PAS III flow cytometer equipped with FloMax software. Similar TUNEL staining was performed in the sections of spleen tissue [30].

Histopathological studies of hepatic and intestinal tissues

The hepatic and jejunal tissues were fixed in 10% neutral-buffered formalin, dehydrated by passing through a graded series of alcohol, and embedded in paraffin blocks and 5-μm sections were prepared, stained successively in eosin and Harris hematoxylin, and examined using an upright trinocular microscope attached to a CCD camera [30].

Survival studies

Animals were divided into four groups of 20 each, as described under experimental design for radioprotection studies. Radiation control groups received 10 Gy of radiation, whereas treated groups received DSePA at 2 and 4 mg/kg/ip for 5 consecutive days before 10 Gy irradiation. The animals were monitored daily for 30 days after irradiation, and mortality was recorded. Survival curves were drawn by plotting percentage survival as a function of postirradiation day.

Statistical analysis

Experiments were performed in triplicate and the results are presented as means ± SEM. The data were analyzed by one-way ANOVA using Origin (version 6.1) software to confirm the variability of data and validity of results. Paired *t* test from Origin (version 6.1) software was used for the comparison of means and $P<0.05$ was considered statistically significant.

Results

Acute toxicity studies

Administration of DSePA at a dose of 0.25–40 mg/kg did not produce any noticeable signs of toxicity within 30 days. However,

Table 1
Hepatoprotective effects of DSePA against γ-radiation (3 Gy)-induced biochemical changes ($n=5$)

Assay	Treatment			
	Control	DSePA control	Radiation (3 Gy)	Radiation (3 Gy) + DSePA
SOD (U/mg protein)	18.76 ± 2.93	18.32 ± 2.51	9.8 ± 1.49*	13.88 ± 1.69*,†
Catalase (U/mg protein)	77.3 ± 12.55	69.1 ± 6.56	60.5 ± 4.93	69.5 ± 7.35
GPx (U/mg protein)	59.8 ± 4.23	73.3 ± 6.33*	42.6 ± 6.12*	68.5 ± 5.66†
GSH (nmol/mg protein)	9.07 ± 0.45	7.87 ± 0.39*	5.07 ± 0.25*	10.8 ± 0.54*,†
Total thiol (μmol/mg protein)	0.71 ± 0.03	0.67 ± 0.03	0.54 ± 0.02*	0.62 ± 0.03*,†
TBARS (nmol/mg protein)	0.26 ± 0.01	0.21 ± 0.01*	0.35 ± 0.01*	0.23 ± 0.01*,†
Protein carbonyls (nmol/mg protein)	1.05 ± 0.10	1.09 ± 0.10	1.73 ± 0.16*	1.49 ± 0.14*,†
ALT (U/L)	41 ± 9.05	52 ± 8.6	94 ± 17.7*	64 ± 8.2*,†
AST (U/L)	27 ± 6.35	35 ± 5.75	75 ± 17.75*	42 ± 9.1†

Results are presented as means ± SEM ($n=5$).
* $P<0.05$ compared to control group.
† $P<0.05$ compared to irradiated group.

increasing the dosage to 120 mg/kg resulted in the death of mice within 24 h. Therefore, the effects of graded doses between 40 and 120 mg/kg on the survival of the mice were studied. The average percentage mortality ($n=10$) was converted into probit values according to published procedures [31,32]. LD_{50} was estimated as 88.6 mg/kg ip from a plot of probit values against logarithmic dose of DSePA (Fig. 1). Furthermore, as per convention, 1/10 of the LD_{50} is considered the maximum tolerated dose (MTD) [32], which is equivalent to 8.6 mg/kg body wt (ip). Therefore, safe and nontoxic doses of 2.0 and 4.0 mg/kg were selected for the survival studies. The most effective dose of 2.0 mg/kg was subsequently employed for the detailed radioprotection studies in the mice.

Hepatoprotection

The effects of DSePA on the enzymatic and nonenzymatic intracellular antioxidant status were investigated in the hepatic tissues of the mice at 24 h after exposure to a radiation dose of 3 Gy. Irradiation decreased the activities of the enzymes such as GPx, catalase, and SOD by 29, 22, and 48%, respectively, compared to the sham controls (Table 1). DSePA pretreatment ameliorated the effects of the radiation exposure and resulted in a significant increase in the activities of GPx, catalase, and SOD enzymes by 62, 15, and 44%, respectively, compared to the radiation control group. The DSePA control group showed negligible change in the activities of SOD and catalase

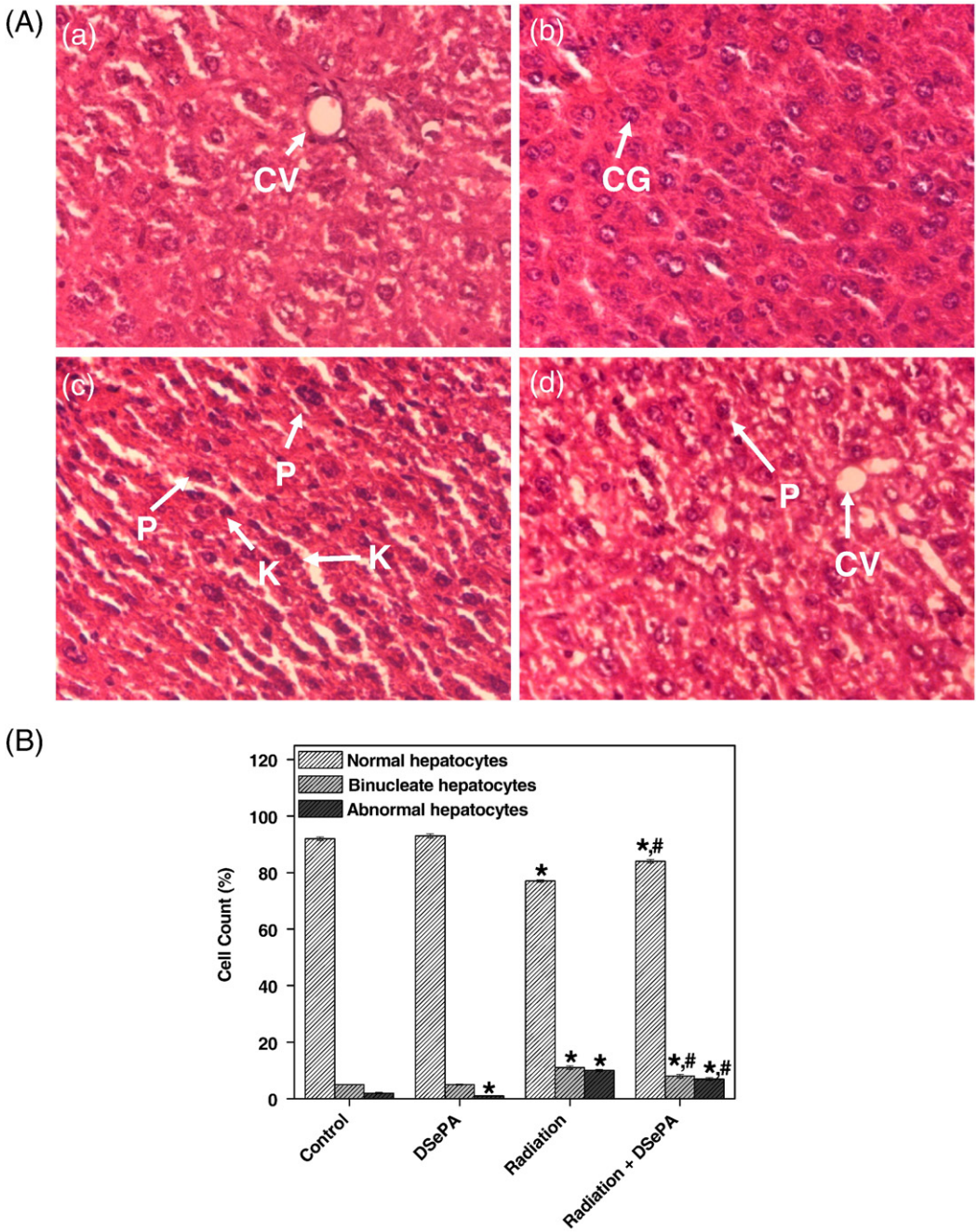

Fig. 2. Histopathological analysis of hepatic tissue sections performed on day 7 postirradiation (5 Gy). (A) Images a, normal control; b, DSePA control; c, radiation control; d, DSePA pretreated and exposed to γ-radiation. CV, central vein; K, inflammatory Kupffer cell; CG, chromatin granule; P, pyknotic nucleus; 400× original magnification. (B) Bar graph showing percentage variation in the count of normal, binucleate, and abnormal hepatic cells under the above treatment conditions. Results are presented as means ± SEM ($n=5$). $^{*}P<0.05$ compared to the control group, $^{\#}P<0.05$ compared to the irradiated group.

enzymes; however, there was a significant increase (1.5-fold) in the GPx activity compared to the sham control group. Table 1 also lists the levels of total thiols and GSH in the hepatic tissues of the treatment groups. It can be seen that irradiation led to a significant decrease in the total thiols and GSH levels; however, DSePA pretreatment prevented this. The DSePA control group showed negligible changes in total thiols and GSH levels compared to the sham control group.

The values presented in Table 1 also indicate that exposure to γ-radiation caused significant increases in the levels of protein carbonyls and TBARS in the hepatic tissues compared to the sham control group. DSePA pretreatment reduced lipid peroxidation and protein carbonyls by 34 and 14%, respectively, compared to the radiation control group. There was neither oxidation of proteins nor lipid peroxidation in the DSePA control group. The effect of DSePA pretreatment on hepatic function was evaluated on day 7 postirradiation from the levels of serum ALT and AST (Table 1). Exposure to γ-radiation significantly increased both serum ALT (130%) and serum AST (179%), whereas DSePA pretreatment ameliorated the irradiation-induced elevations in serum ALT and AST. Although DSePA treatment was unable to restore the enzyme levels to normal, that of ALT was reduced from 130 to 58% and AST from 179 to 55%. On the other hand, DSePA by itself did not increase the ALT and AST levels noticeably (Table 1).

The effects of DSePA on the γ-radiation-induced hepatic architectural changes were studied on day 3 of exposure to an absorbed dose of 5 Gy. Liver histopathology in the radiation control groups indicated fragmentation of the hepatic cells along with the appearance of pyknotic and inflammatory Kupffer cells (Figs. 2A, image c, and 2B). The hepatocytes appeared normal in the DSePA control group (Figs. 2A, image b, and 2B). Further, pretreatment with DSePA not only improved the morphology of the irradiated hepatocytes but also decreased the number of pyknotic and Kupffer cells (Figs. 2A, image d, and 2B). Therefore, the results indicate a prophylactic action of DSePA against the γ-radiation induced hepatic damage.

Hematopoietic protection

Effects of DSePA on the spleen index, spleen cellularity, and spleen colony formation were studied on day 11 of exposure to an absorbed dose of 7.5 Gy and the results are shown in Figs. 3A–C, respectively. Irradiation significantly reduced the spleen index to 0.19 ± 0.01 compared to the sham control (0.53 ± 0.03), whereas the DSePA pretreatment improved the spleen index to 0.36 ± 0.06. The spleen cellularity improved from 32% in the irradiated group to 60% with the DSePA pretreatment. Another important indicator of hematopoietic protection is the abundance of macroscopic colonies (measured as CFUs) that form in the irradiated spleens. DSePA pretreatment enhanced CFUs by a factor of 2.5 (8.50 ± 1.18 in DSePA vs 3.20 ± 0.37 in radiation control). However, DSePA, by itself did not significantly alter the spleen index, spleen weight, or CFUs.

GI protection

Results in Fig. 4 show the effects of DSePA against γ-radiation-induced GI damage, studied on day 3 of exposure to 7.5 Gy γ-radiation. A significant decrease in the number of villi, villus height, crypts, and goblet cells per crypt was observed in the radiation control group compared to the sham control group. Also, increases in the number of dead cells, number of inflammatory cells, and infiltration of fibroblasts were noticed in intestinal (jejunum) tissue of the radiation control group. DSePA pretreatment protected the crypts, the villi, and the villus height from the radiation damage, whereas there was no noticeable change in the goblet cells and the dead cells postirradiation (Figs. 4A, B). No anatomical changes were observed in the DSePA control group.

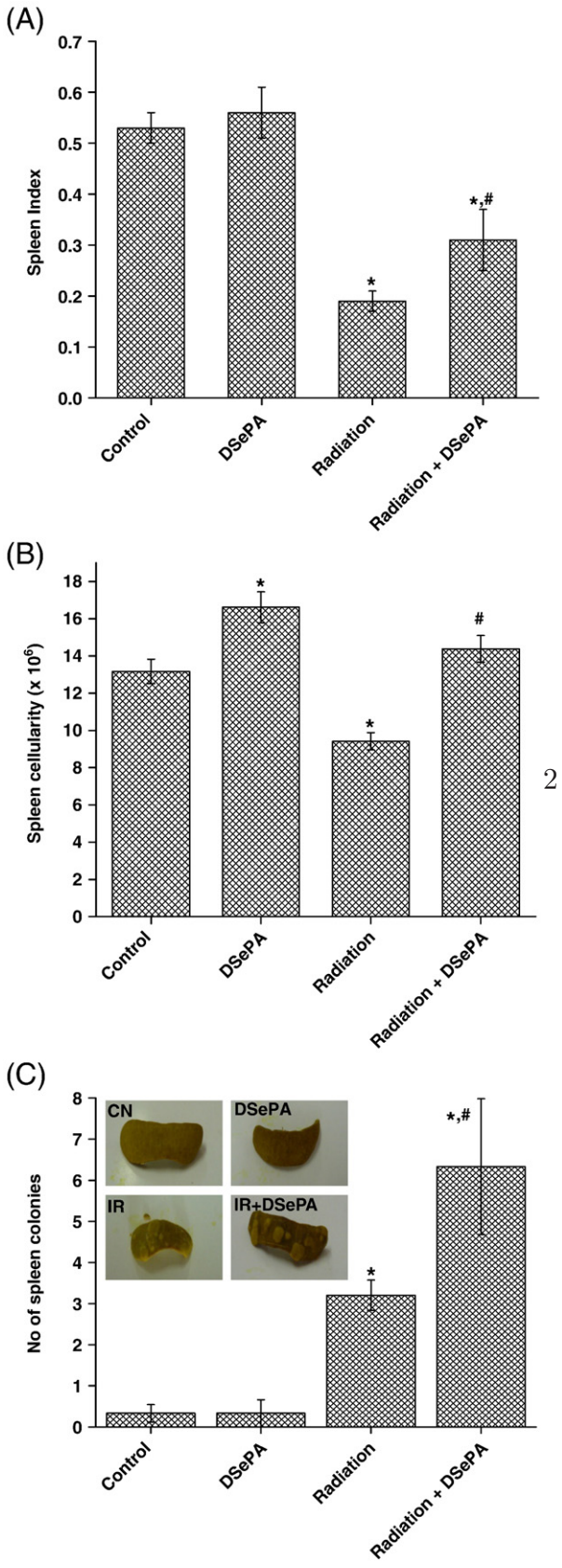

Fig. 3. Effects of DSePA on spleen parameters as monitored on day 11 after irradiation at 7.5 Gy. (A) Spleen index; (B) spleen cellularity; (C) spleen colonies. Results are presented as means ± SEM ($n = 5$). *$P < 0.05$ compared to the control group, $^{\#}P < 0.05$ compared to the irradiated group. IR, irradiation.

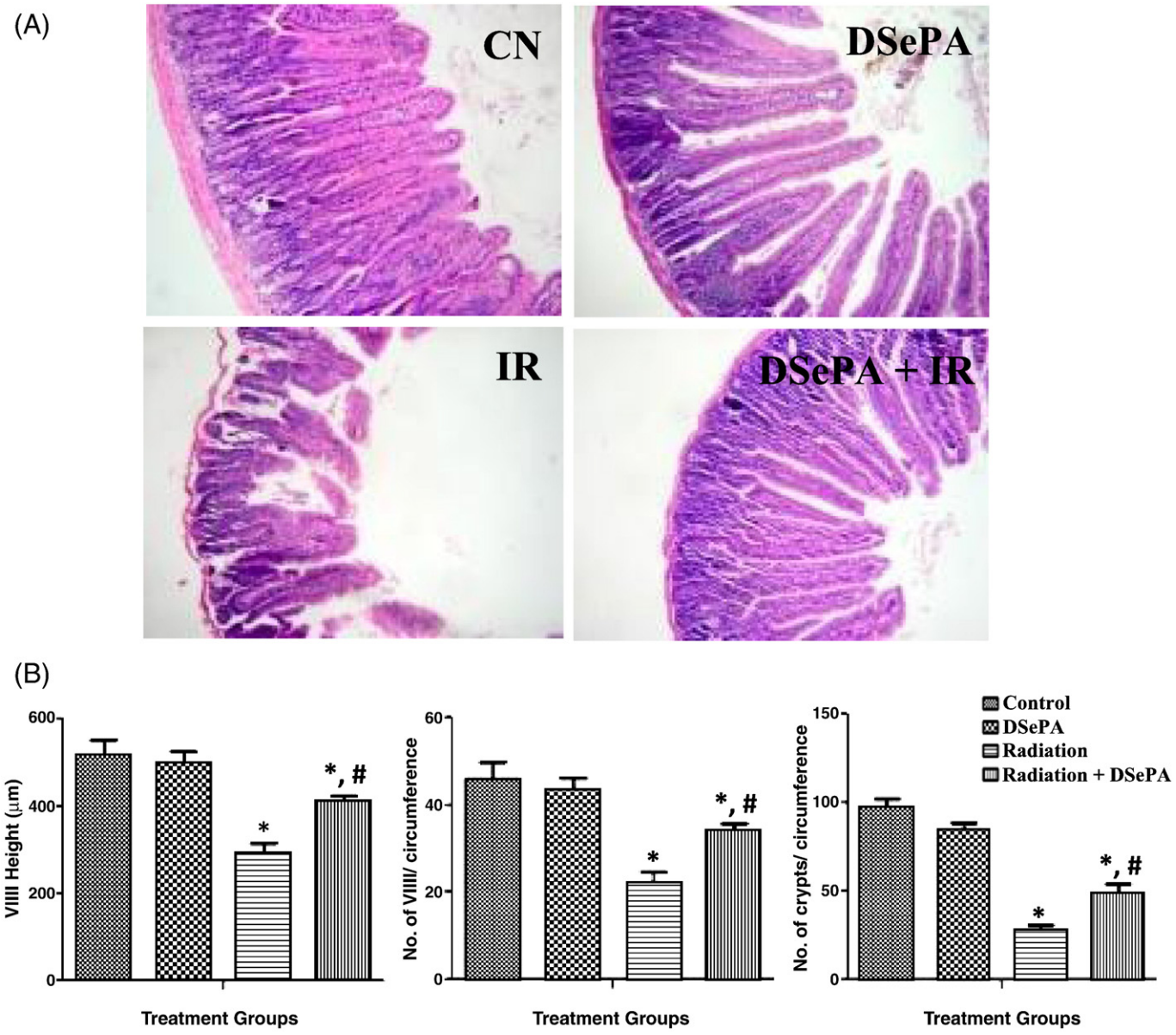

Fig. 4. Effects on DSePA on GI (jejunum) parameters as monitored on day 3 postirradiation (7.5 Gy). (A) Histopathology of jejunum excised from animals of the various groups. CN, control; IR, irradiation. (B) Bar graph showing average villus height, No. of villi, and No. of crypts obtained by analyzing 10 sections/mouse ($n = 5$). *$P<0.05$ compared to the control group, $^{\#}P<0.05$ compared to the irradiated group.

Inhibition of DNA damage in peripheral blood leukocytes and hepatic tissue

The effects of DSePA against radiation-induced DNA damage in peripheral blood leukocytes were investigated using single-cell gel electrophoresis at 30 min after exposure to a radiation dose of 3 Gy. Nucleoids of the cells in the sham control appeared circular, whereas those in the radiation control looked like comets, with fluorescence intensity diminishing from the head to the tail, indicating DNA damage. Fig. 5A shows the frequency distribution histograms of TL, TM, OTM, and percentage of DNA in the tail of leukocytes isolated from the animals of the treatment groups. DSePA pretreatment significantly decreased TL, TM, OTM, and the percentage DNA in the irradiated cells compared to those observed in the radiation control. All the comet parameters in the DSePA control group were similar to those of the sham control, indicating that DSePA by itself does not induce any DNA damage.

The integrity of genomic DNA from hepatic tissue under similar treatment conditions was also evaluated using agarose gel electrophoresis (Fig. 5B). The damaged DNA in the radiation control appeared as a smear of a few low-molecular-weight fragments. DSePA pretreatment reduced the shearing of DNA caused by the radiation.

Modulation in the mRNA expression of DNA damage-responsive genes and inhibition of apoptosis

The modulatory effects of DSePA on the DNA damage-responsive genes were studied by evaluating the mRNA expression levels of the *p21* and *GADD45α* genes in the spleen and the liver at 3 h after exposure to 3 Gy γ-irradiation. Fig. 6 shows the RT-PCR analysis of *p21* and *GADD45α*, along with their relative expression levels. DSePA treatment per se significantly increased the expression of *GADD45α* in the spleen but not in the liver. On the other hand, DSePA, by itself, significantly decreased the expression of *p21* in the liver but not in the spleen. The results also show that irradiation substantially increased the levels of *p21* and *GADD45α* in both the spleen and the liver compared to the sham control group. However, the levels of induction were lower in the former, probably resulting in greater radiation sensitivity in the spleen than in the liver. DSePA pretreatment significantly attenuated the radiation-induced

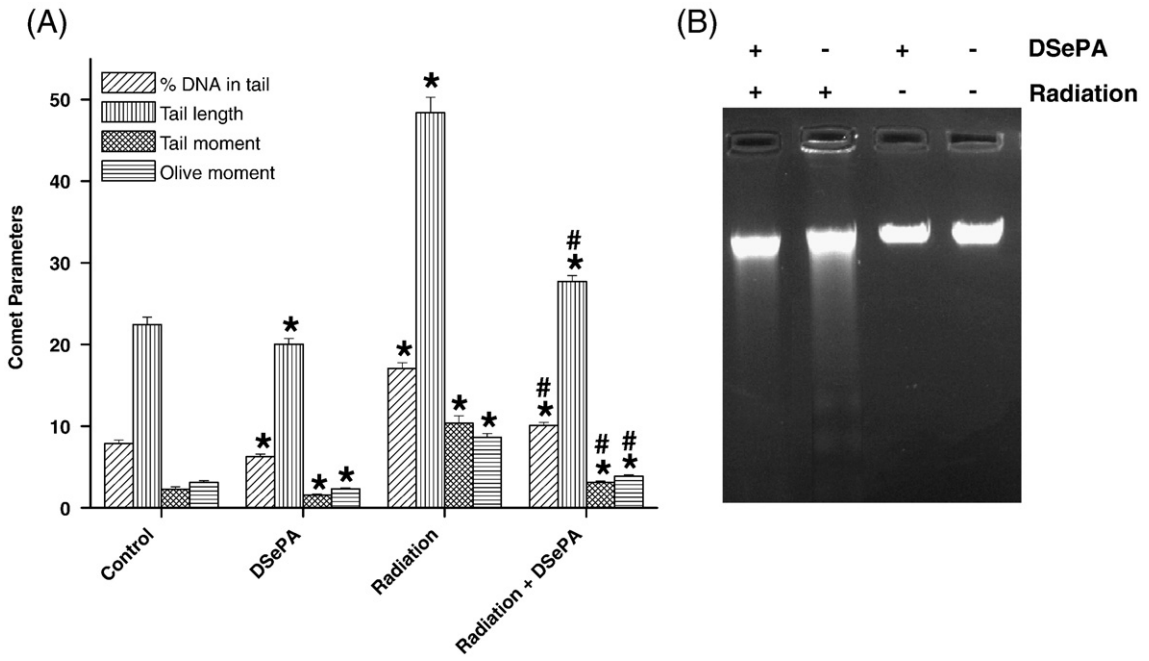

Fig. 5. Effects of DSePA on γ-radiation-induced DNA damage at 30 min postirradiation (3 Gy). (A) Alkali comet assay of peripheral leukocytes. Bar graph represents means ± SEM obtained by analyzing 100 cells/mouse ($n = 5$). *$P < 0.05$ compared to the control group, #$P < 0.05$ compared to the irradiated group. (B) DNA fragmentation in mouse hepatic tissue by agarose gel electrophoresis ($n = 5$).

p21 expression in both tissues, but did not reverse it to the normal levels of the sham control group. Additionally, DSePA augmented the expression level of *GADD45α* in both tissues postirradiation.

The above changes in the expression of cell cycle and DNA repair genes should lead to a decrease in radiation-induced apoptosis. To establish this, we monitored the mRNA expression levels of a

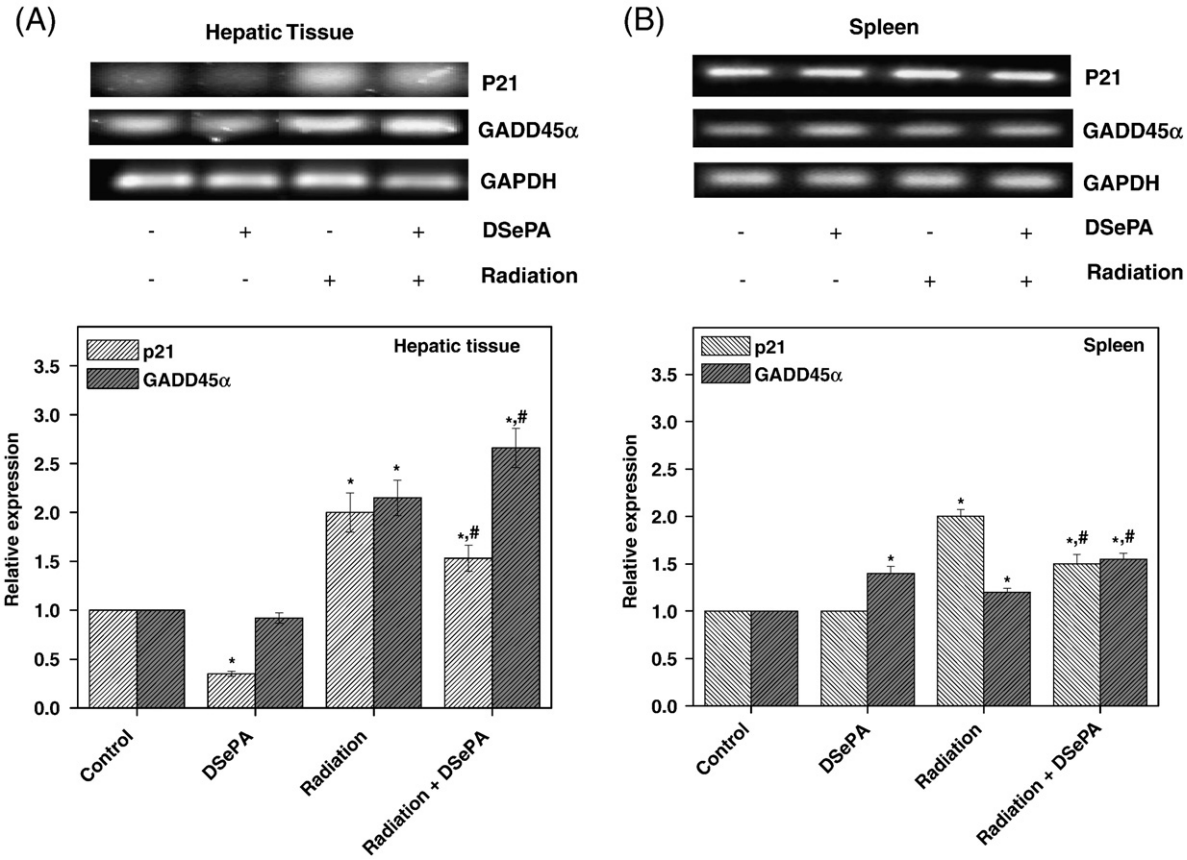

Fig. 6. Effects of DSePA on the mRNA expression of *p21* and *GADD45α* genes at 3 h postirradiation (3 Gy). (A) RT-PCR analysis and bar graph showing variation in the relative mRNA expression of *p21* and *GADD45α* in hepatic tissue. (B) RT-PCR analysis and bar graph showing variation in the relative mRNA expression of *p21* and *GADD45α* in spleen. Results are presented as means ± SEM ($n = 5$). *$P < 0.05$ compared to the control group, #$P < 0.05$ compared to the irradiated group.

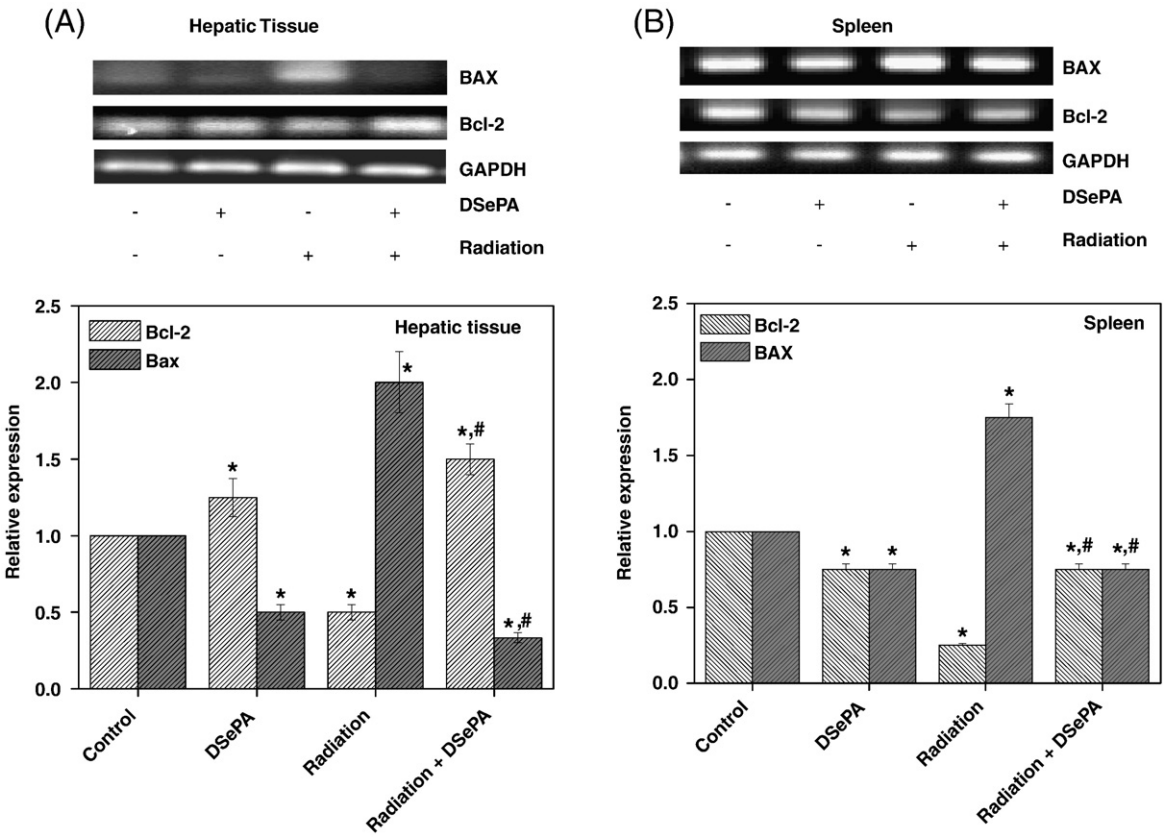

Fig. 7. Effects of DSePA on the mRNA expression of *Bcl-2* and *BAX* genes at 24 h postirradiation (3 Gy). (A) RT-PCR analysis and bar graph showing variation in the relative mRNA expression of *BAX* and *Bcl-2* in hepatic tissue. (B) RT-PCR analysis and bar graph showing variation in the relative mRNA expression of *BAX* and *Bcl-2* in spleen. Results are presented as means ± SEM ($n = 5$). *$P<0.05$ compared to the control group, $^{\#}P<0.05$ compared to the irradiated group.

proapoptotic (*BAX*) and an antiapoptotic (*Bcl-2*) gene in both the spleen and the liver at 24 h postirradiation. Fig. 7 shows the RT-PCR analysis of these two genes and their relative expression levels. Results indicate that irradiation decreased *Bcl-2* expression and increased the expression of *BAX* (notably) in both the spleen and the liver compared to the sham controls. DSePA pretreatment reversed these changes by increasing the *Bcl-2* and reducing the *BAX* levels. The DSePA control group showed a significant increase in *Bcl-2* expression and decrease in *BAX* expression in the liver, whereas in the spleen the expression of both genes was significantly reduced.

Furthermore, the effects of DSePA on cellular markers of apoptosis were studied in splenocytes and spleen tissue at 18 h after irradiation as shown by the fluorescence images of TUNEL-labeled cells in Figs. 8A and B, respectively. The figures indicate that DSePA pretreatment significantly attenuated the radiation-induced increase in apoptotic cells. This was also verified by the flow cytometric acquisition of TUNEL-labeled cells under similar treatment conditions as shown in Figs. 9A–D. Analysis of these data, as shown in the bar graph in Fig. 9E, suggested that pretreatment with DSePA reduced the radiation-induced apoptosis by ~20%. Cellular apoptosis is accompanied by the activation of terminal proteases such as caspase-3; therefore its activity was also determined under similar treatment conditions. The results, represented as a bar graph in Fig. 10, showed an approximately three-fold increase in caspase-3 activity in the irradiated group compared to the control group, which was significantly reduced in the DSePA-pretreated group. Here, the drug control group showed an ~19% induction of apoptosis compared to the control group.

Survival studies

The effects of DSePA on the survival of the mice were evaluated after whole-body γ-irradiation at a lethal dose of 10 Gy and the survival curve is shown in Fig. 11. The radiation control group exhibited signs of radiation sickness such as reduced intake of food and water, irritability, lethargy, ruffling of hair, weight loss, diarrhea, emaciation, and epilation, with median survival of only 9 days. DSePA pretreatment lowered the radiation sickness characteristics and increased the median survival time to 14 days. In the DSePA-treated group, the survival of animals at the end of 30 days after irradiation increased by 35.3%. The DSePA control group did not show any toxic effects during the study period. A similar study at an increased dose of 4 mg/kg/ip did not show much improvement in the survival of the animals (results not shown).

Discussion

The similarities in the chemical properties of selenium and sulfur compounds prompted researchers to explore selenium compounds as new class of radioprotectors [20,33–35]. Sodium selenite and selenomethionine were the first few compounds examined for in vivo radioprotection [33–35]. The results indicated that selenium in the organic form is more effective than in the inorganic form. Our earlier publications reported the antioxidant and in vitro radioprotective effects of DSePA that established that DSePA was nontoxic and showed potent radioprotective activity [18,36]. This encouraged us to evaluate DSePA for in vivo radioprotection.

Acute toxicity is an important parameter to be assessed before performing in vivo experiments [31,32]. As the MTD for DSePA was 8 mg/kg/ip, we chose two nontoxic and safe doses of 2 and 4 mg/kg/ip for the survival studies. Subsequently the most appropriate dose of 2 mg/kg from the survival data was selected for assessing the protection to various organs against γ-radiation.

As anticipated, the irradiation increased lipid peroxidation and protein carbonyl levels while depleting the antioxidant enzymes and

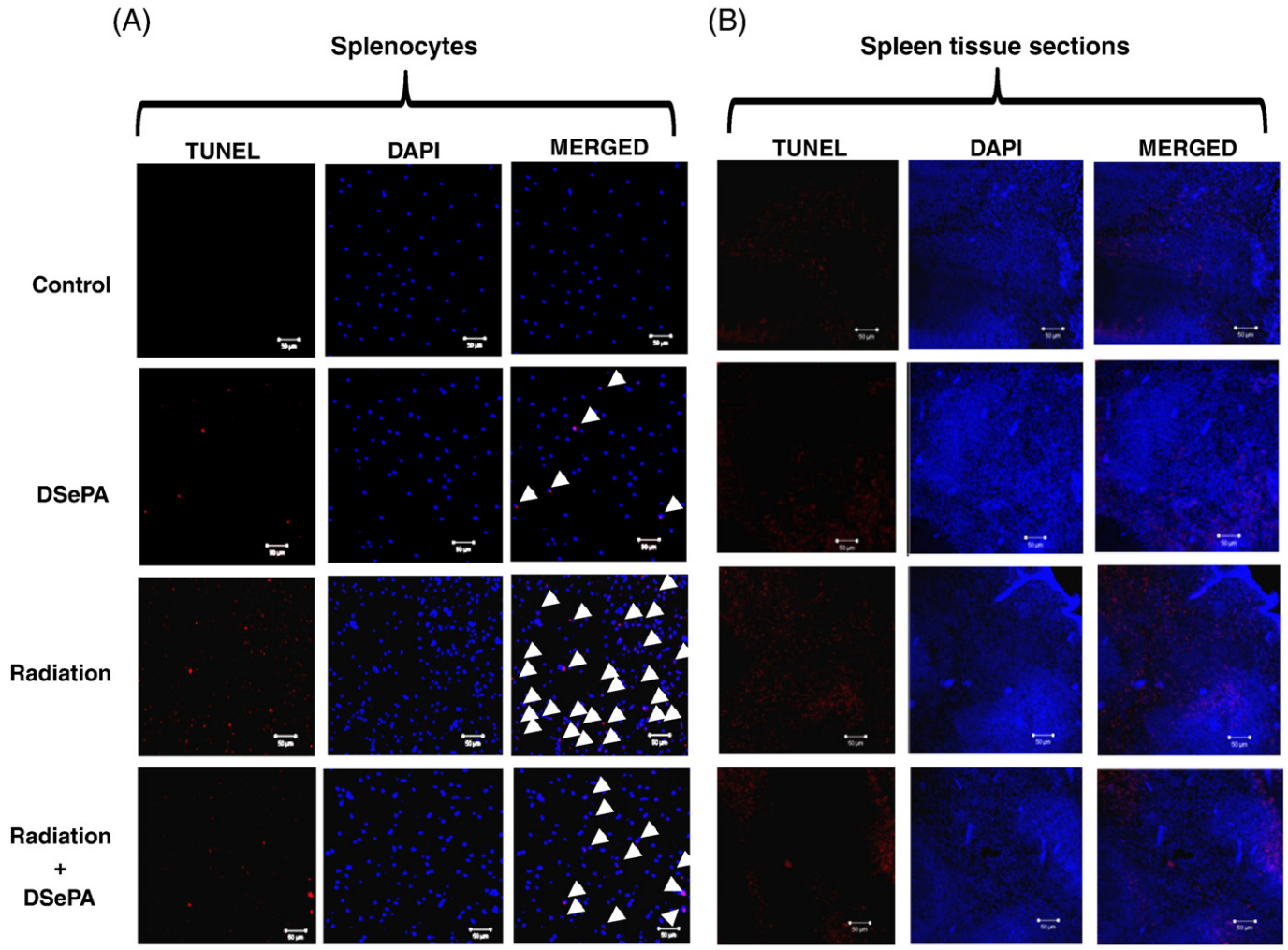

Fig. 8. Effects of DSePA against γ-radiation (3 Gy)-induced apoptosis at 18 h postirradiation as monitored by fluorescence confocal microscopy after TUNEL staining of (A) splenocytes and (B) sections of spleen tissue. The counterstaining by the nucleus-specific DAPI probe indicates the total number of cells. (The fluorescence emissions from TUNEL-positive cells are pseudocolored red; 20× original magnification; arrows point to TUNEL-positive cells.)

the total thiols [21,37–39]. Furthermore, irradiation also resulted in DNA damage and histological abnormalities in the liver [28]. Most importantly, the leakage of hepatic enzymes into the plasma is a critical parameter indicating hepatic injury [40]. The radiation-induced increase in serum AST and ALT levels indicating hepatic structural damage was reversed by DSePA pretreatment, suggesting a significant hepatoprotective effect against radiation [40]. Restoration of the normal hepatic architecture by DSePA indicates a possible prophylactic mechanism of action.

The hematopoietic system and the GI tract, two critically important systems for survival, are also susceptible to radiation-induced damage [41,42]. The spleen index is an important marker to monitor damage to the hematopoietic system. In this study, DSePA pretreatment protected the mice from hematopoietic injury as seen from the increase in the spleen index, the number of spleen colonies, and the cellularity, with respect to the radiation control. Additionally, DSePA prevented DNA damage in the peripheral leukocytes as shown by the decrease in the comet parameters. Similarly, DSePA attenuated radiation-induced damage to the crypts and the villus cells and maintained the villus height. It also prevented the infiltration of inflammatory cells, dead cells, mitotic cells, and hypertrophy of the muscularis mucosa, confirming its ability to protect the GI tract.

An attempt was made to understand the mechanisms responsible for the observed radioprotection. Important molecular mechanisms responsible for radioprotection are free radical scavenging, repair of free radical-induced damage, and inhibition of free radical-initiated apoptosis [2,37]. Our earlier reports indicated that DSePA effectively scavenged peroxyl and hydroxyl radicals with rate constants comparable to those of well-known antioxidants [18,43]. Therefore, this radical-scavenging power of DSePA may be responsible for the inhibition of lipid peroxidation, protein carbonylation, and DNA damage and also the maintenance of the tissue antioxidant status. DSePA itself had no effect on the activity of SOD and catalase; however, being a selenium compound, it was able to increase the levels of GPx [20,35].

In response to radiation-induced DNA damage, cells activate the *p21* and *GADD45α* genes, which regulate the cell cycle arrest at G1/S and G2/M, respectively. GADD45α is specifically associated with DNA repair and the prevention of apoptosis in normal cells [44–50]. If DNA repair is not successful, the cells undergo apoptosis by activation of the intrinsic pathway involving the induction of the proapoptotic gene *BAX* and suppression of the antiapoptotic gene *Bcl-2* [51]. Therefore, studying the effects of DSePA on the expression of the above genes postirradiation can provide insight into the pathways involved in radioprotection. Accordingly, we observed that DSePA pretreatment augmented the *GADD45α* gene and attenuated the *p21* gene in the irradiated tissues. The decrease in *p21* expression indicated that DSePA prevented radiation-induced DNA damage in the early stages of the cell cycle. However, the augmentation of *GADD45α* by DSePA may have a role in postirradiative DNA repair [44–50]. Also, in accordance

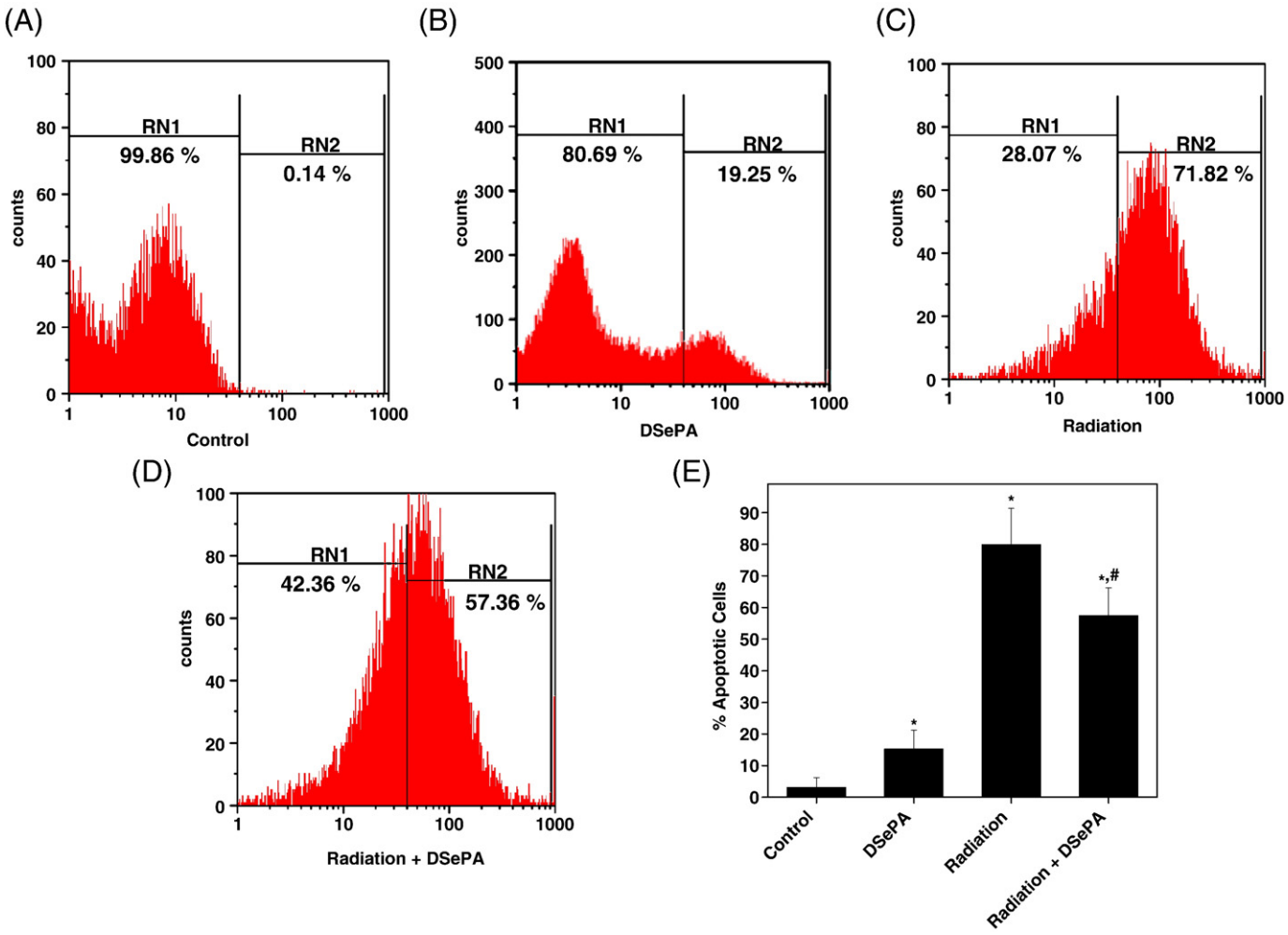

Fig. 9. Flow cytometry acquisition of splenocytes labeled with the TUNEL method at 18 h postirradiation. (A) Control group; (B) drug or DSePA control group; (C) radiation (3 Gy) control group; (D) DSePA-pretreated group. (E) Bar graph showing percentage apoptotic (TUNEL-positive) cells under the various treatment conditions. The gated regions RN1 and RN2 represent distributions of TUNEL-negative and -positive cells, respectively. $^{*}P<0.05$ compared to the control group, $^{\#}P<0.05$ compared to the irradiated group.

with the modulation in the expression of the above genes, DSePA pretreatment significantly reduced the expression of *BAX* and simultaneously increased the expression of *Bcl-2* in both the spleen and the liver. Previous reports suggest that proliferating cells such as lymphocytes are more sensitive to radiation-induced apoptosis, possibly resulting from inefficient DNA repair [51,52]. In agreement with this, we observed a slightly diminished level of the induction of the *GADD45α* gene and a much higher BAX/Bcl-2 ratio (a determinant of the apoptotic

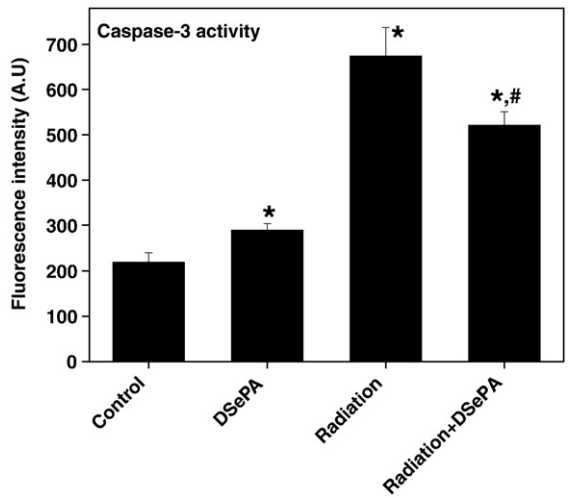

Fig. 10. Bar graph showing caspase-3 activity in splenocytes under the various treatment conditions as determined by spectrofluorimetry at 18 h postirradiation (3 Gy). Results are presented as means ± SEM ($n=5$). $^{*}P<0.05$ compared to the control group, $^{\#}P<0.05$ compared to the irradiated group.

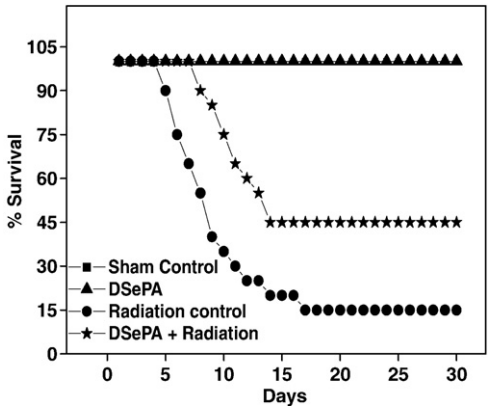

Fig. 11. Kaplan–Meier estimate of 30-day survival of whole-body γ-irradiated (10 Gy) mice preadministered DSePA in comparison to other groups. Results are presented as means ± SEM ($n=20$). The survival curve comparisons between the groups were performed using GraphPad Prism version 5.02, using the log-rank (Mantel–Cox) test at $P<0.05$ and $P<0.001$.

potential of a cell) in the irradiated spleen than in the irradiated liver [53]. The treatment with DSePA itself showed marginal induction of the *GADD45α* and the *Bcl-2* genes, whereas the expression of *p21* and *BAX* was differentially modulated in spleen and liver tissues. All these results imply that DSePA has a regulatory effect on the expression of the genes involved in the cell cycle, DNA repair, and cell survival at the transcriptional level. Our future experiments will focus on understanding these effects in greater detail. Furthermore, the results from the analysis of the apoptotic markers clearly showed that pretreatment with DSePA effectively suppressed apoptosis in spleen by decreasing the activation of caspase-3. However, DSePA, by itself, induced marginal apoptosis in splenocytes.

Finally, the protection conferred to radiosensitive organs by DSePA should naturally manifest in an improvement in the survival of irradiated animals. Indeed, DSePA clearly enhanced the survival of mice exposed to a lethal whole-body dose of 10 Gy by 35.3%. However, doubling the dose of DSePA to 4.0 mg/kg did not enhance the survival percentage, warranting future detailed studies.

In conclusion, all these results confirm that DSePA shows effective protection against γ-radiation-induced mortality in animal models. DSePA may be considered a promising prototype in the design and development of organoselenium antioxidants with lower toxicity and better radioprotective profile.

Acknowledgments

The authors are thankful to Drs. K.B. Sainis, T. Mukherjee, S.K. Sarkar, and D. Das for their encouragement and support of this work. Support from the Board of Research in Nuclear Sciences in the form of a research grant under the Prospective Research Fund Scheme (Grant BRNS/2007/3815) is acknowledged.

References

[1] Andreassen, C. N.; Grau, C.; Lindegaard, J. C. Chemical radioprotection: a critical review of amifostine as a cytoprotector in radiotherapy. *Semin. Radiat. Oncol.* **13:** 62–72; 2008.
[2] Riley, P. A. Free radicals in biology: oxidative stress and the effects of ionizing radiation. *Int. J. Radiat. Biol.* **65:**27–33; 1994.
[3] Weiss, J. F.; Simic, M. G. Perspectives in radioprotection. *Pharmacol. Ther.* **39:** 1–414; 1988.
[4] Weiss, J. F.; Kumar, K. S.; Walden, T. L.; Neta, R.; Landauer, M. R.; Clark, E. P. Advances in radioprotection through the use of combined agent regimens. *Int. J. Radiat. Biol.* **57:**709–722; 1990.
[5] Weiss, J. F.; Landauer, M. R. Protection against ionizing radiation by antioxidant nutrients and phytochemicals. *Toxicology* **189:**1–20; 2003.
[6] Rosenfield, I.; Beath, O. A. Selenium: Geotoxicity, Biochemistry, Toxicity and Nutrition. Academic Press, New York; 1964.
[7] Brenneisen, P.; Steinbrenner, H.; Sies, H. Selenium, oxidative stress, and health aspects. *Mol. Aspects Med.* **26:**256–267; 2005.
[8] Rayman, M. P. The importance of selenium to human health. *Lancet* **356:**233–241; 2000.
[9] Tapiero, H.; Townsen, D. M.; Tew, K. D. The antioxidant role of selenium and selenol-compounds. *Biomed. Pharmacother.* **57:**134–144; 2003.
[10] Venardos, K.; Harrison, G.; Headrick, J.; Perkins, A. Effects of dietary selenium on glutathione peroxidase and thioredoxin reductase activity and recovery from cardiac ischemia–reperfusion. *J. Trace Elem. Med. Biol.* **18:**81–88; 2004.
[11] Nichter, M.; Thompson, J. J. For my wellness, not just my illness: North Americans use of dietary supplements. *Cult. Med. Psychiatry* **30:**175–222; 2006.
[12] Bradburn, M. J.; Deeks, J. J.; Berlin, J. A.; Localio, A. R. Effects of selenium supplementation for cancer prevention in patients with carcinoma of the skin: a randomized controlled trial. *JAMA* **276:**1957–1963; 1996.
[13] Vunta, H.; Davis, F.; Palempalli, U. D.; Bhat, D.; Arne, R. J.; Thompson, J. T.; Peterson, D. G.; Reddy, C. C.; Prabhu, K. S. The anti-inflammatory effects of selenium are mediated through 15-deoxy-$\Delta^{12,14}$-prostaglandin J_2 in macrophages. *J. Biol. Chem.* **282:**17964–17973; 2007.
[14] Arteel, G. E.; Sies, H. The biochemistry of selenium and the glutathione system. *Environ. Toxicol. Pharmacol.* **10:**153–158; 2001.
[15] Sies, H.; Arteel, G. E. Interaction of peroxynitrite with selenoproteins and glutathione peroxidase mimics. *Free Radic. Biol. Med.* **28:**1451–1455; 2000.
[16] Papp, L. V.; Lu, J.; Holmgren, A.; Khanna, K. K. From selenium to selenoproteins: synthesis, identity and their role in human health. *Antioxid. Redox Signaling* **9:** 775–806; 2007.
[17] Mugesh, G.; du Mont, W. -W.; Sies, H. Chemistry of biologically important synthetic organoselenium compounds. *Chem. Rev.* **101:**2125–2179; 2001.
[18] Kunwar, A.; Mishra, B.; Barik, A.; Kumbhare, L. B.; Pandey, R.; Jain, V. K.; Priyadarsini, K. I. 3,3′-Diselenodipropionic acid, an efficient peroxyl radical scavenger and a GPx mimic, protects erythrocytes (RBCs) from AAPH-induced hemolysis. *Chem. Res. Toxicol.* **20:**1482–1487; 2007.
[19] Mishra, B.; Barik, A.; Kunwar, A.; Kumbhare, L. B.; Priyadarsini, K. I.; Jain, V. K. Correlating the GPx activity of selenocystine derivatives with one-electron redox reactions. *Phosphorus Sulfur Silicon* **183:**1018–1025; 2008.
[20] Tak, J. K.; Park, J. W. The use of ebselen for radioprotection in cultured cells and mice. *Free Radic. Biol. Med.* **46:**1177–1185; 2009.
[21] Prabhakar, K. R.; Veerapur, V. P.; Bansal, P.; Parihar, V. K.; Reddy, K. M.; Kumar, P. B.; Priyadarsini, K. I.; Unnikrishnan, M. K. Antioxidant and radioprotective effect of the active fraction of *Pilea microphylla* (L.) ethanolic extract. *Chem. Biol. Interact.* **165:** 22–32; 2007.
[22] Kunwar, A.; Narang, H.; Priyadarsini, K. I.; Krishna, M.; Pandey, R.; Sainis, K. B. Delayed activation of PKCδ and NFκB and higher radioprotection in splenic lymphocytes by copper(II)–curcumin (1:1) complex as compared to curcumin. *J. Cell. Biochem.* **102:**1214–1224; 2007.
[23] Abei, H. Catalase in vitro. *Methods Enzymol.* **105:**121–126; 1984.
[24] Sreejayan, N.; Rao, M. N. A.; Priyadarsini, K. I.; Devasagayam, T. P. A. Inhibition of radiation induced lipid peroxidation by curcumin. *Int. J. Pharm.* **151:**127–130; 1997.
[25] Sedlak, J.; Lindsay, R. Estimation of total, protein-bound, and nonprotein sulfhydryl groups in tissue with Ellman's reagent. *Anal. Biochem.* **25:**192–205; 1968.
[26] Oliver, C. N.; Ahn, B.; Moerman, E. J.; Goldstein, S.; Stadtman, E. R. Age-related changes in oxidized proteins. *J. Biol. Chem.* **262:**5488–5491; 1987.
[27] Reitman, S.; Frankel, S. A. Colourimetric method for the determination of serum oxaloacetic and glutamic pyruvic transaminases. *Am. J. Clin. Pathol.* **28:**56–63; 1957.
[28] Mansour, H. H.; Hafez, H. F.; Fahmy, N. M.; Hanafi, N. Protective effect of N-acetylcysteine against radiation induced DNA damage and hepatic toxicity in rats. *Biochem. Pharmacol.* **75:**773–780; 2008.
[29] Sandhya, T.; Lathika, K. M.; Pandey, B. N.; Bhilwade, H. N.; Chaubey, R. C.; Priyadarsini, K. I.; Mishra, K. P. Protection against radiation oxidative damage in mice by Triphala. *Mutat. Res.* **609:**17–25; 2006.
[30] Mehata, S.; Mehata, L.; Mongia, S. P. Effect of whole body X-irradiation on liver of Swiss albino mice. *Int. J. Exp. Biol.* **13:**73–75; 1975.
[31] Samini, M.; Dehpour, A. R.; Hajinabi, K. The effect of lithium on acute toxicity of carbamazepine in mice. *Acta Med. Iran* **35:**74–76; 1997.
[32] Katzung, B. G. Basic and Clinical Pharmacology. Academic Press, London, pp. 404–405; 1988.
[33] Weiss, J. F.; Srinivasan, V.; Kumar, K. S.; Landauer, M. R. Radioprotection by metals: selenium. *Adv. Space Res.* **12:**23–231; 1992.
[34] Weiss, J. F.; Srinivasan, V.; Kumar, K. S.; Landauer, M. R.; Patchen, M. L. Radioprotection by selenium compounds. In: Favier, A.E., Neve, J., Fauve, P. (Eds.), Trace Elements and Free Radicals in Oxidative Diseases. Am. Oil Chem. Soc., Champaign, IL, pp. 211–222; 1994.
[35] Diamond, A. M.; Dale, P.; Murray, J. L.; Gardina, D. J. The inhibition of radiation induced mutagenesis by the combined effects of selenium and the aminothiol WR-1065. *Mutat. Res.* **356:**147–154; 1996.
[36] Kumar, B. S.; Kunwar, A.; Ahmad, A.; Kumbhare, L. B.; Jain, V. K.; Priyadarsini, K. I. In vitro radioprotection studies of organoselenium compounds: differences between mono and diselenides. *Radiat. Environ. Biophys.* **48:**379–384; 2009.
[37] Maclachlan, T.; Narayanan, B.; Gerlach, V. L.; Smithson, G.; Gerwien, R. W.; Folkerts, O.; Fey, E. G.; Watkins, B.; Seed, T.; Alvarez, E. Human fibroblast growth factor 20 (FGF-20; CG53135-05): a novel cytoprotectant with radioprotective potential. *Int. J. Radiat. Biol.* **81:**567–579; 2005.
[38] Jagetia, G. C.; Reddy, T. K. Modulation of radiation induced alteration in the antioxidant status of mice by naringin. *Life Sci.* **77:**780–794; 2005.
[39] Han, Y.; Son, S. -J.; Akhalaia, M.; Platonov, A.; Son, H. -J.; Lee, K. -H.; Yun, Y. -S.; Song, J. -Y. Modulation of radiation induced disturbances of antioxidant defense systems by ginsan. *eCAM* **2:**529–536; 2005.
[40] Ramadan, L. A.; Roushdy, H. M.; Abusenna, G. M.; Amin, N. E.; El-Deshw, O. A. Radioprotective effect of silymarin against radiation induced hepatotoxicity. *Pharmacol. Res.* **45:**447–454; 2002.
[41] Weiss, J. F.; Landauer, M. R.; Gunter-Smith, P. J.; Hanson, W. R. Effect of radioprotective agents on survival after acute intestinal radiation injury. In: Dubois, A., King, G.L., Livengood, D.R. (Eds.), Radiation and the Gastrointestinal Tract. CRC Press, Boca Raton, FL, pp. 183–199; 1995.
[42] Weiss, J. F.; Landauer, M. R.; Hogan, J. B.; Gunter-Smith, P. J.; Benson, K. A.; Neta, R.; Hanson, W. R. Modification of radiation-induced gastrointestinal and hematopoietic injury in mice by combinations of agents: effects of indomethacin and caffeine. *Adv. Exp. Med. Biol.* **400B:**865–872; 1997.
[43] Mishra, B.; Kumbhare, L. B.; Jain, V. K.; Priyadarsini, K. I. Pulse radiolysis studies on reactions of hydroxyl radicals with selenocystine derivatives. *J. Phys. Chem. B* **112:** 4441–4446; 2008.
[44] Zhang, Y.; Rohde, L. H.; Emami, K.; Hammond, D.; Casey, R.; Mehta, S. K.; Jeevarajan, A. S.; Pierson, D. L.; Wu, H. Suppressed expression of non DSB repair genes inhibits gamma radiation induced cytogenetic repair and cell cycle arrest. *DNA Repair* **7:**1835–1845; 2008.
[45] Amanullah, A.; Azam, N.; Balliet, A.; Hollander, C.; Hoffman, B.; Fornace, A.; Liebermann, D. Cell signalling: cell survival and a Gadd45-factor deficiency. *Nature* **424:**741–742; 2003.
[46] Smith, M. L.; Kontny, H. U.; Zhan, Q.; Sreenath, A.; O'Connor, P. M.; Fornace Jr, A. J. Antisense GADD45 expression results in decreased DNA repair and sensitizes cells to U.V. irradiation or cisplatin. *Oncogene* **13:**2255–2263; 1996.
[47] Fornace Jr., A. J.; Nebert, D. W.; Hollander, M. C.; Luethy, J. D.; Papathanasiou, M.; Fargnoli, J.; Holbrook, N. J. Induction by ionizing radiation of the gadd45 gene in

cultured human cells: lack of mediation by protein kinase C. *Mol. Cell. Biol.* **11:** 1009–1016; 1991.

[48] Gupta, M.; Gupta, S. K.; Hoffman, B.; Liebermann, D. A. Gadd45a and gadd45b protect hematopoietic cells from UV induced apoptosis via distinct signaling pathways including p38 activation and JNK inhibition. *J. Biol. Chem.* **281:**17552–17558; 2006.

[49] Xiong, Y.; Hannon, G. J.; Zhang, H.; Casso, D.; Kobayashi, R.; Beach, D. p21 is a universal inhibitor of cyclin kinases. *Nature* **366:**701–714; 1993.

[50] Smith, M. L.; Ford, J. M.; Hollander, M. C.; Bortnick, R. A.; Amundson, S. A.; Seo, Y. R.; Deng, C. X.; Hanawalt, P. C.; Fornace Jr., A. J. p53-mediated DNA repair responses to UV radiation: studies of mouse cells lacking p53, p21, and/or gadd45 genes. *Mol. Cell. Biol.* **20:**3705–3714; 2000.

[51] Radford, I. R. Initiation of ionizing radiation-induced apoptosis: DNA damage-mediated or does ceramide have a role? *Int. J. Radiat. Biol.* **75:**521–528; 1999.

[52] Mantena, S. K.; Unnikrishnan, S. K.; Joshi, R.; Radha, V.; Uma Devi, P.; Mukharjee, T. In vivo radioprotection by 5-amino salicylic acid. *Mutat. Res.* **650:**63–79; 2008.

[53] Shi, Y. -Q.; Liao, Y. -X.; Qu, X. -J.; Yuan, H. -Q.; Li, S.; Qu, J. -B.; Lou, H. -X. Marchantin C, a macrocyclic bisbibenzyl, induces apoptosis of human glioma A172 cells. *Cancer Lett.* **262:**173–182; 2008.